Value-added products by optimization of hydrothermal liquefaction of wastes

Arturi, Katarzyna Ratajczyk

DOI (link to publication from Publisher):
10.5278/vbn.phd.eng.00004

Publication date:
2017

Document Version
Publisher's PDF, also known as Version of record

VALUE-ADDED PRODUCTS BY OPTIMIZATION OF HYDROTHERMAL LIQUEFACTION OF WASTES

BY
KATARZYNA R. ARTURI

DISSERTATION SUBMITTED 2017

AALBORG UNIVERSITY
DENMARK

Value-added products by optimization of hydrothermal liquefaction of wastes

PhD Dissertation

Katarzyna R. Arturi

Aalborg University
Department of Chemistry and Bioscience
Niels Bohrs Vej 8
DK-6700 Esbjerg

Dissertation submitted: March 3, 2017

PhD supervisor: Prof. Erik G. Søgaard
Department of Chemistry and Bioscience
Aalborg University, Denmark

PhD committee: Professor Donghong Yu (chairman)
Department of Chemistry and Bioscience
Aalborg University, Denmark

Professor Shuguang Deng
School of Engineering of Matter, Transport and Energy
Arizona State University, USA

Professor Peter Westh
Department of Science and Environment, Chemistry
Roskilde University, Denmark

PhD Series: Faculty of Engineering and Science, Aalborg University

ISSN (online): 2446-1636
ISBN (online): 978-87-7112-908-3

Published by:
Aalborg University Press
Skjernvej 4A, 2nd floor
DK – 9220 Aalborg Ø
Phone: +45 99407140
aauf@forlag.aau.dk
forlag.aau.dk

Printed in Denmark by Rosendahls, 2017

Curriculum Vitae

Katarzyna R. Arturi

Proffesional Experience

2014-now **PhD fellow**, Aalborg University Esbjerg
2012-2014 **Scientific Assistant**, Aalborg University Esbjerg

Higher Education

2010–2012 **MSc**, Aalborg University Esbjerg, Removal of Fe from groundwater
2007–2010 **BSc**, Aalborg University Esbjerg, Hydrothermal biomass processing

Teaching Experience

2014–2016 Products, processes, and applied chemistry
2014 Introduction to colloidal chemistry in laboratory
2015 Introduction to X-ray diffraction in laboratory
2012–2016 Supervision of student projects (semesters II-IX)

Conferences

June 2016 Poster presentation "*Hydrothermal processing of waste into value*", 24th EUBCE (European Biomass Conference and Exhibition), Amsterdam, Netherlands.

Sept. 2016 Oral presentation "*Advanced oxidation of water soluble organics (WSO) from near- and supercritical liquefaction (HTL) of biomass*", 1st International Conference on Sustainable Water Processing, Sitges, Spain.

Abstract

The need to replace fossil-based fuels, materials, and chemicals has spurred intense research in dozens of biomass conversion fields. Hydrothermal liquefaction is a thermochemical technique that utilizes the unique properties of near- and supercritical fluids to convert complex biomass feeds into a spectrum of value-added products. The process is versatile in terms of feedstocks, it can process moisture-rich streams unsuitable for the traditional pyrolysis and gasification conversions, and it can utilize wastes incompatible with biochemical processing methods. The outlined advantages make liquefaction an excellent potential addition to a biorefinery.

Optimization of different aspects of liquefaction is crucial for further development and commercialization of this conversion technique. This thesis deals with a number of liquefaction challenges including I) Development of multivariate models for prediction of liquefaction outputs as a function of process parameters; II) Improving the analytical characterization of liquefaction products; III) Design of batch systems and experimental procedures with control over all crucial process parameters as a platform for the development of continuous liquefaction processes; IV) Hydrothermal liquefaction of different wastes (lignin, lignocellulose, and plastic) as potential feedstocks for production of value-added products: drop-in energy carriers, transportation biofuels, and chemicals.

Due to variations in the applied experimental liquefaction procedures and product separation schemes, the pool of results reported in the literature is very heterogeneous. Application of multivariate data analysis as a tool for determination of universally valid guidelines for prediction of liquefaction showed that each biomass type requires its own optimized parameters. The quality of the models varied depending on the biomass type and response. Algae as feed resulted in maximized biofuel yields and enhanced energy content. A combination of concentrations of the homogeneous catalyst, heating time, and residence time controlled the distribution of the products between the aqueous fraction and the biocrude. The energy content in the biocrude was dependent on the biomass properties, but not on the process conditions.

Abstract

With production of valuable chemicals as a partial aim of liquefaction, there is a need for improved characterization of the composition of the reaction products. The challenge today is that the constituents of the aqueous phase and the biocrude are either too polar or not volatile enough to be identified and quantified by standard analytical tools. Transfer and analysis of analytes by combination of solid-phase microextraction (SPME) with gas chromatography-mass spectrometry (GC-MS) was an excellent low-tech method providing detailed characterization of organics present in the aqueous phase and the biocrude from liquefaction. Application of high-resolution liquid chromatography mass spectrometry (LC-ESI-MS/MS) enhanced separation and identification of the samples' constituents and was crucial for an accurate quantification of the produced chemicals.

A small batch reactor is the most common system used for liquefaction studies. These systems have the advantage of minimizing practical challenges common for the continuous systems, and are therefore preferred in the initial stages of liquefaction screening. However, using typical batch reactors can be troublesome with regard to the control of certain process parameters such as medium density, heating rates, and reaction time. The reactor used in this study incorporated injection of biomass slurries into a pre-heated and pre-pressurized reaction medium. This procedure guaranteed fast heating of the feed, which served to avoid unwanted pathways in the conversion chemistry, and precise residence times. In addition to that, the reactor also included a pressure control feature, which made the obtained results comparable to the results from typical continuous liquefaction reactors.

Selection of the right biomass for liquefaction is essential for process sustainability and maximizing resource efficiency. Wastes, which do not compete with food, do not require land, water, nutrients, or pesticides, and are available in ample amounts, seem like an excellent candidate. Recovery of energy from waste streams by burning is at the bottom of the waste hierarchy pyramid. These materials could be valorized more efficiently with liquefaction, as showed by the current results. A broad spectrum of chemicals, including aliphatic, cyclic, and light oxygenates were formed as a result of processing. Lignin was converted into a mixture of aromatic monomers, dimers, and heavier repolymerization products. Liquefaction of lignocellulose resulted in a conversion product combination low molecular weight chemicals (LMW), cyclics (C), aromatics (A), and higher molecular weight compounds (HMW). With plastic as a feed, both the monomers from the polymer chains as well as secondary reaction products were recovered for recycling to close the loop on the material life cycle. Process parameters such as temperature and the presence of co-solvents were of paramount importance for the reaction pathways of liquefaction and the obtained yields of monomers. For liquefaction of biomass, the co-solvents increased the production of aromatics and repressed repolymerization leading to biochar. In solvolysis of plastics, the presence of acetone led to an effective polarity-based separation of reaction products, in addition to the formation of other value-added outputs.

Resumé

Behovet for at erstatte fossile brændstoffer, materialer og kemikalier med vedvarende alternativer har medvirket til intens forskning i biomasse konverteringsprocesser. *Hydrothermal liquefaction* er en termokemisk metode, der omdanner kompleks biomasse til værdifulde produkter vha. de unikke egenskaber af nær- og superkritiske væsker. Processen er alsidig mht. råmaterialer, f.eks. både vandholdig biomasse såvel som organisk affald kan udnyttes. Dette gør liquefaction forskellig fra pyrolyse, forgasning, og biokemiske metoder, der stiller høje krav til råmaterialet. Liquefaction har mange fordele og vil være et fremragende bidrag til et moderne bioraffinaderi.

Optimering af liquefaction er afgørende for teknikkens videre udvikling og kommercialisering. Resultater, præsenteret i denne afhandling, vedrører forskellige udfordringer ved processen: I) Udvikling af statistiske modeller til at forudsige produkternes mængder og egenskaber på bagrund af procesparametrene; II) Forbedring af produkt karakterisering vha. analytiske metoder; III) Design af batch reaktorer og eksperimentelle procedurer, der muliggør en høj grad af proceskontrol og udvikling af kontinuerlige processer; IV) Liquefaction af diverse affaldsprodukter (lignin, lignocellulose, og plast) og evaluering af deres potentiale som en kilde til værdifulde produkter: *drop-in* energibærere, biobrændstoffer til transportformål, og kemikalier.

Liquefaction afhænger af talrige procesparametre, og på grund af variationer i eksperimentelle procedurer og produkt separationsprocesser, findes der signifikante afvigelser mellem resultaterne fra forskellige undersøgelser i litteraturen. Anvendelse af multivariabel dataanalyse som redskab gjorde det muligt at identificere de generelle tendenser bag liquefaction. Der blev ikke fundet optimale proces indstillinger for alle typer af biomasse. Derimod blev der observeret, at udbyttet af vandopløselige organiske stoffer kunne forudsiges med nøjagtighed, hvorimod modellerne for biocrude var en mere generel indikering af tendenser. Alger var omdannet mest effektivt i liquefaction og resulterede i det højeste energiindhold i biocrude. Koncentrationer af den homogene katalysator, opvarmningstiden, og opholdstiden i reaktoren kontrollerede fordeling af produkterne mellem vandfasen og biocrude.

Med produktion af værdifulde kemikalier som et mål, er der et behov for bedre karakterisering af sammensætningen af reaktionsprodukterne fra liquefaction. Udfordringen i dag er, at bestanddelene i vandfasen er for polære og i *biocrude* ikke flygtige nok til at kunne identificeres og kvantificeres effektivt ved hjælp af standard analytiske metoder. Anvendelse af avancerede værktøjer som *solid-phase microextraction* (SPME) og høj opløsning væskekromatografi-massespektrometri (LC-ESI-MS/MS) forbedrede identifikationen af prøverne signifikant. Kombination af SPME med gaskromatografi-massespektrometri (GC-MS) er en lavteknologisk metode der giver en detaljeret karakterisering af organiske forbindelser fra liquefaciton af lignocellulose i både vandfasen og biocrude. Anvendelse af LC-ESI-MS/MS var afgørende for en nøjagtig kvantificering af de producerede kemikalier.

Små batch reaktorer er de mest almindelige værktøjer til undersøgelser af liquefaction. Optimering af processen i disse typer af systemer kræver en streng kontrol over procesparametre, især densitet, opvarmningshastighed, og reaktionstid. Reaktorsystemer med injektion af biomasse til et forvarmet reaktionsmedium sikrede hurtig opvarmning af biomassen, hvorved man undgik den uønskede konvertering af biomasse ved lave temperaturer. Der var desuden i disse systemer mulighed for en nøjagtig styring af reaktionstiden, hvilket gør dem sammenlignelige med kontinuerlige anlæg.

Med hensyn til processens bæredygtighed, er det vigtigt at vælge det rigtige råmateriale til *liquefaction*. Affald konkurrerer ikke med fremstilling af madvarer, kræver ingen land, vand, næringsstoffer eller pesticider, og er tilgængeligt i rigelige mængder. Hvert år dannes der store mængder af industrielt affald. Disse ressourcer bliver normalt forbrændt for at genvinde energien. Dette er en form for genbrug, men disse strømme vil kunne valoriseres yderligere ved at bruge dem til fremstilling af mere værdifulde produkter vha. f.eks. *liquefaction*. Omdannelse af affald resulterede i produktion af mange potentielt nyttige kemikalier. Lignin omdannedes til en blanding af aromatiske monomerer, dimere, og høj molekylevægt komponenter. Liquefaction af lignocellulose resulterede i en blanding af lavmolekylære produkter (LMW), cykliske komponenter (C), aromater (A), og høj molekylevægt produkter (HMW). Med plastik som råvare, blev der dannet monomerer og sekundære reaktionsprodukter, der kan genindvindes og genanvendes til at lukke cirklen på materialets livscyklus. Procesparametre såsom temperatur og tilstedeværelse af co-solventer var af afgørende betydning for produktionen af kemikalier. Ved omdannelse af biomasse, øgede co-solventer dannelsen af aromatiske forbindelser og forhindrede repolymerisering af reaktive mellemprodukter. I tilfælde af plast, resulterede acetone i en polaritet-basereret separation af monomerer (vandfasen) og sekundære reaktionsprodukter (olien). Udover dette, var co-solventen også kilde til vædrifulde kemikalier.

Thesis Details

Thesis title:	Value-added products by optimization of hydrothermal liquefaction of wastes
PhD student:	Katarzyna R. Arturi
Supervisor:	Prof. Erik G. Søgaard, Aalborg University

The main body of this thesis consist of the following papers (in the order of appearance and logical narrative of the thesis):

[A] **Katarzyna R. Arturi**, Sergey Kucheryavskiy, and Erik G. Søgaard, "Performance of hydrothermal liquefaction (HTL) of biomass by multivariate data analysis", *Fuel Processing Technology*, Vol. 150, pp. 94–103, 2016.

[B] **Katarzyna R. Arturi**, Kathrine R. Toft, Rudi P. Nielsen, Lasse A. Rosendahl, and Erik G. Søgaard, "Characterization of liquid products from hydrothermal liquefaction (HTL) of biomass via solid-phase microextraction (SPME)", *Biomass and Bioenergy*, Vol. 88, pp. 116–125, 2016.

[C] **Katarzyna R. Arturi**, Morten Strandgaard, Rudi P. Nielsen, Erik G. Søgaard, and Marco Maschietti, "Hydrothermal liquefaction of lignin in near-critical water in a new batch reactor: Influence of phenol and temperature", *Journal of Supercritical Fluids*, Vol. 123, pp. 28–39, 2017.

[D] **Katarzyna R. Arturi**, Sergey Kucheryavskiy, Marco Maschietti, Rudi P. Nielsen, and Erik G. Søgaard, "Hydrothermal conversion of *Fallopia japonica* in near-critical water: A study of liquefaction routes in the presence of co-solvents", Under peer review in *Bioresource Technology*.

[E] **Katarzyna R. Arturi**, Hülya U. Sokoli, Erik G. Søgaard, Frédéric Vogel, and Saša Bjelić, "Recovery of value-added chemicals by solvolysis of unsaturated polyester resin", Under peer review in *Journal of Cleaner Production*.

In addition to the main papers, contributions to the following publications about hydrothermal conversion have also been made:

[I] Hülya U. Sokoli, Morten E. Simonsen, Rudi P. Nielsen, **Katarzyna R. Arturi**, and Erik G. Søgaard, "Conversion of the matrix in glass fiber reinforced composites into a high heating value oil and other valuable feedstocks", *Fuel Processing Technology*, Vol. 149, pp. 29–39, 2016.

[II] Thomas H. Pedersen, Jessica F. Hoffman, Saquib S. Toor, Iulia M. Daraban, Claus U. Jensen, Rudi P. Nielsen, **Katarzyna R. Arturi**, Erik G. Søgaard, and Lasse A. Rosendahl, "Continuous hydrothermal co-liquefaction of aspen wood and glycerol with water phase recirculation," *Applied Energy*, Vol. 162, pp. 1034–1041, 2016.

[III] Ionela Florentina Grigoras; **Katarzyna R. Arturi**, Donghong Yu, Saqib S Toor, and Lasse A. Rosendahl, "Effect of heating stage severity on the formation of products resulting from hydrothermal liquefaction of meadow grass", Under preparation.

In addition to the papers related to solvothermal liquefaction, the following publications in other research fields have also been made:

[IV] **Katarzyna R. Arturi**, Henrik Jepsen, Jesper N. Callsen, Erik G. Søgaard, and Morten E. Simonsen, "Superhydrophilicity and durability of fluoropolymer-TiO_2 coatings", *Progress in Organic Coatings*, Vol. 90, pp. 132–138, 2016.

[V] **Katarzyna R. Arturi**, Christian B. Koch, and Erik G. Søgaard, "Characterization and comparison of iron oxyhydroxide precipitates from biotic and abiotic groundwater treatments", *Journal of Water Supply: Research and Technology*, In press, 2017.

This thesis has been submitted for assessment in partial fulfillment of the PhD degree. The thesis is based on the submitted or published scientific papers which are listed above. Parts of the papers are used directly or indirectly in the extended summary of the thesis. As part of the assessment, co-author statements have been made available to the assessment committee and are also available at the Faculty. The thesis in its present form is not acceptable for open publication but only in limited and closed circulation as copyright may not be ensured.

Acknowledgments

Firstly, I would like to express my sincere gratitude to my supervisor Prof. Erik G. Søgaard for believing in me and for the continuous support for my research. Thank you Erik for your guidance and for providing me with the freedom to pursue my interests on this extraordinary journey to becoming a PhD.

I thank my fellow PhD students, research associates, and other co-workers, namely: Dorte Spangsmark, Linda B. Madsen, Lisbeth Skou, and Morten Strandgaard for assistance with experimental and analytical work in the laboratory; Adeel N. Sohal, Hülya U. Sokoli, and Anita Asamoah for fruitful discussions and fun we have had in the last three years; Marco Maschietti, Morten E. Simonsen, Kathrine R.T. Hansen, Rudi P. Nielsen, and Jens Muff for the cooperation on various projects and papers; Heidi Thomsen for administrative support. Sergey Kucheryavskiy deserves special thanks for all the time and brilliant help provided in producing and reviewing numerous publications. Your help with Matlab and R has been invaluable.

During my studies I was fortunate to spent three months at Paul Scherrer Institute, Switzerland, with the group of Prof. Frédéric Vogel. To him and my colleagues at PSI I would like to express my sincere gratitude for welcoming me into their scientific circle and making me feel at home. To my supervisor at PSI, Dr. Saša Bjelić, I would like to say this: working with you has been an amazing experience. You have inspired me to always strive towards excellence. For that, I will be forever grateful.

Last but not the least, I would like to express my gratitude to my family and friends. Thank you for supporting my dreams, through good and bad times, and believing in the impossible.

Preface

This thesis is submitted to the International Doctoral School of Technology and Science at Aalborg University in a partial fulfillment of the requirements for the degree of Doctor of Philosophy. The work was carried out in the period spanning from March 2014 to February 2017 at the Department of Chemistry and Bioscience at Aalborg University Esbjerg.

The thesis is concerned with optimization of hydrothermal liquefaction of wastes for production of value-added products and is divided into three parts. In the first part, the framework of the thesis and its research objectives are presented. It includes an introduction to the challenges of replacing fossil resources with renewable and sustainable solutions, places liquefaction in perspective to the other biomass conversion technologies, and presents the state-of-the-art knowledge in the fields of processing in near- and supercritical fluids in general, and liquefaction in particular. This is followed, in Part II, by the presentation of the current results with the focus on the core conclusions of the experimental work. Each chapter of this part tackles an individual research goal, starting with a background, followed by the main findings, and ending with an outline for future work. For the information on the applied materials and methods and a more detailed description of the results, I will refer the reader to the main body of the thesis, i.e. Part III. This part consists of a number of papers, which have been published in or submitted to peer-reviewed journals. The papers have been ordered according to the logical narrative of the thesis and were incorporated into its native typography.

Katarzyna R. Arturi
Aalborg University, February 28, 2017

Contents

Curriculum Vitae iii

Abstract v

Resumé vii

Thesis Details ix

Acknowledgments xi

Preface xiii

I Framework 1

1 Introduction 3
1 Challenges of tomorrow . . . 3
2 Biomass conversion processes . . . 5
3 Biorefinery concept . . . 15
References . . . 17

2 Near- and supercritical fluids 21
1 Water as a reaction medium . . . 21
2 Co-solvents addition . . . 24
References . . . 25

3 Hydrothermal liquefaction 29
1 Historical perspective . . . 29
2 Conversion parameters . . . 30
3 Conversion mechanisms . . . 33
4 Characterization of products . . . 34
References . . . 34

Research objectives 41

II Results **43**

4 Statistical modelling **45**
1 Background . . . 45
2 Modeling of literature data . . . 46
3 PCA and chromatography . . . 48
4 Outlook . . . 48
References . . . 49

***5* Product characterization** **53**
1 Background . . . 53
2 Solid-phase microextraction . . . 54
3 Liquid chromatography-mass spectrometry . . . 57
4 Outlook . . . 57
References . . . 58

6 Reactor **61**
1 Background . . . 61
2 Cold-injection system . . . 61
3 Outlook . . . 64
References . . . 64

7 Conversion of lignin **65**
1 Background . . . 65
2 Production of monomers . . . 68
3 Outlook . . . 69
References . . . 69

8 Conversion of lignocellulose **71**
1 Background . . . 71
2 Influence of co-solvents . . . 74
3 Outlook . . . 74
References . . . 75

9 Conversion of polyester resin **77**
1 Background . . . 77
2 Value-added chemicals . . . 78
3 Outlook . . . 80
References . . . 80

Conclusions **83**

III Papers **87**

A *Performance of hydrothermal liquefaction (HTL) of biomass by multivariate data analysis* **89**
1 Introduction . . . 91
2 Theory . . . 92
3 Materials and Methods . . . 95
4 Results and Discussion . . . 98
5 Conclusions . . . 105
6 Acknowledgements . . . 105
References . . . 106

B *Characterization of liquid products from hydrothermal liquefaction (HTL) of biomass via solid-phase microextraction (SPME)* **113**
1 Introduction . . . 115
2 Materials and Methods . . . 117
3 Results and Discussion . . . 119
4 Conclusions . . . 126
5 Acknowledgements . . . 127
6 Supporting Information . . . 127
References . . . 130

C *Hydrothermal liquefaction of lignin in near-critical water in a new batch reactor: Influence of phenol and temperature* **135**
1 Introduction . . . 137
2 Materials and Methods . . . 140
3 Results and Discussion . . . 145
4 Conclusions . . . 154
5 Acknowledgments . . . 154
6 Supporting Information . . . 155
References . . . 156

D *Hydrothermal conversion of Fallopia japonica in near-critical water: A study of liquefaction routes in the presence of co-solvents* **159**
1 Introduction . . . 161
2 Materials and Methods . . . 163
3 Results and Discussion . . . 167
4 Conclusions . . . 173
5 Acknowledgments . . . 173
6 Supporting Information . . . 173
References . . . 177

E *Recovery of value-added chemicals by solvolysis of unsaturated polyester resin* **179**
1 Introduction 181
2 Materials and Methods 183
3 Results and Discussion 185
4 Conclusions 189
5 Acknowledgments 189
6 Supporting information 190
References 193

Part I

Framework

The motivation behind the current thesis is the need for optimization of thermochemical techniques for the production of sustainable value-added products from biomass and other wastes. A short historical introduction to the problem is followed by the presentation of biomass conversion techniques with the focus on thermochemical conversion in near- and supercritical fluids, water and organic solvents. Potential strategies for obtaining bioenergy, biofuels, and biochemicals are compared and evaluated in terms of the sustainable biorefinery concept. This is followed by a presentation of the state-of-the-art in near- and supercritical processing in general, and liquefaction in particular. The part is concluded with an outline of the research goals and aims.

Chapter 1

Introduction

1 Challenges of tomorrow

The humanity has reached a decisive juncture in its history. While the population has surpassed 7.5 billion, the available natural resources, such as minerals, water, and fossil fuels shrink at an alarming rate due to over-exploiting, pollution, and their finite amounts. Even clean air have become a scarce commodity, with smog covering most of the world's metropolises. At the same time, the geographical distribution of the fossil resources raises serious geopolitical concerns about our dependency on foreign sources for energy and commodities. In addition to that, the climate is going haywire exposing the consequences of the *Homo sapiens'* ruthless exploitation of the environment over hundreds of years. The global climate change caused by human activity can only be mitigated by stopping the flow of greenhouse gasses (GHG) into the atmosphere. GHG encompass a broad spectrum of chemical species, including, beside the main offender, CO_2, also water vapour, methane (CH_4), nitrous oxide (N_2O), ozone (O_3), and chlorofluorocarbons (CFCs). CO_2's leading role, despite its rather low global warming potential (GWP) factor, can be attributed to the sheer size of the emissions (35 669 000 kt in 2014 [1]). The levels of carbon dioxide in the atmosphere have risen from 260 ppm at the beginning of the industrial age, through 320 ppm at the end of the WWII, and over 400 ppm today, a concentration considered by many a point of no return [2]. The consequences of climate change have so far included rising temperatures; the collapse of natural ecosystems; melting of mountain glaciers, the Arctic ice, and the Greenland ice sheet; a rising sea level, acidification of oceans; an increase in frequency and intensity of severe weather, and disturbed bird migration patterns [3]. In recent years, various renewable technologies have been developed to mitigate the human impact on the environment and avert a global disaster. Despite their fast development and commercialization, these techniques, encompassing hydroelectricity, solar energy, wind power, geothermal heat, and biofuels, were in 2013 responsible for less than 20 % of the total world energy consumption (Figure 1.1).

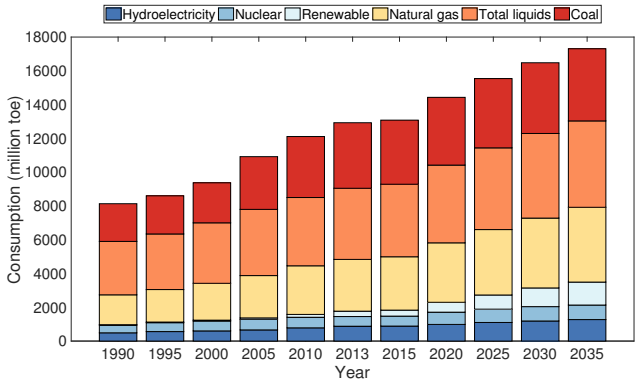

Fig. 1.1: Global energy consumption by source. The "Total liquid" group encompasses also liquid biofuels (i.e. bioethanol and biodiesel). The group "Renewable" includes all remaining types of sustainable sources, including combustion of biomass. Source: [4].

Mitigating climate change can be achieved in a number of ways, including by reducing the consumption of energy, sequestering the discharges, and reducing the emissions. The first solution would be challenging to implement on a global scale due to the development differences across the world. The energy consumption in most of the developed Western countries and regions (e.g. EU and USA) has been decreasing since 2008 due to a lower economic activity after the global economic crisis. Meanwhile, the corresponding consumption in Asia has been increasing steadily by 3 % a year [4], driven mainly by the fast development of China and India (Figure 1.2).

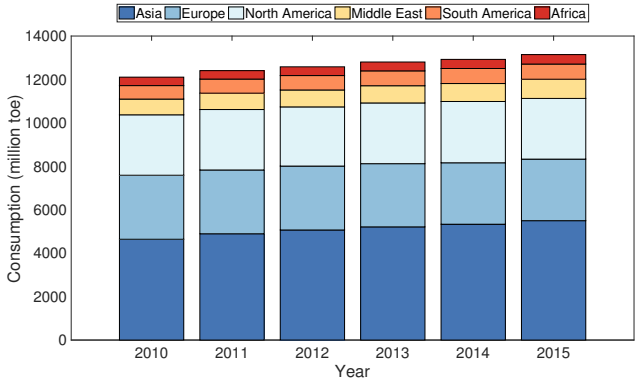

Fig. 1.2: Global consumption of energy by world's regions in the years 2010-2015. Source: [4].

CO_2 sequestration, commonly referred to as carbon dioxide capture and storage (CCS), is an interesting option, but it works best at large fossil and biomass energy facilities and industries with major point emissions [5]. Since transportation is responsible for a large part of the global energy consumption (Figure 1.3), a viable, renewable, and CO_2-neutral solution for this sector is imperative for achieving a real and perceptible change in the atmospheric CO_2 levels.

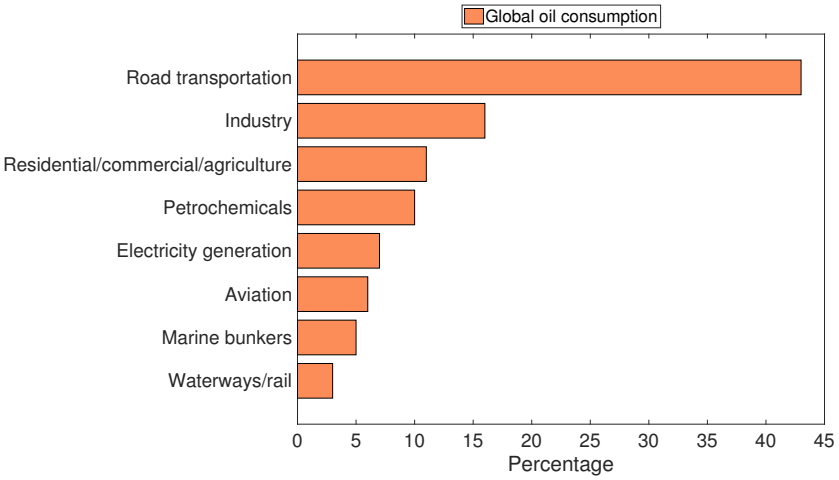

Fig. 1.3: Distribution of global energy consumption by sector in 2013. Source: [4].

The research in renewable forms of transportation is centered around two separate strategies: harnessing and utilization of renewable electrical energy and production of biomass-based fuels. A third, less established solution includes hydrogen powered cars. All of these strategies have been developed independently of each other by different actors. While both the electricity as well as hydrogen gather more and more attention, biomass-based fuels are the cheapest short-term solution for getting off fossil fuels. Utilization of biomass has another positive side effect. It allows the technologies to easily branch up into additional research areas, e.g. development of value-added chemicals and materials.

2 Biomass conversion processes

Utilization of biomass for production of energy, fuels, polymers, and chemicals from biomass is by no means a new phenomenon. Before the introduction of fossil fuels during the Industrial Revolution of the 18th century, numerous large-scale processes utilized raw materials of biological origin. An excellent example is the production of furfural, a precursor to Nylon 6.6 and one of the most common polymers in the textile industry, by distillation of hemicellulose-rich materials in the presence

of acids [6]. The explosive expansion of the petroleum based products in the 20th century has made the previously diverse group of biomass applications nearly obsolete. In recent years, the interest towards utilization of biomass as a raw material has returned as shown by the boom in the development of various biomass conversion methods. Some have been known and utilized for centuries, e.g. combustion. Others, such as biogas, biodiesel, and bioethanol production, have been developed and commercialized in the more recent past. Besides the outlined main biomass conversion processes, a plethora of other techniques in varying stages of studies or commercialization is available. An overview of the main biomass conversion methods and the resulting products is given in Figure 1.4. The thermochemical, biochemical, and physico-chemical conversion routes cover a broad spectrum of miscellaneous methods from extraction, through utilization of bacteria, to application of high temperatures and pressure values.

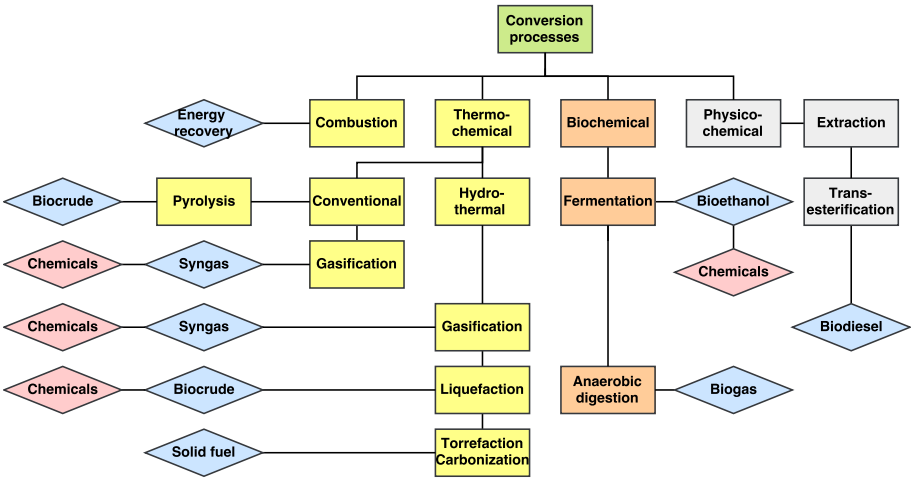

Fig. 1.4: Biomass conversion processes. The colors indicate different families of conversions (yellow - thermochemical, orange - biochemical, and gray - physico-chemical) and products (blue - energy carriers, pink - chemicals).

2.1 Biofuel sustainability

Fuel energy carriers are the most common products from biomass conversion. The drive behind the development of biofuels for transportation purposes is evident. While heat and electricity can be provided by a number of renewable techniques (geothermal energy, wind energy, solar energy), supplying the market with liquid fuels is far more complicated and limited in options due to the presence of a rigid infrastructure based on petroleum. Fermentation of sugary/starchy crops and transesterification of oils (e.g. palm oil or soybean) result in the production of bioethanol and biodiesel, respectively, the two primary liquid biofuels used in the transport industry on a commercial scale. While the former is mostly produced in the America,

the latter is widespread in the European Union (Figure 1.5). Both can be blended with their fossil equivalents (gasoline and diesel) and be used as liquid fuels in conventional engines.

Large scale utilization of biomass for production of biofuels has been discussed widely regarding the process sustainability, which, according to the International Energy Agency, is defined as "a development that meets the needs of the present without compromising the ability of future generations to meet their own needs" [7]. The main sustainability concerns include redirecting resources from food and into fuels and commodities, increasing global food prices, deforestation, and poor GHG savings. All these are related to utilization of the first generation biofuels, which today represent the overwhelming majority of the commercial solutions [8]. Alternative technologies and solutions based on non-food feedstocks, typically of lignocellulosic origin, are being currently developed. However, application of e.g. forest products is also of concern. As recently pointed out by Cornwall et al. [9]: ”the moves by governments to designate biomass as a carbon-neutral resource have spurred a fierce debate”. A letter penned in February 2016 by a group of 65 scientists from some of the largest universities across the U.S. warned that labeling biomass as carbon-neutral would encourage deforestation. A month later, a letter from over 100 other scientists expressed an opposite view to the U.S. Environmental Protection Agency (EPA), stating that "the benefits of sustainable forest biomass energy are well established" [9].

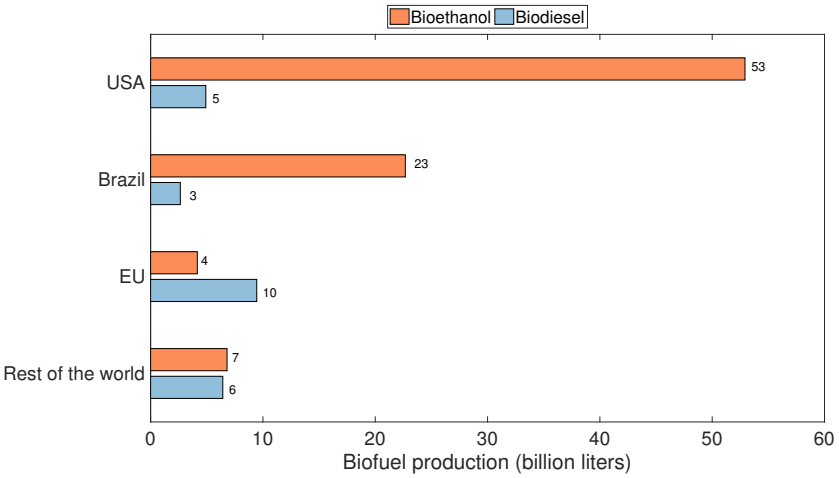

Fig. 1.5: Global biofuel production by region. Source: [4].

2.2 Liquefaction in near- and supercritical water

Thermochemical dry and wet biomass reforming processes represent an alternative source of energy carriers such as biochar, biocrude, and biogas, in addition to value-added chemicals and materials. The focus of this thesis is on wet liquefaction in near-critical water, demonstrated as early as in 1920's by an Austrian scientist Ernst Berl and co-workers [10–13]. The authors proposed and then proceeded to demonstrate that liquid fuel similar to crude oil can be produced by conversion of plants at high temperature and pressure values in water. When the process is carried out in water, it is typically referred to as "hydrothermal". In the presence of organic solvents, the description "solvothermal" can also be used.

Liquefaction can be described in simple terms as pressure cooking at high temperature and pressure values. From a technical point of view, the process involves hydrothermal treatment of a pumpable biomass slurry followed by product cooling and depressurization (Figure 1.6). From a chemical perspective, biomass is depolymerized into monomers which are then converted into intermediates and secondary reaction products distributed upon cooling between the various reaction fractions: biocrude oil, water soluble organics (WSO), gasses, and solids. While the first two are considered the main product and by-product, respectively, the latter two are produced in limited amounts. The exact distribution of the products depends on the reaction conditions and the applied feed.

The liquid biocrudes from liquefaction are fundamentally different from bioethanol, biodiesel, and biogas. The latter represent chemically pure substances or well-defined classes of compounds, while the biocrudes are heterogeneous mixtures containing hundreds of chemical species similar in composition and properties to the crude oil. Biocrude can be used directly as a drop-in boiler fuel, heavy transport fuel, it can be upgraded to lighter transportation products, or it could replace crude oil as the source of chemicals and materials in a biorefinery context [14, 15]. The presence of reactive functional groups containing oxygen in the biocrude prevents its direct use as a conventional transportation fuel without upgrading [16]. The majority of biomass liquefaction research today focuses on breaching the gap between the composition (oxygen, water, nitrogen) and properties (energy, density, viscosity) of biocrude and crude oil (Figure 1.6), which would enable its direct use as a drop-in biofuel with limited changes to the current infrastructure. In recent years, intense research has resulted in a continuous refinement of the produced biocrudes by means of process parameters, additives, and upgrading. The oxygen content, viscosity, density, and water content have all been decreased while the energy content increased [17]. The aqueous phase fraction is sometimes recirculated in the process [18], but is mostly considered to be a waste stream. This fraction contains a large portion of the converted biomass and is a potential source of chemical feedstocks, in addition to the biocrude. The biochar from liquefaction could be used as a fertilizer.

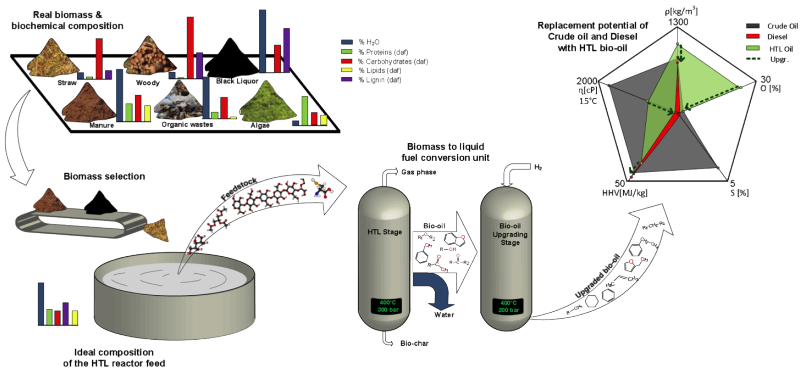

Fig. 1.6: An overview of liquefaction procedure: selection of biomass, preparation of slurry, treatment, and upgrading. In the right top corner of the figure, the properties of biocrude and crude oil are compared. Credit: Iulia-Maria Sintamarean.

The advantages of liquefaction compared to other conversion processes are numerous. Regarding the process products, pyrolysis is the dry equivalent of liquefaction. It involves high temperatures (300 - 600 °C) atmospheric pressure conversion of biomass into liquid biofuels in the absence of water and oxygen. Both liquefaction and pyrolysis are flexible regarding the raw feed used, but the biomass has to be relatively dry in the latter case. In addition to the energy intensive drying, pyrolysis biocrude has inferior quality (lower thermal stability, higher water content, lower energy content). Liquefaction and biochemical processes do not share any processing features, except that the former can be utilized as a pre-treatment before the application of the latter. The largest advantage of liquefaction over biochemical conversion lies in its raw feed versatility [19–21]. Any biomass type and content are suitable, be it wood residues, algae, manure, municipal waste, or organic-rich industrial wastewater. Waste is of particular interest, as it represents a huge underutilized resource [22] (Figure 1.7).

Liquefaction does not compete with the production of food, and its valorization of waste results in high GHG reductions combined with decreasing competition of biomass for land and water, thus taking care of an environmental burden instead of creating an additional water demand. The water footprint is, in addition to biomass price and transport costs, is considered to be a significant factor influencing the economic viability of every biomass conversion technology. As was proposed for pyrolysis [23], liquefaction could be performed in small-scale plants transported to the biomass instead of the other way around. Skeptics of liquefaction point to the process' high capital cost investments and significant energy requirements as the biggest challenges decreasing the sustainability and preventing commercialization.

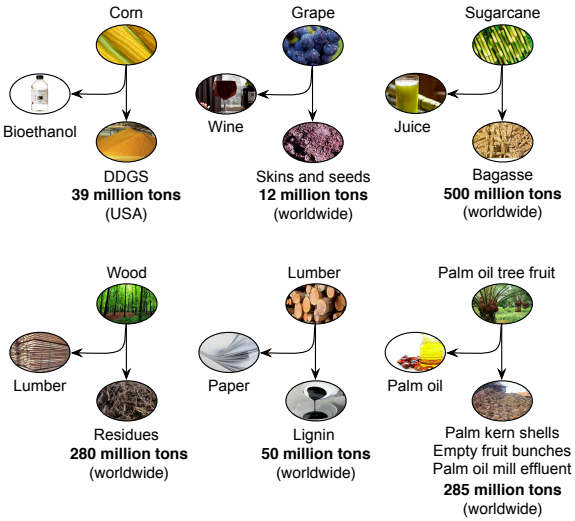

Fig. 1.7: Examples of residual biomass resources. Source [22, 24–27].

2.3 Biochemicals

More than 16 % of the oil produced each year (and more than 9 % of all fossil fuels) is used for the manufacture of chemicals and raw materials [28]. Another 5 % of the global energy consumption is spent in the manufacture processes [29]. A significant part of this produce is channeled into the polymer industry, which in 2015 alone resulted in 322 million tons of plastic materials [30]. Different recycling strategies exist today to increase the sustainability of plastics as materials. One of the most promising methods includes chemical monomer recycling, which offers a potential of closing the loop on the polymer life cycle by perpetually reusing the raw materials. Other significant applications for petrochemicals include agrochemicals, cosmetics, dyes, flavorings, pharmaceuticals, all of which must be manufactured. The most basic platform chemicals used in petrochemical industry can be divided into two groups: olefins (ethylene, propylene, C4 olefins: butadiene, 1-butene, 2-butene, isobutene) and aromatics (benzene, toluene, and xylens, commonly referred to as BTX chemicals). Production of the former involves fluid catalytic cracking of petroleum fractions. Production of the latter takes place through catalytic reforming of naphtha. The subsequent processing includes the conversion of the hydrocarbons and formation of small oxygenates with various functional groups. Figure 1.8 shows a summary of the petroleum-based platform chemicals, intermediates, and commodity products.

Taking into account the market worth of the petrochemical industry, it is easy to understand why the idea of biomass as a renewable source of chemicals is so attractive. Strategies for development of biochemicals can be divided into two distinctive groups: 1) Finding pathways for conversion of biomass into platform chemicals that are produced today from the petroleum, i.e. a drop-in "business as usual" solution; and 2) Finding new platform chemicals that can be easily manufactured from the biomass and exploring their potential. The first approach has been inherently more popular, as the solutions are customized to the current infrastructure and needs. The second approach, which was applied for the development of petrochemicals back in time, is more uncertain and thus far less common. An excellent example of this strategy is discovery and utilization of polyethylene furan dicarboxylate (PEF) [31], which combines replacement of non-renewable materials and energy, reductions in GHG emissions, with superior material properties.

Chemical and biochemical routes The most commonly utilized strategies for production of platform chemicals from biomass can be divided into two groups: chemical and biochemical. The chemical platform is dominated by acid assisted hydrolysis of C5 and C6 sugars, with results in the formation of furfural and hydroxymethylfurfural, two important platform molecules for the production of both fuels as well as chemicals [33, 34]. The biggest challenge of this technology lies in preventing secondary reactions resulting in relatively low yields of the main products. The biochemical production of chemicals is based on the processing of water-soluble sugars and starch, which can be metabolized by bacteria to produce certain chemical compounds, typically alcohols, diols, and acids. These products are typically dehydrated into corresponding olefins linking the biorefinery with the conventional petrochemical conversion routes [35]. Examples include production of bioethylene from bioethanol [36], biopropylene from bioisopropanol [37], and biobutene from bioisobutanol [38]. The biochemical routes for the manufacture of chemicals are well developed and in numerous instances also commercialized. Leading world producers of fermentative biochemicals include Braskem, DuPont, BP, Butamax Advanced Technologies, Cobalt Technologies, Green Biologics, Gevo, Global Bioenergies, Genencor, and Amyris [35]. In addition to the production of hydrocarbons, certain oxygenates produced by fermentation of carbohydrates can be the main goal of biotechnological processes. The most common examples include 1,3-propane diol, 1,3-butane diol, 2,3-butane diol, lactic acid, and acrylic acid, all of which have a plethora of industrial applications including production of various polyesters and other polymer materials [35]. While each of the discussed pathways follows a different procedure, all biochemical processes share similar challenges. They are based on sugary/starch biomass thus resulting in a competition between the production of commodities and food. For utilization of lignocellulosic biomass, although very limited in practice, extensive pre-treatment is required, either enzymatic of thermochemical degradation of the present lignin. Furthermore, the produced stream of products is heavily diluted in water, increasing the cost of post-processing.

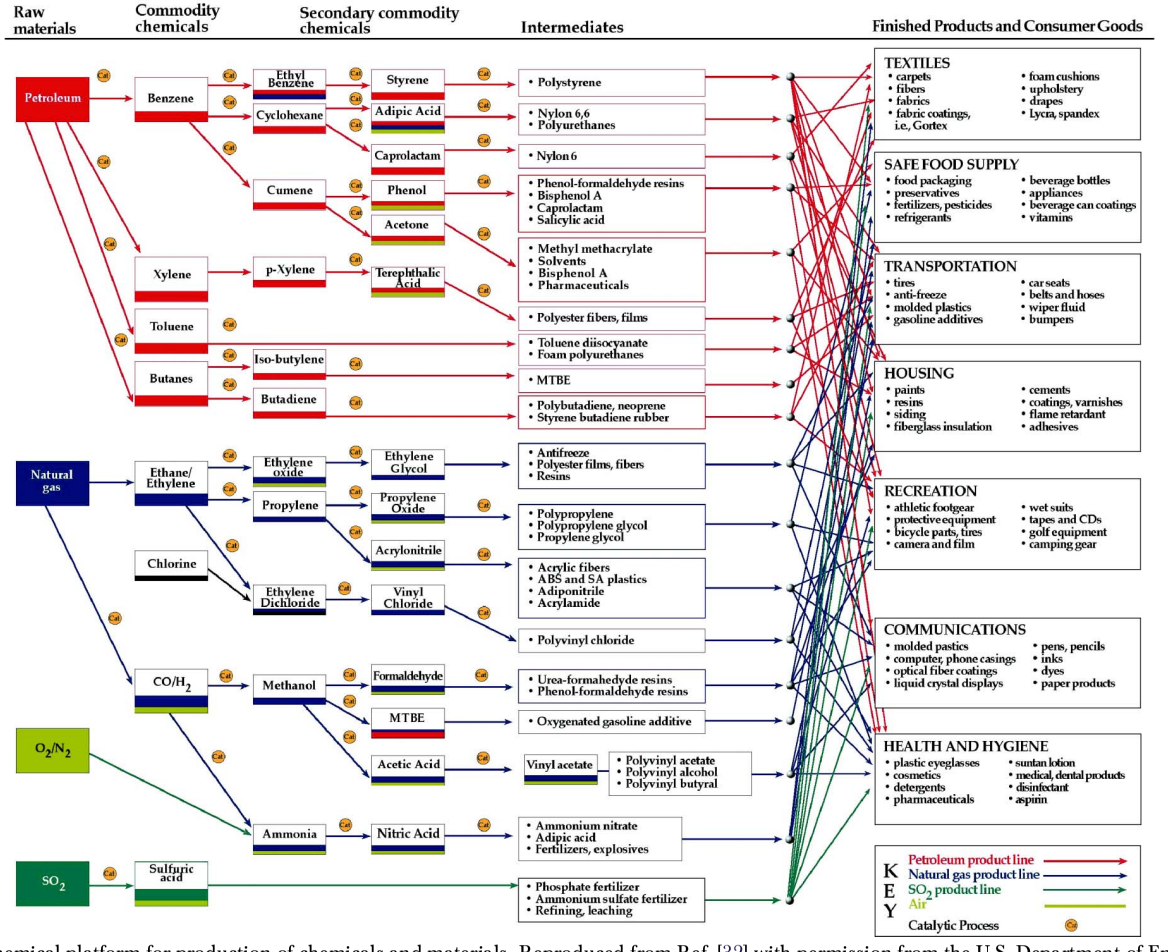

Fig. 1.8: Petrochemical platform for production of chemicals and materials. Reproduced from Ref. [32] with permission from the U.S. Department of Energy Efficiency and Renewable Energy.

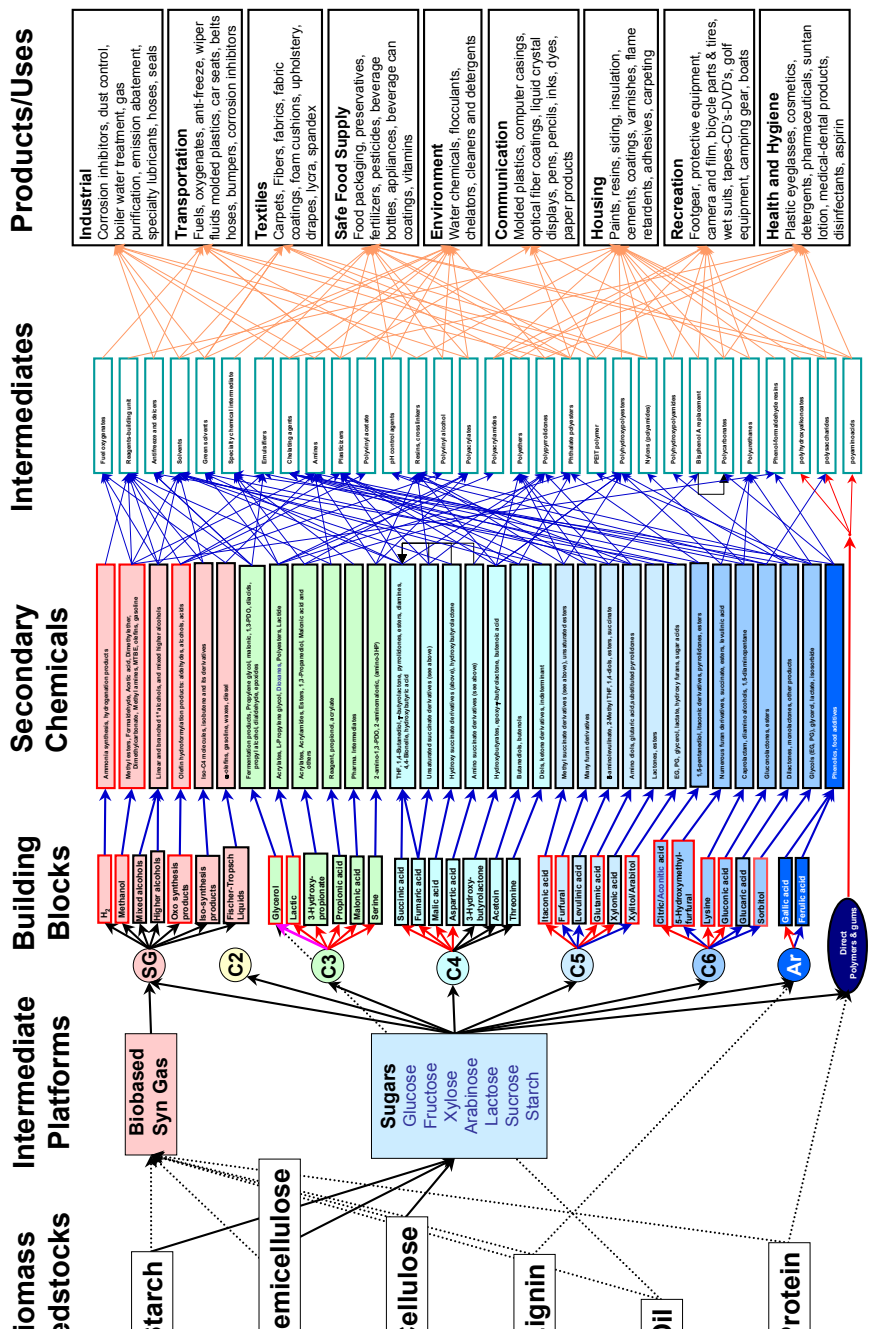

Fig. 1.9: Biomass platform for production of chemicals and materials. Reproduced from Ref. [32] with permission from the U.S. Department of Energy Efficiency and Renewable Energy.

Aqueous phase reforming Beside the biological and chemical pathways, carbohydrates can also be converted into hydrocarbons by means of an aqueous phase reforming (APR), a hydrothermal conversion method at moderate temperatures (200 - 250 °C) and pressures (15 - 50 bar) in the presence of solid nickel- or platinum-based catalyst [39]. The process results in the conversion of oxygenated hydrocarbons into hydrogen and light alkanes and has been proposed to be a solution for maximizing the sustainability of biorefinery by converting water soluble by-products and waste streams from processes such as gasification, pyrolysis, and liquefaction into valuable hydrocarbons that could be utilized as platform chemicals. APR proceeds by three main transformations: water-gas shift reaction ($CO + H_2O \rightarrow CO_2 + H_2$), methanation ($CO + 3H_2 \rightarrow CH_4 + H_2O$, $CO_2 + 4H_2 \rightarrow CH_4 + 2H_2O$), and Fischer-Tropsch ($(2n+1)H_2 + nCO \rightarrow C_nH_{2n+2} + nH_2O$) to produce short-chain (C1 - C6) gaseous alkanes. Liquefaction of biomass results in the formation of WSO, a relatively small and polar mixture of oxygen-rich aromatics, cyclics, aliphatic ketones, aldehyde, alcohols, and acids. WSO typically constitute approx. 10 - 40 wt.% of the treated biomass, representing an enormous unused resource and a potential source of significant amounts of wastewater. This organics present in the aqueous phase would be a perfect organic-rich feed to an APR application. The largest challenge of the process lies in the stability and effectiveness of the solid catalysts, in addition to relatively large amounts of by-products produced (alcohols, glycols, glyceraldehyde, hydroxyacetone, ketones, and aldehydes).

Syngas based methods Gasification of biomass is another conversion method leading to chemicals. The process takes place in the presence of oxygen or air at high temperatures (≥ 700 °C). The biomass is converted into a syngas mixture consisting mainly of carbon monoxide and hydrogen (full composition: CO, H_2, CO_2, and CH_4). After cleaning, the syngas can be used directly as an energy source, as a fuel, or as a chemical intermediate for the production of fuels (Fischer-Tropsch diesel) and chemicals (methanol, ethanol, organic acids, ammonia). Methanol is an important chemical feedstock for production of acetic acid, formaldehyde, methyl methacrylate, and methyl tertiary-butyl ether (MTBE) [40]. The main disadvantages of the dry gasification include: 1) Only relatively dry streams can be converted because of the high water enthalpy of evaporation; 2) High energy inputs are required; 3) Production of by-products, mostly solids; 4) Gas cleaning is required. Some of the challenges were solved by application of wet gasification in supercritical water.

Direct production of oxygenates Production of chemicals from petroleum and syngas is performed by reduction of complex feedstocks into relatively simple building blocks, which are then synthesized into larger compounds, typically by adding oxygen to obtain certain chemical functionalities. The practice, which involves numerous chemical rearrangements of the precursors into light oxygenates, has been optimized over the decades, and yet it seems backward concerning the green chemistry principles, which recommend that the number of conversion steps in a process should be minimized. A process, which results in a direct formation of light oxygenates similar to platform chemicals and chemical building blocks, would seem

more energetically profitable. Hydrothermal liquefaction is an example of biomass conversion technique leading to the formation of a broad spectrum of partially oxygenated compounds with various functional groups. While the complexity of the liquefaction products can be a serious analytic challenge, it also represents a potential source of platform oxygenates for the chemical industry. It is a relatively new, but promising, research angle [41–45]. The U.S. Department of Energy Efficiency and Renewable Energy (EERE) conducted studies about possible venues for production of chemicals by utilization of biomass conversion processes, including liquefaction and similar technologies [32, 46]. According to the results, the primary platform chemicals in this approach would involve phenols, organic acids, furfurals, and levoglucosan. The challenges here include non-selective depolymerization routes leading to the formation of hundreds of different compounds instead of selected few, the lack of analytical tools for detailed characterization of the products, and the need for an extensive downstream separation and purification. An alternative route could involve identification of new platform chemicals and building blocks easily available from liquefaction of biomass. Figure 1.9 shows a summary over the biomass-based platform chemicals, intermediates, and commodity products.

3 Biorefinery concept

The biorefinery concept is one of the most central pillars of the biomass-based economy of the future. Biorefining is defined as "sustainable processing of biomass into a spectrum of marketable products (food, feed, materials, chemicals) and energy (fuels, power, heat). A biorefinery can be a concept, a facility, a process, a plant, or even a cluster of facilities" [4]. The idea behind biorefineries is to integrate biomass conversion processes and maximize the output from each raw material stream, analogously to the today's petroleum refinery. Biorefinery concepts and guidelines have been established by IEA Bioenergy Task 42, an international platform set up in order to assess the global potential of biorefineries as a cornerstone of a new biomass-based economy and to create a program for their development. The major aims of Task 42 included the development of classification systems, mapping, defining policies, and bringing together stakeholders, with the ultimate goal to replace the modern day fossils refineries with biorefineries processing biomass.

The aim of biorefining is to separate the biomass into its building blocks and convert them into a range of value-added commodities (food- and feedstuffs, bioenergy, biofuels, biochemicals, and biomaterials) by using an integrated series of conversion techniques. However, since the expansion of renewable transportation fuels has been the central drive of the biorefinery development, the currently formulated biorefinery systems are centered around the concept of fuel supported with bio-based products providing additional economic and environmental benefits. As can be seen in Figure 1.10, the biorefinery concept is not bound by a single conversion technique or biomass type but is meant to be a mix of supplementing components, utilizing and valorizing all material flows and biomass components [47].

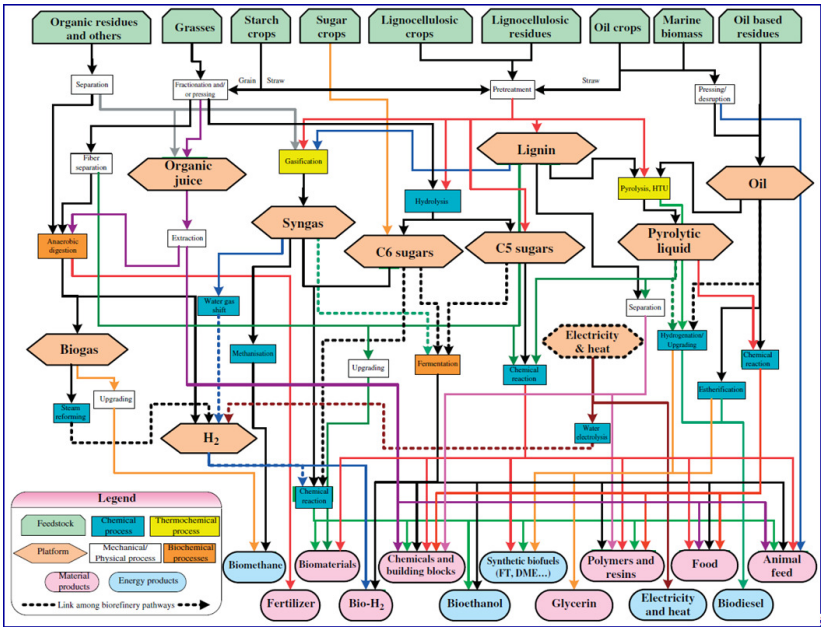

Fig. 1.10: Biorefinery classification systems according to IEA Bioenergy Task 42. Reproduced from Ref. [4] with permission from the International Energy Agency.

The four main parts of biorefinery key characteristics can be classified as following:

1. Platforms (core intermediates, e.g. C5, C6, lignin, syngas, biocrude)
2. Products (energy, fuels, chemicals, materials)
3. Feedstocks (biomass from forestry, agriculture, energy crops, etc.)
4. Processes (chemical, biochemical, thermochemical, mechanical)

A nearly infinite combination of the different classifying features in biorefinery is possible, and although some can claim to utilize biorefinery concepts (e.g. Borregaard, Norway), no real-life examples of fully integrated biorefineries exist today. Most biomass-based commercial solutions today are single-chain productions based on one type of biomass. A biorefinery is not meant to be a large plant facility corresponding in size, and operational extend to the current refineries. A biorefinery should represent a local production unit, unique in its setup and using local resources. Liquefaction in near- and supercritical fluids is versatile regarding raw feed, and as such it represents an excellent potential addition to a biorefinery.

References

[1] European Commission, "Joint Research Centre, Emissions Database for Global Atmospheric Research: CO_2 time series 1990-2014 per region/country." http://edgar.jrc.ec.europa.eu, 2017. [Online].

[2] J. Hansen, M. Sato, P. Kharecha, D. Beerling, R. Berner, V. Masson-Delmotte, M. Pagani, M. Raymo, D. L. Royer, and J. C. Zachos, "Target atmospheric CO_2: Where should humanity aim?," *Open Atmos. Sci. J.*, vol. 2, pp. 217–231, 2008.

[3] W. Thuiller, S. Lavergne, C. Roquet, I. Boulangeat, B. Lafourcade, and M. B. Araujo, "Consequences of climate change on the tree of life in Europe," *Nature*, vol. 470, no. 7335, pp. 531–534, 2011.

[4] International Energy Agency, "Energy & Environmental Technology." https://www.iea.org, 2017. [Online].

[5] D. Y. Leung, G. Caramanna, and M. M. Maroto-Valer, "An overview of current status of carbon dioxide capture and storage technologies," *Renew. Sustainable Energy Rev.*, vol. 39, pp. 426–443, 2014.

[6] A. Castellan, J. C. J. Bart, and S. Cavallaro, "Industrial production and use of adipic acid," *Catal. Today*, vol. 9, no. 3, pp. 237–254, 1991.

[7] Statista, "The portal for statistics." https://www.statista.com, 2017. [Online].

[8] T. Searchinger, R. Heimlich, R. A. Houghton, F. Dong, A. Elobeid, J. Fabiosa, S. Tokgoz, D. Hayes, and T.-H. Yu, "Use of US croplands for biofuels increases greenhouse gases through emissions from land-use change," *Science*, vol. 319, no. 5867, pp. 1238–1240, 2008.

[9] W. Cornwall, "The burning question," *Science*, vol. 355, no. 6320, pp. 18–21, 2017.

[10] E. Berl and A. Schmidt, "Über das Verhalten der Cellulose bei der Druckerhitzung mit Wasser," *Eur. J. Org. Chem.*, vol. 461, no. 1, pp. 192–220, 1928.

[11] E. Berl, A. Schmidt, H. Biebesheimer, and W. Dienst, "Die Entstehung von Erdöl, Asphalt und Steinkohle," *Sci. Nat.*, vol. 20, no. 35, pp. 652–655, 1932.

[12] E. Berl and H. Biebesheimer, "Zur Frage der Entstehung des Erdöls," *Liebigs Ann.*, vol. 504, no. 1, pp. 38–61, 1933.

[13] E. Berl, "Production of oil from plant material," *Science*, vol. 99, no. 2573, pp. 309–312, 1944.

[14] D. Elliott, D. Beckman, A. Bridgwater, J. Diebold, S. Gevert, and Y. Solantausta, "Developments in direct thermochemical liquefaction of biomass: 1983-1990," *Energy Fuels*, vol. 5, no. 3, pp. 399–410, 1991.

[15] B. lent Sahin, "Upgrading of biomass materials as energy sources: Liquefaction of mosses from Turkey," *Energy Sources*, vol. 22, no. 5, pp. 403–408, 2000.

[16] S. Xiu and A. Shahbazi, "Bio-oil production and upgrading research: A review," *Renew. Sust. Energ. Rev.*, vol. 16, no. 7, pp. 4406–4414, 2012.

[17] T. H. Pedersen, I. Grigoras, J. Hoffmann, S. S. Toor, I. M. Daraban, C. U. Jensen, S. Iversen, R. B. Madsen, M. Glasius, K. R. Arturi, R. P. Nielsen, E. G. Søgaard, and L. A. Rosendahl, "Continuous hydrothermal co-liquefaction of aspen wood and glycerol with water phase recirculation," *Appl. Energ.*, vol. 162, pp. 1034–1041, 2016.

[18] Z. Zhu, L. Rosendahl, S. S. Toor, D. Yu, and G. Chen, "Hydrothermal liquefaction of barley straw to bio-crude oil: Effects of reaction temperature and aqueous phase recirculation," *Appl. Energ.*, vol. 137, pp. 183–192, 2015.

[19] K. Anastasakis and A. Ross, "Hydrothermal liquefaction of the brown macro-alga Laminaria Saccharina: Effect of reaction conditions on product distribution and composition," *Bioresource Technol.*, vol. 102, no. 7, pp. 4876–4883, 2011.

[20] D. L. Barreiro, W. Prins, F. Ronsse, and W. Brilman, "Hydrothermal liquefaction (HTL) of microalgae for biofuel production: State of the art review and future prospects," *Biomass Bioenergy*, vol. 53, pp. 113–127, 2013.

[21] D. C. Elliott, "Historical developments in hydroprocessing bio-oils," *Energy Fuels*, vol. 21, no. 3, pp. 1792–1815, 2007.

[22] C. Tuck, E. Pérez, I. Horváth, R. Sheldon, and M. Poliakoff, "Valorization of biomass: deriving more value from waste," *Science*, vol. 337, no. 6095, pp. 695–699, 2012.

[23] J. Rogers and J. G. Brammer, "Analysis of transport costs for energy crops for use in biomass pyrolysis plant networks," *Biomass Bioenergy*, vol. 33, no. 10, pp. 1367–1375, 2009.

[24] Plastics Europe, "Agricultural marketing resource center." http://www.agmrc.org, 2017. [Online].

[25] M. Oliveira and E. Duarte, "Integrated approach to winery waste: waste generation and data consolidation," *Front. Env. Sci. Eng.*, vol. 10, no. 1, pp. 168–176, 2016.

[26] N. Yanli, L. Yong-guo, L. Ya, Z. Yong-hong, and L. Yuan, "Report on utilization and prospect of sugar cane bagasse resources," *Forest. Econom.*, vol. 5, pp. 61–63, 2007.

[27] A. J. Ragauskas, G. T. Beckham, M. J. Biddy, R. Chandra, F. Chen, M. F. Davis, B. H. Davison, R. A. Dixon, P. Gilna, M. Keller, P. Langan, A. K. Naskar, J. N. Saddler, T. J. Tschaplinski, G. A. Tuskan, and C. E. Wyman, "Lignin valorization: Improving lignin processing in the biorefinery," *Science*, vol. 344, no. 6185, p. 1246843, 2014.

[28] L. Shen, J. Haufe, and M. K. Patel, "Product overview and market projection of emerging bio-based plastics PRO-BIP 2009," 2009.

[29] Energy Information Agency, "Bulk chemical feedstock use a key part of increasing industrial energy demand." https://www.iea.org, 2017. [Online].

[30] Plastics Europe, "World Plastic Production 1950–2015." https://committee.iso.org, 2016. [Online].

[31] G. J. M. Gruter and F. Dautzenberg, "Method for the synthesis of 5-alkoxymethyl furfural ethers and their use," Mar. 13 2012. US Patent 8,133,289.

[32] T. Werpy, G. Petersen, A. Aden, J. Bozell, J. Holladay, J. White, A. Manheim, D. Eliot, L. Lasure, and S. Jones, "Top value added chemicals from biomass. Volume I - Results of screening for potential candidates from sugars and synthesis gas," tech. rep., Report prepared by members of NREL, PNNL and University of Tennessee, 2004.

[33] R. Mariscal, P. Maireles-Torres, M. Ojeda, I. Sadaba, and M. L. Granados, "Furfural: a renewable and versatile platform molecule for the synthesis of chemicals and fuels," *Energy Environ. Sci.*, vol. 9, no. 4, pp. 1144–1189, 2016.

[34] R. J. van Putten, J. C. van der Waal, E. De Jong, C. B. Rasrendra, H. J. Heeres, and J. G. de Vries, "Hydroxymethylfurfural, a versatile platform chemical made from renewable resources," *Chem. Rev.*, vol. 113, no. 3, pp. 1499–1597, 2013.

[35] R. A. Sheldon, "Green and sustainable manufacture of chemicals from biomass: State of the art," *Green Chem.*, vol. 16, no. 3, pp. 950–963, 2014.

[36] P. L. de Andrade Coutinho, A. T. Morita, L. F. Cassinelli, A. Morschbacker, and R. Werneck Do Carmo, "Braskem's Ethanol to Polyethylene Process Development," *Catal. Process Dev. Renew. Mater.*, pp. 149–165, 2013.

[37] K. Inokuma, J. C. Liao, M. Okamoto, and T. Hanai, "Improvement of isopropanol production by metabolically engineered Escherichia coli using gas stripping," *J. Biosci. Bioeng.*, vol. 110, no. 6, pp. 696–701, 2010.

[38] G. K. Donaldson, A. C. Eliot, D. Flint, L. A. Maggio-Hall, and V. Nagarajan, "Fermentive production of four carbon alcohols," Dec. 14 2010. US Patent 7,851,188.

[39] I. Coronado, M. Stekrova, M. Reinikainen, P. Simell, L. Lefferts, and J. Lehtonen, "A review of catalytic aqueous-phase reforming of oxygenated hydrocarbons derived from biorefinery water fractions," *Int. J. Hydrogen Energy*, vol. 41, no. 26, pp. 11003–11032, 2016.

[40] M. Balat, M. Balat, E. Kırtay, and H. Balat, "Main routes for the thermo-conversion of biomass into fuels and chemicals. Part 2: Gasification systems," *Energy Convers. Manage.*, vol. 50, no. 12, pp. 3158–3168, 2009.

[41] C. Amen-Chen, H. Pakdel, and C. Roy, "Production of monomeric phenols by thermochemical conversion of biomass: A review," *Bioresour. Technol.*, vol. 79, no. 3, pp. 277–299, 2001.

[42] P. Azadi, O. R. Inderwildi, R. Farnood, and D. A. King, "Liquid fuels, hydrogen and chemicals from lignin: A critical review," *Renew. Sustainable Energy Rev.*, vol. 21, pp. 506–523, 2013.

[43] S. Kang, X. Li, J. Fan, and J. Chang, "Hydrothermal conversion of lignin: A review," *Renew. Sustainable Energy Rev.*, vol. 27, pp. 546–558, 2013.

[44] A. Corma, S. Iborra, and A. Velty, "Chemical routes for the transformation of biomass into chemicals," *Chem. Rev.*, vol. 107, no. 6, pp. 2411–2502, 2007.

References

[45] J.-M. Lavoie, W. Baré, and M. Bilodeau, "Depolymerization of steam-treated lignin for the production of green chemicals," *Bioresour. Tèchnol.*, vol. 102, no. 7, pp. 4917–4920, 2011.

[46] J. Holladay, J. Bozell, J. White, and D. Johnson, "Top value-added chemicals from biomass. Volume II–Results of screening for potential candidates from biorefinery lignin," tech. rep., 2007.

[47] F. Cherubini, "The biorefinery concept: using biomass instead of oil for producing energy and chemicals," *Energy Convers. Manage.*, vol. 51, no. 7, pp. 1412–1421, 2010.

Chapter 2

Near- and supercritical fluids

1 Water as a reaction medium

1.1 Properties

Water is a benign and cheap solvent with a relatively low critical point (T_{cr} = 374 °C, p_{cr} = 22.1 MPa). Due to its unique properties in the near- and the supercritical region (near-critical water - NCW, and supercritical water - SCW), water is utilized in a variety of biomass conversion processes [1]. With increasing temperature, the hydrogen bonds in water are disrupted along with the tetrahedral coordination of the single molecules [2]. The regular network is replaced with clusters of 5 - 20 hydrogen-bound H_2O units [2]. Since the hydrogen bond is the most important feature of water as a solvent, the alterations to the H-bonding leads to profound modifications in the properties.

Ionic product (K_w), which expresses the degree of water auto-dissociation and controls the extent of ionic reactions, increases steadily from 10^{-14} to 10^{-11} in the temperature range 25 - 280 °C, and then decreases up to the supercritical point and beyond, a phenomenon explained by the decreasing stabilization power of the ionic species [1]. K_w increases with pressure at constant temperature values [3] . In addition to K_w, density (ρ) and viscosity (μ) are also severely altered at NCW and SCW conditions. Both parameters influence transport properties, and their decreasing values yield in increased mobilities of analytes and an enhancement in mass transfer and diffusion-controlled chemical reactions. The low density and viscosity values in NCW and SCW are typically referred to as a high fluidity region [4]. Last, but not least, the values of dielectric constant (the relative dielectric permittivity, ϵ) decrease from approx. 80 at T = 25 °C to 10 - 25 in the near-critical region. The modification in ϵ, which controls dissociation of salts, entails that the aqueous medium is still capable of dissolving and ionizing electrolytes, while it also becomes miscible with non-polar solutes. The value of ϵ for water in the near-critical region corresponds to the relative permittivity of dipolar organic solvents

such as acetone and acetonitrile at ambient conditions. In the supercritical region, the dielectric constant decreases further (ϵ = 1 - 2), and the medium loses its ability to dissolve salts, while it becomes miscible with increasingly non-polar compounds, e.g. hexane [2, 5, 6]. Figure 2.1 shows the values of K_w, ρ, and ϵ as a function of temperature and density.

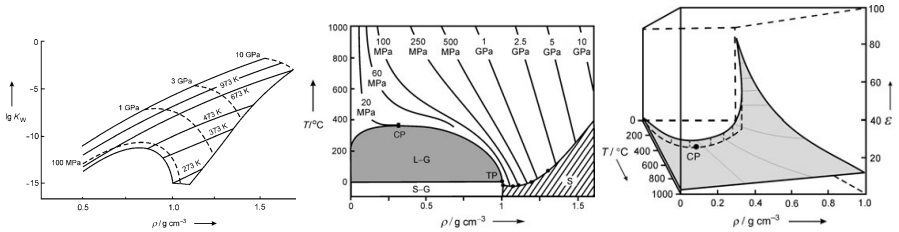

Fig. 2.1: Ionic constant K_w (left) and water density ρ (middle), and dielectric constant ϵ (right) as a function of temperature and pressure. Reproduced from Ref. [4], Copyright (2005), with permission from John Wiley and Sons.

As can be seen in Figure 2.2, the properties of water as a solvent and reaction medium can be fine-tuned with changes in pressure and temperature, typically expressed collectively as density. With varying values of K_w, ρ, μ, and ϵ, the reactions mechanisms dominating biomass conversion can be controlled and directed towards specific targets. In the near-critical region, the high K_w values enhance ionic reactions, while radical reaction mechanisms govern the supercritical region. In addition to being reaction medium, water molecules act as reactants, reacting products, and catalyst. Furthermore, while both the reactants and the products (biomass and degradation intermediates) are soluble during the reaction time, they are, upon cooling, spontaneously separated and distributed between different product fractions according to their boiling points, molecular weight, and polarity.

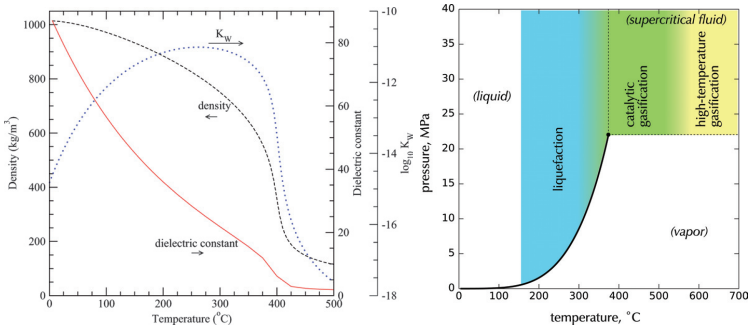

Fig. 2.2: Water properties. Reproduced from Ref. [7], Copyright (2008), with permission from The Royal Society of Chemistry.

1.2 Role of water

Reactant The most common reactions of water molecules in the near-critical region include hydrolysis and pyrolysis. Hydrolysis involves cleavage of a bond between a carbon and a heteroatom, e.g. oxygen or nitrogen, of a functional group, i.e. compounds such as ester, ethers, and amines are most susceptible to this reaction. Hydrolysis of ester leads to carboxylic acids, which are then decarboxylated or otherwise thermally degraded by the present water. Alternatively, carboxylic acids can act as an acid catalyst (autocatalysis) and help to hydrolyze other molecules [2]. Hydrolysis is competing with pyrolysis, and each dominates at different conditions. Hydrolysis has been shown to be promoted at high densities, while high temperatures (decreasing densities) seem to enhance pyrolysis pathways, i.e. dehydration and decarboxylation [8].

Hydrogen donor Numerous authors have shown that water can act as a hydrogen donor during liquefaction [9]. These effects are most pronounced at low-density values, i.e. closer to the radically driven supercritical range [10]. Diverse pathways have been proposed for the production of H_2, including hydrolysis, conversion of alcohols into ketones, water-gas shift reaction, and oxidation of carbon [2]. However, the reactions resulting in hydrogen could be similar to the mechanisms responsible for the formation of hydroxyl radicals, protons, and hydrogen gas in any advanced oxidation process (Reactions 2.1 - 2.4). In addition to the presented reactions, a similar pathway for formation of hydrogen could be set-up for H_2O_2, which is produced during liquefaction from e.g. methanol. Generation of hydrogen in-situ is expected to have significant consequences for the overall reaction pathways during liquefaction and the final product distribution. In addition to the role of H_2, the proposed pathway for formation of hydrogen also includes radicals, which can result in fragmentation by oxidation and formation of gaseous products.

$$H_2O \rightarrow H^\bullet + HO^\bullet \tag{2.1}$$
$$H_2O + H^\bullet \rightarrow H_2 + HO^\bullet \tag{2.2}$$
$$O_2 + H^\bullet \rightarrow O^\bullet + HO^\bullet \tag{2.3}$$
$$O^\bullet + H_2O \rightarrow 2HO^\bullet \tag{2.4}$$

Catalyst The high concentrations of H^+ and OH^- in the high-density regions of liquefaction promote all types of ionic reactions, including acid/base catalyzed hydrolysis, alcohol dehydration, addition of water, rearrangements, Friedel-Crafts alkylation, aldol condensation, and Cannizzaro reaction [2]. This results in high reaction rates at relatively low catalyst concentrations or even in its absence, with water acting as a acid/base catalyst, in addition to its role as a conjugated acid or base. Most of the mentioned reactions can be catalyzed by both acids as well as bases. In the near-critical region and the absence of catalyst, the majority are acid-catalyzed (hydrolysis, dehydration, addition of water, Friedel-Crafts, rearrangements), while only a few are base-catalyzed (aldol condensation and Cannizzaro).

2 Co-solvents addition

The use of organic co-solvents in hydrothermal liquefaction leads to the reduction of char formation during conversion of biomass, an effect that was explained by increased stabilization of biomass and its conversion products, as well as scavenging of unstable fragments produced in the course of depolymerization [11–14]. Numerous co-solvents have been applied for the purpose, including methanol [15], ethanol [16], butanol [17], and propylene glycol [18]. Small alcohols work best for reduction of char production [17], but also have the tendency to evaporate. The alcohols methanol and ethanol and some other organics including 1,4-dioxane have also been studied as the main reaction fluid [19–21]. The studies of liquefaction of various materials have shown, that by application of organic solvents as a reaction medium, liquefaction could be performed in at significantly milder conditions, improving the economic viability of the conversion [22].

2.1 Phenol

Phenol is one of the most common co-solvents applied for liquefaction of lignin and its key reaction intermediates [23–27]. According to the findings, its presence results in reduced char formation due to the compound's role as a capping agent [11–13] and solubilizer [13]. Studies on the valorization of Kraft lignin in the presence of phenol showed that the compound plays a role in increasing the yields of aromatic monomers from liquefaction of lignin [28–30]. The critical point of phenol lies at T_c = 421 °C and p_c = 60 bar. Depending on the ratio between the water and co-solvent, the phase change parameters of the reaction mixture are shifted.

2.2 Acetone

Acetone has been studied both as the main reaction solvent [22] as well as a co-solvent [16] in liquefaction. The results indicated that application of acetone enhances the yields and the quality of the produced biocrude. In general, polar solvents are expected to be more efficient liquefaction conversion media and co-solvents than non-polar compounds [31]. The supercritical point of acetone lies at T_c = 235 °C and p_c = 48 bar. In addition to the conversion of biomass, acetone has also been applied for liquefaction of the polymer resins in composites. The technology is used as a chemical recycling strategy for recovery of both the monomers as well as the production of additional value-added chemicals [22, 32, 33]. Acetone is considered a relatively harmless, non-toxic, and cheap solvent compared to e.g. methanol.

2.3 Tetralin

Tetralin is a non-polar compound that has shown potential as the solvent for liquefaction of both coal [34] as well as different biomass types (lignin, cellulose, waste) [35–37]. The presence of phenol results in increasing conversion yields and

enahnced qualities of the products. A study by Duan et al. [31] revealed that, while the processing in tetralin improves liquefaction to a certain extent, a generally better outcome can be achieved with polar solvents. Other study concluded that the non-polar compounds such as tetralin, 1-methyl naphthalene, and toluene, are most effective when used as co-solvents in combination with water [38]. In addition to the traditional role of co-solvents as solubilizers and scavaengers, tetralin and similar compounds also act as a hydrogen source. In a very recent study by Koriakin et al. [39], the efficiency of different hydrogen donor solvents (tetralin, decalin, and m-xylene) has been compared and tetralin was concluded to be the most efficient regarding the overall conversion yields. The supercritical point of tetralin lies at T_c = 174 °C and p_c = 36 bar.

References

[1] A. Kruse and E. Dinjus, "Hot compressed water as reaction medium and reactant: Properties and synthesis reactions," *J. Supercrit. Fluids*, vol. 39, no. 3, pp. 362–380, 2007.

[2] N. Akiya and P. E. Savage, "Roles of water for chemical reactions in high-temperature water," *Chem. Rev.*, vol. 102, no. 8, pp. 2725–2750, 2002.

[3] C. A. Meyer, R. McClintock, and G. Silvestri, *ASME Steam Tables: Thermodynamic and Transport Properties of Steam: Comprising Tables and Charts for Steam and Water, Calculated Using the 1967 IFC Formulation for Industrial Use, in Conformity with the 1963 International Skeleton Tables, as Adopted by the Sixth International Conference on the Properties of Steam.* American Society of Mechanical Engineers, 1993.

[4] H. Weingärtner and E. U. Franck, "Supercritical water as a solvent," *Angew. Chem. Int. Ed.*, vol. 44, no. 18, pp. 2672–2692, 2005.

[5] N. Matubayasi and M. Nakahara, "Super-and subcritical hydration of nonpolar solutes. I. Thermodynamics of hydration," *J. Chem. Phys*, vol. 112, no. 18, pp. 8089–8109, 2000.

[6] R. P Nielsen and E. G Søgaard, "Features of near-and supercritical water," *Curr. Phys. Chem.*, vol. 3, no. 4, pp. 501–507, 2013.

[7] A. A. Peterson, F. Vogel, R. P. Lachance, M. Fröling, M. J. Antal Jr, and J. W. Tester, "Thermochemical biofuel production in hydrothermal media: A review of sub-and supercritical water technologies," *Energy Environ. Sci.*, vol. 1, no. 1, pp. 32–65, 2008.

[8] S. H. Townsend, M. A. Abraham, G. L. Huppert, M. T. Klein, and S. C. Paspek, "Solvent effects during reactions in supercritical water," *Ind. Eng. Chem. Res.*, vol. 27, no. 1, pp. 143–149, 1988.

[9] O. M. Ogunsola, "Decomposition of isoquinoline and quinoline by supercritical water," *J. Hazard. Mater.*, vol. 74, no. 3, pp. 187–195, 2000.

[10] A. Kruse and K. Ebert, "Chemical reactions in supercritical water - 1. Pyrolysis of tert.-butylbenzene," *Ber. Bunsenges. Phys. Chem.*, vol. 100, no. 1, pp. 80–83, 1996.

[11] M. Saisu, T. Sato, M. Watanabe, T. Adschiri, and K. Arai, "Conversion of lignin with supercritical water-phenol mixtures," *Energy Fuels*, vol. 17, no. 4, pp. 922–928, 2003.

[12] K. Okuda, M. Umetsu, S. Takami, and T. Adschiri, "Disassembly of lignin and chemical recovery–rapid depolymerization of lignin without char formation in water–phenol mixtures," *Fuel Process. Technol.*, vol. 85, no. 8, pp. 803–813, 2004.

[13] Z. Fang, T. Sato, R. L. Smith, H. Inomata, K. Arai, and J. A. Kozinski, "Reaction chemistry and phase behavior of lignin in high-temperature and supercritical water," *Bioresour. Technol.*, vol. 99, no. 9, pp. 3424–3430, 2008.

[14] T. H. Pedersen, I. Grigoras, J. Hoffmann, S. S. Toor, I. M. Daraban, C. U. Jensen, S. Iversen, R. B. Madsen, M. Glasius, K. R. Arturi, R. P. Nielsen, E. G. Søgaard, and L. A. Rosendahl, "Continuous hydrothermal co-liquefaction of aspen wood and glycerol with water phase recirculation," *Appl. Energ.*, vol. 162, pp. 1034–1041, 2016.

[15] E. Jakab, K. Liu, and H. L. Meuzelaar, "Thermal decomposition of wood and cellulose in the presence of solvent vapors," *Ind. Eng. Chem. Res.*, vol. 36, no. 6, pp. 2087–2095, 1997.

[16] Z. Liu and F. Zhang, "Effects of various solvents on the liquefaction of biomass to produce fuels and chemical feedstocks," *Energ. Convers. and Manage.*, vol. 49, no. 12, pp. 3498–3504, 2008.

[17] S. P. Mun and M. H. El Barbary, "Liquefaction of lignocellulosic biomass with dioxane/polar solvent mixtures in the presence of an acid catalyst," *J. Ind. Eng. Chem.*, vol. 10, no. 3, pp. 473–477, 2004.

[18] A. Kržan, M. Kunaver, and V. Tišler, "Wood liquefaction using dibasic organic acids and glycols," *Acta Chim. Slov*, vol. 52, pp. 253–258, 2005.

[19] X. Yuan, J. Wang, G. Zeng, H. Huang, X. Pei, H. Li, Z. Liu, and M. Cong, "Comparative studies of thermochemical liquefaction characteristics of microalgae using different organic solvents," *Energy*, vol. 36, no. 11, pp. 6406–6412, 2011.

[20] H. Huang, X. Yuan, G. Zeng, J. Wang, H. Li, C. Zhou, X. Pei, Q. You, and L. Chen, "Thermochemical liquefaction characteristics of microalgae in sub-and supercritical ethanol," *Fuel Process. Technol.*, vol. 92, no. 1, pp. 147–153, 2011.

[21] P. D. Patil, V. G. Gude, A. Mannarswamy, S. Deng, P. Cooke, S. Munson-McGee, I. Rhodes, P. Lammers, and N. Nirmalakhandan, "Optimization of direct conversion of wet algae to biodiesel under supercritical methanol conditions," *Bioresour. Technol.*, vol. 102, no. 1, pp. 118–122, 2011.

[22] B. Jin, P. Duan, C. Zhang, Y. Xu, L. Zhang, and F. Wang, "Non-catalytic liquefaction of microalgae in sub-and supercritical acetone," *Chem. Eng. J.*, vol. 254, pp. 384–392, 2014.

[23] C. C. Xu, H. Su, and D. Cang, "Liquefaction of corn distillers dried grains with solubles (DDGS) in hot-compressed phenol," *BioResources*, vol. 3, no. 2, pp. 363–382, 2008.

[24] D. Maldas and N. Shiraishi, "Liquefaction of biomass in the presence of phenol and H_2O using alkalies and salts as the catalyst," *Biomass Bioenenergy*, vol. 12, no. 4, pp. 273–279, 1997.

[25] L. Lin, Y. Yao, M. Yoshioka, and N. Shiraishi, "Liquefaction mechanism of lignin in the presence of phenol at elevated temperature without catalysts. Studies on ß-o-4 lignin model compound. I. Structural characterization of the reaction products," *Holzforschung-Int. J. Biol. Chem. Phys. Technol. Wood*, vol. 51, no. 4, pp. 316–324, 1997.

[26] L. Lin, M. Yoshioka, Y. Yao, and N. Shiraishi, "Liquefaction mechanism of lignin in the presence of phenol at elevated temperature without catalysts. Studies on ß-0-4 lignin model compound. III. Multi-condensation," *Holzforschung-Int. J. Biol. Chem. Phys. Technol. Wood*, vol. 51, no. 4, pp. 333–337, 1997.

[27] L. Lin, M. Yoshioka, Y. Yao, and N. Shiraishi, "Liquefaction mechanism of lignin in the presence of phenol at elevated temperature without catalysts. Studies on ß-o-4 lignin model compound. II. Reaction pathway," *Holzforschung-Int. J. Biol. Chem. Phys. Technol. Wood*, vol. 51, no. 4, pp. 325–332, 1997.

[28] T. D. H. Nguyen, M. Maschietti, T. Belkheiri, L.-E. Åmand, H. Theliander, L. Vamling, L. Olausson, and S.-I. Andersson, "Catalytic depolymerisation and conversion of Kraft lignin into liquid products using near-critical water," *J. Supercrit. Fluids*, vol. 86, pp. 67–75, 2014.

[29] M. Maschietti, T. D. H. Nguyen, T. Belkheiri, L.-E. Åmand, H. Theliander, L. Vamling, L. Olausson, and S.-I. Andersson, "Catalytic hydrothermal conversion of LignoBoost Kraft lignin for the production of bio-oil and aromatic chemicals," in *Proceedings of the International Chemical Recovery Conference*, vol. 2, pp. 252–261, 2014.

[30] T. D. H. Nguyen, M. Maschietti, L.-E. Åmand, L. Vamling, L. Olausson, S.-I. Andersson, and H. Theliander, "The effect of temperature on the catalytic conversion of Kraft lignin using near-critical water," *Bioresource Technol.*, vol. 170, pp. 196–203, 2014.

[31] P. Duan, B. Jin, Y. Xu, Y. Yang, X. Bai, F. Wang, L. Zhang, and J. Miao, "Thermo-chemical conversion of Chlorella pyrenoidosa to liquid biofuels," *Bioresour. Technol.*, vol. 133, pp. 197–205, 2013.

[32] C. Morin, A. Loppinet-Serani, F. Cansell, and C. Aymonier, "Near-and supercritical solvolysis of carbon fibre reinforced polymers (CFRPs) for recycling carbon fibers as a valuable resource: State of the Art," *J. Supercrit. Fluids*, vol. 66, pp. 232–240, 2012.

[33] H. U. Sokoli, M. E. Simonsen, R. P. Nielsen, K. R. Arturi, and E. G. Søgaard, "Conversion of the matrix in glass fiber reinforced composites into a high heating value oil and other valuable feedstocks," *Fuel Process. Technol.*, vol. 149, pp. 29–39, 2016.

[34] S. Sangon, S. Ratanavaraha, S. Ngamprasertsith, and P. Prasassarakich, "Coal liquefaction using supercritical toluene–tetralin mixture in a semi-continuous reactor," *Fuel Process. Technol.*, vol. 87, no. 3, pp. 201–207, 2006.

[35] R. W. Thring, E. Chornet, and R. P. Overend, "Thermolysis of glycol lignin in the presence of tetralin," *Can. J. Chem. Eng.*, vol. 71, no. 1, pp. 107–115, 1993.

[36] R. Maggi and D. Elliott, "Upgrading overview," in *Developments in thermochemical biomass conversion*, pp. 575–588, Springer, 1997.

[37] S. B. Lalvani, P. Rajagopal, B. Akash, J. A. Koropchak, and C. B. Muchmore, "Liquefaction of newsprint and cellulose in tetralin under moderate reaction conditions," *Fuel Process. Technol.*, vol. 35, no. 3, pp. 219–232, 1993.

[38] T.-o. Matsui, A. Nishihara, C. Ueda, M. Ohtsuki, N.-o. Ikenaga, and T. Suzuki, "Liquefaction of micro-algae with iron catalyst," *Fuel*, vol. 76, no. 11, pp. 1043–1048, 1997.

[39] A. Koriakin, H. V. Nguyen, D.-W. Kim, and C.-H. Lee, "Thermochemical decomposition of microcrystalline cellulose using sub-and supercritical tetralin and decalin with Fe_3O_4," *Ind. Eng. Chem. Res.*, vol. 54, no. 18, pp. 5184–5194, 2015.

Chapter 3

Hydrothermal liquefaction

1 Historical perspective

Liquefaction of biomass into valuable products was demonstrated for the first time nearly 100 years ago [1–4]. Since then, the process has been studied extensively in both small batch reactors [5–7] as well as in continuous pilot plants [8–11]. The first industrial scale liquefaction plant was developed at the Pittsburgh Energy Research Center (PERC, Oregon, USA) by Appell and co-workers [12, 13], and later at the Lawrence Berkeley Laboratory (LBL, California, USA) [14]. The former process, which was performed in the presence of CO and Na_2CO_3, converted 100 kg/h wood powder at T = 350 °C, p = 20.8 MPa, and reaction time of 20 - 60 min. The resulting product was a biocrude with 12 - 14 % oxygen content, 3 - 5 % water content, and a melting point close to the room temperature [15]. The latter process added a slurry pretreatment step involving a mild acid hydrolysis (T = 180 °C, τ = 45 min) of the lignocellulosic biomass prior to the hydrothermal processing. The pre-treatment tackled some of the technical processing challenges of the pioneering work done at PERC, including decreasing biomass slurry viscosity and preventing precipitation of solids.

In Europe, Shell Research Laboratories (Amsterdam, Netherlands) developed hydrothermal upgrading based on liquefaction (HTU®) [16]. Processing was based on the PERC procedure, except for the addition of CO and Na_2CO_3, which resulted in a biocrude with increased oxygen content (18 %) and a melting point close to 80 °C [17]. The plant operated at 300 - 350 °C, p = 12 - 18 MPa, and τ = 5 - 20 min. Other liquefaction-based continuous bench scale plants included thermo-depolymerization process (TDP, Missouri, USA) [18] and CatLiq® conversion (Copenhagen, Denmark) [19]. The former converted turkey offal and fats (conditions unknown) into renewable fuels. The latter operated at a 20 L/h capacity for conversion of organic waste streams in near critical water (T = 280 °C, p = 22.5 - 25 MPa) and in the presence of catalysts (K_2CO_3 and ZrO_2).

The efforts to develop liquefaction into an industrial conversion technique started as a reaction to the oil crisis of 1973. All of the projects as mentioned above have since been halted, due to technical challenges, low prices of petroleum, and lack of competitiveness. The technical difficulties most common for high pressure and temperature systems include issues with slurry pumping, precipitation of salts, and corrosion. High dry matter contents are required to maximize the oil yields and energy efficiency, but such mixtures are not easy to pump. Furthermore, the formation of stable slurries requires small particles, which makes an extensive mechanical pretreatment of the raw feed necessary [14]. With regard to the corrosion problems, research has shown that only costly alloys of Ni (e.g. Inconel 625 and Hastelloy C-276) and Ti are resistant to hydrothermal conditions, although the latter has limited mechanical strength [20]. The effort of commercializing liquefaction today are carried out by few companies including Steeper Energy (Hydrofaction^{TM}, Aalborg, Denmark) [21] and Licella Cat-HTR (Catalytic Hydrothermal Reactor, Sydney, Australia) [22].

2 Conversion parameters

Numerous process parameters influence the output of liquefaction, including temperature, pressure, the presence of additives (type and amounts of homogeneous and heterogeneous catalysts and co-solvents), reaction time, biomass heating rates, product cooling rates, type of biomass used, the morphology of the biomass, and pre-treatment. An overview of inputs and outputs of a liquefaction process, in addition to the conditions applied and mechanisms behind the conversion, are outlined in Figure 3.1. In the following text, the state-of-the-art in liquefaction is reported. The role of co-solvents is left out, since it has been discussed in Section 2 of Chapter 2.

Biomass Laboratory liquefaction studies have been performed on numerous types of feeds from key compounds such as glucose [24, 25], biopolymers (cellulose [26–29], hemicellulose [30, 31], and lignin [32–34]), and complex biomass feeds (lignocellulose [35, 36], algae [37–41], waste [39, 39, 42–45]). All biomass types can be liquefied, but waste products have been of special interest due to their low cost and high sustainability [46–49]. Since biomass type, along with processing costs and transport, is one the most significant expenses essential to the economic viability of a biomass conversion process, a cheap feedstock is a requirement. Biomass is not only important in terms of economics, but also with regard to the obtained yields. Studies have shown that biocrude from algae and other lipid-rich raw feedstocks contains more fatty acid than the corresponding product from lignocellulose [50]. Biocrude from lignin, on the other hand, tends to result in relatively high yields of biochar [51]. Liquefaction of lignocellulose has been studied in detail [14] and was shown to yield a broad spectrum of species with the output depending heavily on process conditions [14]. Conversion of protein rich biomass tends to result in

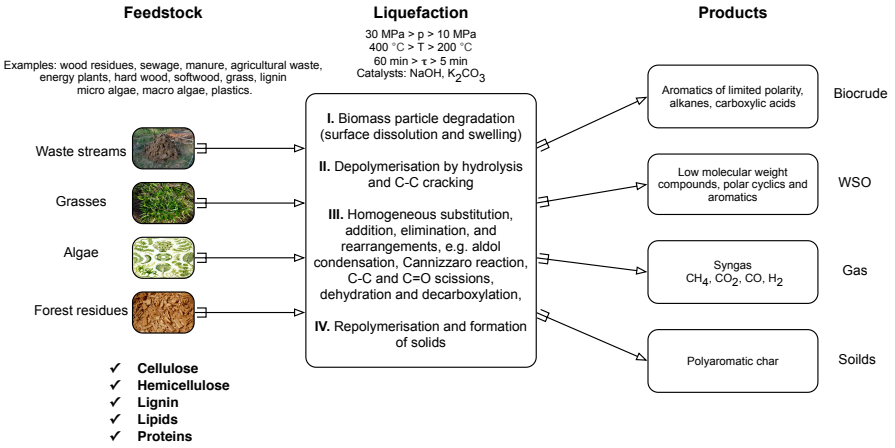

Fig. 3.1: An overview of the feedstocks, conditions, and outputs from hydrothermal processing of biomass. Based on data from [23].

nitrogen-rich products [39, 39].

Temperature and pressure Temperature influences the properties of fluids, and therefore also the course of liquefaction, significantly. Increasing temperatures raise K_w and result in an enhanced hydrolysis of biopolymers, as well as a number of other ionically-driven acid/base catalyzed reactions (Section 1.2 of Chapter 2). The conversion in NCW is further facilitated by the low viscosity and density conditions which result in high mobility of the analytes and a lack of mass transfer barriers. Furthermore, due to the low dielectric constant, the reactions are homogeneous, and both reactants, catalysts, and the formed products are soluble in the reaction medium. With the temperatures increasing above the supercritical temperature, the properties are transformed further, enhancing radical reaction pathways and formation of gaseous products. The influence of pressure is secondary compared to the effect of temperature, but it affects the values of K_w, ρ, ϵ, μ to a certain degree, especially in the supercritical region, where the reaction medium becomes highly compressible. In NCW, this effect is smaller, although not without importance. Pressure is one of the variables that is typically overlooked when reporting the liquefaction process parameters and a limited number of studies have dealt with the direct influence of pressure on liquefaction of biomass. Kruse et al. [52] reported augmentation of ionic reactions and suppression of radical reactions at high pressures. The former was attributed to the increasing K_w values, while the latter was explained by solvent cage effects. Temperature is the most widely examined parameter of liquefaction, and the number of studies dealing with temperature is large [14, 53]. The most commonly reported liquefaction temperature and pressure values are in the range 300 - 400 °C and 20 - 30 MPa. Temperatures between 300 - 350 °C are considered the most optimal range for production of biocrude by

liquefaction [14], but there is no consensus on the issue, and a broad spectrum of results are available in the literature.

Catalysts Catalysts have been used in liquefaction from the very beginning, especially the homogeneous catalysts in the form of alkali salts, e.g. sodium and potassium carbonates (Na_2CO_3 and K_2CO_3 [54]) and hydroxides (NaOH and KOH [55]). As was demonstrated by the Shell results in the 1980's, the absence of alkali catalyst resulted in lower product yields and inferior product qualities [16]. Similar conclusions were drawn from numerous batch studies on liquefaction performed since [56–59]. The influence of alkali salts has not been entirely explained, but it was proposed that increasing pH suppresses dehydration reactions and favours removal of oxygen through decarboxylation [14]. Uncontrolled dehydration can lead to formation of unsaturated intermediates prone to repolymerization. Another explanations points to the promotion of water-gas shift reaction ($CO + H_2O \rightarrow CO_2 + H_2$) in the presence of alkali salts [60]. However, this mechanism is most relevant in the supercritical region of conversion. For liquefaction performed in the near-critical region, the yields of gaseous products are low. According to Karagöz et al. [61] the catalytic efficiency of alkali salts and hydroxides decreases in the following order $K_2CO_3 \geq KOH \geq Na_2CO_3 \geq NaOH$. In addition to the alkali salts, a number of other catalysts have been tested ($Ba(OH)_2$ [62], $RbCO_3$ [63, 64], $FeSO_4$ [65], FeS [65], organic acids [66]). The subject of catalysts concentrations has not been studied in detail. Anastasakis et al. [67] reported that increasing the amounts of KOH actually decrease the yields of biocrude from liquefaction of algae. According to Nguyen et al. [32], the concentration of the catalyst has no influence on hydrothermal conversion of lignin into oil, but it results in increasing amounts of monomers.

Heterogeneous catalysts are commonly used in supercritical gasification where they have been shown to enhance biomass conversion yields and rates and to reduce required energy inputs [24, 68]. In liquefaction, heterogeneous catalysts have been used combined with hydrogenation to produce transport grade fuels in a single step [69]. Research has also been done on upgrading the biocrudes from liquefaction in a separate treatment step [70]. The results have varied depending on the raw material, and the type of catalyst applied [71]. Typical examples of heterogeneous catalysts include an active metal on a support bed of an inert material: Pd/C, Pt/C, Ru/C, Ni/SiO_2-Al_2O_3, CoMo/γ-Al_2O_3 [69, 71–75]. In recent years, application of rare metals has been replaced with low-cost alternatives such as metal oxides, e.g. ZrO_2 [32, 33, 76].

Reaction time and heating rate Reaction time during liquefaction is relatively short. It typically varies between 5 and 60 min [14], depending on the combination of the process parameters and the feed. Shorter reaction times are considered sufficient for conversion of biomass into biocrudes at severe reaction condition, i.e. with high reaction temperatures [67, 77, 78]. Lignin, which at high temperatures can be carbonized even over short reaction times, is an exception from this rule [51]. Reaction time is typically defined as the steady state period between reaching the

reaction temperature and stopping the influx of heat. This definition is not accurate without the information about the accompanying rates of reactant heating and product cooling, which can vary widely depending on the experimental setup. Typical heating rates during liquefaction are in the range 5 - 250 K/min. Slow heating is typical for large (1 - 2 L) batch reactors using electrical jackets. Fast heating is usually achieved in micro-reactors (1 - 2 mL) heated in sand beds, continuous systems with inductive heating or product recirculation, and in sequential-feed batch reactors. The heating rate is considered a critical process parameter that severely affects the liquefaction conversion chemistry [5, 79–82]. According to the literature, while slow heating results in increased amounts of solid products formed by repolymerization and condensation reactions, fast heating ensures increased yields of biocrude [81–83].

3 Conversion mechanisms

The idea of biomass liquefaction originates from and is meant to mimic the geological formation of fossil fuels from algae and trees. While liquefaction takes place in near- or supercritical water, the formation of fossil resources was achieved at moderate temperatures (200 - 250 °C) and high pressure values (approx. 100 MPa) [84]. By increasing the temperature during liquefaction, the conversion time is shortened from millions of years to minutes. However, the reaction mechanisms behind those two processes are quite different. Formation of oil, gas, and coal took place at anoxic conditions and resulted in the conversion of burried biomass into lignite and kerogen (type I and II - oil and gas, type III - coal) [85]. The reactions responsible for the transformation included condensation, deoxygenation, and aromatization and the resulting product could be described as a high molecular weight network of organic compounds. The kerogens were then decomposed through dehydration, dehydrogenation, alkylation, and elimination reactions into fossil fuels. In liquefaction, the opposite happens. The biomass is depolymerized into monomers, which are converted into intermediates that continue to react and repolymerize into higher molecular weight products.

The three steps of liquefaction include depolymerization of biopolymers, secondary reactions of intermediates, and repolymerization of unstable compounds. Depolymerization processes are heterogeneous and take place inside and on the surface of biomass particles. The first step involves the release (through hydrolysis, C-C scission, or water elimination) of monomers (glucose from cellulose, xylose, arabinose, and mannose from hemicellulose, glycerol and fatty acids from lipids, and amino acids from proteins). Lignin is not hydrolyzed into any repeating monomers, but into a broad spectrum of aromatic units. Biomass is relatively easy to depolymerize at hydrothermal conditions (e.g. 180 °C for hemicellulose, 200 °C for lignin, and 240 °C for cellulose) [86]. Some of the primary reaction products are stable under hydrothermal conditions, while other will react further to form intermediates [27, 87–90]. The chemistry behind the subsequent conversion pathways is

complex due to the complicated makeup of the depolymerization products as well as interactions between them. The major groups of secondary reactions pathways include dehydration, dehydrogenation, rearrangements, retro-aldol condensation, Cannizzaro reaction, and Friedel-Crafts alkylation. Dehydration, decarboxylation, and decarbonylation are the major pathways for oxygen removal. Dehydration of the intermediates leads to low molecular weight components. Decarboxylation and decarbonylation are of minor significance in liquefaction, as indicated by low yields of gaseous products from the process [91]. While it is impossible to explain liquefaction with well defined and clear reaction pathways, the studies have shown that in the near-critical region, the conversion is ionically driven. E.g. dehydration in the near-critical water is a condensation reaction, and it can take place through many ionic mechanisms, including elimination (E1, E2), substitution (S_N2), and addition (Ad_E1, Ad_E2) [92]. As the conditions approach the supercritical region, radical reactions become more significant.

4 Characterization of products

The product from liquefaction is typically a two-phase mixture of biocrude and process water with suspended char particles. Minor amounts of synthesis gas are produced as well. The aqueous phase contains mainly polar compounds typically referred to as the water soluble organics (WSO). WSO include alcohols, acids, and ketones of both aliphatic and aromatic nature. In addition to that, various cyclic and aromatic compounds (cresols, phenols, pyrans, and furans) are present as well [93]. Biocrude consists of aliphatic, cyclic, and aromatic units of limited polarity, but minor amounts of the polar organics can be present as well.

Various analytical techniques can be applied for characterization of the liquefaction products' composition as well as their general structure and properties. The latter group includes methods such as Fourier transform infra-red spectroscopy (FT-IR) for determination of functional groups, nuclear magnetic resonance (NMR) for assessment of the aromaticity and saturation, higher heating value (HHV) for measurements of the energy content, and total organic carbon (TOC) for estimation of the organic content. On the other hand, it is considered an analytical challenge to accurately identify and quantify specific constituents present in the aqueous and biocrude fractions [94–96]. Similar difficulties have been reported with regard to pyrolysis oil [50, 96–98].

References

[1] E. Berl and A. Schmidt, "Über das Verhalten der Cellulose bei der Druckerhitzung mit Wasser," *Eur. J. Org. Chem.*, vol. 461, no. 1, pp. 192–220, 1928.

[2] E. Berl, A. Schmidt, H. Biebesheimer, and W. Dienst, "Die Entstehung von Erdöl, Asphalt und Steinkohle," *Sci. Nat.*, vol. 20, no. 35, pp. 652–655, 1932.

[3] E. Berl and H. Biebesheimer, "Zur Frage der Entstehung des Erdöls," *Liebigs Ann.*, vol. 504, no. 1, pp. 38–61, 1933.

[4] E. Berl, "Production of oil from plant material," *Science*, vol. 99, no. 2573, pp. 309–312, 1944.

[5] A. Sinag, A. Kruse, and J. Rathert, "Influence of the heating rate and the type of catalyst on the formation of key intermediates and on the generation of gases during hydropyrolysis of glucose in supercritical water in a batch reactor," *Ind. Eng. Chem. Res.*, vol. 43, no. 2, pp. 502–508, 2004.

[6] J. Barbier, N. Charon, N. Dupassieux, A. Loppinet-Serani, L. Mahé, J. Ponthus, M. Courtiade, A. Ducrozet, A. Fonverne, and F. Cansell, "Hydrothermal conversion of glucose in a batch reactor. A detailed study of an experimental key-parameter: The heating time," *J. Supercrit. Fluids*, vol. 58, no. 1, pp. 114–120, 2011.

[7] K. R. Arturi, M. Strandgaard, R. P. Nielsen, E. G. Søgaard, and M. Maschietti, "Hydrothermal liquefaction of lignin in near-critical water in a new batch reactor: Influence of phenol and temperature," *J. Supercrit. Fluids*, vol. 123, pp. 28–39, 2017.

[8] D. C. Elliott, "Historical developments in hydroprocessing bio-oils," *Energy Fuels*, vol. 21, no. 3, pp. 1792–1815, 2007.

[9] L. J. Sealock Jr, D. C. Elliott, E. G. Baker, and R. S. Butner, "Chemical processing in high-pressure aqueous environments. 1. Historical perspective and continuing developments," *Ind. Eng. Chem. Res.*, vol. 32, no. 8, pp. 1535–1541, 1993.

[10] C. Jazrawi, P. Biller, A. B. Ross, A. Montoya, T. Maschmeyer, and B. S. Haynes, "Pilot plant testing of continuous hydrothermal liquefaction of microalgae," *Algal Res.*, vol. 2, no. 3, pp. 268–277, 2013.

[11] T. H. Pedersen, I. Grigoras, J. Hoffmann, S. S. Toor, I. M. Daraban, C. U. Jensen, S. Iversen, R. B. Madsen, M. Glasius, K. R. Arturi, R. P. Nielsen, E. G. Søgaard, and L. A. Rosendahl, "Continuous hydrothermal co-liquefaction of aspen wood and glycerol with water phase recirculation," *Appl. Energ.*, vol. 162, pp. 1034–1041, 2016.

[12] H. R. Appell, Y. Fu, S. Friedman, P. Yavorsky, and I. Wender, "Converting organic wastes to oil," *Agr. Eng.*, 1972.

[13] J. Bouvier, M. Gelus, and S. Maugendre, "Wood liquefaction - An overview," *Appl. Energy*, vol. 30, no. 2, pp. 85–98, 1988.

[14] S. S. Toor, L. Rosendahl, and A. Rudolf, "Hydrothermal liquefaction of biomass: a review of subcritical water technologies," *Energy*, vol. 36, no. 5, pp. 2328–2342, 2011.

[15] P. Thigpen, W. Berry, and D. Klass, "Energy from biomass and wastes VI," *IGT, Chicago*, p. 1057, 1982.

[16] F. Goudriaan and D. Peferoen, "Liquid fuels from biomass via a hydrothermal process," *Chem. Eng. Sci.*, vol. 45, no. 8, pp. 2729–2734, 1990.

[17] F. Goudriaan, J. Zeevalkink, and J. Naber, *HTU process design and development: Innovation involves many disciplines*. CPL Press: Newbury Berks, UK, 2006.

[18] E. J. Daniels, J. A. Carpenter, C. Duranceau, M. Fisher, C. Wheeler, and G. Winslow, "Sustainable end-of-life vehicle recycling: R&D collaboration between industry and the US DOE," *JOM*, vol. 56, no. 8, pp. 28–32, 2004.

[19] R. P. Nielsen, G. Olofsson, and E. G. Søgaard, "CatLiq–High pressure and temperature catalytic conversion of biomass: The Catliq technology in relation to other thermochemical conversion technologies," *Biomass Bioenergy*, vol. 39, pp. 399–402, 2012.

[20] P. Kritzer and E. Dinjus, "An assessment of supercritical water oxidation (SCWO): Existing problems, possible solutions and new reactor concepts," *Chem. Eng. J.*, vol. 83, no. 3, pp. 207–214, 2001.

[21] M. W. Huang, "Biomass liquefaction process," May 5 1981. US Patent 4,266,083.

[22] M. N. Nabi, M. M. Rahman, M. A. Islam, F. M. Hossain, P. Brooks, W. N. Rowlands, J. Tulloch, Z. D. Ristovski, and R. J. Brown, "Fuel characterisation, engine performance, combustion and exhaust emissions with a new renewable Licella biofuel," *Energy Convers. Manage.*, vol. 96, pp. 588–598, 2015.

[23] M. Balat, "Mechanisms of thermochemical biomass conversion processes. Part 3: Reactions of liquefaction," *Energ. Source. Part A*, vol. 30, no. 7, pp. 649–659, 2008.

[24] T. Minowa, Z. Fang, T. Ogi, and G. Várhegyi, "Decomposition of cellulose and glucose in hot-compressed water under catalyst-free conditions," *J. Chem. Eng. Jpn.*, vol. 31, no. 1, pp. 131–134, 1998.

[25] B. M. Kabyemela, T. Adschiri, R. M. Malaluan, and K. Arai, "Glucose and fructose decomposition in subcritical and supercritical water: Detailed reaction pathway, mechanisms, and kinetics," *Ind. Eng. Chem. Res.*, vol. 38, no. 8, pp. 2888–2895, 1999.

[26] T. Minowa, F. Zhen, T. Ogi, and G. Varhegyi, "Liquefaction of cellulose in hot compressed water using sodium carbonate: products distribution at different reaction temperatures," *J. Chem. Eng. Jpn.*, vol. 30, no. 1, pp. 186–190, 1997.

[27] M. Sasaki, Z. Fang, Y. Fukushima, T. Adschiri, and K. Arai, "Dissolution and hydrolysis of cellulose in subcritical and supercritical water," *Ind. Eng. Chem. Res.*, vol. 39, no. 8, pp. 2883–2890, 2000.

[28] W. S. Mok, M. J. Antal Jr, and G. Varhegyi, "Productive and parasitic pathways in dilute acid-catalyzed hydrolysis of cellulose," *Ind. Eng. Chem. Res.*, vol. 31, no. 1, pp. 94–100, 1992.

[29] M. Sasaki, B. Kabyemela, R. Malaluan, S. Hirose, N. Takeda, T. Adschiri, and K. Arai, "Cellulose hydrolysis in subcritical and supercritical water," *J. Supercrit. Fluids*, vol. 13, no. 1, pp. 261–268, 1998.

[30] W. Shu-Lai Mok and M. Antal, "Uncatalyzed solvolysis of whole biomass hemicellulose by hot compressed liquid water," *Ind. Eng. Chem. Res.*, vol. 31, no. 4, pp. 1157–1161, 1992.

[31] S. E. Jacobsen and C. E. Wyman, "Xylose monomer and oligomer yields for uncatalyzed hydrolysis of sugarcane bagasse hemicellulose at varying solids concentration," *Ind. Eng. Chem. Res.*, vol. 41, no. 6, pp. 1454–1461, 2002.

[32] T. D. H. Nguyen, M. Maschietti, T. Belkheiri, L.-E. Åmand, H. Theliander, L. Vamling, L. Olausson, and S.-I. Andersson, "Catalytic depolymerisation and conversion of Kraft lignin into liquid products using near-critical water," *J. Supercrit. Fluids*, vol. 86, pp. 67–75, 2014.

[33] T. D. H. Nguyen, M. Maschietti, L.-E. Åmand, L. Vamling, L. Olausson, S.-I. Andersson, and H. Theliander, "The effect of temperature on the catalytic conversion of Kraft lignin using near-critical water," *Bioresource Technol.*, vol. 170, pp. 196–203, 2014.

[34] M. Maschietti, T. D. H. Nguyen, T. Belkheiri, L.-E. Åmand, H. Theliander, L. Vamling, L. Olausson, and S.-I. Andersson, "Catalytic hydrothermal conversion of LignoBoost Kraft lignin for the production of bio-oil and aromatic chemicals," in *Proceedings of the International Chemical Recovery Conference*, vol. 2, pp. 252–261, 2014.

[35] F. Taner, A. Eratik, and I. Ardic, "Identification of the compounds in the aqueous phases from liquefaction of lignocellulosics," *Fuel Process. Technol.*, vol. 86, no. 4, pp. 407–418, 2005.

[36] S. P. Mun and M. H. El Barbary, "Liquefaction of lignocellulosic biomass with dioxane/polar solvent mixtures in the presence of an acid catalyst," *J. Ind. Eng. Chem.*, vol. 10, no. 3, pp. 473–477, 2004.

[37] S. Zou, Y. Wu, M. Yang, C. Li, and J. Tong, "Thermochemical catalytic liquefaction of the marine microalgae Dunaliella tertiolecta and characterization of bio-oils," *Energy Fuels*, vol. 23, no. 7, pp. 3753–3758, 2009.

[38] D. L. Barreiro, W. Prins, F. Ronsse, and W. Brilman, "Hydrothermal liquefaction (HTL) of microalgae for biofuel production: State of the art review and future prospects," *Biomass Bioenergy*, vol. 53, pp. 113–127, 2013.

[39] T. Minowa, M. Murakami, Y. Dote, T. Ogi, and S.-y. Yokoyama, "Oil production from garbage by thermochemical liquefaction," *Biomass Bioenergy*, vol. 8, no. 2, pp. 117–120, 1995.

[40] A. Marcilla, L. Catalá, J. García-Quesada, F. Valdés, and M. Hernández, "A review of thermochemical conversion of microalgae," *Renew. Sustainable Energy Rev.*, vol. 27, pp. 11–19, 2013.

[41] P. Biller and A. B. Ross, "Hydrothermal processing of algal biomass for the production of biofuels and chemicals," *Biofuels*, vol. 3, no. 5, pp. 603–623, 2012.

[42] Y. Qian, C. Zuo, J. Tan, and J. He, "Structural analysis of bio-oils from sub-and supercritical water liquefaction of woody biomass," *Energy*, vol. 32, no. 3, pp. 196–202, 2007.

[43] A. Demirbaş, "Conversion of wood to liquid products using alkaline glycerol," *Fuel Sci. Technol. Int.*, vol. 10, no. 2, pp. 173–184, 1992.

[44] R. Eager, J. Mathews, and J. Pepper, "Liquefaction of aspen poplar wood," *Can. J. Chem. Eng.*, vol. 60, no. 2, pp. 289–294, 1982.

[45] A. Demirbaş, M. Balat, and K. Bozbaş, "Direct and catalytic liquefaction of wood species in aqueous solution," *Energ. Source.*, vol. 27, no. 3, pp. 271–277, 2005.

[46] S. Itoh, A. Suzuki, T. Nakamura, and S. Yokoyama, "Production of heavy oil from sewage sludge by direct thermochemical liquefaction," *Desalination*, vol. 98, no. 1, pp. 127–133, 1994.

[47] B. He, Y. Zhang, Y. Yin, T. Funk, and G. Riskowski, "Operating temperature and retention time effects on the thermochemical conversion process of swine manure," *T. ASAE*, vol. 43, no. 6, pp. 1821–1826, 2000.

[48] L. Zhang, P. Champagne, and C. Xu, "Bio-crude production from secondary pulp/paper-mill sludge and waste newspaper via co-liquefaction in hot-compressed water," *Energy*, vol. 36, no. 4, pp. 2142–2150, 2011.

[49] S. Xiu, Y. Zhang, and A. Shahbazi, "Swine manure solids separation and thermochemical conversion to heavy oil," *Bioresources*, vol. 4, no. 2, pp. 458–470, 2009.

[50] Z. Shuping, W. Yulong, Y. Mingde, I. Kaleem, L. Chun, and J. Tong, "Production and characterization of bio-oil from hydrothermal liquefaction of microalgae Dunaliella tertiolecta cake," *Energy*, vol. 35, no. 12, pp. 5406–5411, 2010.

[51] A. Demirbaş, "Effect of lignin content on aqueous liquefaction products of biomass," *Energy Convers. Manage.*, vol. 41, no. 15, pp. 1601–1607, 2000.

[52] A. Kruse and E. Dinjus, "Hot compressed water as reaction medium and reactant: Properties and synthesis reactions," *J. Supercrit. Fluids*, vol. 39, no. 3, pp. 362–380, 2007.

[53] K. Tekin, S. Karagöz, and S. Bektaş, "A review of hydrothermal biomass processing," *Renew. Sustainable Energy Rev.*, vol. 40, pp. 673–687, 2014.

[54] H. Mazaheri, K. T. Lee, and A. R. Mohamed, "Influence of temperature on liquid products yield of oil palm shell via subcritical water liquefaction in the presence of alkali catalyst," *Fuel Process. Technol.*, vol. 110, pp. 197–205, 2013.

[55] F. Behrendt, Y. Neubauer, M. Oevermann, B. Wilmes, and N. Zobel, "Direct liquefaction of biomass," *Chem. Eng.Technol.*, vol. 31, no. 5, pp. 667–677, 2008.

[56] S. Karagöz, T. Bhaskar, A. Muto, and Y. Sakata, "Hydrothermal upgrading of biomass: Effect of K_2CO_3 concentration and biomass/water ratio on products distribution," *Bioresource Technol.*, vol. 97, no. 1, pp. 90–98, 2006.

[57] C. Song, H. Hu, S. Zhu, G. Wang, and G. Chen, "Nonisothermal catalytic liquefaction of corn stalk in subcritical and supercritical water," *Energy Fuels*, vol. 18, no. 1, pp. 90–96, 2004.

[58] D. Maldas and N. Shiraishi, "Liquefaction of biomass in the presence of phenol and H_2O using alkalies and salts as the catalyst," *Biomass Bioenenergy*, vol. 12, no. 4, pp. 273–279, 1997.

[59] S. Karagöz, T. Bhaskar, A. Muto, and Y. Sakata, "Catalytic hydrothermal treatment of pine wood biomass: effect of RbOH and CsOH on product distribution," *J. Chem. Technol. Biotechnol.*, vol. 80, no. 10, pp. 1097–1102, 2005.

[60] H. Schmieder, J. Abeln, N. Boukis, E. Dinjus, A. Kruse, M. Kluth, G. Petrich, E. Sadri, and M. Schacht, "Hydrothermal gasification of biomass and organic wastes," *J. Supercrit. Fluids*, vol. 17, no. 2, pp. 145–153, 2000.

[61] S. Karagöz, T. Bhaskar, A. Muto, Y. Sakata, T. Oshiki, and T. Kishimoto, "Low-temperature catalytic hydrothermal treatment of wood biomass: analysis of liquid products," *Chem. Eng. J.*, vol. 108, no. 1, pp. 127–137, 2005.

[62] C. Xu and N. Lad, "Production of heavy oils with high caloric values by direct liquefaction of woody biomass in sub/near-critical water," *Energy Fuels*, vol. 22, no. 1, pp. 635–642, 2007.

[63] C. C. Xu, H. Su, and D. Cang, "Liquefaction of corn distillers dried grains with solubles (DDGS) in hot-compressed phenol," *BioResources*, vol. 3, no. 2, pp. 363–382, 2008.

[64] K. Tekin and S. Karagöz, "Non-catalytic and catalytic hydrothermal liquefaction of biomass," *Res. Chem. Intermediat.*, vol. 39, no. 2, pp. 485–498, 2013.

[65] C. Xu and T. Etcheverry, "Hydro-liquefaction of woody biomass in sub-and super-critical ethanol with iron-based catalysts," *Fuel*, vol. 87, no. 3, pp. 335–345, 2008.

[66] A. Ross, P. Biller, M. Kubacki, H. Li, A. Lea-Langton, and J. Jones, "Hydrothermal processing of microalgae using alkali and organic acids," *Fuel*, vol. 89, no. 9, pp. 2234–2243, 2010.

[67] K. Anastasakis and A. Ross, "Hydrothermal liquefaction of the brown macro-alga Laminaria Saccharina: Effect of reaction conditions on product distribution and composition," *Bioresource Technol.*, vol. 102, no. 7, pp. 4876–4883, 2011.

[68] T. Minowa and T. Ogi, "Hydrogen production from cellulose using a reduced nickel catalyst," *Catal. Today*, vol. 45, no. 1, pp. 411–416, 1998.

[69] P. Duan and P. E. Savage, "Hydrothermal liquefaction of a microalga with heterogeneous catalysts," *Ind. Eng. Chem. Res.*, vol. 50, no. 1, pp. 52–61, 2010.

[70] D. Elliott, "Hydrodeoxygenation of phenolic components of wood-derived oil," *Am. Chem. Soc., Div. Pet. Chem.*, vol. 28, no. Conf. 830303, 1983.

[71] P. Biller, R. Riley, and A. Ross, "Catalytic hydrothermal processing of microalgae: Decomposition and upgrading of lipids," *Bioresour. Technol.*, vol. 102, no. 7, pp. 4841–4848, 2011.

[72] B. Yoosuk, D. Tumnantong, and P. Prasassarakich, "Amorphous unsupported ni–mo sulfide prepared by one step hydrothermal method for phenol hydrodeoxygenation," *Fuel*, vol. 91, no. 1, pp. 246–252, 2012.

[73] W. Wang, Y. Yang, H. Luo, and W. Liu, "Effect of additive (Co, La) for Ni–Mo–B amorphous catalyst and its hydrodeoxygenation properties," *Catal. Commun.*, vol. 11, no. 9, pp. 803–807, 2010.

[74] A. Hammerschmidt, N. Boukis, E. Hauer, U. Galla, E. Dinjus, B. Hitzmann, T. Larsen, and S. D. Nygaard, "Catalytic conversion of waste biomass by hydrothermal treatment," *Fuel*, vol. 90, no. 2, pp. 555–562, 2011.

[75] D. Elliott, L. J. Sealock Jr, and E. G. Baker, "Chemical processing in high-pressure aqueous environments. 2. Development of catalysts for gasification," *Ind. Eng. Chem. Res.*, vol. 32, no. 8, pp. 1542–1548, 1993.

[76] M. Watanabe, T. Iida, and H. Inomata, "Decomposition of a long chain saturated fatty acid with some additives in hot compressed water," *Energ. Convers. Manag.*, vol. 47, no. 18, pp. 3344–3350, 2006.

[77] L. Garcia Alba, C. Torri, C. Samorì, J. van der Spek, D. Fabbri, S. R. Kersten, and D. W. Brilman, "Hydrothermal treatment (HTT) of microalgae: Evaluation of the process as conversion method in an algae biorefinery concept," *Energy Fuels*, vol. 26, no. 1, pp. 642–657, 2011.

[78] Y. Qu, X. Wei, and C. Zhong, "Experimental study on the direct liquefaction of Cunninghamia lanceolata in water," *Energy*, vol. 28, no. 7, pp. 597–606, 2003.

[79] E. Kamio, S. Takahashi, H. Noda, C. Fukuhara, and T. Okamura, "Effect of heating rate on liquefaction of cellulose by hot compressed water," *Chem. Eng. J.*, vol. 137, no. 2, pp. 328–338, 2008.

[80] Q.-V. Bach, M. V. Sillero, K.-Q. Tran, and J. Skjermo, "Fast hydrothermal liquefaction of a Norwegian macro-alga: Screening tests," *Algal Res.*, vol. 6, pp. 271–276, 2014.

[81] S. Saka and T. Ueno, "Chemical conversion of various celluloses to glucose and its derivatives in supercritical water," *Cellulose*, vol. 6, no. 3, pp. 177–191, 1999.

[82] Z. Fang, T. Minowa, R. Smith, T. Ogi, and J. Kozinski, "Liquefaction and gasification of cellulose with Na_2CO_3 and Ni in subcritical water at 350 °C," *Ind. Eng. Chem. Res.*, vol. 43, no. 10, pp. 2454–2463, 2004.

[83] B. Zhang, M. von Keitz, and K. Valentas, "Thermochemical liquefaction of high-diversity grassland perennials," *J. Anal. Appl. Pyrolysis*, vol. 84, no. 1, pp. 18–24, 2009.

[84] H. Weingärtner and E. U. Franck, "Supercritical water as a solvent," *Angew. Chem. Int. Ed.*, vol. 44, no. 18, pp. 2672–2692, 2005.

[85] M. Siskin and A. R. Katritzky, "Reactivity of organic compounds in hot water: Geochemical and technological implications," *Science*, vol. 254, no. 5029, p. 231, 1991.

[86] O. Bobleter, "Hydrothermal degradation of polymers derived from plants," *Prog. Polym. Sci.*, vol. 19, no. 5, pp. 797–841, 1994.

[87] Z. Srokol, A.-G. Bouche, A. van Estrik, R. C. Strik, T. Maschmeyer, and J. A. Peters, "Hydrothermal upgrading of biomass to biofuel: Studies on some monosaccharide model compounds," *Carbohydr. Res.*, vol. 339, no. 10, pp. 1717–1726, 2004.

[88] G. Brunner, "Near critical and supercritical water. Part I. Hydrolytic and hydrothermal processes," *J. Supercrit. Fluids*, vol. 47, no. 3, pp. 373–381, 2009.

[89] G. Brunner, "Near and supercritical water. Part II: Oxidative processes," *J. Supercrit. Fluids*, vol. 47, no. 3, pp. 382–390, 2009.

[90] B. M. Kabyemela, T. Adschiri, R. M. Malaluan, and K. Arai, "Kinetics of glucose epimerization and decomposition in subcritical and supercritical water," *Ind. Eng. Chem. Res.*, vol. 36, no. 5, pp. 1552–1558, 1997.

[91] J. Akhtar and N. A. S. Amin, "A review on process conditions for optimum bio-oil yield in hydrothermal liquefaction of biomass," *Renew. Sustainable Energy Rev.*, vol. 15, no. 3, pp. 1615–1624, 2011.

[92] A. A. Peterson, F. Vogel, R. P. Lachance, M. Fröling, M. J. Antal Jr, and J. W. Tester, "Thermochemical biofuel production in hydrothermal media: A review of sub-and supercritical water technologies," *Energy Environ. Sci.*, vol. 1, no. 1, pp. 32–65, 2008.

[93] C. Xu and J. Lancaster, "Conversion of secondary pulp/paper sludge powder to liquid oil products for energy recovery by direct liquefaction in hot-compressed water," *Water Res.*, vol. 42, no. 6, pp. 1571–1582, 2008.

[94] N. Sudasinghe, B. Dungan, P. Lammers, K. Albrecht, D. Elliott, R. Hallen, and T. Schaub, "High resolution FT-ICR mass spectral analysis of bio-oil and residual water soluble organics produced by hydrothermal liquefaction of the marine microalga Nannochloropsis salina," *Fuel*, vol. 119, pp. 47–56, 2014.

[95] S. R. Villadsen, L. Dithmer, R. Forsberg, J. Becker, A. Rudolf, S. B. Iversen, B. B. Iversen, and M. Glasius, "Development and application of chemical analysis methods for investigation of bio-oils and aqueous phase from hydrothermal liquefaction of biomass," *Energy Fuels*, vol. 26, no. 11, pp. 6988–6998, 2012.

[96] E. A. Smith, S. Park, A. T. Klein, and Y. J. Lee, "Bio-oil analysis using negative electrospray ionization: Comparative study of high-resolution mass spectrometers and phenolic versus sugaric components," *Energy Fuels*, vol. 26, no. 6, pp. 3796–3802, 2012.

[97] M. Garcia-Perez, A. Chaala, H. Pakdel, D. Kretschmer, and C. Roy, "Characterization of bio-oils in chemical families," *Biomass Bioenergy*, vol. 31, no. 4, pp. 222–242, 2007.

[98] B. Scholze and D. Meier, "Characterization of the water-insoluble fraction from pyrolysis oil (pyrolytic lignin). Part I. PY–GC/MS, FTIR, and functional groups," *J. Anal. Appl. Pyrol.*, vol. 60, no. 1, pp. 41–54, 2001.

Research objectives

Liquefaction in near- or supercritical water is one of many biomass conversion techniques for the production of renewable value-added products, energy carriers, fuels, chemicals, and materials. The field of biomass valorization has been dominated by chemical and biochemical methods resulting in a landscape with nearly all commercial roads leading to either bioethanol or biodiesel.

The sustainability of utilizing particular types of biomass as a raw material for the production of biofuels and other commodities raise concerns. The skeptics point to the "food vs. fuels" debate and overall poor GHG savings as the main arguments against the first generation biofuels. Utilization of second generation biomass types, e.g. forest residues, is not considered a significantly more sustainable solution, due to the fears of deforestation and soil erosion.

The sustainability of biomass-based products can be improved by utilizing conversion processes, which can use waste streams. Millions of tons of organic wastes are produced every year. The sustainability of the future bioeconomy will depend on the valorization of these resources. Liquefaction is a process that is extremely versatile regarding the used raw feed. It is a processing method for production of drop-in biofuels and chemicals from all types of biomass, including water-rich, complex wastes. As such, liquefaction would be an excellent addition handling multiple streams on a biorefinery.

Liquefaction is versatile and extremely promising biomass conversion technique, and yet, due to to the lack of investments, the method has not been commercialized. In addition to the production of biofuels, the focus should be shifted to include additional products, especially chemicals. The approach of supplementing the production of transportation fuels with high-value products would help increase the process sustainability and make the biocrudes profitable. Based on the presented framework, several challenges and areas of concern in the field of liquefaction were identified and laid out as the cornerstones of this work. The overall goal is:

To optimize hydrothermal processing of wastes into value-added products.

To fulfill this objective, the following specific tasks are addressed:

1. Significant variations in liquefaction data reported in the literature have resulted in a slow progress of liquefaction optimization.

Identify the general trends behind the hydrothermal conversion of biomass by using multivariate data analysis on a large sample of liquefaction data. Find hidden patterns and predict liquefaction outputs (yields and product quality) as a function of process parameters.

2. Challenges in characterization of liquefaction products have limited our knowledge about the process.

Develop analytical procedures for detailed characterization of the liquefaction products, both the biocrude and the aqueous phase. Use analytical tools that result in improved identification and quantification of the complex liquefaction products.

3. Batch processing without control over all crucial parameters does not provide an accurate basis for the development of large-scale continuous processes.

Optimize liquefaction in batch to obtain full control over process parameters and obtain reliable experimental results.

4. Waste is s vast resource, and there is a need for more studies about valorization of particular types of waste streams.

Evaluate liquefaction of various wastes (lignin, lignocellulose, polymers) and assess their potential as a source for value-added products by hydrothermal liquefaction in near-critical water. Study reaction mechanisms and the role of different co-solvents.

Part II

Results

In this part, the background for the studies performed as a part of the current work, their main findings, and an outlook for further work are presented. The Conclusion section sums up the obtained results in a larger perspective.

Chapter 4

Statistical modelling

This chapter covers applications of multivariate data analysis (MDA) for the description of liquefaction and its products. MDA is utilized to find general trends in the yields of products and their quality as reported in the literature. The aim was to develop tools for prediction of outputs from liquefaction as a function of process parameters. Furthermore, MDA was also applied to explore its potential application in combination with chromatography. The novelty of this work lies in the application of advanced statistical tools for modeling of liquefaction as a process. The reader is referred to Papers A and E for more details.

1 Background

As mentioned in the introduction, due to the variations in hydrothermal processing, the liquefaction results reported in the literature are very heterogeneous. The yield of the produced biocrude is the most central quantitative response from liquefaction, and an extensive amount of data is available. Figure 4.1 shows of a compilation of biocrude yields obtained as a function of reaction temperatures for different biomass types. The observed differences can be attributed to the variations in processing, both the controlled process parameters as well as those typically unreported, e.g. heating rates and reaction medium density. The spread is very wide, and it's clear that it would be difficult to draw any generally valid conclusions from these data. A similar conclusion can be made for other process outputs, or responses, including the yields of other products and their quality. The results tend to be more consistent within the same type of biomass (Figure 4.2), but significant differences still occur. The situation has contributed to a widespread confusion in the field and slow progress in process optimization. Utilization of univariate and multivariate statistical tools on a large set of liquefaction data (more than 400 records) aimed at determination of overall trends and hidden patterns including the interactions and correlations between the process conditions (biomass type, biomass content, lignin content, catalyst amount, reaction temperature, heating rate, reac-

tion time, energy content of the biomass, and C/H ratio of the biomass) and the outputs (yields of the biocrude, yields of the water soluble organics, and energy content in the biocrude). MDA is an multidisciplinary tool used widely in many fields of science for analysis of large experimental data sets.

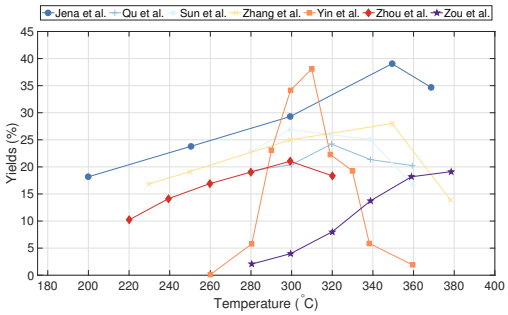

Fig. 4.1: HTL yields as a function of temperature. Data source: Jena et al. [1], Qu et a. [2], Sun et al. [3], Yin et al. [4], Zhang et al. [5], Zhou et al. [6], Zou et al. [7]. Reproduced from Ref. [8], Copyright (2012), with permission from the American Chemical Society.

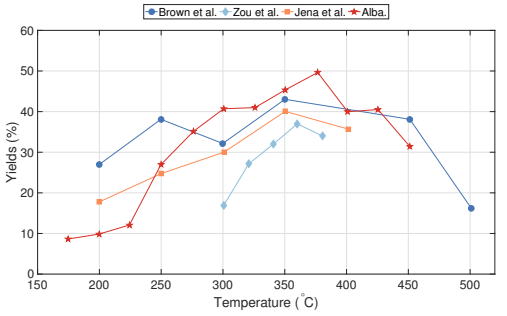

Fig. 4.2: HTL yields for algae biomass as a function of temperature. Data source: Brown et al. [9], Zou et al. [10], Jena et al. [1], Alba et al. [11]. Reprinted with permission from Ref. [12]. Copyright (2013), with permission from Elsevier.

2 Modeling of literature data

The experimental data was collected from 34 peer-reviewed studies [2, 4, 8, 10, 13–42] available in the literature. The data was assessed by principal component analysis - PCA, partial least squares - PLS, and traditional statistical methods (analysis of variance - ANOVA, Tukey's test, and Spearman's correlation with bootstrap confidence intervals). The strategy was to assess the general patterns by PCA, examine the found trends by ANOVA, Tukey's, and Spearman's tests, and finally to build a regression model. Although the quality of the statistical models obtained in this study varied depending on the response and analysis parameters, MDA was shown

to be a promising tool for compiling and extracting useful information from the heterogeneous pool of liquefaction results. It was shown that few trends are common for all biomass types. Algae showed the highest biocrude yields and enhanced biocrude energy content, while lignocellulose resulted in most reliable models. The findings confirmed certain axioms of liquefaction in addition to uncovering new trends. High yields of WSO were obtained at conditions involving increasing concentrations of catalyst, fast heating, and longer reaction times. The opposite was true for the biocrude. The energy content in the biocrude was ruled not by the process parameters, but the properties of the biomass. The PCA and PLS-R results for WSO for all biomass types are presented in Figure 4.3 and 4.4.

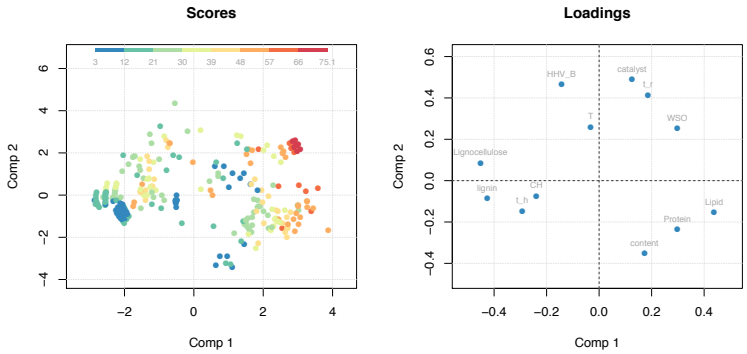

Fig. 4.3: PC1 (34.94 %) vs. PC2 (15.57 %) score and loading plots (PCA model of factors and WSO for all groups of biomass). The color gradient on the scores plot corresponds to different yields of WSO (blue-low, red-high). The loading plot shows which factors are related to WSO yields. Reproduced from Paper A, Copyright (2016), with permission from Elsevier.

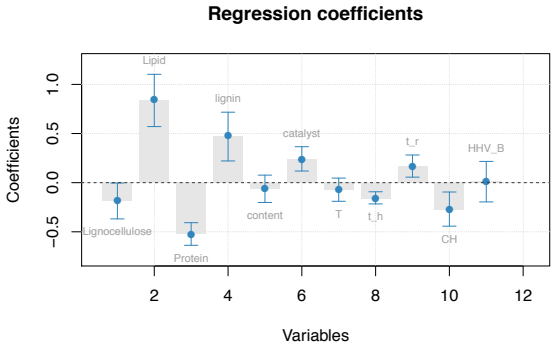

Fig. 4.4: Regression coefficients with 95 % confidence interval for WSO values (calculated with PLS for all biomass groups). The size, sign, and the confidence intervals are used to judge the importance of each factor. Reproduced from Paper A, Copyright (2016), with permission from Elsevier.

3 PCA and chromatography

Chromatographic data was analyzed with PCA in the same way as the liquefaction results obtained from the literature. Here, we reduced the number of dimensions (chromatographic data points, i.e. the counts for each retention time value - RT to the number of principal components - PCs) while exposing the information about the variation patterns in the data. In this case, each data point in the scores plot represents a chromatogram, while the loadings estimate how much each of the old coordinates (peaks) contributes to each of the new coordinates (PCs). Due to the high number of variables in this analysis, the loadings are presented as a line plot instead of a scatter plot. Exploration of chromatographic data with multivariate tools proved to be an excellent tool for finding hidden patterns in the obtained GC-MS data. The results confirmed that the presence of tetralin resulted in reaction pathways shift leading to increased amounts of aromatics and decreased high molecular weight products (HMW). These findings were collaborated by yields of reaction products (lower solid content and higher BC yields in the presence of co-solvents, especially tetralin) and the semi-quantitative GC-MS results obtained from analysis of chemical class distribution (increased yields of A and decreased HMW).

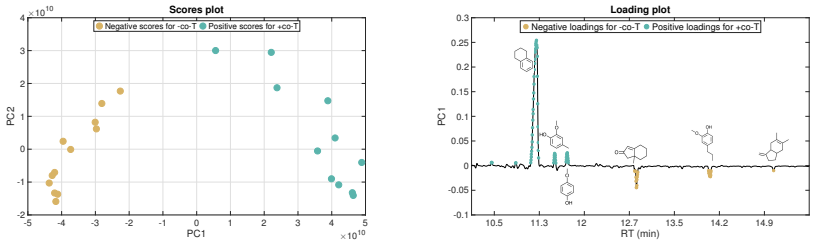

Fig. 4.5: PC1 vs. PC2 score plot (top) and PC1 line loading plot (bottom) colored according to the presence of tetralin co-solvent. Reproduced from Paper D.

4 Outlook

MDA is an excellent tool for identifying hidden patterns in large data sets. The obtained multivariate models were of varying statistical significance depending on the type of response and biomass. For models of high statistical quality (low RMSE and high R^2), the calculated regression coefficients can be used directly to make predictions based on the input variables, as was the case for the WSO yields. With reduced regression parameters, the models can only be applied for observation of loose tendencies in the data. In addition to the differences in experimental procedures, variations in the pre-analytical handling and separation of the reaction products (separation schemes, organic solvents used, filtration, evaporation, assisted extraction, etc.) introduced a second set of unaccounted for variables and could explain the poor quality of some of the models. The obtained MDA models could

be improved further by collecting and analyzing a larger random sample, and by the introduction of additional requirements to the data, e.g. closed mass and carbon balances combined with a single separation scheme.

References

[1] U. Jena, K. Das, and J. Kastner, "Effect of operating conditions of thermochemical liquefaction on biocrude production from Spirulina platensis," *Bioresource Technol.*, vol. 102, no. 10, pp. 6221–6229, 2011.

[2] Y. Qu, X. Wei, and C. Zhong, "Experimental study on the direct liquefaction of Cunninghamia lanceolata in water," *Energy*, vol. 28, no. 7, pp. 597–606, 2003.

[3] P. Sun, M. Heng, S.-H. Sun, and J. Chen, "Analysis of liquid and solid products from liquefaction of paulownia in hot-compressed water," *Energ. Convers. Manage.*, vol. 52, no. 2, pp. 924–933, 2011.

[4] S. Yin, R. Dolan, M. Harris, and Z. Tan, "Subcritical hydrothermal liquefaction of cattle manure to bio-oil: Effects of conversion parameters on bio-oil yield and characterization of bio-oil," *Bioresour. Technol.*, vol. 101, no. 10, pp. 3657–3664, 2010.

[5] L. Zhang, P. Champagne, and C. Xu, "Bio-crude production from secondary pulp/paper-mill sludge and waste newspaper via co-liquefaction in hot-compressed water," *Energy*, vol. 36, no. 4, pp. 2142–2150, 2011.

[6] D. Zhou, S. Zhang, H. Fu, and J. Chen, "Liquefaction of macroalgae Enteromorpha prolifera in sub-/supercritical alcohols: direct production of ester compounds," *Energy Fuels*, vol. 26, no. 4, pp. 2342–2351, 2012.

[7] S. Zou, Y. Wu, M. Yang, C. Li, and J. Tong, "Thermochemical catalytic liquefaction of the marine microalgae Dunaliella tertiolecta and characterization of bio-oils," *Energy Fuels*, vol. 23, no. 7, pp. 3753–3758, 2009.

[8] A. J. Mørup, P. R. Christensen, D. F. Aarup, L. Dithmer, A. Mamakhel, M. Glasius, and B. B. Iversen, "Hydrothermal liquefaction of dried distillers grains with solubles: A reaction temperature study," *Energy Fuels*, vol. 26, no. 9, pp. 5944–5953, 2012.

[9] T. M. Brown, P. Duan, and P. E. Savage, "Hydrothermal liquefaction and gasification of Nannochloropsis sp.," *Energy Fuels*, vol. 24, no. 6, pp. 3639–3646, 2010.

[10] S. Zou, Y. Wu, M. Yang, C. Li, and J. Tong, "Bio-oil production from sub-and supercritical water liquefaction of microalgae Dunaliella tertiolecta and related properties," *Energy Environ. Sci.*, vol. 3, no. 8, pp. 1073–1078, 2010.

[11] L. Garcia Alba, C. Torri, C. Samorì, J. van der Spek, D. Fabbri, S. R. Kersten, and D. W. Brilman, "Hydrothermal treatment (HTT) of microalgae: Evaluation of the process as conversion method in an algae biorefinery concept," *Energy Fuels*, vol. 26, no. 1, pp. 642–657, 2011.

[12] D. L. Barreiro, W. Prins, F. Ronsse, and W. Brilman, "Hydrothermal liquefaction (HTL) of microalgae for biofuel production: State of the art review and future prospects," *Biomass Bioenergy*, vol. 53, pp. 113–127, 2013.

[13] C. Zhong and X. Wei, "A comparative experimental study on the liquefaction of wood," *Energy*, vol. 29, no. 11, pp. 1731–1741, 2004.

[14] L. Zhang, C. C. Xu, and P. Champagne, "Energy recovery from secondary pulp/paper-mill sludge and sewage sludge with supercritical water treatment," *Bioresource Technol.*, vol. 101, no. 8, pp. 2713–2721, 2010.

[15] A. Demirbaş, "Thermochemical conversion of biomass to liquid products in the aqueous medium," *Energ. Source.*, vol. 27, no. 13, pp. 1235–1243, 2005.

[16] S. Karagöz, T. Bhaskar, A. Muto, and Y. Sakata, "Comparative studies of oil compositions produced from sawdust, rice husk, lignin and cellulose by hydrothermal treatment," *Fuel*, vol. 84, no. 7, pp. 875–884, 2005.

[17] T. D. H. Nguyen, M. Maschietti, T. Belkheiri, L.-E. Åmand, H. Theliander, L. Vamling, L. Olausson, and S.-I. Andersson, "Catalytic depolymerisation and conversion of Kraft lignin into liquid products using near-critical water," *J. Supercrit. Fluids*, vol. 86, pp. 67–75, 2014.

[18] T. D. H. Nguyen, M. Maschietti, L.-E. Åmand, L. Vamling, L. Olausson, S.-I. Andersson, and H. Theliander, "The effect of temperature on the catalytic conversion of Kraft lignin using near-critical water," *Bioresource Technol.*, vol. 170, pp. 196–203, 2014.

[19] X. Pei, X. Yuan, G. Zeng, H. Huang, J. Wang, H. Li, and H. Zhu, "Co-liquefaction of microalgae and synthetic polymer mixture in sub-and supercritical ethanol," *Fuel Process. Technol.*, vol. 93, no. 1, pp. 35–44, 2012.

[20] K. Anastasakis and A. Ross, "Hydrothermal liquefaction of the brown macro-alga Laminaria Saccharina: Effect of reaction conditions on product distribution and composition," *Bioresource Technol.*, vol. 102, no. 7, pp. 4876–4883, 2011.

[21] D. R. Vardon, B. Sharma, J. Scott, G. Yu, Z. Wang, L. Schideman, Y. Zhang, and T. J. Strathmann, "Chemical properties of biocrude oil from the hydrothermal liquefaction of Spirulina algae, swine manure, and digested anaerobic sludge," *Bioresource Technol.*, vol. 102, no. 17, pp. 8295–8303, 2011.

[22] P. Biller, A. B. Ross, S. Skill, A. Lea-Langton, B. Balasundaram, C. Hall, R. Riley, and C. Llewellyn, "Nutrient recycling of aqueous phase for microalgae cultivation from the hydrothermal liquefaction process," *Algal Res.*, vol. 1, no. 1, pp. 70–76, 2012.

[23] P. Biller and A. Ross, "Potential yields and properties of oil from the hydrothermal liquefaction of microalgae with different biochemical content," *Bioresource Technol.*, vol. 102, no. 1, pp. 215–225, 2011.

[24] M. K. Akalın, K. Tekin, and S. Karagöz, "Hydrothermal liquefaction of cornelian cherry stones for bio-oil production," *Bioresource Technol.*, vol. 110, pp. 682–687, 2012.

[25] B. He, Y. Zhang, Y. Yin, T. Funk, and G. Riskowski, "Preliminary characterization of raw oil products from the thermochemical conversion of swine manure," *T. ASAE.*, vol. 44, no. 6, pp. 1865–1872, 2001.

[26] X. Yuan, J. Wang, G. Zeng, H. Huang, X. Pei, H. Li, Z. Liu, and M. Cong, "Comparative studies of thermochemical liquefaction characteristics of microalgae using different organic solvents," *Energy*, vol. 36, no. 11, pp. 6406–6412, 2011.

[27] X. Yuan, J. Tong, G. Zeng, H. Li, and W. Xie, "Comparative studies of products obtained at different temperatures during straw liquefaction by hot compressed water," *Energy Fuels*, vol. 23, no. 6, pp. 3262–3267, 2009.

[28] P. R. Christensen, A. J. Mørup, A. Mamakhel, M. Glasius, J. Becker, and B. B. Iversen, "Effects of heterogeneous catalyst in hydrothermal liquefaction of dried distillers grains with solubles," *Fuel*, vol. 123, pp. 158–166, 2014.

[29] S. Cheng, I. D'cruz, M. Wang, M. Leitch, and C. Xu, "Highly efficient liquefaction of woody biomass in hot-compressed alcohol- water co-solvents," *Energy Fuels*, vol. 24, no. 9, pp. 4659–4667, 2010.

[30] W.-T. Chen, Y. Zhang, J. Zhang, G. Yu, L. C. Schideman, P. Zhang, and M. Minarick, "Hydrothermal liquefaction of mixed-culture algal biomass from wastewater treatment system into bio-crude oil," *Bioresource Technol.*, vol. 152, pp. 130–139, 2014.

[31] Y. H. Chan, S. Yusup, A. T. Quitain, Y. Uemura, and M. Sasaki, "Bio-oil production from oil palm biomass via subcritical and supercritical hydrothermal liquefaction," *J. Supercrit. Fluid.*, vol. 95, pp. 407–412, 2014.

[32] D. Zhou, L. Zhang, S. Zhang, H. Fu, and J. Chen, "Hydrothermal liquefaction of macroalgae Enteromorpha prolifera to bio-oil," *Energy Fuels*, vol. 24, no. 7, pp. 4054–4061, 2010.

[33] X. Yuan, H. Li, G. Zeng, J. Tong, and W. Xie, "Sub-and supercritical liquefaction of rice straw in the presence of ethanol–water and 2-propanol–water mixture," *Energy*, vol. 32, no. 11, pp. 2081–2088, 2007.

[34] S.-y. Yokoyama, A. Suzuki, M. Murakami, T. Ogi, K. Koguchi, and E. Nakamura, "Liquid fuel production from sewage sludge by catalytic conversion using sodium carbonate," *Fuel*, vol. 66, no. 8, pp. 1150–1155, 1987.

[35] C. Xu and J. Lancaster, "Conversion of secondary pulp/paper sludge powder to liquid oil products for energy recovery by direct liquefaction in hot-compressed water," *Water Res.*, vol. 42, no. 6, pp. 1571–1582, 2008.

[36] D. R. Vardon, B. K. Sharma, G. V. Blazina, K. Rajagopalan, and T. J. Strathmann, "Thermochemical conversion of raw and defatted algal biomass via hydrothermal liquefaction and slow pyrolysis," *Bioresource Technol.*, vol. 109, pp. 178–187, 2012.

[37] P. J. Valdez, M. C. Nelson, H. Y. Wang, X. N. Lin, and P. E. Savage, "Hydrothermal liquefaction of Nannochloropsis sp.: Systematic study of process variables and analysis of the product fractions," *Biomass Bioenergy*, vol. 46, pp. 317–331, 2012.

[38] M. Tymchyshyn and C. C. Xu, "Liquefaction of bio-mass in hot-compressed water for the production of phenolic compounds," *Bioresource Technol.*, vol. 101, no. 7, pp. 2483–2490, 2010.

[39] S. S. Toor, L. Rosendahl, M. P. Nielsen, M. Glasius, A. Rudolf, and S. B. Iversen, "Continuous production of bio-oil by catalytic liquefaction from wet distiller's grain with solubles (WDGS) from bio-ethanol production," *Biomass Bioenenergy*, vol. 36, pp. 327–332, 2012.

[40] S. Sawayama, S. Inoue, T. Minowa, K. Tsukahara, and T. Ogi, "Thermochemical liquidization and anaerobic treatment of kitchen garbage," *J. Fermen. Bioeng.*, vol. 83, no. 5, pp. 451–455, 1997.

[41] G. van Rossum, W. Zhao, M. Castellvi Barnes, J.-P. Lange, and S. R. Kersten, "Liquefaction of lignocellulosic biomass: Solvent, process parameter, and recycle oil screening," *ChemSusChem*, vol. 7, no. 1, pp. 253–259, 2014.

[42] A. Ross, P. Biller, M. Kubacki, H. Li, A. Lea-Langton, and J. Jones, "Hydrothermal processing of microalgae using alkali and organic acids," *Fuel*, vol. 89, no. 9, pp. 2234–2243, 2010.

Chapter 5

Product characterization

This chapter covers optimization of analysis of liquefaction products performed as a part of the current work. The aim was to improve characterization of both the aqueous phase as well as the biocrude fractions. The focus was split between an enhanced transfer of analytes and their separation and identification. The novelty of this work lies in the utilization of advanced state-of-the tools for characterization of complex mixtures. The reader is referred to Papers B and E for more details.

1 Background

There is no doubt that the parameters of the analytical processing are of the uttermost importance for the results. Application of different separation schemes for the products from liquefaction is very common [1–4], and it ends in variations based not on the processing conditions, but on the analytical strategy. For extraction of biocrude and dissolved solids, tetrahydrofuran and acetone are the most applied solvents [5–8], but a significant number of other organics have been used. The influence of the solvent on the yields of extracted products was studied by Valdez et al. [9]. According to the results, extraction with hexadecane and decane provided the highest gravimetric yields of oil, while the highest amounts of organic carbon were extracted with the polar solvents. Furthermore, the most efficient gas chromatography-mass spectrometry (GC-MS) identification of biocrudes was obtained with chlorinated solvents, e.g. chloroform.

The composition of liquefaction products is complex, and an accurate assessment of their content can be challenging. The two main analytical challenges regard a successful transfer of the analytes from the samples to the instruments and their following separation and identification. The most commonly applied technique for identification of the biocrude and aqueous phase from liquefaction is GC-MS [8–20]. The major challenge of this technique is the pre-requisite for analyte volatility. According to a study on the composition of pyrolytic biocrude by Garcia et al. [12], the

composition of the product could be described as following: 49 wt.% GC-detectable compounds, 15 wt.% non-volatile HPLC detectable compounds, and 15 wt.% high molar mass non-detectable compounds. The results obtained by Bridgwater et al. [21] for pyrolytic oil specified that the content could be divided into 5 - 10 wt.% hydrocarbons, 10 - 25 wt.% oxygenated compounds including phenols, aldehydes, ketones and moderately polar alcohols, and 30 - 45 wt.% highly polar compounds with low, moderate and high molecular weights. According to a similar study by Valdez et al. [9] on the composition of biocrude from liquefaction, only 10 - 35 wt. % of the compounds can be identified with GC-MS. Villadsen et al. [5] concluded that the method is inadequate for determining highly polar compounds such as sugars and fatty acids. Concluding, the constituents of the aqueous phase are too polar to be efficiently analyzed, while the biocrude components lack the necessary volatility. However, due to the complexity of the liquefaction products, a typical biocrude chromatogram contains more than 200 peaks, with approx. 30 of the peaks responsible for the principal part of the signal [5]. With such a large number of peaks, the separation and identification of the compounds become involved. In order to improve analyte transfer and separation, methods such as solid-phase microextraction (SPME) [22], thin layer chromatography (TLC) [23], acid-base extraction [24], and derivatization [5, 25], have been applied.

2 Solid-phase microextraction

Solid phase microextraction (SPME) is a solvent-free alternative to liquid-liquid extraction (LLE) for transfer of the analytes from the sample and into the instrument. SPME is concerned with equilibrium between the sample and a fiber covered with an adsorbent (or absorbent) material, and not with the exhaustive transfer of compounds typical for LLE [26]. The technique has been used in a number of applications [27–29], including liquefaction [22], although to a very limited extent. SPME is based on the mass of conservation, according to which, in the equilibrium regime, the absorbed/adsorbed amount of an analyte is linearly proportional to its concentration in the sample (Equation 5.1) [26]). The exact ratio between the present and extracted amounts of analytes are expressed in terms of the partition coefficient K_{fs} (Equation 5.2). The value of K_{fs} is compound-specific, dependent on the present matrix, and the used fiber. Higher K_{fs} values entail longer equilibrium times (Equation 5.3). The values of distribution coefficients are similar for similar compounds (in structure and properties). In general, very little data is available on the experimental values for distribution coefficients of different organics and fibers types [30]. For a three-phase system in a head-space (HS) extraction the mathematical expression for SPME changes to (Equation 5.4). A simplified version of the equation can be written for large volume samples as Equation 5.5. The value of K_{hs} represents a head-space/fiber distribution coefficient that can be calculated from Henry's constant and the retention times of the analytes ($K_{hs} = H/(RT)$).

$$C_0 \cdot V_s = C_f^{\infty} \cdot V_f + C_s^{\infty} \cdot V_s \tag{5.1}$$

$$K_{fs} = \frac{C_f^{\infty}}{C_s^{\infty}} \tag{5.2}$$

$$n = C_f^{\infty} \cdot V_f = C_0 \cdot \frac{K_{fs} \cdot V_f \cdot V_s}{K_{fs} \cdot V_f + V_s} \tag{5.3}$$

$$n = \frac{K_{fs} \cdot V_f \cdot V_s \cdot C_0}{K_{fs} \cdot V_f + K_{hs} \cdot V_h + V_s} \tag{5.4}$$

$$n = K_{fs} \cdot V_f \cdot C_0 \tag{5.5}$$

Where:

n	Extracted mol
C_0	Initial concentration of analyte
V_s	Volume of the sample
C_s	Concentration of the analyte in the sample
C_f	Concentration of the analyte on the fiber
K_{fs}	Distribution coefficient fiber/sample
K_{hs}	Distribution coefficient head-space/sample

In this study, SPME in combination with GC-MS were applied to improve the transfer of analytes from the samples to the instrument. For the aqueous phase, description of the composition was accompanied by a systematic method development. SPME can be influenced by a number of parameters, including extraction time and temperature, stirring rates, changes in pH, and the addition of salt. In the pre-equilibrium region, small variations in the process parameters lead to significant changes in the results. To maximize the accuracy and reproducibility of the results, the applied time of extraction should be sufficient for reaching equilibrium. The influence of temperature is expressed through the changes to the partition (Equation 5.6) and diffusion coefficients of the analytes. From the kinetic point of view, diffusion rates grow with temperatures, increasing the mass transfer and reducing the time necessary for obtaining an equilibrium. From the thermodynamic point of view, the extraction is an exothermal process (when K_{fs}>1, as is the case for most analytes, ΔH>0 in Equation 5.6), and the transferred amounts decrease with increasing temperatures. An optimal temperature is a compromise between these two opposing effects. The addition of salt reduces the solubility and raises the volatility of the analytes, especially the polar ones, resulting in enhanced extraction rates. The theory behind the salting-out effects has been explained previously (Setchenow's theory, Equation 5.7) for LLE, and the general aspects are expected to be similar for SPME. For changes in pH, since only neutral species can be extracted by SPME, changes in $[H^+]$ and $[OH^-]$ influence the partition of dissociable species according to Equation 5.8. As pH decreases, increasing amounts of neutral acids can be adsorbed onto the coating, resulting in a better extraction sensitivity. The transfer of bases is enhanced at the opposite conditions.

$$K_{fs} = K_0 \cdot exp\left[-\frac{\Delta H}{R} \cdot \left(\frac{1}{T} - \frac{1}{T_0}\right)\right] \tag{5.6}$$

$$K_{fs} = K_0 \cdot e^{k_s \cdot C_s} = K_0 \cdot \left[1 + k_s \cdot C_s + \frac{(k_s \cdot C_s)^2}{2!} + \frac{(k_s \cdot C_s)^3}{3!} + \cdots\right] \tag{5.7}$$

$$K_{fs} = K_0 \cdot \frac{[H^+]}{K_a + [H^+]} \tag{5.8}$$

In this study, the following method parameters were studied: type of fiber (7 and 100 μm PDMS - poly(dimethylsiloxane), 65 μm PDMS/DVB - poly(dimethylsiloxane) divinylbenzene, and 85 μm PA - poly(acrylate), extraction method (HS - head space and. DI - direct immersion), extraction temperature (T_{ext} = 25 °C and 50 °C), extraction time (t_{ext} = 10 min and 20 min), pH (pH below 2, ≈6, and above 12), and salting out effect (±1). Utilization of SPME as a sample preparation technique is an excellent low-tech method resulting in an in-depth qualitative description of the biocrude's and the aqueous' phase compositions, which were more complex than previously reported in the literature (Figure 5.1).

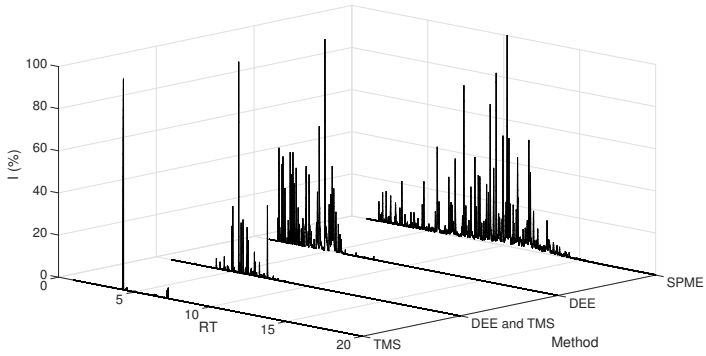

Fig. 5.1: Comparison between LLE results for the water phase (extraction with DEE and TMS) and the current SPME results (HS, 65 μm PDMS/DVB, T_{ext} = 50 °C, no salt, pH≈6, t_{ext} = 10 min). Reproduced from Paper B, Copyright (2016), with permission from Elsevier.

The four main classes of compounds identified in the current samples included low molecular weight compounds (LMW), cyclics (C), aromatics (A), and high molecular weight (HMW) products. The polarity divergence between the compositions of biocrude and the aqueous phase was easily observed. While the SPME extraction from the aqueous phase was adjustable with process parameters, the biocrude yielded similar results independently of the modifications to the extraction temperature, time, etc. Fiber type was the only factor affecting the transfer of the biocrude's constituents. The 65 μm PDMS/DVB fiber was the most efficient coating for both fractions. Optimal conditions for SPME extraction of WSO were achieved by HS at neutral pH, T_{ext} = 50 °C, and t_{ext} = 10 min.

3 Liquid chromatography-mass spectrometry

Due to the limitations of the standard analytical methods such as GC-MS and their requirements for analyte volatility and polarity, alternative analytical tools for characterization of organics in complex mixtures have been developed, e.g. liquid chromatography-mass spectrometry (LC-MS). Numerous instrument configurations of chromatographic columns, ion sources, ion analyzers, and detectors are available on the marked, and the right choice is a critical prerequisite for a successful analysis. The most common sources include electron ionization (EI), chemical ionization (CI), and field ionization (FI). Although they serve their purpose, specialized applications may require more sophisticated solutions, e.g. electrospray ionization (ESI), a soft ionization technique preventing decomposition of fragile, large organics. Another emerging technique for characterization of liquefaction (and similar) products include matrix-assisted laser desorption/ionization (MALDI) [31, 32]. Ion analyzers are also found in numerous variations, the most common being ion traps and quadrupole ion analyzers. For improved analysis of the liquefaction products, analyzers such as time of flight (TOF) [5] and FTICR [16, 33–38] were also shown to be useful.

The assessment of the products from liquefaction presented in this part was performed by application of liquid chromatography with electrospray ionization and a hybrid orbitrap-quadrupole mass spectrometric detection (LC-ESI-MS/MS), which includes a quadrupole precursor ion selection and an Orbitrap mass analyzer. The instrument is a state-of-the-art equipment combining superb separation of analytes, high resolution, mass accuracy, and sensitivity. The raw data were processed with Compound Discoverer^{TM} 2.0 software (Thermo Fisher Scientific, Switzerland). The applied workflow is shown in Figure 5.2. The analyzed samples were produced by liquefaction of a resin from a glass fiber reinforced composite (GFRC). The obtained results were of excellent quality, as was confirmed by closing the carbon balances in the aqueous phase and explaining a significant part of the oil fraction. The compounds identified in both phases represented a broad range of chemical species of varying volatility including acetone (highly volatile), isophorone (semi-volatile), and non-volatile (phthalic acid). The obtained quantification data were of high-quality thanks to the combination of the cutting-edge analytic methodology with verified quantification procedures. More details about the products follow in Chapter 9. The described methods can be used to identify and quantify a broad spectrum of chemical species with different polarity and volatility typical for the products from liquefaction of biomass.

4 Outlook

Analytics is a field often considered to be a mere tool for an assessment of a primary goal, be it characterization of the products from a conversion process, reporting the reaction rates, or conversion yields. More often than not, the applied

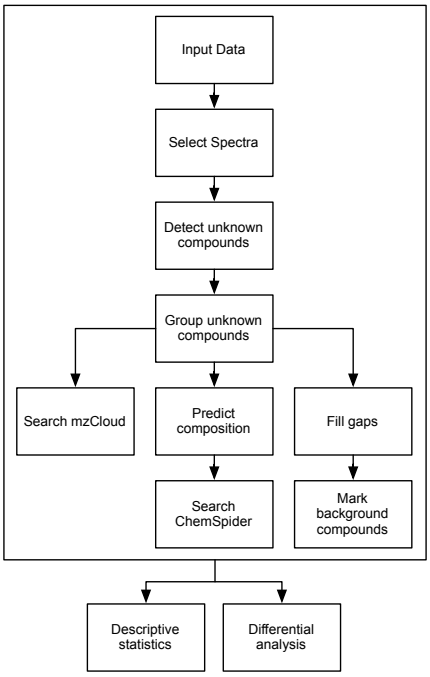

Fig. 5.2: Work flow used to process the obtained data in Compound Discoverer^{TM} 2.0 (Thermo Fisher Scientific Inc.). A standard method was applied except for the values of intensity threshold for precursors (10^5 counts), maximum shift alignment (0.1 min), mass tolerance (2.5 ppm). Reproduced from Paper E.

analytical methods are standard, not optimized for the purpose, techniques. As demonstrated here, optimizing analytical procedures and application of superior analytical equipment should be at the core of any scientific reporting. The field is severely underdeveloped, and yet, we can never actually exploit the results from the studies if we do not optimize the analytical procedures by which they were obtained. Lots of research is needed in order to accurately quantify the reaction products from the conversion and to finally be able to give a true description of the liquefaction process. Exploration of non-standard analytical tools is crucial for the continuous improvement of the characterization of the complex liquefaction products. The challenge of instrumental diversity lies in the lack of libraries and databases for identification purposes. A great deal of resources are available on-line in e.g. mzCloud [39] and ChemSpider [40]. However, those resources are limited compared to the NIST GC-MS mass spectral library.

References

[l] S. Yin, R. Dolan, M. Harris, and Z. Tan, "Subcritical hydrothermal liquefaction of cattle manure to bio-oil: Effects of conversion parameters on bio-oil yield and characterization of bio-oil," *Bioresour. Technol.*, vol. 101, no. 10, pp. 3657–3664, 2010.

[2] M. Tymchyshyn and C. C. Xu, "Liquefaction of bio-mass in hot-compressed water for the production of phenolic compounds," *Bioresource Technol.*, vol. 101, no. 7, pp. 2483–2490, 2010.

[3] S. Karagöz, T. Bhaskar, A. Muto, and Y. Sakata, "Comparative studies of oil compositions produced from sawdust, rice husk, lignin and cellulose by hydrothermal treatment," *Fuel*, vol. 84, no. 7, pp. 875–884, 2005.

[4] S. Karagöz, T. Bhaskar, A. Muto, Y. Sakata, T. Oshiki, and T. Kishimoto, "Low-temperature catalytic hydrothermal treatment of wood biomass: analysis of liquid products," *Chem. Eng. J.*, vol. 108, no. 1, pp. 127–137, 2005.

[5] S. R. Villadsen, L. Dithmer, R. Forsberg, J. Becker, A. Rudolf, S. B. Iversen, B. B. Iversen, and M. Glasius, "Development and application of chemical analysis methods for investigation of bio-oils and aqueous phase from hydrothermal liquefaction of biomass," *Energy Fuels*, vol. 26, no. 11, pp. 6988–6998, 2012.

[6] T. D. H. Nguyen, M. Maschietti, T. Belkheiri, L.-E. Åmand, H. Theliander, L. Vamling, L. Olausson, and S.-I. Andersson, "Catalytic depolymerisation and conversion of Kraft lignin into liquid products using near-critical water," *J. Supercrit. Fluids*, vol. 86, pp. 67–75, 2014.

[7] C. Xu and J. Lancaster, "Conversion of secondary pulp/paper sludge powder to liquid oil products for energy recovery by direct liquefaction in hot-compressed water," *Water Res.*, vol. 42, no. 6, pp. 1571–1582, 2008.

[8] Y. Qian, C. Zuo, J. Tan, and J. He, "Structural analysis of bio-oils from sub-and supercritical water liquefaction of woody biomass," *Energy*, vol. 32, no. 3, pp. 196–202, 2007.

[9] P. J. Valdez, J. G. Dickinson, and P. E. Savage, "Characterization of product fractions from hydrothermal liquefaction of Nannochloropsis sp. and the influence of solvents," *Energy Fuels*, vol. 25, no. 7, pp. 3235–3243, 2011.

[10] P. Sun, M. Heng, S.-H. Sun, and J. Chen, "Analysis of liquid and solid products from liquefaction of paulownia in hot-compressed water," *Energ. Convers. Manage.*, vol. 52, no. 2, pp. 924–933, 2011.

[11] Z. Shuping, W. Yulong, Y. Mingde, I. Kaleem, L. Chun, and J. Tong, "Production and characterization of bio-oil from hydrothermal liquefaction of microalgae Dunaliella tertiolecta cake," *Energy*, vol. 35, no. 12, pp. 5406–5411, 2010.

[12] M. Garcia-Perez, A. Chaala, H. Pakdel, D. Kretschmer, and C. Roy, "Characterization of bio-oils in chemical families," *Biomass Bioenergy*, vol. 31, no. 4, pp. 222–242, 2007.

[13] F. Taner, A. Eratik, and I. Ardic, "Identification of the compounds in the aqueous phases from liquefaction of lignocellulosics," *Fuel Process. Technol.*, vol. 86, no. 4, pp. 407–418, 2005.

[14] J. Li, C. Wang, and Z. Yang, "Production and separation of phenols from biomass-derived bio-petroleum," *J. Anal. Appl. Pyrolysis*, vol. 89, no. 2, pp. 218–224, 2010.

[15] X. Yuan, J. Wang, G. Zeng, H. Huang, X. Pei, H. Li, Z. Liu, and M. Cong, "Comparative studies of thermochemical liquefaction characteristics of microalgae using different organic solvents," *Energy*, vol. 36, no. 11, pp. 6406–6412, 2011.

[16] I. Leonardis, S. Chiaberge, T. Fiorani, S. Spera, E. Battistel, A. Bosetti, P. Cesti, S. Reale, and F. De Angelis, "Characterization of bio-oil from hydrothermal liquefaction of organic waste by NMR spectroscopy and FTICR mass spectrometry," *ChemSusChem*, vol. 6, no. 1, pp. 160–167, 2013.

[17] S. Chiaberge, I. Leonardis, T. Fiorani, P. Cesti, S. Reale, and F. D. Angelis, "Bio-oil from waste: A comprehensive analytical study by soft-ionization FTICR mass spectrometry," *Energy Fuels*, vol. 28, no. 3, pp. 2019–2026, 2014.

[18] T. T. Kekäläinen, T. Venäläinen, and J. Jänis, "Characterization of birch wood pyrolysis oils by ultrahigh-resolution FT-ICR mass spectrometry: Insights into thermochemical conversion," *Energy Fuels*, 2014.

[19] J. M. Jarvis, A. M. McKenna, R. N. Hilten, K. Das, R. P. Rodgers, and A. G. Marshall, "Characterization of pine pellet and peanut hull pyrolysis bio-oils by negative-ion electrospray ionization Fourier transform ion cyclotron resonance mass spectrometry," *Energy Fuels*, vol. 26, no. 6, pp. 3810–3815, 2012.

[20] L. A. Stanford, S. Kim, G. C. Klein, D. F. Smith, R. P. Rodgers, and A. G. Marshall, "Identification of water-soluble heavy crude oil organic-acids, bases, and neutrals by electrospray ionization and field desorption ionization Fourier transform ion cyclotron resonance mass spectrometry," *Environ. Sci. Technol.*, vol. 41, no. 8, pp. 2696–2702, 2007.

[21] A. Bridgwater, D. Meier, and D. Radlein, "An overview of fast pyrolysis of biomass," *Org. Geochem.*, vol. 30, no. 12, pp. 1479–1493, 1999.

[22] A. Kruse and A. Gawlik, "Biomass conversion in water at 330 - 410 °C and 30 - 50 MPa. Identification of key compounds for indicating different chemical reaction pathways," *Ind. Eng. Chem. Res.*, vol. 42, no. 2, pp. 267–279, 2003.

[23] P. Desbene, M. Essayegh, B. Desmazieres, and F. Villeneuve, "Analysis of biomass pyrolysis oils by a combination of various liquid chromatographic techniques and gas chromatography-mass spectrometry," *J. Chromatogr. A*, vol. 553, pp. 211–221, 1991.

[24] H. Pan, "Synthesis of polymers from organic solvent liquefied biomass: A review," *Renew. Sustainable Energy Rev.*, vol. 15, no. 7, pp. 3454–3463, 2011.

[25] K. Sipilä, E. Kuoppala, L. Fagernäs, and A. Oasmaa, "Characterization of biomass-based flash pyrolysis oils," *Biomass Bioenergy*, vol. 14, no. 2, pp. 103–113, 1998.

[26] J. Pawliszyn, *Handbook of solid phase microextraction.* Elsevier, 2011.

[27] H. Prosen and L. Zupančič-Kralj, "Solid-phase microextraction," *Trac-Trend. Anal. Chem.*, vol. 18, no. 4, pp. 272–282, 1999.

[28] S. Vichi, A. I. Castellote, L. Pizzale, L. S. Conte, S. Buxaderas, and E. López-Tamames, "Analysis of virgin olive oil volatile compounds by headspace solid-phase microextraction coupled to gas chromatography with mass spectrometric and flame ionization detection," *J. Chromatogr. A*, vol. 983, no. 1, pp. 19–33, 2003.

[29] J. C. Demyttenaere, C. Dagher, P. Sandra, S. Kallithraka, R. Verhé, and N. De Kimpe, "Flavour analysis of Greek white wine by solid-phase microextraction–capillary gas chromatography–mass spectrometry," *J. Chromatogr. A*, vol. 985, no. 1, pp. 233–246, 2003.

[30] J. Brulík, B. Vrana, M. Oravec, and Z. Šimek, "Determination of distribution coefficients of polycyclic aromatic nitrogen heterocycles using solid-phase microextraction," *Int. J. Environ. Anal. Chem.*, vol. 93, no. 5, pp. 511–527, 2013.

[31] T. Kanetake, M. Sasaki, and M. Goto, "Decomposition of a lignin model compound under hydrothermal conditions," *Chem. Eng. Technol*, vol. 30, no. 8, pp. 1113–1122, 2007.

[32] A. A. Herod, K. D. Bartle, and R. Kandiyoti, "Characterization of heavy hydrocarbons by chromatographic and mass spectrometric methods: An overview," *Energy Fuels*, vol. 21, no. 4, pp. 2176–2203, 2007.

[33] E. A. Smith, S. Park, A. T. Klein, and Y. J. Lee, "Bio-oil analysis using negative electrospray ionization: Comparative study of high-resolution mass spectrometers and phenolic versus sugaric components," *Energy Fuels*, vol. 26, no. 6, pp. 3796–3802, 2012.

[34] A. G. Marshall and R. P. Rodgers, "Petroleomics: The next grand challenge for chemical analysis," *Acc. Chem. Res.*, vol. 37, no. 1, pp. 53–59, 2004.

[35] T. M. Schaub, R. P. Rodgers, A. G. Marshall, K. Qian, L. A. Green, and W. N. Olmstead, "Speciation of aromatic compounds in petroleum refinery streams by continuous flow field desorption ionization FT-ICR mass spectrometry," *Energy Fuels*, vol. 19, no. 4, pp. 1566–1573, 2005.

[36] K. Qian, W. K. Robbins, C. A. Hughey, H. J. Cooper, R. P. Rodgers, and A. G. Marshall, "Resolution and identification of elemental compositions for more than 3000 crude acids in heavy petroleum by negative-ion microelectrospray high-field fourier transform ion cyclotron resonance mass spectrometry," *Energy Fuels*, vol. 15, no. 6, pp. 1505–1511, 2001.

[37] K. Qian, R. P. Rodgers, C. L. Hendrickson, M. R. Emmett, and A. G. Marshall, "Reading chemical fine print: Resolution and identification of 3000 nitrogen-containing aromatic compounds from a single electrospray ionization Fourier transform ion cyclotron resonance mass spectrum of heavy petroleum crude oil," *Energy Fuels*, vol. 15, no. 2, pp. 492–498, 2001.

[38] N. Sudasinghe, B. Dungan, P. Lammers, K. Albrecht, D. Elliott, R. Hallen, and T. Schaub, "High resolution FT-ICR mass spectral analysis of bio-oil and residual water soluble organics produced by hydrothermal liquefaction of the marine microalga Nannochloropsis salina," *Fuel*, vol. 119, pp. 47–56, 2014.

[39] HighChem Ltd., Bratislava, Slovakia, "mzCloud - Advanced Mass Spectral Database." https://www.mzcloud.org/, 2016. [Online].

[40] Royal Society of Chemistry, Thomas Graham House, Cambridge, UK, "Chemspider." http://www.chemspider.com/, 2016. [Online].

Chapter 6

Reactor

This chapter covers reactor design and experimental procedure developed as a part of the current work. The aim was to take full control over process parameters during liquefaction in a small scale batch reactor. The novelty of this work lies in the increased process control over heating rates, reaction times, and medium density. The reader is referred to Papers C and D for more details.

1 Background

The majority of liquefaction experiments are performed in small batch reactors. Such tests are straightforward and easy to implement, but they also suffer from numerous limitations such as long heating times and lack of proper pressure control. This results in uncertainties in reaction conditions, such as reaction time and medium density. Fast heating can be achieved in micro-reactors, which entails other practical challenges, such as small amounts of products and high variations in calculations of yields. The results from such studies often do not provide an accurate basis for developing continuous processes [1]. A solution to this challenge was first proposed by Modell et al. [2] and involved fast heating of a biomass slurry by injection into a pre-heated reaction medium. Although similar systems were described since by other authors since [3–5], the procedure has not gained significant popularity due to the associated additional economic costs of such systems. However, an accurate and reproducible assessment of liquefaction from batch experiments is a crucial step for developing and commercialization of continuous large-scale processes.

2 Cold-injection system

Figure 6.1 demonstrates the principle behind the cold injection reactor system designed specifically for hydrothermal liquefaction of biomass and build by SITEC-Sieber Engineering AG (Maur, Switzerland). The reactor (R1, 99 ml, Inconel 625)

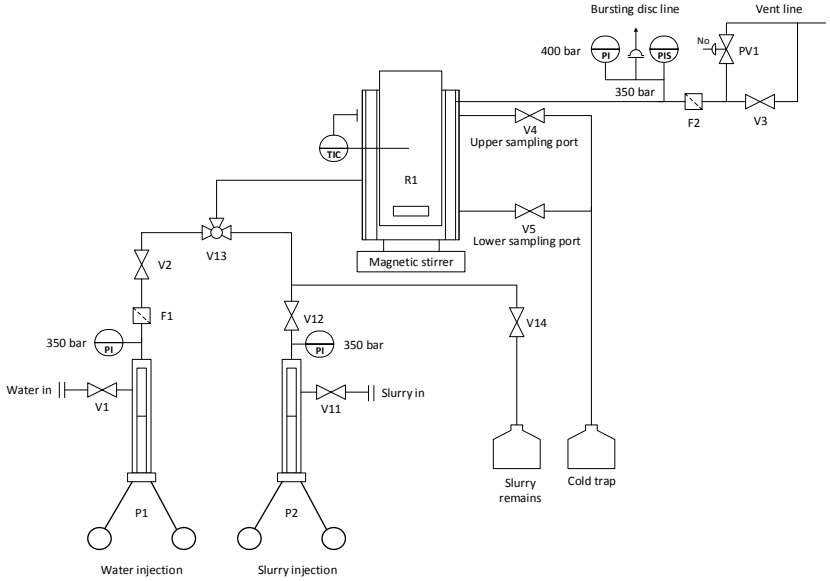

Fig. 6.1: P& I diagram for the applied batch/semi-batch reactor system. R1: reactor, P1, P2: hand-driven pumps; F1, F2: filters; V1-V5, V11-V12: closing valves; V13: three-way valve; PV1: pneumatic safety valve; PI: pressure indicator; PIS: pressure indicator switch; TIC: temperature indicator and controller. Reproduced from Paper C, Copyright (2017), with permission from Elsevier.

can operate up to 400 °C and 300 bar and is equipped with a heating shell wrapped in a high-temperature insulation jacket, heating plate, pressure gauge, and magnetic stirring. The innovative part of the system consists of two high-pressure syringe pumps (P1 and P2, capacity: 100 ml, revolution: 2 ml) connected to the reactor and used to inject the reaction medium (P1) and the biomass slurry (P2), and to control the pressure in the reactor by injection/withdrawal of infinitesimal amounts of water. In addition to that, the reactor is connected to two sampling ports, which are used for quenching of products (Figure 6.2).

In a typical run, an amount of reaction medium was injected through P1 or placed directly in the reactor through a top lid, purged with N_2, and heated to a preheating temperature (T_{PH}) slightly above the reaction temperature (T_R). The biomass slurry was then injected through P2 into the pre-heated and pre-pressurized reactor containing a two-phase vapour-liquid mixture of the reaction medium. The reaction temperature was obtained quickly since injection of the cold biomass slurry resulted in a temperature drop from T_{PH} close to T_R. The temperature drop was limited, as the heating of the slurry was fuelled by the condensation of the vapour in the reactor. Injection of biomass into a homogeneous mixture would have resulted in much more severe temperature drops. Any remaining temperature differences were equilibrated by the fast heating system. Pressure decreased in the first stages of

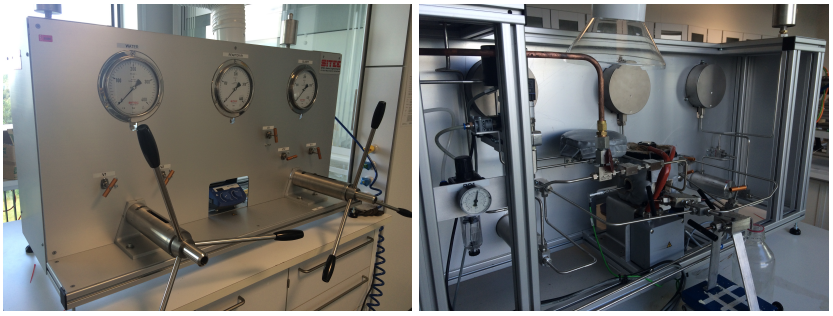

Fig. 6.2: Images of the applied batch/semi-batch reactor system.

the injection and then increased with rising content of liquid in the reactor. When necessary, the pressure was adjusted through P2. The procedure could be modified depending on the progress of each run, e.g. set points of temperature can be adapted to achieve certain conditions. After the reaction time, the reactor content was quenched in a cold-trap through the lower sampling port. The injection, residence, and product quenching times were approx. 3 - 5 min, 10 - 30 min, and 0.5 - 1 min, respectively.

Figure 6.3 shows the pressure and temperature profiles during a typical run. The used equipment and procedure allowed for fine control of reaction time and density of the reaction medium through the combination of fast heating of the biomass, pressure control, and products withdrawal/quenching. The density is important for controlling the reaction conditions, keeping the reaction medium in the liquid phase region, and with regard to the enthalpy penalties associated with reaction medium evaporation.

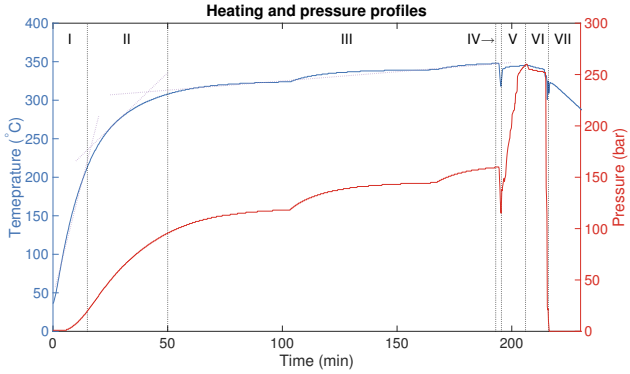

Fig. 6.3: Heating and pressure profiles for the SITEC setup. The regions of interest: I - III: different heating rates, IV - V: cold injection procedure, VI: reaction time, VII: cooling and depressurization. Reproduced from Paper D.

3 Outlook

Strict control of conditions is an absolute prerequisite for studying processes such as liquefaction, which depend on a multitude of parameters. Improvements to the described system could involve reduction of dead volume (approx. 5 ml) and further advancements in the reaction procedure, e.g. shortening the injection time and reduction of temperature fluctuations. In a typical run, the variations in temperature and pressure during the reaction time were ± 5 °C and ± 10 bar, respectively. However, the temperature and pressure values during the injection could vary between different runs. In the example shown on Figure 6.3, the reaction temperature was over-reached and then approached from the ”above”. Otherwise, the reaction temperature could have been achieved from "below" or right "on spot" with the set point.

References

[1] A. Kruse, T. Henningsen, A. Sinag, and J. Pfeiffer, “Biomass gasification in supercritical water: Influence of the dry matter content and the formation of phenols,” *Ind. Eng. Chem. Res.*, vol. 42, no. 16, pp. 3711–3717, 2003.

[2] M. Modell, “Gasification and liquefaction of forest products in supercritical water,” in *Fundamentals of Thermochemical Biomass Conversion*, pp. 95–119, Springer, 1985.

[3] H. Schmieder, J. Abeln, N. Boukis, E. Dinjus, A. Kruse, M. Kluth, G. Petrich, E. Sadri, and M. Schacht, “Hydrothermal gasification of biomass and organic wastes,” *J. Supercrit. Fluids*, vol. 17, no. 2, pp. 145–153, 2000.

[4] J. Barbier, N. Charon, N. Dupassieux, A. Loppinet-Serani, L. Mahé, J. Ponthus, M. Courtiade, A. Ducrozet, A. Fonverne, and F. Cansell, “Hydrothermal conversion of glucose in a batch reactor. A detailed study of an experimental key-parameter: The heating time,” *J. Supercrit. Fluids*, vol. 58, no. 1, pp. 114–120, 2011.

[5] J. Barbier, N. Charon, N. Dupassieux, A. Loppinet-Serani, L. Mahé, J. Ponthus, M. Courtiade, A. Ducrozet, A.-A. Quoineaud, and F. Cansell, “Hydrothermal conversion of lignin compounds. A detailed study of fragmentation and condensation reaction pathways,” *Biomass Bioenergy*, vol. 46, pp. 479–491, 2012.

Chapter 7

Conversion of lignin

This chapter focuses on catalyzed (K_2CO_3) hydrothermal conversion of Kraft lignin as a function of varying temperature (T = 280 - 350 °C) and phenol mass fraction (w_{Ph} = 0 - 9.7 wt.%) in the reaction mixture. The main aim of this work was to assess the role of phenol on the hydrothermal conversion of lignin, especially with regard to the production of value-added products, i.e. the biocrude and chemical building blocks. The novelty of this work lies in the utilization of a cutting-edge laboratory batch reactor encompassing fast biomass heating, pressure control, and product quenching for studies on the influence of phenol amounts on liquefaction. The reader is referred to Paper C for more details.

1 Background

1.1 Structure

Lignin in its natural form is a complex amorphous polymer of cross-linked phenyl propane units with a composition varying from species to species. As a biopolymer, lignin is unusual in its lack of defined or ordered structure, which can be roughly described as cross-linked p-hydroxyphenyl, guaiacyl, and syringyl phenylpropanoids formed from the p-coumaryl, coniferyl, and sinapyl alcohol precursors. The monolignol syringol is only found in hardwood. The role of lignin in plants is to cross-link the plant polysaccharides, provide mechanical strength and chemical resistivity to the cell walls and, by extension, to the plant as a whole. The most common chemical bonds in lignin include C-O (β-O-4) and C-C linkages (β-1 and β-β). Figure 7.1 shows the general structure of lignin [1].

Lignin is, next to cellulose and hemicellulose, the third bio-polymer making up the lignocellulosic biomass. Lignin constitutes 30 wt.% of the biomass on the mass basis and up to 40 wt.% on the energy basis [3]. Lignin is the second most abundant organic polymer on Earth, exceeded only by cellulose. No future biomass-based

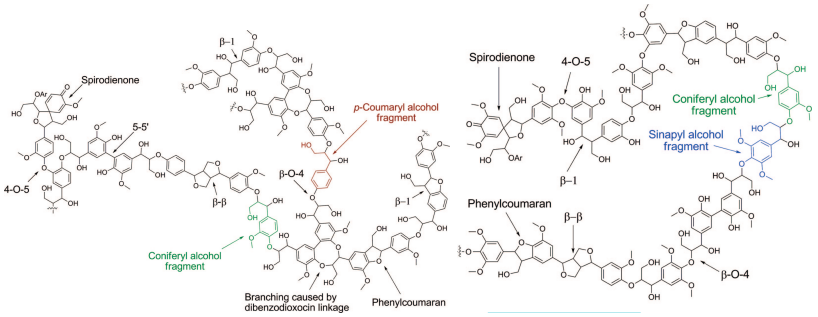

Fig. 7.1: Lignin structure. Reprinted with permission from [2], Copyright (2010), American Chemical Society.

biorefinery could ever claim sustainability without a reasonable lignin valorization. The largest source of lignin waste stream today is the paper industry, where the biopolymer is produced as a by-product of the pulping process. Significant amounts of lignin waste are also contained in dried distillers grains with solubles (DDGS) produced as a distillation by-product from brewers and ethanol plants. Most of the lignin produced today is used as an energy source for the manufacturing process from which it originates, e.g. burning of lignin provides the power for the pulping process. While this strategy makes use of a by-product and recovers energy at the same time, it does not realize the true potential of lignin. A limited amount of lignin is extracted from the pulping liquors for alternative purposes, e.g. production of chemicals (e.g. vanillin, dimethyl sulfoxide, xylitol), use as dispersants, textile dyes, additives in the oil industry, and as a dust suppressor for the roads [4]. Taking the aromatic structure of lignin into account, the compound could be a potential large-scale source of precursors for aromatic monomers for the chemical industry.

1.2 Recovery

Lignin found in the biomass is called proto-lignin. Different separations methods have been applied for the separation of lignocellulose into its building blocks by removal of the molecular glue, i.e. lignin. The tree most common processes are kraft, sulfite, and organosolv processes. The first two techniques involve the formation of a liquor product, which is a mixture of dissolved lignin residues, hemicellulose, and the inorganic chemicals used in the treatment. In the case of the organosolv process, lignin is dissolved in an organic solvent added NaOH. The typical approach for each of the streams includes concentration by evaporation of solvents and recovery of cooking chemicals involved in the process followed by burning. The three main commercial processes for separation of lignin from the black liquor include LignoBoost (Sweden) [5–7], LignoForce (Canada) [8], and SLRP (U.S.A) [9], each being chemically invasive procedure involving further modifications to the lignin structure. The lignin after the extraction, although still called lignin, technically speaking has little in common to the macromolecular proto-lignin found in living flora [2].

1.3 Conversion

Development of depolymerization procedures resulting in high yields of aromatic monomers would maximize the output from lignin and thus significantly improve biorefinery sustainability. Due to this enormous potential, lignin has been a long-standing focus of scientific studies in search of an efficient method for production of aromatics. While several bacteria and fungi have been observed to be able to metabolize lignin, commercial application of this approach is considered expensive and ineffective [10, 11].

The thermochemical platform for lignin deconstruction has been studied extensively during the latest 20 years, resulting in a broader understanding of lignin decomposition under the influence of chemicals, changing temperature, and pressure conditions. The main challenges facing the thermochemical routes involve the structure of the lignin itself, or more precisely the presence of inter-units C-C bonds in both the proto-lignin as well as the extracted lignin. Furthermore, the non-selective and oxidative nature of the reactions results in an erratic depolymerization into unstable intermediates that are dehydrated and condensed further into solid products. The reaction pathway responsible for this unwanted effect has been previously recognized as an attack of reactive benzylic side chain carbocations on electron rich aromatic rings in lignin [11–13].

As shown recently by Shuai et al. [11], biomass pretreatment with formaldehyde separates lignin from the polysaccharides and neutralizes the active carbocation sites, thus preventing the formation of C-C linkages and char production during thermal treatment. The combination of the pretreatment with hydrogenolysis resulted in monomeric yields in the range 47 - 78 %, which is a significant improvement over the commonly achieved yields of 5 - 27 %. However, the method can only be applied on lignin from biomass, and will not work for e.g. the waste Kraft lignin from the pulping process, in which the reactive sites have already been stabilized by increasing the density of C-C bonds. For those raw feeds, alternative valorization routes must be applied.

Hydrothermal liquefaction in near- and supercritical water has been studied widely for the purpose. According to the results, liquefaction of lignin occurs through hydrolysis and alkylation yielding low molecular weight compounds that can by cross-linked into high molecular weight products resulting in solids [14]. Most of the lignin liquefaction studies use phenol as an additive or co-solvent, which is expected to increase solubilization of lignin in addition to its role as a scavenger and capping agent of unstable intermediates with reactive sites prone to repolymerization [15]. According to Nguyen et al. [5, 6] the primary products from the liquefaction include alkylphenols, guaiacols, catechols, and methoxybenzenes, all of which could be used as platform chemicals for the production of a broad spectrum of aromatics (Figure 7.2).

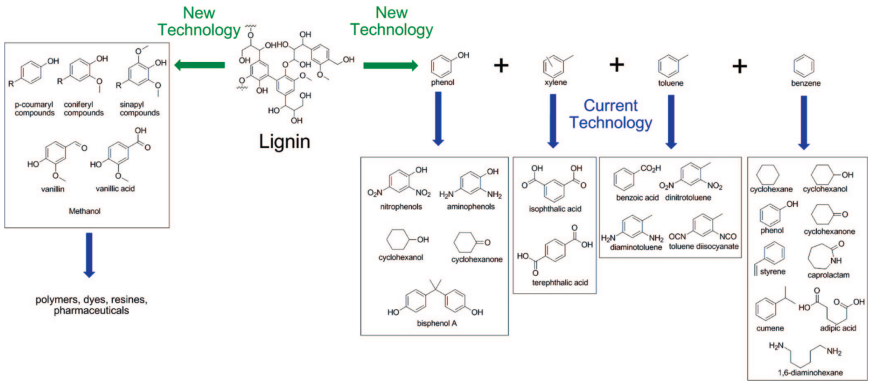

Fig. 7.2: Lignin structure. Reprinted from Ref. [2], Copyright (2010), with permission from American Chemical Society.

2 Production of monomers

The majority of the compounds identified among the conversion products obtained in the current work could be classified into six main groups of compounds: methoxybenzenes (M), guaiacols (G), catechols (C), alkylphenols (A), anisolic/phenolic dimers (APD), and 2-ring non-condensed aromatics (2-NCAR). Compounds such as guaiacols and catechols were derived directly from the lignin structure by hydrolysis of ether bonds attached to phenolic benzene rings [14]. Alkylphenols and methoxybenzenes were produced by reactions of phenol with small molecular weight compounds such as propanol as reported previously [16]. The formation of dimers was previously attributed to the reactions of phenol and reaction intermediates with formaldehyde and other reactive species [14]. The overall yields of monomers ranged between 7 - 11 %, varying with temperature and the phenol mass fraction (Figures 7.3).

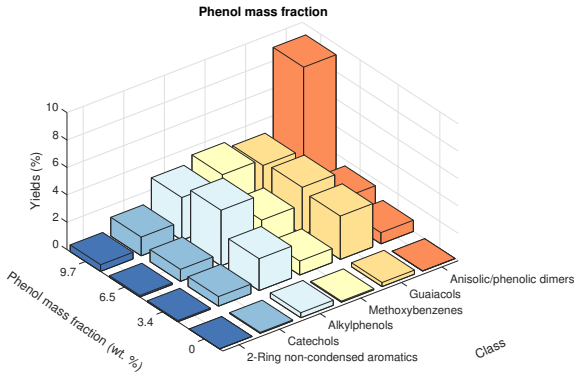

Fig. 7.3: Overall yields of the main chemical families as a function of phenol mass fraction (T = 300 °C). Reproduced from Paper C, Copyright (2017), with permission from Elsevier.

As can be seen in Figure 7.3, in the absence of phenol, the production of monomers and dimers was largely non-existent and insolubles, which were formed due to cross-linking of reactive intermediates, were the major part of the reaction products. The addition of phenol up to 6.5 wt.% to the reacting system led to a substantial increase in the obtained yields of chemicals. At even higher mass fractions of phenol, the monomers yields remained virtually unchanged, but the amounts of anisolic/phenolic dimers increased drastically, which indicates the predominance of reactions of phenol and 1-ring aromatic monomers.

3 Outlook

In order to make a sustainable valorization of lignin a reality, specific and selective pathways must be developed to convert it into high-value products, i.e. platform chemicals and building blocks. The conversion must be further optimized and remodeled to maximize the yields of the monomeric aromatics and decrease the formation of solids. This could be achieved by a combination of pretreatments of the extracted lignin such as described by Shuai et al. [11] with liquefaction outlined in this study. There is no doubt that this will be one of many researching focus areas for the discovery of methods for production of aromatics from lignin.

References

[1] M. P. Pandey and C. S. Kim, "Lignin depolymerization and conversion: A review of thermochemical methods," *Chem. Eng. Technol.*, vol. 34, no. 1, pp. 29–41, 2011.

[2] J. Zakzeski, P. C. A. Bruijnincx, A. L. Jongerius, and B. M. Weckhuysen, "The catalytic valorization of lignin for the production of renewable chemicals," *Chem. Rev.*, vol. 110, no. 6, pp. 3552–3599, 2010.

[3] J. Holladay, J. Bozell, J. White, and D. Johnson, "Top value-added chemicals from biomass. Volume II–Results of screening for potential candidates from biorefinery lignin," tech. rep., 2007.

[4] A. J. Ragauskas, G. T. Beckham, M. J. Biddy, R. Chandra, F. Chen, M. F. Davis, B. H. Davison, R. A. Dixon, P. Gilna, M. Keller, P. Langan, A. K. Naskar, J. N. Saddler, T. J. Tschaplinski, G. A. Tuskan, and C. E. Wyman, "Lignin valorization: Improving lignin processing in the biorefinery," *Science*, vol. 344, no. 6185, p. 1246843, 2014.

[5] T. D. H. Nguyen, M. Maschietti, T. Belkheiri, L.-E. Åmand, H. Theliander, L. Vamling, L. Olausson, and S.-I. Andersson, "Catalytic depolymerisation and conversion of Kraft lignin into liquid products using near-critical water," *J. Supercrit. Fluids*, vol. 86, pp. 67–75, 2014.

[6] T. D. H. Nguyen, M. Maschietti, L.-E. Åmand, L. Vamling, L. Olausson, S.-I. Andersson, and H. Theliander, "The effect of temperature on the catalytic conversion of Kraft lignin using near-critical water," *Bioresource Technol.*, vol. 170, pp. 196–203, 2014.

[7] M. Maschietti, T. D. H. Nguyen, T. Belkheiri, L.-E. Åmand, H. Theliander, L. Vamling, L. Olausson, and S.-I. Andersson, "Catalytic hydrothermal conversion of LignoBoost Kraft lignin for the production of bio-oil and aromatic chemicals," in *Proceedings of the International Chemical Recovery Conference*, vol. 2, pp. 252–261, 2014.

[8] L. Kouisni, P. Holt-Hindle, K. Maki, and M. Paleologou, "The lignoforce system: a new process for the production of high-quality lignin from black liquor," *J. Sci. Technol. For. Prod. Processes*, vol. 2, no. 4, pp. 6–10, 2012.

[9] M. Lake and J. Blackburn, "SLRP–An innovative lignin-recovery technology," *Cellul. Chem. Technol.*, vol. 48, no. 9-10, pp. 799–804, 2014.

[10] M. E. Brown and M. C. Chang, "Exploring bacterial lignin degradation," *Curr. Opin. Chem. Biol.*, vol. 19, pp. 1–7, 2014.

[11] L. Shuai, M. T. Amiri, Y. M. Questell-Santiago, F. Héroguel, Y. Li, H. Kim, R. Meilan, C. Chapple, J. Ralph, and J. S. Luterbacher, "Formaldehyde stabilization facilitates lignin monomer production during biomass depolymerization," *Science*, vol. 354, no. 6310, pp. 329–333, 2016.

[12] K. Shimada, S. Hosoya, and T. Ikeda, "Condensation reactions of softwood and hardwood lignin model compounds under organic acid cooking conditions," *J. Wood Chem. Technol.*, vol. 17, no. 1-2, pp. 57–72, 1997.

[13] M. R. Sturgeon, S. Kim, K. Lawrence, R. S. Paton, S. C. Chmely, M. Nimlos, T. D. Foust, and G. T. Beckham, "A mechanistic investigation of acid-catalyzed cleavage of aryl-ether linkages: Implications for lignin depolymerization in acidic environments," *ACS Sustain. Chem. Eng.*, vol. 2, no. 3, pp. 472–485, 2013.

[14] M. Saisu, T. Sato, M. Watanabe, T. Adschiri, and K. Arai, "Conversion of lignin with supercritical water-phenol mixtures," *Energy Fuels*, vol. 17, no. 4, pp. 922–928, 2003.

[15] Z. Fang, T. Sato, R. L. Smith, H. Inomata, K. Arai, and J. A. Kozinski, "Reaction chemistry and phase behavior of lignin in high-temperature and supercritical water," *Bioresour. Technol.*, vol. 99, no. 9, pp. 3424–3430, 2008.

[16] T. Sato, G. Sekiguchi, T. Adschiri, and K. Arai, "Non-catalytic and selective alkylation of phenol with propan-2-ol in supercritical water," *Chem. Commun.*, no. 17, pp. 1566–1567, 2001.

Chapter 8

Conversion of lignocellulose

This chapter focuses on catalyzed (K_2CO_3) hydrothermal conversion of *Fallopia japonica*, an invasive plant species, in near-critical water as a function of varying temperature (T = 280 - 320 °C) and in the presence of co-solvents of different polarity (acetone and tetralin). The aim was to elaborate on the shifts in reaction mechanisms due to the presence of these additives and to understand their exact function. The novelty of this work lies in the utilization of a new feed, comparing two co-solvents of different polarity, and the use of advanced statistical tools for analysis of the results. The reader is referred to Paper D for more details.

1 Background

1.1 Structure

Despite its complexity, over 95 % of lignocellulosic biomass is build from 8 monomeric building blocks that can be classified as C5 sugars (glucose, mannose, and galactose), C5 sugars (xylose and arabinose), and the primary lignin building blocks (p-coumaryl, coniferyl, and sinapyl alcohols). The schematic structure of biomass is depicted in Figure 8.1.

Cellulose is a linear biopolymer of glucose units bound by β-1,4-glycosidic bonds. Due to its structure and crystallinity, cellulose is difficult to depolymerize under normal conditions and without a catalyst. Hemicellulose is much less crystalline than cellulose and it consists of shorter chains of C5 sugars. Lignin, as described in the previous chapter, is an amorphous structure of phenyl propane units bound together by both C-O as well as C-C bonds. All the biopolymers in lignocellulose represent 75 - 98 % of green plants. The content of each biopolymer, and even its composition, varies widely among different types of plants, e.g. syringol units are normally only present in softwood; hardwood contains less lignin than softwood (23 % vs. 30 %); grasses contain the highest percentage of hemicellulose (37 % vs. 20 -

26 % in other biomass types), the highest percentage of inorganics (6 % vs. 1 %), and the lowest amounts of lignin (17 % vs. 23 - 30 %).

The composition of biomass is one of the most significant factors influencing the output of liquefaction, and even within the field of lignocellulose liquefaction, significant differences may occur, due to small, but crucial, differences in the compositions of the utilized biomass. Due to the doubts about the sustainability of utilization of certain types of biomass including trees, the focus has been shifted towards residual lignocellulosic biomass, e.g. residual forest biomass. Plants such as *Fallopia japnica* are non-indigenous and environmentally malign weeds, that could be turned from an ecological burden into a useful material. *Fallopia japonica* is native to East Asia, but is also emerging in Europe and North America.

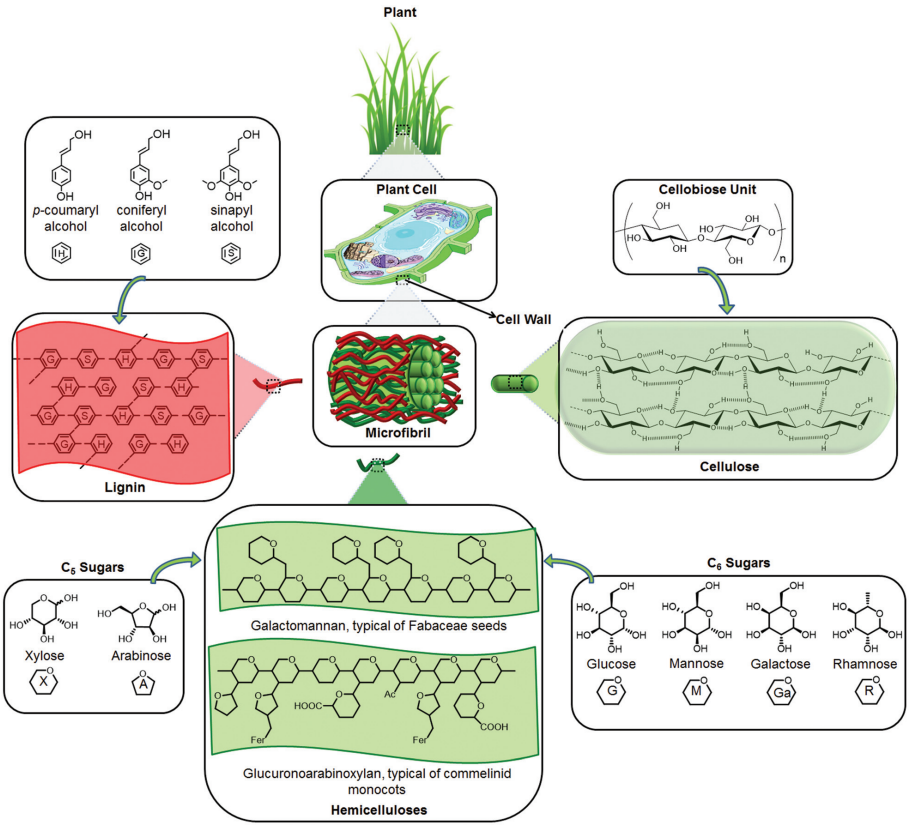

Fig. 8.1: Lignocellulosic biomass structure. Reproduced from [1], Copyright (2015), with permission from The Royal Society of Chemistry.

1.2 Conversion

Numerous studies have focused on liquefaction of both lignocellulose [2, 3], the most abundant raw material in agriculture and forestry sectors worldwide [4], as well as its building blocks [5–10], most commonly glucose. Figure 8.2 summarizes the reaction pathways of glucose during hydrothermal treament in near- and supercritical water. The mechanisms are strongly dependent on the applied reaction conditions, especially the temperature and the presence of a catalyst. The two most important reaction pathways include retro-aldol condensation and dehydration, resulting in low molecular weight compounds and furfurals, respectively. Furfurals can be then dehydrated into phenols [11, 12].

Conversion of complex biomass types gives much more complex results. Carrier et al. [13] studied the reaction products from a number of biopolymers (lignin, holocellulose, and cellulose) and compared it with liquefaction of a real-life lignocellulosic feed (fern). The main products included: aromatic derivatives such as benzene, guaiacol, and phenol from lignin; cyclopentanone and cyclopentenone derivatives from hemicellulose; and furfurals from cellulose. It was interesting that conversion of the lignocellulosic feed did not yield all the corresponding products but was dominated by the cyclics (cyclopentanone and cyclopentenone) and aromatics (phenols and guaiacols). Most notable was the absence of furfural indicating a chemical synergy between hemicellulose and cellulose leading to shifts in reaction pathways.

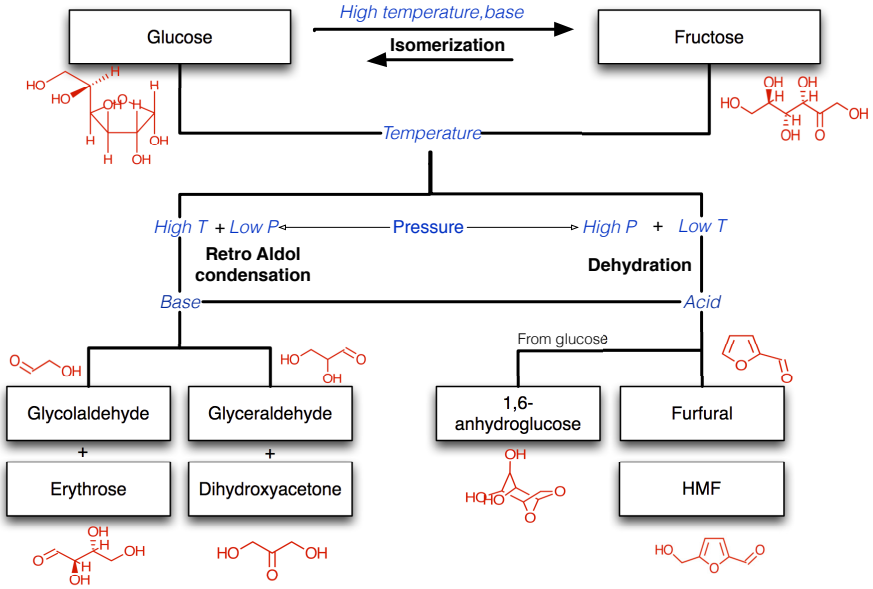

Fig. 8.2: Pathways for conversion of glucose during hydrothermal treatment. Source: [14].

2 Influence of co-solvents

The general patterns in reaction pathways behind the liquefaction of *Fallopia japnica* were in agreement with previously reported liquefaction results for lignocellulosic biomass. Four major groups of compounds were identified among the products: low molecular weight aliphatics (LMW), cyclic carbonyl compounds (C), aromatics (A), and high molecular weight (HMW) compounds. While LMW compounds comprised the smallest part of the products (0.5 - 1.1 %), the aromatics constituted the largest part (33 - 69 %). The cyclics (8 - 23 %) and the high molecular weight compounds (7 - 26 %) accounted for the rest. LMW aldehydes, ketones, alcohols, and acids, were produced through direct retro-aldol condensation of sugars. Under a variety of reaction conditions, those compounds were, in addition to the depolymerization of lignin, also the source of aromatics through aldol- or Michael condensations, cyclization, dehydration, and dehydrogenation [15, 16]. Cyclics identified in this work originated from dehydration of hemicellulose to furfural followed by rearrangements. Condensation and cyclization of intermediates lead to the formation of aromatic compounds. HMW were formed due to recombination of the reactive intermediates and were precursors of char as a consequence of uncontrolled dehydration. The reaction pathways behind liquefaction of lignocellulosic biomass are summarized in Figure 8.3.

The reaction pathways behind liquefaction of *Falopia* could be adjusted by regulation of the reaction temperature as well as the presence of co-solvents. The final result of liquefaction is always a compromise between fragmentation and recombination reactions under certain process conditions. The aim of co-solvent addition was to stabilize the reaction mixture and to enhance the production of monomeric building blocks instead of high molecular weight products ultimately leading to char. While similar tendencies were noted for both co-solvents, only for tetralin could the trends be confirmed statistically. In general, the presence of the non-polar co-solvent resulted in enhanced production of aromatics (enhanced solubilization of lignin and aromatization of glucose) and LMW compounds (retro-aldol condensation). In the absence of co-solvents, the formation of cyclics and repolymerization of HMW leading to solids were of significance. Among the water insoluble products (WIO), the primary constituents included alkanes and alkenes of varying chain length, semi-polar aromatics, and polymerized structures.

3 Outlook

A significant part of the reaction products obtained from liquefaction of *Fallopia* were the aromatics, which could also be used as a source of the chemical building blocks, especially by liquefaction in the presence of co-solvents. Other groups of chemical classes were either produced in small amounts (LMW) or should be avoided as a precursor of biochar (HMW). The cyclics such as cyclopentanone are emerging chemical raw materials used widely as organics solvents and building

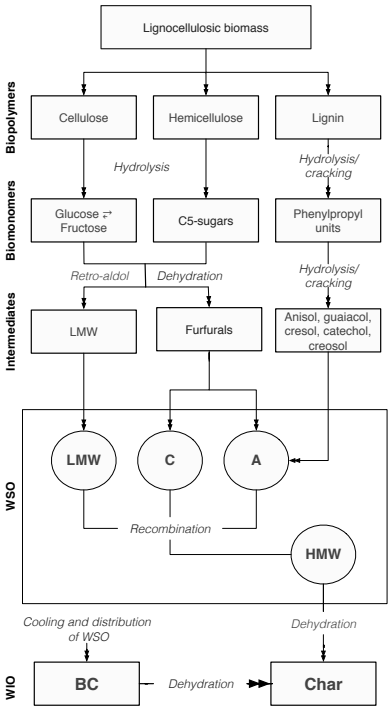

Fig. 8.3: Reaction routes behind HTL of lignocellulose biomass.

blocks for a variety of high-value products, e.g. drugs and fragrances [17, 18] as well as fuel precursors [19]. Production of WIO was poor, so production of value-added chemicals should be the focus of *Fallopia* conversion under the described process conditions. In addition to that, longer reaction times should be explored and studied toward the formation of biofuels, in addition of chemicals.

References

[1] F. H. Isikgor and C. R. Becer, "Lignocellulosic biomass: a sustainable platform for the production of bio-based chemicals and polymers," *Polym. Chem.*, vol. 6, no. 25, pp. 4497–4559, 2015.

[2] S. S. Toor, L. Rosendahl, and A. Rudolf, "Hydrothermal liquefaction of biomass: a review of subcritical water technologies," *Energy*, vol. 36, no. 5, pp. 2328–2342, 2011.

[3] J. Akhtar and N. A. S. Amin, "A review on process conditions for optimum bio-oil yield in hydrothermal liquefaction of biomass," *Renew. Sustainable Energy Rev.*, vol. 15, no. 3, pp. 1615–1624, 2011.

[4] A. J. Ragauskas, C. K. Williams, B. H. Davison, G. Britovsek, J. Cairney, C. A. Eckert, W. J. Frederick, J. P. Hallett, D. J. Leak, and C. L. Liotta, "The path forward for biofuels and biomaterials," *Science*, vol. 311, no. 5760, pp. 484–489, 2006.

[5] T. Minowa, Z. Fang, T. Ogi, and G. Várhegyi, "Decomposition of cellulose and glucose in hot-compressed water under catalyst-free conditions," *J. Chem. Eng. Jpn.*, vol. 31, no. 1, pp. 131–134, 1998.

[6] W. S. Mok, M. J. Antal Jr, and G. Varhegyi, "Productive and parasitic pathways in dilute acid-catalyzed hydrolysis of cellulose," *Ind. Eng. Chem. Res.*, vol. 31, no. 1, pp. 94–100, 1992.

[7] M. Sasaki, B. Kabyemela, R. Malaluan, S. Hirose, N. Takeda, T. Adschiri, and K. Arai, "Cellulose hydrolysis in subcritical and supercritical water," *J. Supercrit. Fluids*, vol. 13, no. 1, pp. 261–268, 1998.

[8] W. Shu-Lai Mok and M. Antal, "Uncatalyzed solvolysis of whole biomass hemicellulose by hot compressed liquid water," *Ind. Eng. Chem. Res.*, vol. 31, no. 4, pp. 1157–1161, 1992.

[9] S. E. Jacobsen and C. E. Wyman, "Xylose monomer and oligomer yields for uncatalyzed hydrolysis of sugarcane bagasse hemicellulose at varying solids concentration," *Ind. Eng. Chem. Res.*, vol. 41, no. 6, pp. 1454–1461, 2002.

[10] T. D. H. Nguyen, M. Maschietti, L.-E. Åmand, L. Vamling, L. Olausson, S.-I. Andersson, and H. Theliander, "The effect of temperature on the catalytic conversion of Kraft lignin using near-critical water," *Bioresource Technol.*, vol. 170, pp. 196–203, 2014.

[11] A. A. Peterson, F. Vogel, R. P. Lachance, M. Fröling, M. J. Antal Jr, and J. W. Tester, "Thermochemical biofuel production in hydrothermal media: A review of sub-and supercritical water technologies," *Energy Environ. Sci.*, vol. 1, no. 1, pp. 32–65, 2008.

[12] M. Watanabe, Y. Aizawa, T. Iida, T. M. Aida, C. Levy, K. Sue, and H. Inomata, "Glucose reactions with acid and base catalysts in hot compressed water at 473 vk," *Carbohydr. Res.*, vol. 340, no. 12, pp. 1925–1930, 2005.

[13] M. Carrier, A. Loppinet-Serani, C. Absalon, C. Aymonier, and M. Mench, "Degradation pathways of holocellulose, lignin and α-cellulose from Pteris vittata fronds in sub-and super critical conditions," *Biomass Bioenergy*, vol. 43, pp. 65–71, 2012.

[14] A. Kruse, A. Krupka, V. Schwarzkopf, C. Gamard, and T. Henningsen, "Influence of proteins on the hydrothermal gasification and liquefaction of biomass. 1. Comparison of different feedstocks," *Ind. Eng. Chem. Res.*, vol. 44, no. 9, pp. 3013–3020, 2005.

[15] J. Russell, R. Miller, and P. Molton, "Formation of aromatic compounds from condensation reactions of cellulose degradation products," *Biomass*, vol. 3, no. 1, pp. 43–57, 1983.

[16] M. Balat, "Mechanisms of thermochemical biomass conversion processes. Part 3: Reactions of liquefaction," *Energ. Source. Part A*, vol. 30, no. 7, pp. 649–659, 2008.

[17] X.-L. Li, J. Deng, J. Shi, T. Pan, C.-G. Yu, H.-J. Xu, and Y. Fu, "Selective conversion of furfural to cyclopentanone or cyclopentanol using different preparation methods of Cu–Co catalysts," *Green Chem.*, vol. 17, no. 2, pp. 1038–1046, 2015.

[18] J. Guo, G. Xu, Z. Han, Y. Zhang, Y. Fu, and Q. Guo, "Selective conversion of furfural to cyclopentanone with CuZnAl catalysts," *ACS Sustain. Chem. Eng.*, vol. 2, no. 10, pp. 2259–2266, 2014.

[19] M. Hronec, K. Fulajtárova, T. Liptaj, M. Štolcová, N. Prónayová, and T. Soták, "Cyclopentanone: A raw material for production of C15 and C17 fuel precursors," *Biomass Bioenergy*, vol. 63, pp. 291–299, 2014.

Chapter 9

Conversion of polyester resin

This chapter covers production of value-added chemicals by catalyzed (KOH) solvothermal (T = 275 - 350 °C) liquefaction of polyester-based resin material from glass fiber reinforced composites (GFRC) in 50/50 vol.% water/acetone reaction mixtures. The main aim of this work was to characterize the products from the conversion and to assess the material's and method's potential for production of chemicals. The novelty lies in the utilization of state-of-the-art analytical equipment for analysis of the non-volatile and semi-volatile compounds from the conversion. The reader is referred to Paper E for more details.

1 Background

Waste biomass is a promising resource for production of value-added products, and so are all types of garbage materials. They are generated in large amounts, and their utilization turns an environmental burden into value. Plastic is an excellent example of such a resource. Only in 2015, 322 million tons of polymer materials were created [1]. Since most of the plastic is packaging, which is likely to be discarded within the year of its synthesis, it results in an enormous pollution. Diverse recycling methods have been developed to fight this issue, and one of the most promising ones is a liquefaction-based treatment in near- and supercritical fluids (typically water and alcohols) for recovery of the monomers. This has been applied successfully for a number of plastics and was shown to be challenging for other types [2]. The latter group includes composite materials consisting of an organic resin reinforced with fibers (e.g. fiberglass) and fillers. In contrast to thermoplastics such as polyethylene terephthalate (PET), thermoset resin matrix of GFRC do not consist of tidy repeating polymer units, but of chains cross-linked into an amorphous structure. GFRC are strong, lightweight materials used in numerous applications, especially in transportation, construction, and oil & gas industries [3].

2 Value-added chemicals

A recent study by Sokoli et al. [4] showed that GFRC materials can be chemically recycled by the recovery of the fibers combined with the production of a high heating value biocrude. However, to entirely close the loop on the polymer life cycle and maximize the sustainability of the process, the products must be assessed as a source to value-added chemicals [5]. The only difference between liquefaction of biomass and plastics lies in the relative simplicity of the polymer feed. Utilization of organic solvents instead of pure water enables a reduction in reaction temperature, which, besides decreasing the energy required for conversion, also serves to protect the fibers. In addition to that, organic solvents are expected to increase the flowability of the reaction products. The resin used in this study was a styrene cross-linked polymer of unsaturated polyester (UP) chains polymerized from two types of dibasic acids (phthalic and maleic acids) and a polyhydric alcohol (propylene glycol). The principle behind the curing is shown in Figure 9.1.

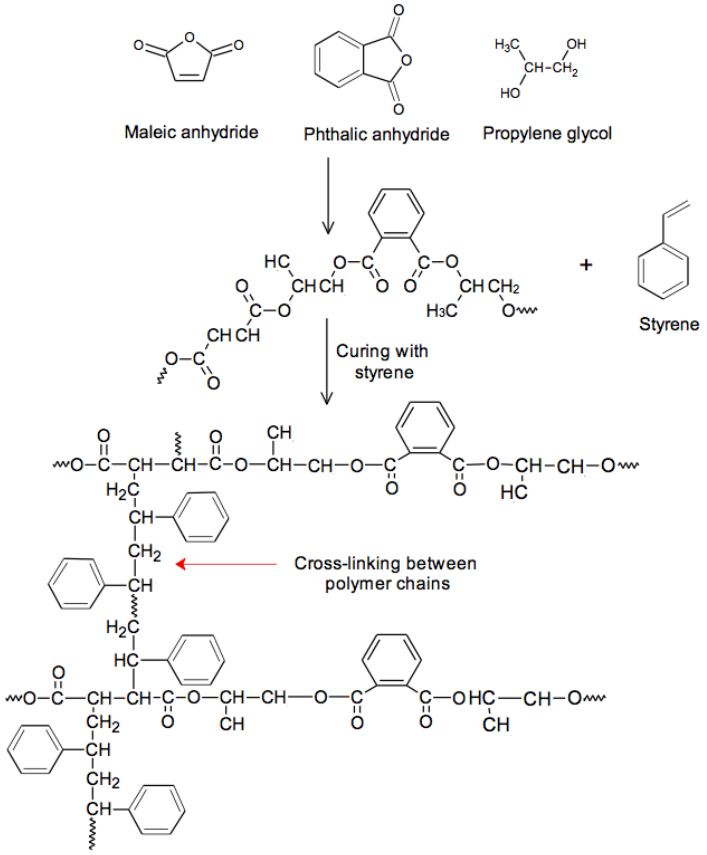

Fig. 9.1: Cross-linking of unsaturated polyester resin. Reproduced with permission from Ref. [6].

The conversion procedure was described in detail by Sokoli et al. [4]. In this study, we focused on characterization and quantification of the liquid products from the process to assess its potential as a source of value-added chemicals. In light of the growing demand and mounting legislative pressure preventing land-filling, methods for characterization of the products from chemical recycling and recovery of valuable chemicals from GFRC must be developed. According to the results of this study, reaction products from the conversion of the polyester resin were either the monomers from the polyester chain or secondary reaction products. Also, those two groups were separated along their polarity in an aqueous and an oil fraction. The identified monomers included phthalic acid ($[PHTHA]_{max}$ = 39 g/L) and dipropylene glycol ($[DPG]_{max}$ = 17 g/L)). The application of the analytic methodology described in Chapter 5 with verified quantification resulted in an explanation of nearly 100 % of the organic carbon in the aqueous phase (Figure 9.2).

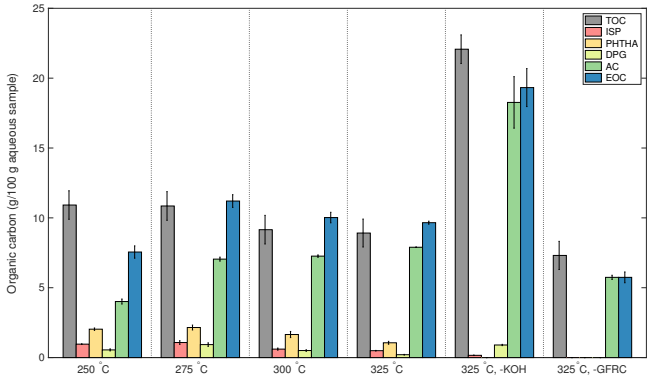

Fig. 9.2: Carbon content present in the aqueous phase and the fractions of carbon explained by the quantification of individual compounds. EOC - explained organic carbon. Groups 1 - 4 (250 - 325 °C) represent runs with GFRC, AC, and KOH. Run 325 °C, -KOH was performed with GFRC and AC (without KOH). Run 325 °C, -GFRC was performed with AC and KOH (without GFRC). Reproduced from Paper E.

In addition to the hydrolyzable building blocks, which could be reused directly and were found exclusively in the aqueous phase, the second group of chemicals was identified as secondary reaction products including isophorone ($[ISP]_{max}$ = 300 g/L), dihydroisophorone ($[DHISP]_{max}$ = 90 g/L), and 3,3,6,8-tetramethyl-1-tetralone ($[TMTL]_{max}$ = 500 g/L). While minor amounts of these compounds were found in the aqueous phase, they completely dominated the content of the oil fraction. Self-condensation of acetone through the competitive paths of addition and dehydration was identified as the origin of these compounds (Figure 9.3). The yields of both the monomers as well as the secondary reaction products decreased with reaction temperature.

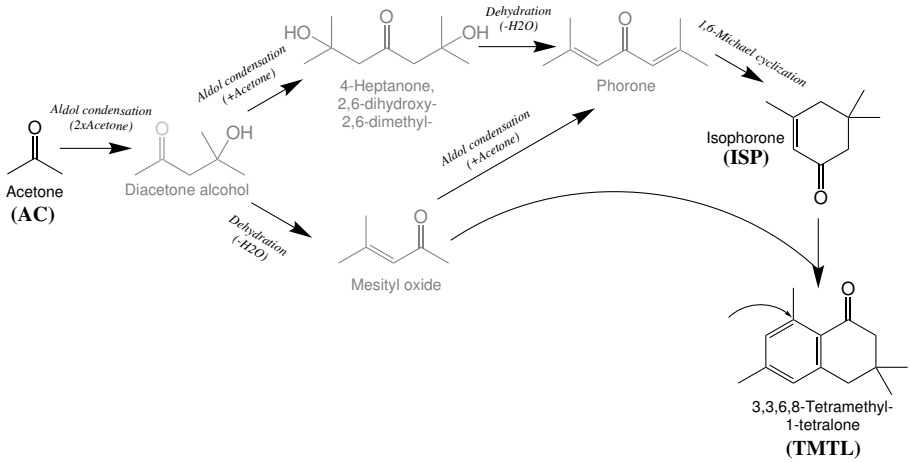

Fig. 9.3: Reaction pathways for acetone self-condensation leading to formation of isophorone and 3,3,6,8-tetramethyl-1-tetralone [7]. The grayed out compounds represent the reaction intermediates not identified in this study. Reproduced from Paper E.

3 Outlook

With increasing amounts of plastic waste in general and composite materials in particular, methods such as the presented solvothermal liquefaction of polymers gather more and more attention. The approach described in the current work results in three separate value-added products streams: fiberglass, oil for heating purposes as well as the source of valuable chemicals and monomers. The conversion of acetone into ISP, DHISP, TMTL, and the subsequent loss of the co-solvent is not disconcerting at all. It represents an additional value chain from the process. Acetone self-condensation takes usually place high temperature and pressure, and in the presence of both homogeneous as well as heterogeneous catalysts. The reaction products is a mixture of diacetone alcohol, mesityl oxide, phorone, mesitylene, isophorone and 3,5-xylenol and still, numerous other products are possible. Solvothermal liquefaction in the presence of KOH results in high yields of the final product TMTL. In the absence of the catalyst, the reaction takes place anyway to a certain extent, but it leads to ISP. Dihydroisophorone has been identified for the first time as a by-product of this pathway. Incorporation of liquefaction into the modern biorefinery concept would make it possible to valorize GFRC along with biomass waste streams.

References

[1] Plastics Europe, "World Plastic Production 1950–2015." https://committee.iso.org, 2016. [Online].

[2] M. Goto, "Chemical recycling of plastics using sub-and supercritical fluids," *J. Supercrit. Fluids*, vol. 47, no. 3, pp. 500–507, 2009.

[3] H. U. Sokoli, M. E. Simonsen, R. P. Nielsen, J. Henriksen, M. L. Madsen, N. H. Pedersen, and E. G. Søgaard, "Characterization of the liquid products from hydrolyzed epoxy and polyester resin composites using solid-phase microextraction and recovery of the monomer phthalic acid," *Ind. Eng. Chem. Res.*, vol. 55, no. 34, pp. 9118–9128, 2016.

[4] H. U. Sokoli, M. E. Simonsen, R. P. Nielsen, K. R. Arturi, and E. G. Søgaard, "Conversion of the matrix in glass fiber reinforced composites into a high heating value oil and other valuable feedstocks," *Fuel Process. Technol.*, vol. 149, pp. 29–39, 2016.

[5] G. Oliveux, J.-L. Bailleul, and E. L. G. La Salle, "Chemical recycling of glass fibre reinforced composites using subcritical water," *Composites Part A*, vol. 43, no. 11, pp. 1809–1818, 2012.

[6] H. U. Sokoli, *Chemical Solvolysis as an Approach to Recycle Fibre Reinforced Thermoset Polymer Composites and Close the End-of the Life Cycle.* PhD thesis, Aalborg University, September 2016.

[7] K. Ramanamurty and G. Salvapati, "New dimensions on value added aldol chemicals of acetone," *J. Sci. Ind. Res.*, vol. 59, no. 5, pp. 339–349, 2000.

Conclusions

Hydrothermal liquefaction is a technique utilizing the unique properties of near- and supercritical fluids to produce value-added products, namely energy carriers, transportation biofuels, and chemical feedstocks, from biomass. The process is versatile in terms of feedstocks; it can handle both moisture-rich streams as well as wastes unsuitable for pyrolysis and biochemical processing methods, respectively. These advantages make liquefaction an excellent potential addition to the future biorefinery.

Liquefaction is performed in a relatively compact equipment, which could be transported on site to the available biomass resources, just as it was proposed for pyrolysis. Following the concepts of biorefining, the future bioeconomy will not be a one-technology solution but will be based on a plethora of conversion applications. In this study, numerous aspects of liquefaction processing and analysis were investigated and optimized. Based on the statistical analysis and experimental work, it can be concluded that:

- Due to the heterogeneity of the liquefaction results reported in the literature, optimization of the process has been slow. The situation originates from the unaccounted for variations in processing (pressure, heating rates, cooling rates), product separation (different schemes and settings), and analysis (types of methods and instruments). Development of standard approaches and minimal requirements for liquefaction processing would promote the progress and commercialization of this technique. Utilization of the approach of biomass cold-injection into a pre-heated and pre-pressurized reaction medium maximizes the control over control parameters while minimizing the effort and technical challenges typically associated with continuous processing. The main advantages of this approach include fast heating of biomass, pressure and reaction time control, and rapid quenching of the products. These features made the obtained results directly comparable to results obtained with continuous liquefaction units. Cold-injection batch reactors can, therefore, be treated as a basis for the development of liquefaction from a lab-scale to pilot plant and towards commercialization.

- According to the statistical analysis, biomass type had the largest impact on the yields and the quality of liquefaction the products, with algae producing the best results. The analysis of the literature data showed that there were few tendencies in the conversion trends common for all biomass types. This indicated that the process should be optimized individually according to the feed's composition. While combining increasing concentrations of the homogeneous catalyst, fast heating rates, and longer reaction times resulted in rising WSO yields, the exact opposite conditions were optimal for the production of biocrude. The heating value of the produced biocrude was dependent on the biomass properties, and not the reaction conditions.

- The results showed that the characterization of liquefaction products could be improved significantly by application of advanced analytical tools for both an enhanced transfer of the analytes (SPME), as well as their improved separation and identification (LC-ESI-MS/MS). SPME, which is a low-tech extraction method that can be used with most of the standard GC-MS equipment, did not require organic solvent and could be optimized for a broad spectrum of analytes of varying molecular weight, polarity, and volatility. Application of high-resolution LC-ESI-MS/MS expanded product characterization even further beyond the samples' volatile constituents. The combination of a carefully designed analytic methodology with verified quantification procedures was crucial for an accurate quantification of the samples' composition.

- Hydrothermal liquefaction of Kraft lignin resulted in of a broad spectrum of products. Production of monomers was maximized at phenol/lignin ratio of approx. 1. With increasing phenol mass fractions (9.7 wt.%), the formation of phenolic/anisolic dimers dominated the conversion mechanisms. In the absence of the co-solvent, the production of chemicals was very poor. Similar trends were noted at low reaction temperatures. With regard to the production of monomers, the yields of guaiacols and alkylphenols were maximized at phenol mass fraction of w_{Ph} = 6.5 %, whereas the amounts of catechols and methoxybenzenes increased progressively. At w_{Ph} = 3.4 wt.%, the highest yields of monomers were achieved at T = 320 °C.

- Hydrothermal conversion of lignocellulose resulted in water soluble and insoluble products consisting of low molecular weight (LMW) compounds, cyclics (C), aromatics (A), and high molecular weight (HMW) products. The addition of co-solvents resulted in significant reaction shifts, including increased production of A (enhanced solubilization of lignin and aromatization of glucose) and LMW (retro-aldol condensation), while repressing the formation of HMW, often considered precursors of biochar. Both aromatics, as well as the cyclic compounds, could be utilized as platform chemicals and chemical building blocks in the chemical industry.

- Polymer materials were effectively depolymerized in water/acetone mixtures at hydrothermal conditions. The products were divided into two fractions according to the compounds polarity and included monomers from the polyester chains (aqueous phase) and secondary reaction products (oil fraction). The former group consisted of compounds such as phthalic acid and dipropylene glycol. The latter group consisted of isophorone, dihydroisophorone, and 3,3,6,8-tetramethyl-1-tetralone, all of which were formed due to self-condensation of acetone. By liquefaction-based recycling of the monomeric building blocks and production of valuable chemicals, it will be possible to close the loop on the composites' life-cycle.

Part III

Papers

This part is the main body of the thesis. It consists of a number of papers which have been published in or submitted to peer-reviewed journals. The papers have been ordered according to the logical narrative of the thesis and were incorporated into its native typography.

Paper A

Performance of hydrothermal liquefaction (HTL) of biomass by multivariate data analysis

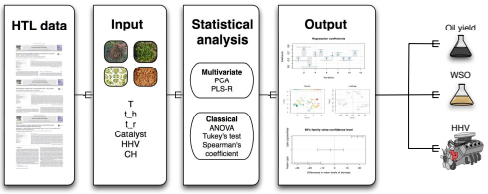

Katarzyna R. Arturi, Sergey Kucheryavskiy, and Erik G. Søgaard

The paper has been published in the
Fuel Processing Technology Vol. 150, pp. 94–103, 2016.

Abstract

Hydrothermal liquefaction (HTL) is one of the most promising biomass reforming processes for production of drop-in biofuels. The technique has been under development for a number of years, and yet, due to its complexity, it has always been difficult to generalize information about the optimal conditions. The main issue regards to the limited knowledge available from batch studies evaluating HTL by a finite number of process conditions in certain combinations. In this study, multivariate statistical methods were applied for investigation of HTL data available in the literature. The aim was to determine a set of generally valid rules for prediction of the output from the process (yields and the energy content) on the basis of relatively few process parameters. The results have shown that multivariate data analysis can be used to make predictions about HTL and increase our understanding of the process, despite the fact that the input data constituted a very broad spectrum of values. In general, biomass type and properties were the most significant parameters controlling both the obtained yields and the energy content in the produced biocrude. Regression models calculated for all groups of biomass were relatively poor, due to the lack of common trends. However, a number of statistically sound models was obtained for selected combinations of biomass and responses. The drawn conclusions supported the pre-understood axioms of HTL, but also indicated a number of new associations. It was shown that the overall conversion rates are governed by biomass properties and the applied heating velocities, while the amount of homogeneous catalyst and the reaction time control the distribution of the products between the water phase and the biocrude. The energy content in the biocrude produced from lignocellulose was dependent mostly on the biomass content and properties, and not the process conditions.

1 Introduction

Conversion of biomass into bio-fuels for transport purposes has a history spanning over 100 years and covering a great number of different routes that can be roughly divided into physicochemical, biochemical, and thermochemical processes. For many years, biodiesel and bioethanol have been focal points of the bio-fuel research, resulting in the development of many practical applications. However, all of these applications are fundamentally flawed because they use food resources as feed, thereby decreasing the food security. While the second generation biomass conversion technologies are under strong development, the bulk of the industrial methods still focuses on the first generation of biomass [1]. Over the last 25 years, a number of thermochemical conversion methods, including hydrothermal liquefaction (HTL), for production of drop-in fuels for transport purposes has come into focus [2–6]. HTL is a promising technique utilizing the unique properties of near- or supercritical water (T_{cr} = 374 °C, p_{cr} = 22.1 MPa, and ρ_{cr} = 320 kg/m^3), including high reaction rates, increased solubility of organics, and the lack of mass transport barriers [7–12]. Near critical water (hot compressed water, HCW) and supercritical water (SCW) behave similarly to a number of organic solvents, i.e. they can dissolve biomass and its degradation products [13]. HLT does not require strong bases or

acids and can utilize any type of biomass (lignocellulose, algae, waste) for production of a crude oil-like product [14–17]. Utilization of waste, which may be one of the most lucrative resources in the future [18], increases the sustainability of the process.

The idea of HTL used for conversion of biomass into biocrude has been experimented with as early as in the 1940s [19]. The first large scale application of the process was developed in the late 1970s at the Pittsburgh Energy Research Center (PERC) [16]. Today, a number of similar large scale facilities is operating [20–23], but the main bulk of the HTL research is still done on a lab-scale. A typical batch study examines a finite number of process conditions in a pre-selected set of combinations without using e.g. a full or fractional factorial design based on all parameters [24–26]. Because HTL depends on numerous variables, including both conversion conditions and the employed biomass type [27–29], the insight into the process based on this standard procedure is limited. It is not easy to predict the output, generalize the conclusions, or to understand the chemical transformations behind it [30–33]. While reaction mechanisms for HTL have been explained in detail for one-component feeds, e.g. pure glucose [34], real life biomasses are typically complex mixtures. The aim of this study was to compare HTL data available in the literature and to build generally valid statistical models for prediction of the yields and the quality of the products from the process as a function of the applied process parameters. To achieve this goal, both univariate and multivariate data analysis (MDA) tools were employed. MDA is an interdisciplinary mixture of statistics, applied mathematics, and computer science, used widely in chemistry, medicine, biology, and chemical engineering for analysis of experimental data with many parameters and factors [35–38]. Simple univariate models for determination of biocrude yield for one type of feed have been previously computed as a function of feed composition [39] or lignin content [40], but were shown to be of limited applicability. This is, as far as the authors were able to discover, the first study about multivariate modeling of HTL, and also one of the very few systematic statistical appraisals of the process performance of such extend and complexity.

2 Theory

2.1 Reaction mechanisms

Conversion of biomass during HTL is a combination of an initial heterogeneous degradation of the biomass particles, an ionic driven hydrolysis of the biopolymers, and a number of secondary pathways involving the hydrolysis products [41–44]. In addition to hydrolysis, depolymerization also takes place by radical C-C scission. The secondary reactions depend on the process conditions and include dehydration, dehydrogenation, rearrangements, retro aldol condensation, Cannizzaro reaction, cyclization, and polymerization [45, 46]. Lignocellulosic biomass is converted into its monomers: glucose (from cellulose), xylose, arabinose, and mannose (from hemicellulose). The amorphous lignin, which is not broken down into any repeating

units, is typically decomposed into small phenylpropane entities soluble in supercritical water. Similarly to carbohydrates, lipids and proteins are depolymerized into monomers (glycerol, fatty acids, and amino acids). The fatty acids tend to be stable at elevated temperatures, especially in HCW, but are thermally degraded above the supercritical point [47]. Alternatively, long chain fatty acids can also be reformed to long chain hydrocarbons [48]. Glycerol can be transformed to a number of products including methanol, ethanol, formaldehyde, acetaldehyde, propionaldehyde, acrolein, and small gas molecules [49–51]. Two of the most common routes for conversion of amino acids formed by hydrolysis of proteins are: I) decarboxylation into carbonic acid and amines, and II) deamination into ammonia and organic acids [21, 52–56]. The products from hydrolysis of proteins and the primary reactions of amino acids will typically undergo secondary reactions including repolymerization and condensation. The converted compounds are upon cooling redistributed between a two-phase product consisting of process water and biocrude. Relatively small amounts of solid particles and gas products are also formed. The organic content of the aqueous phase, which is referred to as the water soluble organics (WSO), consists of relatively polar compounds: small molecular weight (MW) aliphatics, short fatty acids, phenolics, cyclic compounds, and unreacted sugars [57]. Biocrude contains both the cyclic compounds and phenolics that are commonly found in WSO and heavy MW compounds of lower polarity, including short and long chained aliphatic alkanes and alkenes as well as polymerized aromatic and cyclic units.

2.2 State of the art

The range of the reported pressure and temperature values for HTL is quite broad (150 - 600 °C and 5 - 40 MPa), but most processes are executed under temperatures 300 - 400 °C, with T = 350 °C being reported as the most optimal value [58]. With temperature increasing, dehydration reactions become thermodynamically favorable, and the water soluble biocrude precursors are converted into phenolics, long chained carboxylic acids, esters and other hydrocarbons [57]. However, as the temperature approaches the critical point, radical cracking and condensation reactions begin to dominate, thus decreasing the yield of biocrude and increasing the formation of gas and solid products [59–64]. The impact of pressure must be considered in terms of its ability to influence the overall water density in the near- and supercritical region.

It has been shown, that the velocity of heating is very important for conversion of lignocellulosic biomass [25, 65], for which high heating rates support fragmentation reactions and prevent char formation. If the heating is slow, the secondary reactions, i. e.repolymerization and condensation reactions dominate, thereby increasing the amount of solid residues [66, 67]. Similar effect was demonstrated for algae [68], but it has not been studied in detail for other feedstocks. The residence time in HTL varies normally between 5 and 120 min, depending on the feed, presence of catalysts, pressure and temperature values. Generally, a short reaction

time is expected to degrade all types of biomass more effectively at high temperatures [14, 69, 70], while lower temperatures require significantly longer residence times [71]. This is not the case for lignin-based biomasses, which are converted more easily into solid char with increasing temperatures and residence times [40].

Both homogeneous and heterogeneous catalysts have been used in HTL. The early experiments on the pilot plant scale were performed with K_2CO_3 as homogeneous catalyst [72], and later, it was shown that hydrothermal processing without the presence of alkali gives rise to a much higher content of char and oxygen in the biocrude [73]. A great number of different homogeneous catalysts has been tried in HTL: (NaOH [24], Na_2CO_3 [20, 24], KOH [20], K_2CO_3 [24], $Ba(OH)_2$ [74], $RbCO_3$ [75, 76], $FeSO_4$ [77], FeS [77]). The most common heterogeneous catalysts include Pd/C, Pt/C, Ru/C, Ni/SiO_2-Al_2O_3, CoMo/γ-Al_2O_3 [39, 78–80], and ZrO_2 [81]. In general, numerous advantages have been associated with the use of homogeneous catalysts, including decreasing the amount of produced solids [82], increasing the yield of biocrude [83], and improving the biocrude properties [84, 85]. Addition of alkali salts increases pH, thus decreasing possibility for dehydration reactions, which typically leads to increased amounts of unstable unsaturated compounds prone to repolymerization. The heterogeneous catalysts influence the gasification in low-temperature processes [86], while the reports of its effects on HTL have been mixed [54]. Co-solvents act as scavengers of the unsaturated compounds, which are formed by dehydration and also likely to repolymerize. Their presence reduces the amount of undesired products (char and tar) and to direct the transformations towards desired pathways. The most common examples of organic solvents are phenol [75, 84], methanol [60], ethanol [87], acetone [87], butanol [88], propylene glycol [89]. Small alcohols work best for reduction of char production [88], but have also tendency to evaporate.

HTL can use different feeds, but waste products, e. g.agricultural and industrial waste, have always been of particular interest [62, 90–92]. A cheap feed is a requirement, if the biocrude shall be able to compete against both the petrochemical and other bio-conversion processes. Studies on the liquefaction of cellulose [93–96], its degradation product glucose [97] and hemicellulose [98, 99] focused on unlocking the mysteries behind the conversion mechanisms. Conversion of pure compounds is interesting from a theoretical point of view, but the applicability of HTL can only be tested with complex biomass feeds such as lignocellulosic biomass, including agricultural and industrial waste streams [100–103]. Lignin [104] and algae [15, 105–108] have also been a popular selection for HTL in the recent years. The oil yields produced from HTL typically range between 20 and 40 wt.%. Lipid rich biomass tends to produce higher yields. Biocrude produced from algae was reported to contain more fatty acids and fatty acid methyl esters, ketones and aldehydes [109], than biocrude produced from lignocellulose. The nature of the products, biocrude and the produced water, has been shown to be highly dependent on the composition of the feed.

3 Materials and Methods

3.1 Data

The data for the analysis was collected from 34 peer-reviewed studies [14, 26, 53, 57, 70, 103, 110–137] to give more than 400 records. The articles were selected to include a wide range of feeds and process conditions and to characterize the yields of the biocrude (OY), yields of the water soluble organics (WSO), and energy content in the biocrude (higher heating value, HHV) most broadly. The statistics of the continuous factors used in the analysis can be found in Table A.1.

Table A.1: The most important statistic parameters (minimum and maximum values, mean and median, 1st and 3rd quartiles) of the continuous factors used in the analysis. The acronyms correspond to the names of the variables used in statistical analysis and the results.

Variable	Biomass % (wt.%)	Lignin (wt. %)	Catalyst (wt.%)	Temp. (K)	Heating t (min)	Reaction t (min)	HHV (MJ/kg)	C/H ratio (-)
Acronym	content	lignin	catalyst	T	t_h	t_r	HHV_F	CH
Minimum	2.8	0.0	0.00	473	0.0	0	8.0	4.87
1st quuartile	8.9	0.0	0.00	573	10.0	15	14.8	7.25
Median	10.0	9.2	0.00	603	37.5	30	18.0	7.86
Mean	11.8	15.5	2.19	600	42.2	35	17.3	7.83
3rd quuartile	13.3	27.6	2.20	623	60.0	60	19.2	8.45
Maximum	66.7	100.0	13.45	823	120.4	120	39.5	17.00

The data was additionally characterized with a categorical factor ”biomass type“, which identified the chemical composition of the used feed as lignocellulose, lipid, and/or protein. Algae were categorized as both a lipid and protein-rich feed. The used HTL output parameters, also called the responses, are summarized in Table A.2. Analysis of the data according to the ”study“, i.e. the different papers used, was performed and no tendencies or groupings were found. A number of process conditions, including pressure, type of reactor, presence of co-solvent and heterogeneous catalyst, type of atmosphere, and extraction solvent was removed from the analysis due to the their low abundance as parameters in the studies. The yields were expressed as wt.% (on the dry biomass basis). The heating time was, when not stated in the studies, approximated according to the literature data for reactors with similar properties (type and volume). HHV values of the biocrude was either taken directly from the studies or calculated from the measured CHO composition (Dulong formula, Equation, A.1). HHV can be estimated by a number of mathematical models based on the content of different elements, among others carbon, hydrogen, oxygen, nitrogen, sulphur, chlorine, and phosphorus [138, 139]. Formula A.1 is considered a fair approximation for estimation of HHV for biocrudes, as their main constituents are limited to C, H, and O [110, 121, 127, 140]. Alternatively, an equation based on CHNSO and ash content of biocrudes could be used [141].

$$\mathrm{HHV} = 0.3383 \cdot \mathrm{C} + 1.442 \cdot \left(\mathrm{H} - \frac{\mathrm{O}}{8}\right) \tag{A.1}$$

Table A.2: The most important statistic parameters (minimum and maximum values, mean and median, 1st and 3rd quartiles) of the responses. The acronyms correspond to the names of the responses used in statistical analysis and the results. NaN describes the number of missing values for each response.

Response	Biocrude yield (wt.%)	HHV biocrude (MJ/kg)	WSO (wt.%)
Acronym	OY	HHV_O	WSO
Minimum	0.0	3.1	2.0
1st quartile	16.4	28.8	12.8
Median	22.0	31.0	26.0
Mean	25.9	31.4	28.6
3rd quartile	34.0	35.2	40.0
Maximum	85.0	39.9	75.0
NaN	6	219	140

3.2 Modeling

Due to the relatively large number of missing values in the responses, each of them was analyzed separately, thus reducing the number of removed NaN-containing samples for each analysis. Outliers constituted no more than 3 % of all data points. Prior to multivariate analysis the data columns were autoscaled by subtracting mean and dividing to standard deviation calculated for the values of each column. The applied methods encompassed: I) Principal Component Analysis (PCA), II) Traditional statistical methods including Analysis of Variance (ANOVA), Tukey's test, and Spearman's correlation with bootstrap confidence intervals, and III) Partial Least Squares Regression (PLS-R). The qualitative data was analyzed with ANOVA combined with Tukey's test, while Spearman's correlation analysis was used for the quantitative data. In PCA and PLS all the qualitative variables (factors) were converted into "dummy" ("+1" and "-1") variables. PCA was used to look for the general patterns, which thereafter were examined with ANOVA, Tukey's, and Spearman's tests. Following that, a regression model was build and examined. Analysis was performed both on all available records with biomass type as an additional factor, as well as on sets of records categorized according to the three biomass groups appearing in the study: lignocellulose, algae, and protein waste. All calculations were made in R (version 3.2.2), a free software environment for statistical computing and graphics, supported by mdatools and boot packages.

PCA PCA is the simplest of the eigenvector-based multivariate methods for exploratory assessment of large data sets [142]. It projects the original data to a set of orthogonal vectors (principal components, PC) oriented in the original variable space along directions of maximum spread of the data points. Often, PCA allows to find hidden structures in the data-objects relationship, such as groups, trends, and outliers. The results of PCA are evaluated with score plots and loading plots. Score plots show the projection of data objects to the principal components while loading plots show contribution of each variable to orientation of the components. Objects

positioned close to each other on a score plot are considered similar according to the variable (or a set of variables) which dominates the loading where the samples had high scores. All PCA models in this study used six compounds (comp = 6) as standard.

Classic statistical tools Analysis of Variance (ANOVA) is a statistical method used for quantitative assessment of association between a response and a number of factors [142]. ANOVA is also often used as an input for post hoc multiple comparison of means, also called Tukey's test. The requirements for the use of ANOVA include normal distribution of the data, homogeneity of variance and statistical independence of the samples. When the data used in this study did not fulfill the conditions for normality or variance homogeneity, the results were examined additionally using non-parametric Welch's ANOVA with Games-Howell test for multiple comparison. Spearman's coefficient is a non-parametric measure of statistical dependence between two variables. The perfect monotone correlation between two variables is expressed with correlation of "-1" or "+1". The confidence intervals for the quantitative Spearman's test were calculated with bootstrapping [143].

PLS-R PLS is a multivariate regression method similar to PCA that uses the structure of Y (response) as a guide to decompose the X-matrix (predictors), thus giving superior interpretation possibilities. The basic tools of PLS are common to all regression algorithms. The quality of a PLS model is evaluated by a number of parameters for both calibration (CAL) and cross-validation (CV). Root Mean Square Error (RMSE) is used as an estimate of how close the values, predicted by a PLS model, are to the actual values (Eq. A.2). Another parameter assessing the quality of the model is the slope of least squared line points on predicted vs. measured plot. Additionally, bias and ratio of performance to deviation (RPD) values can be calculated and analyzed as a measure of the goodness of fit. The evaluation of each model in this study was performed based on RMSE, slope, and R^2 values calculated for predictions obtained using a random cross-validation with ten segments.

$$RMSE = \sqrt{\frac{\sum_n^{t=1}(\hat{y}_t - y)^2}{n}} \tag{A.2}$$

The meaning of each PLS-R model calculated in this study was interpreted by analyzing regression coefficients and their confidence intervals, calculated using Jack-Knife approach [144]. This allowed to estimate a direct influence of each variable on the response. Generally, when a model has low RMSE and high R^2 values, the calculated regression coefficients can be used directly to predict the response. With poor regression parameters, the models can not be used for more than observation of loose tendencies in the data.

4 Results and Discussion

4.1 Oil yield

An initial PCA analysis of the factors combined with the oil yield (OY) has shown that both were spread over a great range of values. The samples with the most extreme values were removed as outliers in order to improve the quality of the models. The final composition of the data sets was a compromise between the precision and the "real life" applicability of the calibrated statistical models. As many as 9 PCs were required in order to explain 95 % of the variance in the data, most of which could be attributed to the variations in the variables, and not the OY itself. PC1 represented the variability caused by the presence of different groups of biomass (lignocellulose, algae, and protein waste), while PC2 outlined an interaction between the time of reaction and the time of heating, i.e. there was a tendency in the studies to use short reaction time, when the heating was slow. This can be clearly seen from the two bottom scores plots in Figure A.1 where the points are colored with a color gradient according to the values of these two parameters - points with large values for heating time (orange and red colors on the right plot) have short reaction time (blue and green points on the left plot) and vice versa.

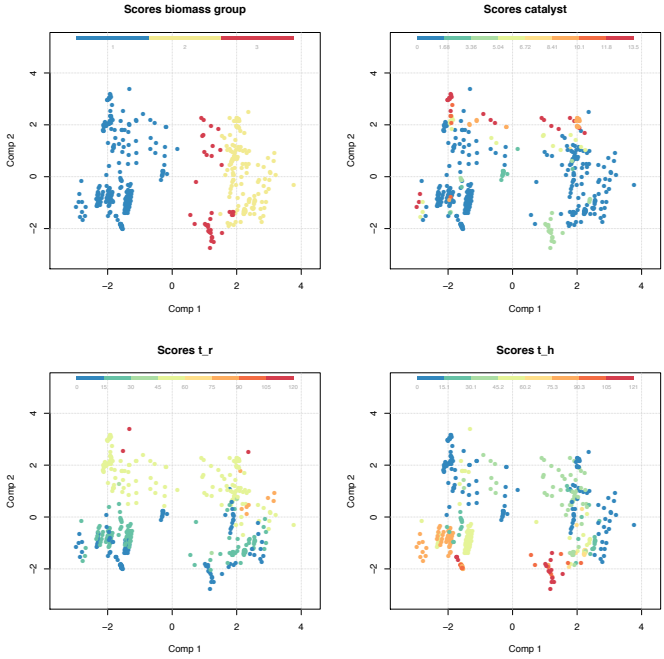

Fig. A.1: PC1 (29.99 %) vs. PC2 (16.68 %) scores plots (PCA model of factors and OY for all groups of biomass). The color gradient corresponds to different levels of selected factors. Top-left: biomass group (1-Lignocellulose, 2-Algae, 3-Protein waste). Top-right: catalyst amount (blue-low, red-high). Bottom-left: reaction time (blue-short, red-long). Bottom-right: heating time (blue-short, red-long).

Similarly, PC3 could be explained by the variations in reaction temperature and biomass content (low temperature with large loadings and opposite). An interesting detail was discovered during the analysis of PC4, in which OY had large negative loading, as demonstrated by PC1 vs. PC4 score and loading plots in Figure A.2. OY did not seem to be correlated to any of the other variables, i.e. the process conditions, indicating a hidden structure governing the variability of OY. Similar results were achieved with calculation of Spearman's correlation with bootstrap confidence intervals between OY and each variable. There may have been a tentative positive correlation between OY, biomass content, and HHV of the feed.

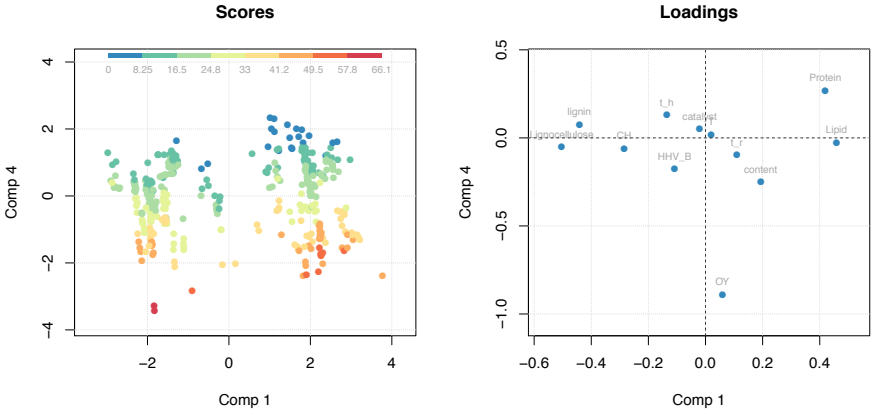

Fig. A.2: PC1 (29.99 %) vs. PC4 (8.76%) score and loading plots (PCA model of factors and OY for all groups of biomass). The color gradient on the scores plot corresponds to the different levels of oil yield (blue-low, red-high). The loading plot shows a corresponding compilation of factors and OY.

This was, to a certain extent, confirmed by PLS regression, according to which the highest OY values were achieved with lipid-rich biomass, i.e. algae, high biomass content in the reactor, long heating time, and short reaction time. The regression coefficients are displayed in Figure A.3. The relationship between the OY and biomass type was verified by Tukey's test, in which the differences between the mean values of OY for different types of biomass were compared and presented in Figure A.4. Additionally, while high HHV values of the biomass and low catalyst concentrations seemed to produce larger oil yields, the temperature did not have any statistically significant influence. It must be noted that the model was quite poor statistically speaking (RMSE = 10.60, R^2 = 0.15, Slope = 0.17), most probably due to the lack of trends common for all biomass groups. Other, less certain tendencies, e.g. a possible positive correlation between lignin content and OY, were noted as well. The large variation in the data was due to the disregarded process conditions (pressure, heterogeneous catalysts, presence of co-solvents) and additional differences in the pre-processing and chemical analysis of the biocrudes (application of different solvents and extraction methods).

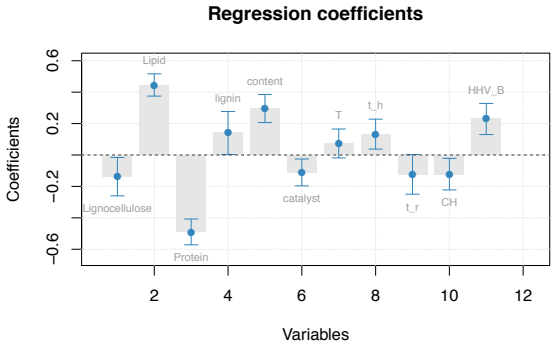

Fig. A.3: Regression coefficients with 95 % confidence interval for OY values (calculated with PLS for all biomass groups). The size, sign, and the confidence intervals are used to judge the importance of each factor.

Statistical analysis of the data according to biomass group had improved the performance of the regression models for the algae (RMSE = 10.31, R^2 = 0.43, Slope = 0.47), but not for the lignocellulose, nor the protein waste feed. The PLS regression model for the algae, which is summarized with the regression coefficients in Figure A.5, indicated that OY depends on the biomass properties, reaction temperature, and the amount of homogeneous catalyst. While the influence of temperature was expected, no studies have ever proposed a negative relationship between the yields of biocrude and the amount of homogeneous catalyst.

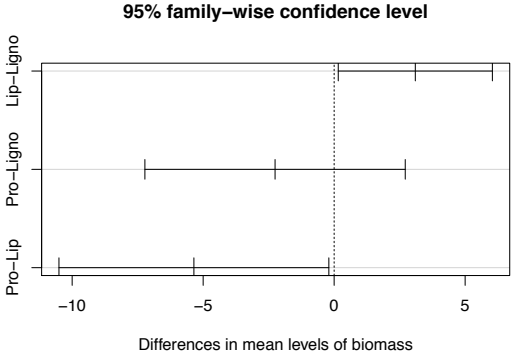

Fig. A.4: The differences in the average OY values for the different biomass types. Bottom: OY(Protein)-OY(Lipid). Middle: OY(Protein)-OY(Lignocellulose). Top: OY(Lipid)-OY(Lignocellulose). When the confidence intervals cross 0, there is no significant difference between the groups.

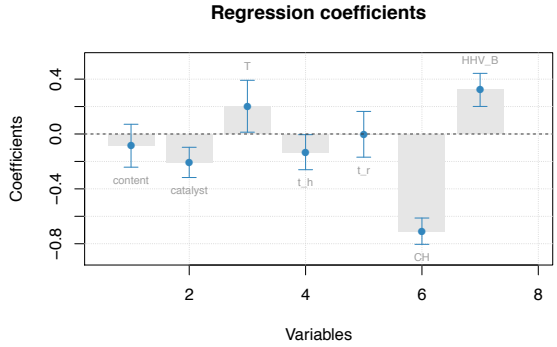

Fig. A.5: Regression coefficients with 95 % confidence intervals for OY (calculated with PLS for algae biomass). The size, sign, and the confidence intervals are used to judge the importance of each factor.

4.2 WSO

A PCA analysis of the factors combined with the WSO values was significantly easier to interpret than the corresponding analysis of OY. Several of the variables were correlated to WSO along the directions of largest variation, as shown by PC1 vs. PC2 score and loading plots in Figure A.6. The tendency on the score plot went clearly from left bottom corner of the plots to the right top one, indicating that the WSO can be explained by a linear combination of PC1 and PC2.

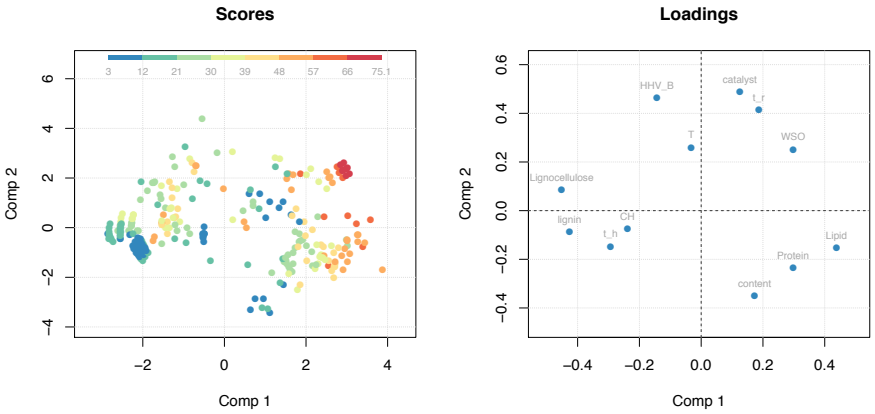

Fig. A.6: PC1 (34.94 %) vs. PC2 (15.57 %) score and loading plots (PCA model of factors and WSO for all groups of biomass). The color gradient on the scores plot corresponds to different yields of WSO (blue-low, red-high). The loading plot shows which factors are related to WSO yields.

The correlation between WSO and the variables positioned close to it on the loading plot was additionally confirmed by calculation of Spearman's correlations with bootstrap confidence intervals. The following PLS regression model, summarized with the regression coefficient plot in Figure A.7, was better than the corresponding model for OY (RMSE = 13.1, R^2 = 0.44, Slope = 0.50). According to the results, the production and accumulation of WSO in the water phase was favored for lipid-rich feeds (algae), high lignin contents, high concentrations of catalyst, long reaction times, fast heating rates, and low C/H ratios. This indicates, that algae biomass with low C/H ratios is easier to convert into water soluble organics and oil in HTL when combined with fast heating rates. On the other hand, the amount of homogeneous catalyst and the reaction time seem to control the distribution of the products between the water and the biocrude phases. As described in Section 4.1, the OY values are maximized at lower amounts of catalysts and short reaction times. The dependence of WSO on the biomass type was confirmed by Tukey's test, the results of which are summarized in Figure A.8. There was no significant difference in the average WSO yields produced from lignocellulose and protein-rich feeds, while utilization of lipid-rich biomass (algae) as feed resulted in increased WSO yields. The performance of the PLS regression model for WSO was improved significantly for lignocellulosic biomass (RMSE = 6.43, R^2 = 0.76, Slope = 0.78). According to this model, in addition to the amounts of homogeneous catalyst, WSO is also governed by the biomass composition and properties. The regression coefficient plot shown in Figure A.9 demonstrated that high HHV values, low C/H ratios, and high lignin contents decrease WSO production when lignocellulose is applied as feed.

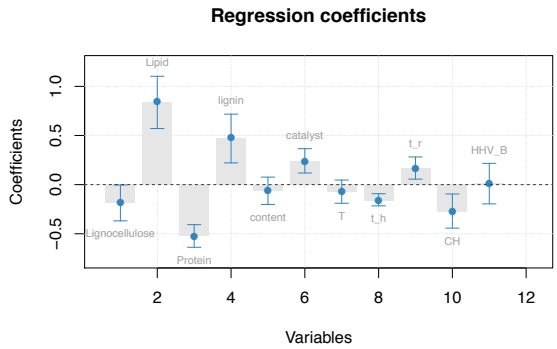

Fig. A.7: Regression coefficients with 95 % confidence interval for WSO values (calculated with PLS for all biomass groups). The size, sign, and the confidence intervals are used to judge the importance of each factor.

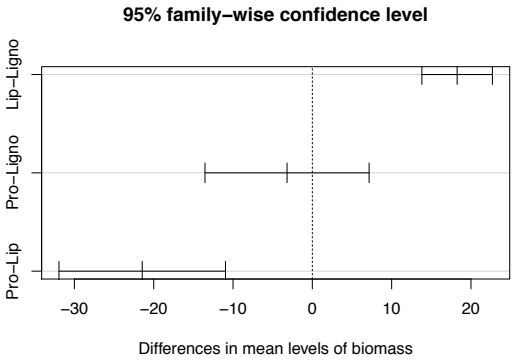

Fig. A.8: The differences in the average WSO values for the different biomass types. Bottom: OY(Protein)-OY(Lipid). Middle: OY(Protein)-OY(Lignocellulose). Top: OY(Lipid)-OY(Lignocellulose). When the confidence intervals cross 0, there is no significant difference between the groups.

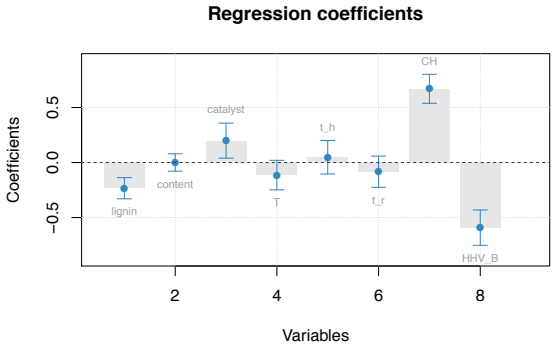

Fig. A.9: Regression coefficients with 95 % confidence intervals for WSO values (calculated with PLS for lignocellulosic biomass). The size, sign, and the confidence intervals are used to judge the importance of each factor.

4.3 HHV

A PCA analysis of the factors combined with HHV values did not show any clear connections between the biocrude energy content and the process parameters, as demonstrated by the score and loading plots in Figure A.10. However, according to the Spearman's correlation values, there was a measurable correlation between HHV, biomass content, reaction temperature, and reaction time. As indicated by Tukey's test results shown in Figure A.11, the biocrude from algae tended to be more energy-rich than the biocrude from the other two types of biomass. The PLS regression model for HHV and all groups of biomass was quite poor (RMSE = 6.54, R^2 = 0.24, Slope = 0.28). An improved regression model for lignocellulose only (RMSE = 3.10, R^2 = 0.74, Slope = 0.77) showed that the biocrude energy content depends mostly on the biomass content and properties, and not the process condi-

tions. However, as evidenced by the regression coefficients displayed in Figure A.12, heating time influences the HHV of the biocrude as well. OY and HHV can be considered together as a direct measure energy recovery from HTL. On the whole, most energy is recovered from HTL with algae as feed, at high reaction temperatures, fast heating rates, and relatively small homogeneous catalyst amounts.

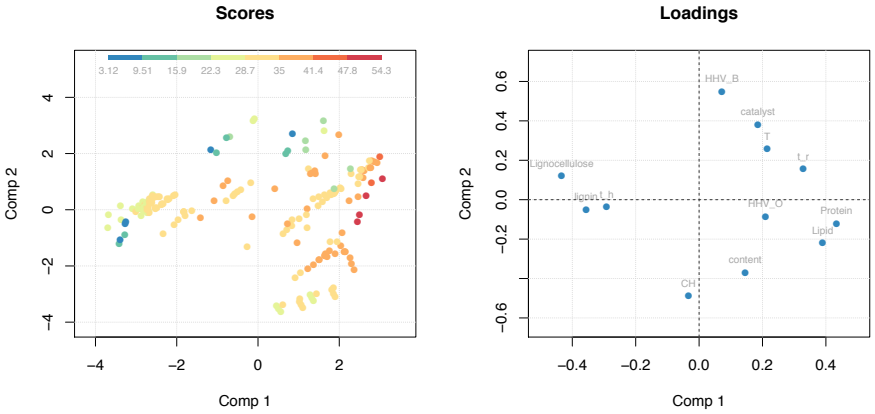

Fig. A.10: PC1 (37.96 %) vs. PC2 (17.65 %) score and loading plots (PCA model of factors and HHV for all groups of biomass). The color gradient on the scores plot corresponds to different values of HHV (blue-low, red-high). The loading plot shows which factors are related to HHV.

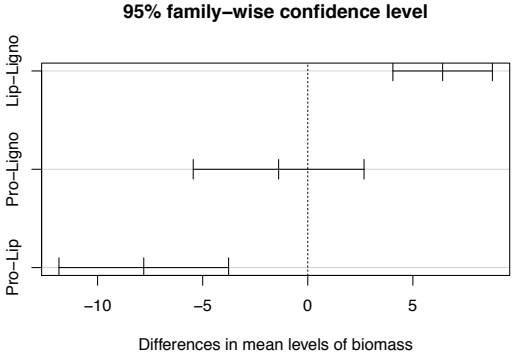

Fig. A.11: The differences in the average HHV values for the different biomass types. Bottom: OY(Protein)-OY(Lipid). Middle: OY(Protein)-OY(Lignocellulose). Top: OY(Lipid)-OY(Lignocellulose). When the confidence intervals cross 0, there is no significant difference between the groups.

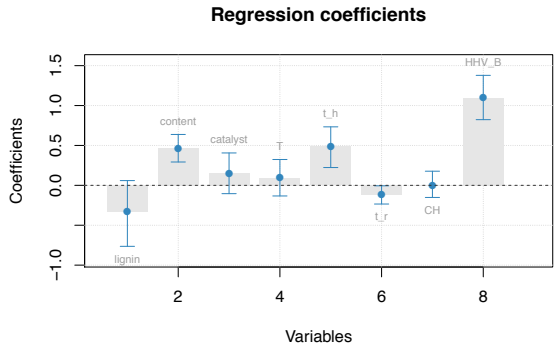

Fig. A.12: Regression coefficients with 95% confidence intervals for HHV values (calculated with PLS for lignocellulosic biomass). The size, sign, and the confidence intervals are used to judge the importance of each factor.

5 Conclusions

The multivariate approach used in this study was proven to be useful for analysis and prediction of the output from HTL. Generally, the regression models combining all groups of biomass were of poor statistical quality, most probably due to the lack of trends common for lignocellulose, algae, and protein waste. This indicates that each biomass requires a different approach for an optimal biocrude production. Several successful regression models, e.g. OY for algae, WSO for lignocellulose, and HHV for lignocellulose, were obtained. The composition of the feed was the most significant factor, with algae yielding the largest conversion rates, oil yields, and energy contents. The conclusions supported known axioms of HTL, including the influence of temperature, heating, and reaction times on the production of biocrude and WSO. While the overall conversion rates seemed to be governed by biomass properties and the applied heating rates, the amount of homogeneous catalyst and reaction time controlled the distribution of the products between WSO and biocrude. The yields of biocrude and WSO were maximized at the opposite reaction conditions with regard to the homogeneous catalyst amount and the time of reaction. The energy content in the biocrude from HTL of lignocellulose has been shown to be dependent mostly on the biomass content and properties.

6 Acknowledgements

The authors gratefully acknowledge the financial support from the Danish Council for Strategic Research (DSF grant no. 1305-00030B).

References

[1] S. Naik, V. V. Goud, P. K. Rout, and A. K. Dalai, "Production of first and second generation biofuels: A comprehensive review," *Renew. Sust. Energ. Rev.*, vol. 14, no. 2, pp. 578–597, 2010.

[2] L. Zhang, C. C. Xu, and P. Champagne, "Overview of recent advances in thermo-chemical conversion of biomass," *Energ. Convers. Manag.*, vol. 51, no. 5, pp. 969–982, 2010.

[3] Z. Zhu, L. Rosendahl, S. S. Toor, D. Yu, and G. Chen, "Hydrothermal liquefaction of barley straw to bio-crude oil: Effects of reaction temperature and aqueous phase recirculation," *Appl. Energ.*, vol. 137, pp. 183–192, 2015.

[4] A. Demirbaş, "Current technologies for the thermo-conversion of biomass into fuels and chemicals," *Energ. Source.*, vol. 26, no. 8, pp. 715–730, 2004.

[5] D. Elliott, D. Beckman, A. Bridgwater, J. Diebold, S. Gevert, and Y. Solantausta, "Developments in direct thermochemical liquefaction of biomass: 1983-1990," *Energy Fuels*, vol. 5, no. 3, pp. 399–410, 1991.

[6] A. Demirbaş, "Recent advances in biomass conversion technologies," *Energy Educ. Sci. Tech.*, vol. 6, pp. 19–40, 2000.

[7] A. Kruse and E. Dinjus, "Hot compressed water as reaction medium and reactant: Properties and synthesis reactions," *J. Supercrit. Fluids*, vol. 39, no. 3, pp. 362–380, 2007.

[8] R. P Nielsen and E. G Søgaard, "Features of near-and supercritical water," *Curr. Phys. Chem.*, vol. 3, no. 4, pp. 501–507, 2013.

[9] C. A. Meyer, R. McClintock, and G. Silvestri, *ASME Steam Tables: Thermodynamic and Transport Properties of Steam: Comprising Tables and Charts for Steam and Water, Calculated Using the 1967 IFC Formulation for Industrial Use, in Conformity with the 1963 International Skeleton Tables, as Adopted by the Sixth International Conference on the Properties of Steam.* American Society of Mechanical Engineers, 1993.

[10] H. Weingärtner and E. U. Franck, "Supercritical water as a solvent," *Angew. Chem. Int. Ed.*, vol. 44, no. 18, pp. 2672–2692, 2005.

[11] A. A. Galkin and V. V. Lunin, "Subcritical and supercritical water: a universal medium for chemical reactions," *Russ. Chem. Rev.*, vol. 74, no. 1, p. 21, 2005.

[12] D. Broell, C. Kaul, A. Kraemer, P. Krammer, T. Richter, M. Jung, H. Vogel, and P. Zehner, "Chemistry in supercritical water," *Angew. Chem. Int. Ed.*, vol. 38, no. 20, pp. 2998–3014, 1999.

[13] N. Matubayasi and M. Nakahara, "Super-and subcritical hydration of nonpolar solutes. I. Thermodynamics of hydration," *J. Chem. Phys*, vol. 112, no. 18, pp. 8089–8109, 2000.

[14] K. Anastasakis and A. Ross, "Hydrothermal liquefaction of the brown macro-alga Laminaria Saccharina: Effect of reaction conditions on product distribution and composition," *Bioresource Technol.*, vol. 102, no. 7, pp. 4876–4883, 2011.

[15] D. L. Barreiro, W. Prins, F. Ronsse, and W. Brilman, "Hydrothermal liquefaction (HTL) of microalgae for biofuel production: State of the art review and future prospects," *Biomass Bioenergy*, vol. 53, pp. 113–127, 2013.

[16] D. C. Elliott, "Historical developments in hydroprocessing bio-oils," *Energy Fuels*, vol. 21, no. 3, pp. 1792–1815, 2007.

[17] L. J. Sealock Jr, D. C. Elliott, E. G. Baker, and R. S. Butner, "Chemical processing in high-pressure aqueous environments. 1. Historical perspective and continuing developments," *Ind. Eng. Chem. Res.*, vol. 32, no. 8, pp. 1535–1541, 1993.

[18] C. Tuck, E. Pérez, I. Horváth, R. Sheldon, and M. Poliakoff, "Valorization of biomass: deriving more value from waste," *Science*, vol. 337, no. 6095, pp. 695–699, 2012.

[19] E. Berl, "Production of oil from plant material," *Science*, vol. 99, no. 2573, pp. 309–312, 1944.

[20] F. Behrendt, Y. Neubauer, M. Oevermann, B. Wilmes, and N. Zobel, "Direct liquefaction of biomass," *Chem. Eng.Technol.*, vol. 31, no. 5, pp. 667–677, 2008.

[21] S. S. Toor, L. Rosendahl, and A. Rudolf, "Hydrothermal liquefaction of biomass: a review of subcritical water technologies," *Energy*, vol. 36, no. 5, pp. 2328–2342, 2011.

[22] T. H. Pedersen, I. Grigoras, J. Hoffmann, S. S. Toor, I. M. Daraban, C. U. Jensen, S. Iversen, R. B. Madsen, M. Glasius, K. R. Arturi, R. P. Nielsen, E. G. Søgaard, and L. A. Rosendahl, "Continuous hydrothermal co-liquefaction of aspen wood and glycerol with water phase recirculation," *Appl. Energ.*, vol. 162, pp. 1034–1041, 2016.

[23] C. Jazrawi, P. Biller, A. B. Ross, A. Montoya, T. Maschmeyer, and B. S. Haynes, "Pilot plant testing of continuous hydrothermal liquefaction of microalgae," *Algal Res.*, vol. 2, no. 3, pp. 268–277, 2013.

[24] H. Mazaheri, K. T. Lee, and A. R. Mohamed, "Influence of temperature on liquid products yield of oil palm shell via subcritical water liquefaction in the presence of alkali catalyst," *Fuel Process. Technol.*, vol. 110, pp. 197–205, 2013.

[25] E. Kamio, S. Takahashi, H. Noda, C. Fukuhara, and T. Okamura, "Effect of heating rate on liquefaction of cellulose by hot compressed water," *Chem. Eng. J.*, vol. 137, no. 2, pp. 328–338, 2008.

[26] T. D. H. Nguyen, M. Maschietti, T. Belkheiri, L.-E. Åmand, H. Theliander, L. Vamling, L. Olausson, and S.-I. Andersson, "Catalytic depolymerisation and conversion of Kraft lignin into liquid products using near-critical water," *J. Supercrit. Fluids*, vol. 86, pp. 67–75, 2014.

[27] S. S. Toor, L. A. Rosendahl, J. Hoffmann, T. H. Pedersen, R. P. Nielsen, and E. G. Søgaard, "Hydrothermal Liquefaction of Biomass," in *Application of Hydrothermal Reactions to Biomass Conversion.* Springer, 2014, pp. 189–217.

[28] F. Goudriaan and D. Peferoen, "Liquid fuels from biomass via a hydrothermal process," *Chem. Eng. Sci.*, vol. 45, no. 8, pp. 2729–2734, 1990.

[29] R. P. Nielsen, G. Olofsson, and E. G. Søgaard, "CatLiq-High pressure and temperature catalytic conversion of biomass: The Catliq technology in relation to other thermochemical conversion technologies," *Biomass Bioenergy*, vol. 39, pp. 399–402, 2012.

[30] A. Demirbaş, "Mechanisms of liquefaction and pyrolysis reactions of biomass," *Energy Convers. Manage.*, vol. 41, no. 6, pp. 633–646, 2000.

[31] S. Xiu and A. Shahbazi, "Bio-oil production and upgrading research: A review," *Renew. Sust. Energ. Rev.*, vol. 16, no. 7, pp. 4406–4414, 2012.

[32] M. Balat, "Mechanisms of thermochemical biomass conversion processes. Part 3: Reactions of liquefaction," *Energ. Source. Part A*, vol. 30, no. 7, pp. 649–659, 2008.

[33] A. Kruse and A. Gawlik, "Biomass conversion in water at 330 - 410 °C and 30 - 50 MPa. Identification of key compounds for indicating different chemical reaction pathways," *Ind. Eng. Chem. Res.*, vol. 42, no. 2, pp. 267–279, 2003.

[34] A. Kruse, A. Krupka, V. Schwarzkopf, C. Gamard, and T. Henningsen, "Influence of proteins on the hydrothermal gasification and liquefaction of biomass. 1. Comparison of different feedstocks," *Ind. Eng. Chem. Res.*, vol. 44, no. 9, pp. 3013–3020, 2005.

[35] H. Keller and D. Massart, "Peak purity control in liquid chromatography with photodiode-array detection by a fixed size moving window evolving factor analysis," *Anal. Chim. Acta*, vol. 246, no. 2, pp. 379–390, 1991.

[36] Q. Miao, W. Kong, X. Zhao, S. Yang, and M. Yang, "GC-FID coupled with chemometrics for quantitative and chemical fingerprinting analysis of Alpinia oxyphylla oil," *J. Pharmaceut. Biomed.*, vol. 102, pp. 436–442, 2015.

[37] M. Farrés, B. Piña, and R. Tauler, "Chemometric evaluation of Saccharomyces cerevisiae metabolic profiles using LC–MS," *Metabolomics*, vol. 11, no. 1, pp. 210–224, 2015.

[38] Y. Liang, P. Xie, and F. Chau, "Chromatographic fingerprinting and related chemometric techniques for quality control of traditional Chinese medicines," *J. Sep. Sci.*, vol. 33, no. 3, pp. 410–421, 2010.

[39] P. Biller, R. Riley, and A. Ross, "Catalytic hydrothermal processing of microalgae: Decomposition and upgrading of lipids," *Bioresour. Technol.*, vol. 102, no. 7, pp. 4841–4848, 2011.

[40] A. Demirbaş, "Effect of lignin content on aqueous liquefaction products of biomass," *Energy Convers. Manage.*, vol. 41, no. 15, pp. 1601–1607, 2000.

[41] Z. Srokol, A.-G. Bouche, A. van Estrik, R. C. Strik, T. Maschmeyer, and J. A. Peters, "Hydrothermal upgrading of biomass to biofuel: Studies on some monosaccharide model compounds," *Carbohydr. Res.*, vol. 339, no. 10, pp. 1717–1726, 2004.

[42] G. Brunner, "Near critical and supercritical water. Part I. Hydrolytic and hydrothermal processes," *J. Supercrit. Fluids*, vol. 47, no. 3, pp. 373–381, 2009.

[43] ——, "Near and supercritical water. Part II: Oxidative processes," *J. Supercrit. Fluids*, vol. 47, no. 3, pp. 382–390, 2009.

[44] B. M. Kabyemela, T. Adschiri, R. M. Malaluan, and K. Arai, "Kinetics of glucose epimerization and decomposition in subcritical and supercritical water," *Ind. Eng. Chem. Res.*, vol. 36, no. 5, pp. 1552–1558, 1997.

[45] E. Chornet and R. P. Overend, "Biomass liquefaction: An overview," in *Fundamentals of thermochemical biomass conversion*. Springer, 1985, pp. 967–1002.

[46] J. Russell, R. Miller, and P. Molton, "Formation of aromatic compounds from condensation reactions of cellulose degradation products," *Biomass*, vol. 3, no. 1, pp. 43–57, 1983.

[47] R. L. Holliday, J. W. King, and G. R. List, "Hydrolysis of vegetable oils in sub-and supercritical water," *Ind. Eng. Chem. Res.*, vol. 36, no. 3, pp. 932–935, 1997.

[48] M. Watanabe, T. Iida, and H. Inomata, "Decomposition of a long chain saturated fatty acid with some additives in hot compressed water," *Energ. Convers. Manag.*, vol. 47, no. 18, pp. 3344–3350, 2006.

[49] W. Bühler, E. Dinjus, H. Ederer, A. Kruse, and C. Mas, "Ionic reactions and pyrolysis of glycerol as competing reaction pathways in near-and supercritical water," *J. Supercrit. Fluid.*, vol. 22, no. 1, pp. 37–53, 2002.

[50] A. Seretis and P. Tsiakaras, "Hydrogenolysis of glycerol to propylene glycol by in situ produced hydrogen from aqueous phase reforming of glycerol over SiO_2-Al_2O_3 supported nickel catalyst," *Fuel Process. Technol.*, vol. 142, pp. 135–146, 2016.

[51] M. Khavarian, S.-P. Chai, and A. R. Mohamed, "Carbon dioxide conversion over carbon-based nanocatalysts," *J. Nanosci. Nanotechnol.*, vol. 13, no. 7, pp. 4825–4837, 2013.

[52] N. Sato, A. T. Quitain, K. Kang, H. Daimon, and K. Fujie, "Reaction kinetics of amino acid decomposition in high-temperature and high-pressure water," *Ind. Eng. Chem. Res.*, vol. 43, no. 13, pp. 3217–3222, 2004.

[53] P. Biller and A. Ross, "Potential yields and properties of oil from the hydrothermal liquefaction of microalgae with different biochemical content," *Bioresource Technol.*, vol. 102, no. 1, pp. 215–225, 2011.

[54] A. A. Peterson, F. Vogel, R. P. Lachance, M. Fröling, M. J. Antal Jr, and J. W. Tester, "Thermochemical biofuel production in hydrothermal media: A review of sub-and supercritical water technologies," *Energy Environ. Sci.*, vol. 1, no. 1, pp. 32–65, 2008.

[55] T. Rogalinski, S. Herrmann, and G. Brunner, "Production of amino acids from bovine serum albumin by continuous sub-critical water hydrolysis," *J. Supercrit. Fluid.*, vol. 36, no. 1, pp. 49–58, 2005.

[56] D. Klingler, J. Berg, and H. Vogel, "Hydrothermal reactions of alanine and glycine in sub-and supercritical water," *J. Supercrit. Fluid.*, vol. 43, no. 1, pp. 112–119, 2007.

[57] C. Xu and J. Lancaster, "Conversion of secondary pulp/paper sludge powder to liquid oil products for energy recovery by direct liquefaction in hot-compressed water," *Water Res.*, vol. 42, no. 6, pp. 1571–1582, 2008.

[58] J. Akhtar and N. A. S. Amin, "A review on process conditions for optimum bio-oil yield in hydrothermal liquefaction of biomass," *Renew. Sustainable Energy Rev.*, vol. 15, no. 3, pp. 1615–1624, 2011.

[59] P. Sun, M. Heng, S.-H. Sun, and J. Chen, "Analysis of liquid and solid products from liquefaction of paulownia in hot-compressed water," *Energ. Convers. Manage.*, vol. 52, no. 2, pp. 924–933, 2011.

[60] E. Jakab, K. Liu, and H. L. Meuzelaar, "Thermal decomposition of wood and cellulose in the presence of solvent vapors," *Ind. Eng. Chem. Res.*, vol. 36, no. 6, pp. 2087–2095, 1997.

[61] H. R. Holgate, J. C. Meyer, and J. W. Tester, "Glucose hydrolysis and oxidation in supercritical water," *AIChE J.*, vol. 41, no. 3, pp. 637–648, 1995.

[62] B. He, Y. Zhang, Y. Yin, T. Funk, and G. Riskowski, "Operating temperature and retention time effects on the thermochemical conversion process of swine manure," *T. ASAE*, vol. 43, no. 6, pp. 1821–1826, 2000.

[63] K. Ocfemia, Y. Zhang, and T. Funk, "Hydrothermal processing of swine manure to oil using a continuous reactor system: Effects of operating parameters on oil yield and quality," *T. ASABE*, vol. 49, no. 6, pp. 1897–1904, 2006.

[64] U. Jena, K. Das, and J. Kastner, "Effect of operating conditions of thermochemical liquefaction on biocrude production from Spirulina platensis," *Bioresource Technol.*, vol. 102, no. 10, pp. 6221–6229, 2011.

[65] A. Sinag, A. Kruse, and J. Rathert, "Influence of the heating rate and the type of catalyst on the formation of key intermediates and on the generation of gases during hydropyrolysis of glucose in supercritical water in a batch reactor," *Ind. Eng. Chem. Res.*, vol. 43, no. 2, pp. 502–508, 2004.

[66] S. Saka and T. Ueno, "Chemical conversion of various celluloses to glucose and its derivatives in supercritical water," *Cellulose*, vol. 6, no. 3, pp. 177–191, 1999.

[67] Z. Fang, T. Minowa, R. Smith, T. Ogi, and J. Kozinski, "Liquefaction and gasification of cellulose with Na_2CO_3 and Ni in subcritical water at 350 °C," *Ind. Eng. Chem. Res.*, vol. 43, no. 10, pp. 2454–2463, 2004.

[68] Q.-V. Bach, M. V. Sillero, K.-Q. Tran, and J. Skjermo, "Fast hydrothermal liquefaction of a Norwegian macro-alga: Screening tests," *Algal Res.*, vol. 6, pp. 271–276, 2014.

[69] L. Garcia Alba, C. Torri, C. Samorì, J. van der Spek, D. Fabbri, S. R. Kersten, and D. W. Brilman, "Hydrothermal treatment (HTT) of microalgae: Evaluation of the process as conversion method in an algae biorefinery concept," *Energy Fuels*, vol. 26, no. 1, pp. 642–657, 2011.

[70] Y. Qu, X. Wei, and C. Zhong, "Experimental study on the direct liquefaction of Cunninghamia lanceolata in water," *Energy*, vol. 28, no. 7, pp. 597–606, 2003.

[71] S. Karagöz, T. Bhaskar, A. Muto, Y. Sakata, T. Oshiki, and T. Kishimoto, "Low-temperature catalytic hydrothermal treatment of wood biomass: analysis of liquid products," *Chem. Eng. J.*, vol. 108, no. 1, pp. 127–137, 2005.

[72] P. Thigpen, W. Berry, and D. Klass, "Energy from biomass and wastes VI," *IGT, Chicago*, p. 1057, 1982.

[73] F. Goudnaan, B. van de Beld, F. Boerefijn, G. Bos, J. Naber, S. van der Wal, and J. Zeevalkink, *Thermal Efficiency of the HTU® Process for Biomass Liquefaction.* Blackwell Science Ltd, 2008, pp. 1312–1325.

[74] C. Xu and N. Lad, "Production of heavy oils with high caloric values by direct liquefaction of woody biomass in sub/near-critical water," *Energy Fuels*, vol. 22, no. 1, pp. 635–642, 2007.

[75] C. C. Xu, H. Su, and D. Cang, "Liquefaction of corn distillers dried grains with solubles (DDGS) in hot-compressed phenol," *BioResources*, vol. 3, no. 2, pp. 363–382, 2008.

[76] K. Tekin and S. Karagöz, "Non-catalytic and catalytic hydrothermal liquefaction of biomass," *Res. Chem. Intermediat.*, vol. 39, no. 2, pp. 485–498, 2013.

[77] C. Xu and T. Etcheverry, "Hydro-liquefaction of woody biomass in sub-and super-critical ethanol with iron-based catalysts," *Fuel*, vol. 87, no. 3, pp. 335–345, 2008.

[78] P. Duan and P. E. Savage, "Hydrothermal liquefaction of a microalga with heterogeneous catalysts," *Ind. Eng. Chem. Res.*, vol. 50, no. 1, pp. 52–61, 2010.

[79] B. Yoosuk, D. Tumnantong, and P. Prasassarakich, "Amorphous unsupported ni–mo sulfide prepared by one step hydrothermal method for phenol hydrodeoxygenation," *Fuel*, vol. 91, no. 1, pp. 246–252, 2012.

[80] W. Wang, Y. Yang, H. Luo, and W. Liu, "Effect of additive (Co, La) for Ni–Mo–B amorphous catalyst and its hydrodeoxygenation properties," *Catal. Commun.*, vol. 11, no. 9, pp. 803–807, 2010.

[81] A. Hammerschmidt, N. Boukis, E. Hauer, U. Galla, E. Dinjus, B. Hitzmann, T. Larsen, and S. D. Nygaard, "Catalytic conversion of waste biomass by hydrothermal treatment," *Fuel*, vol. 90, no. 2, pp. 555–562, 2011.

[82] S. Karagöz, T. Bhaskar, A. Muto, and Y. Sakata, "Hydrothermal upgrading of biomass: Effect of K_2CO_3 concentration and biomass/water ratio on products distribution," *Bioresource Technol.*, vol. 97, no. 1, pp. 90–98, 2006.

[83] C. Song, H. Hu, S. Zhu, G. Wang, and G. Chen, "Nonisothermal catalytic liquefaction of corn stalk in subcritical and supercritical water," *Energy Fuels*, vol. 18, no. 1, pp. 90–96, 2004.

[84] D. Maldas and N. Shiraishi, "Liquefaction of biomass in the presence of phenol and H_2O using alkalies and salts as the catalyst," *Biomass Bioenenergy*, vol. 12, no. 4, pp. 273–279, 1997.

[85] S. Karagöz, T. Bhaskar, A. Muto, and Y. Sakata, "Catalytic hydrothermal treatment of pine wood biomass: effect of RbOH and CsOH on product distribution," *J. Chem. Technol. Biotechnol.*, vol. 80, no. 10, pp. 1097–1102, 2005.

[86] M. Watanabe, Y. Aizawa, T. Iida, T. M. Aida, C. Levy, K. Sue, and H. Inomata, "Glucose reactions with acid and base catalysts in hot compressed water at 473 vk," *Carbohydr. Res.*, vol. 340, no. 12, pp. 1925–1930, 2005.

[87] Z. Liu and F. Zhang, "Effects of various solvents on the liquefaction of biomass to produce fuels and chemical feedstocks," *Energ. Convers. and Manage.*, vol. 49, no. 12, pp. 3498–3504, 2008.

[88] S. P. Mun and M. H. El Barbary, "Liquefaction of lignocellulosic biomass with dioxane/polar solvent mixtures in the presence of an acid catalyst," *J. Ind. Eng. Chem.*, vol. 10, no. 3, pp. 473–477, 2004.

[89] A. Kržan, M. Kunaver, and V. Tišler, "Wood liquefaction using dibasic organic acids and glycols," *Acta Chim. Slov*, vol. 52, pp. 253–258, 2005.

[90] S. Itoh, A. Suzuki, T. Nakamura, and S. Yokoyama, "Production of heavy oil from sewage sludge by direct thermochemical liquefaction," *Desalination*, vol. 98, no. 1, pp. 127–133, 1994.

[91] L. Zhang, P. Champagne, and C. Xu, "Bio-crude production from secondary pulp/paper-mill sludge and waste newspaper via co-liquefaction in hot-compressed water," *Energy*, vol. 36, no. 4, pp. 2142–2150, 2011.

[92] S. Xiu, Y. Zhang, and A. Shahbazi, "Swine manure solids separation and thermochemical conversion to heavy oil," *Bioresources*, vol. 4, no. 2, pp. 458–470, 2009.

[93] T. Minowa, F. Zhen, T. Ogi, and G. Varhegyi, "Liquefaction of cellulose in hot compressed water using sodium carbonate: products distribution at different reaction temperatures," *J. Chem. Eng. Jpn.*, vol. 30, no. 1, pp. 186–190, 1997.

[94] M. Sasaki, Z. Fang, Y. Fukushima, T. Adschiri, and K. Arai, "Dissolution and hydrolysis of cellulose in subcritical and supercritical water," *Ind. Eng. Chem. Res.*, vol. 39, no. 8, pp. 2883–2890, 2000.

[95] W. S. Mok, M. J. Antal Jr, and G. Varhegyi, "Productive and parasitic pathways in dilute acid-catalyzed hydrolysis of cellulose," *Ind. Eng. Chem. Res.*, vol. 31, no. 1, pp. 94–100, 1992.

[96] M. Sasaki, B. Kabyemela, R. Malaluan, S. Hirose, N. Takeda, T. Adschiri, and K. Arai, "Cellulose hydrolysis in subcritical and supercritical water," *J. Supercrit. Fluids*, vol. 13, no. 1, pp. 261–268, 1998.

[97] T. Minowa, Z. Fang, T. Ogi, and G. Várhegyi, "Decomposition of cellulose and glucose in hot-compressed water under catalyst-free conditions," *J. Chem. Eng. Jpn.*, vol. 31, no. 1, pp. 131–134, 1998.

[98] W. Shu-Lai Mok and M. Antal, "Uncatalyzed solvolysis of whole biomass hemicellulose by hot compressed liquid water," *Ind. Eng. Chem. Res.*, vol. 31, no. 4, pp. 1157–1161, 1992.

[99] S. E. Jacobsen and C. E. Wyman, "Xylose monomer and oligomer yields for uncatalyzed hydrolysis of sugarcane bagasse hemicellulose at varying solids concentration," *Ind. Eng. Chem. Res.*, vol. 41, no. 6, pp. 1454–1461, 2002.

[100] Y. Qian, C. Zuo, J. Tan, and J. He, "Structural analysis of bio-oils from sub-and supercritical water liquefaction of woody biomass," *Energy*, vol. 32, no. 3, pp. 196–202, 2007.

[101] A. Demirbaş, "Conversion of wood to liquid products using alkaline glycerol," *Fuel Sci. Technol. Int.*, vol. 10, no. 2, pp. 173–184, 1992.

[102] R. Eager, J. Mathews, and J. Pepper, "Liquefaction of aspen poplar wood," *Can. J. Chem. Eng.*, vol. 60, no. 2, pp. 289–294, 1982.

[103] A. Demirbaş, M. Balat, and K. Bozbaş, "Direct and catalytic liquefaction of wood species in aqueous solution," *Energ. Source.*, vol. 27, no. 3, pp. 271–277, 2005.

[104] M. Kleinert and T. Barth, "Phenols from lignin," *Chem. Eng. Technol.*, vol. 31, no. 5, pp. 736–745, 2008.

[105] S. Zou, Y. Wu, M. Yang, C. Li, and J. Tong, "Thermochemical catalytic liquefaction of the marine microalgae Dunaliella tertiolecta and characterization of bio-oils," *Energy Fuels*, vol. 23, no. 7, pp. 3753–3758, 2009.

[106] T. Minowa, M. Murakami, Y. Dote, T. Ogi, and S.-y. Yokoyama, "Oil production from garbage by thermochemical liquefaction," *Biomass Bioenergy*, vol. 8, no. 2, pp. 117–120, 1995.

[107] A. Marcilla, L. Catalá, J. García-Quesada, F. Valdés, and M. Hernández, "A review of thermochemical conversion of microalgae," *Renew. Sustainable Energy Rev.*, vol. 27, pp. 11–19, 2013.

[108] P. Biller and A. B. Ross, "Hydrothermal processing of algal biomass for the production of biofuels and chemicals," *Biofuels*, vol. 3, no. 5, pp. 603–623, 2012.

[109] Z. Shuping, W. Yulong, Y. Mingde, I. Kaleem, L. Chun, and J. Tong, "Production and characterization of bio-oil from hydrothermal liquefaction of microalgae Dunaliella tertiolecta cake," *Energy*, vol. 35, no. 12, pp. 5406–5411, 2010.

[110] C. Zhong and X. Wei, "A comparative experimental study on the liquefaction of wood," *Energy*, vol. 29, no. 11, pp. 1731–1741, 2004.

[111] L. Zhang, C. C. Xu, and P. Champagne, "Energy recovery from secondary pulp/paper-mill sludge and sewage sludge with supercritical water treatment," *Bioresource Technol.*, vol. 101, no. 8, pp. 2713–2721, 2010.

[112] S. Karagöz, T. Bhaskar, A. Muto, and Y. Sakata, "Comparative studies of oil compositions produced from sawdust, rice husk, lignin and cellulose by hydrothermal treatment," *Fuel*, vol. 84, no. 7, pp. 875–884, 2005.

[113] S. Zou, Y. Wu, M. Yang, C. Li, and J. Tong, "Bio-oil production from sub-and supercritical water liquefaction of microalgae Dunaliella tertiolecta and related properties," *Energy Environ. Sci.*, vol. 3, no. 8, pp. 1073–1078, 2010.

[114] T. D. H. Nguyen, M. Maschietti, L.-E. Åmand, L. Vamling, L. Olausson, S.-I. Andersson, and H. Theliander, "The effect of temperature on the catalytic conversion of Kraft lignin using near-critical water," *Bioresource Technol.*, vol. 170, pp. 196–203, 2014.

[115] X. Pei, X. Yuan, G. Zeng, H. Huang, J. Wang, H. Li, and H. Zhu, "Co-liquefaction of microalgae and synthetic polymer mixture in sub-and supercritical ethanol," *Fuel Process. Technol.*, vol. 93, no. 1, pp. 35–44, 2012.

[116] A. J. Mørup, P. R. Christensen, D. F. Aarup, L. Dithmer, A. Mamakhel, M. Glasius, and B. B. Iversen, "Hydrothermal liquefaction of dried distillers grains with solubles: A reaction temperature study," *Energy Fuels*, vol. 26, no. 9, pp. 5944–5953, 2012.

[117] D. R. Vardon, B. Sharma, J. Scott, G. Yu, Z. Wang, L. Schideman, Y. Zhang, and T. J. Strathmann, "Chemical properties of biocrude oil from the hydrothermal liquefaction of Spirulina algae, swine manure, and digested anaerobic sludge," *Bioresource Technol.*, vol. 102, no. 17, pp. 8295–8303, 2011.

[118] P. Biller, A. B. Ross, S. Skill, A. Lea-Langton, B. Balasundaram, C. Hall, R. Riley, and C. Llewellyn, "Nutrient recycling of aqueous phase for microalgae cultivation from the hydrothermal liquefaction process," *Algal Res.*, vol. 1, no. 1, pp. 70–76, 2012.

[119] M. K. Akalın, K. Tekin, and S. Karagöz, "Hydrothermal liquefaction of cornelian cherry stones for bio-oil production," *Bioresource Technol.*, vol. 110, pp. 682–687, 2012.

[120] B. He, Y. Zhang, Y. Yin, T. Funk, and G. Riskowski, "Preliminary characterization of raw oil products from the thermochemical conversion of swine manure," *T. ASAE.*, vol. 44, no. 6, pp. 1865–1872, 2001.

[121] X. Yuan, J. Wang, G. Zeng, H. Huang, X. Pei, H. Li, Z. Liu, and M. Cong, "Comparative studies of thermochemical liquefaction characteristics of microalgae using different organic solvents," *Energy*, vol. 36, no. 11, pp. 6406–6412, 2011.

[122] X. Yuan, J. Tong, G. Zeng, H. Li, and W. Xie, "Comparative studies of products obtained at different temperatures during straw liquefaction by hot compressed water," *Energy Fuels*, vol. 23, no. 6, pp. 3262–3267, 2009.

[123] P. R. Christensen, A. J. Mørup, A. Mamakhel, M. Glasius, J. Becker, and B. B. Iversen, "Effects of heterogeneous catalyst in hydrothermal liquefaction of dried distillers grains with solubles," *Fuel*, vol. 123, pp. 158–166, 2014.

[124] S. Cheng, I. D'cruz, M. Wang, M. Leitch, and C. Xu, "Highly efficient liquefaction of woody biomass in hot-compressed alcohol- water co-solvents," *Energy Fuels*, vol. 24, no. 9, pp. 4659–4667, 2010.

[125] W.-T. Chen, Y. Zhang, J. Zhang, G. Yu, L. C. Schideman, P. Zhang, and M. Minarick, "Hydrothermal liquefaction of mixed-culture algal biomass from wastewater treatment system into bio-crude oil," *Bioresource Technol.*, vol. 152, pp. 130–139, 2014.

[126] Y. H. Chan, S. Yusup, A. T. Quitain, Y. Uemura, and M. Sasaki, "Bio-oil production from oil palm biomass via subcritical and supercritical hydrothermal liquefaction," *J. Supercrit. Fluid.*, vol. 95, pp. 407–412, 2014.

[127] D. Zhou, L. Zhang, S. Zhang, H. Fu, and J. Chen, "Hydrothermal liquefaction of macroalgae Enteromorpha prolifera to bio-oil," *Energy Fuels*, vol. 24, no. 7, pp. 4054–4061, 2010.

[128] X. Yuan, H. Li, G. Zeng, J. Tong, and W. Xie, "Sub-and supercritical liquefaction of rice straw in the presence of ethanol–water and 2-propanol–water mixture," *Energy*, vol. 32, no. 11, pp. 2081–2088, 2007.

[129] S.-y. Yokoyama, A. Suzuki, M. Murakami, T. Ogi, K. Koguchi, and E. Nakamura, "Liquid fuel production from sewage sludge by catalytic conversion using sodium carbonate," *Fuel*, vol. 66, no. 8, pp. 1150–1155, 1987.

[130] S. Yin, R. Dolan, M. Harris, and Z. Tan, "Subcritical hydrothermal liquefaction of cattle manure to bio-oil: Effects of conversion parameters on bio-oil yield and characterization of bio-oil," *Bioresour. Technol.*, vol. 101, no. 10, pp. 3657–3664, 2010.

[131] D. R. Vardon, B. K. Sharma, G. V. Blazina, K. Rajagopalan, and T. J. Strathmann, "Thermochemical conversion of raw and defatted algal biomass via hydrothermal liquefaction and slow pyrolysis," *Bioresource Technol.*, vol. 109, pp. 178–187, 2012.

[132] P. J. Valdez, M. C. Nelson, H. Y. Wang, X. N. Lin, and P. E. Savage, "Hydrothermal liquefaction of Nannochloropsis sp.: Systematic study of process variables and analysis of the product fractions," *Biomass Bioenenergy*, vol. 46, pp. 317–331, 2012.

[133] M. Tymchyshyn and C. C. Xu, "Liquefaction of bio-mass in hot-compressed water for the production of phenolic compounds," *Bioresource Technol.*, vol. 101, no. 7, pp. 2483–2490, 2010.

[134] S. S. Toor, L. Rosendahl, M. P. Nielsen, M. Glasius, A. Rudolf, and S. B. Iversen, "Continuous production of bio-oil by catalytic liquefaction from wet distiller's grain with solubles (WDGS) from bio-ethanol production," *Biomass Bioenenergy*, vol. 36, pp. 327–332, 2012.

[135] S. Sawayama, S. Inoue, T. Minowa, K. Tsukahara, and T. Ogi, "Thermochemical liquidization and anaerobic treatment of kitchen garbage," *J. Fermen. Bioeng.*, vol. 83, no. 5, pp. 451–455, 1997.

[136] G. van Rossum, W. Zhao, M. Castellvi Barnes, J.-P. Lange, and S. R. Kersten, "Liquefaction of lignocellulosic biomass: Solvent, process parameter, and recycle oil screening," *ChemSusChem*, vol. 7, no. 1, pp. 253–259, 2014.

[137] A. Ross, P. Biller, M. Kubacki, H. Li, A. Lea-Langton, and J. Jones, "Hydrothermal processing of microalgae using alkali and organic acids," *Fuel*, vol. 89, no. 9, pp. 2234–2243, 2010.

[138] R. A. Corbitt, *Standard handbook of environmental engineering, Second Edition.* McGraw Hill, Washington, D.C., 1999.

[139] A. Demirbaş, "Calculation of higher heating values of biomass fuels," *Fuel*, vol. 76, no. 5, pp. 431–434, 1997.

[140] D. Liu, L. Song, P. Wu, Y. Liu, Q. Li, and Z. Yan, "Direct hydro-liquefaction of sawdust in petroleum ether and comprehensive bio-oil products analysis," *Bioresource Technol.*, vol. 155, pp. 152–160, 2014.

[141] S. Channiwala and P. Parikh, "A unified correlation for estimating HHV of solid, liquid and gaseous fuels," *Fuel*, vol. 81, no. 8, pp. 1051–1063, 2002.

[142] K. H. Esbensen, D. Guyot, F. Westad, and L. P. Houmoller, *Multivariate data analysis-in practice: an introduction to multivariate data analysis and experimental design.* CAMO Software, 2002.

[143] J. Larson-Hall, *A guide to doing statistics in second language research using SPSS.* Routledge, 2009.

[144] B. Efron and B. Efron, *The jackknife, the bootstrap and other resampling plans.* SIAM, 1982, vol. 38.

Paper B

Characterization of liquid products from hydrothermal liquefaction (HTL) of biomass via solid-phase microextraction (SPME)

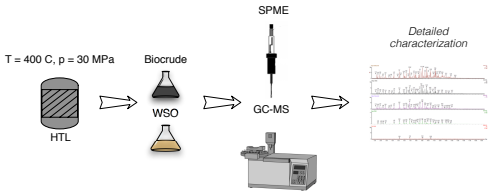

Katarzyna R. Arturi, Kathrine R. Toft, Rudi P. Nielsen, Lasse A. Rosendahl, and Erik G. Søgaard

The paper has been published in the
Biomass and Bioenergy Vol. 88, pp. 116–125, 2016.

Abstract

Although hydrothermal liquefaction of biomass (HTL) is considered one of the most promising techniques for production of drop-in biofuels, the challenges associated with its development and expansion are still significant. One of the issues is concerned with characterization of the liquid product (biocrude) and by-product (aqueous phase), which, due to their complexity and polarity, are considered an analytical challenge. In this study, solid-phase microextraction (SPME) combined with gas chromatography mass spectroscopy (GC-MS) were applied for a qualitative characterization of both the aqueous phase and the biocrude from HTL. Furthermore, a method for an optimal application of SPME on water soluble organics (WSO) was developed with regard to the fiber type and a number of extraction parameters. For the biocrude, the optimization was limited to the fiber type. Four different SPME fibers were used, namely 65 µm poly(dimethylsiloxane) divinylbenzene (PDMS/DVB), 85 µm poly(acrylate) (PA), 7 µm poly(dimethylsiloxane) (PDMS), and 100 µm poly(dimethylsiloxane) (PDMS), covering a wide range of potential compounds. The results have shown that characterization of liquid products from HTL is significantly improved by application of SPME. Four groups of compounds were identified: I) Low molecular weight (MW) aliphatics; II) Cyclic compounds; III) Aromatics; and IV) High MW compounds. The oil phase consisted ofdeoxygenated species of chemicals present in the water phase, including complex polymerized cyclic structures and aromatic-aliphatic assemblies. 65 µm PDMS/DVB fiber was the most efficient one for adsorption of compounds from both the biocrude and the aqueous phase. Keywords: solid-phase microextraction, hydrothermal liquefaction, biomass conversion, liquid products, method development.

1 Introduction

Hydrothermal liquefaction (HTL) is one of the most promising thermochemical techniques [1–6], in which biopolymers are converted by the means of near- or supercritical water (T_{cr} = 647 K and P_{cr} = 22,1 MPa) into a crude oil-like product called biocrude [7–13]. One of the greatest advantages of HTL compared to nearly all other types of biomass conversion techniques is its ability to process any kind of wet biomass, including complex mixtures of lignocellulose, protein, and fats [14–16]. This is significant, as first generation biomass, e.g. starch, required for biochemical production of ethanol or chemicals, are expected in the future to be needed as food for the rapidly growing human population. Waste, on the other hand, is going to be a nearly unlimited resource and thus an attractive choice in the future biorefinery [17], increasing both the sustainability and the economy of the processes such as HTL. Since the feed in HTL is complex, so is its final product, typically a two-phase mixture of biocrude and process water with suspended char particles. Small amounts of synthesis gas are produced as well. The aqueous phase contains a great number of polar water soluble organics (WSO), most commonly aliphatic and aromatic alcohols, acids, and ketones. The derivatives of cresols, phenols, pyrans, and furans are common as well, and so are sugars [18]. Compared to that, biocrude

from HTL contains non-polar short and long chain aliphatic, cyclic, and aromatic units. Functional groups of limited polarity can occur as well. The aqueous phase and biocrude have a common origin, i.e. the biomass and its derivatives dissolved in near- and supercritical water, from which the biocrude is formed during the cooling step.

The complex make-up of the liquid HTL products make them an analytical challenge [19–21]. While a number of techniques can be used for general description of the product properties (e.g. heating value, acid number, viscosity), a more detailed characterization is required for understanding the mechanisms behind HTL, optimizing the process for oil production, and designing an appropriate upgrading route for the biocrude. Additionally, the knowledge about the composition of the water phase is crucial for selection of an optimal waste treatment and disposal procedure. A detailed description of composition can normally be obtained by a combination of chromatography and spectroscopy, e.g. gas chromatography mass spectroscopy (GC-MS), which may be the most common analytical tool for description of liquid HTL products [22–27]. Another popular approach includes the use of liquid chromatography, e.g. high performance liquid chromatography time-of-flight mass spectroscopy (HPLC-TOF-MS) [20]. Both methods have a number of disadvantages including their prerequisite for the analytes to be volatile or soluble in a certain solvent, which limits the number of potential compounds identified. According to [28], not more that half of the compounds present in the biocrude from HTL can be identified with GC-MS. A typical chromatogram of biocrude contains 100-200 peaks, with approx. 30 being the most significant ones [20]. The abundance of peaks leads to bad separation and convolution, and ultimately to a poor identification. A number of approaches has been tried to improve the analysis of biocrudes from thermochemical conversion of biomass, mostly pyrolysis [29–33], and similar conversion routes [34–38]. These studies focus on either an improved separation or a better identification, e.g. thin layer chromatography (TLC) [39], ion-exchange and size-exclusion chromatography [40], Fourier transform ion cyclotron resonance mass spectroscopy (FTICR-MS) [19, 25, 26, 41–43], and pyrolysis coupled to gas chromatography mass spectroscopy (Pyr-GC-MS) [44, 45]. However, a number of simpler possibilities, including solid-phase microextraction (SPME), which has been successful in a number of other applications [46–48], remains unexamined. SPME is an innovative solvent-free extraction method concerned with the equilibrium between the sample and a fiber covered with adsorbent or absorbent material, rather than the exhaustive transfer of compounds known from liquid-liquid extraction (LLE) [49]. The unique mechanism behind SPME makes it interesting as a possible application for analysis of complex and rather concentrated matrices, but so far, it has been used very sparingly in connection with HTL [50]. In this study, the performance of SPME as a tool for sampling of compounds from HTL products, both the aqueous phase and biocrude, for GC-MS was examined qualitatively. Furthermore, a method for an optimal application of SPME on the water phase was systematically developed.

2 Materials and Methods

2.1 Samples and materials

The biocrude and aqueous phase samples used in this study were produced by continuous liquefaction of aspen wood and glycerol with a catalyst (K_2CO_3) in a bench scale reactor (CBS1) at the Department of Energy Technology, Aalborg University. Process conditions were 400 °C and 30 MPa. The properties of the biomass and separation procedure are described previously [51]. Both the aqueous, as well as the biocrude samples, were analyzed with SPME by withdrawing an aliquot with an automatic pipette and placing it in a vial. A number of GC-MS runs with liquid-liquid extraction (ratio 1:1, extraction time 30 min, DEE (diethyl ether) as the solvent for the aqueous phase, hexane for the oil) of the samples was performed for comparison purposes. When indicated, trimethylsilyl trifluoromethanesulfonate (TMS) was used as derivatization agent. For the water phase, TMS derivatization was proceeded by I) drying, or II) DEE extraction. The TMS procedure was as follows: addition of 0.002 cm^3 TMS to 5 mg sample, heating to 75 °C for 1 hr, removal of the solvent, GC-MS analysis in 5 cm^3 hexane. The organic solvents were purchased from Sigma Aldrich: hexane (ACS reagent, anhydrous, ≥ 99.9 %), diethyl ether (DEE, ACS reagent, anhydrous, ≥ 99.9 %), trimethylsilyl trifluoromethanesulfonate (TMS, purum, ≥ 98 %). The used salting-out agent was sodium chloride (NaCl, ACS reagent, anhydrous, free-flowing, ≥ 99 %).

2.2 SPME fibers

The SPME holder (manual sampling), and fibers used in the study were purchased from Supelco (Bellefonte, PA, USA). Four different fibers were tested: 7 and 100 μm poly(dimethylsiloxane) (PDMS), 65 μm poly(dimethylsiloxane) divinylbenzene (PDMS/DVB), and 85 μm poly(acrylate) (PA). The needles were either 3 or 24 gauge. Before the first daily analysis, the fibers were conditioned in the GC injector as recommended by the manufacturer (Table B.1). For the following injections, a cleaning run was performed (30 min at T = 250 °C), followed by a blank run checking for a possible carry-over. The fibers were immersed either in the head-space (HS) or in the liquid phase (direct immersion, DI) of the samples. A fresh sample (5 cm^3 for HS and 10 cm^3 for DI) was placed in a 22 cm^3 glass vial containing a magnetic stirrer (when necessary with added salt, acid, or base), and sealed using a PTFE-coated silicone rubber septum. The vial was placed in a thermostated water bath adjusted to the experiment conditions tested (T_{ext}) and tempered for 2 min. The depth of immersion (reading 4.0 on the holder) was controlled by the screw and was constant through all steps of the process. Once the extraction step was finished after t_{ext}, the fiber was retracted into the SPME syringe and any drop of water attached to the needle was removed with a tissue. The syringe was then injected directly through the GC septum and into the GC injection port at T_{inj} and desorbed for 5 seconds.

Table B.1: Properties and conditioning temperatures for the fibers.

Fiber	Type	Target compounds	m/z	T_{cond} (°C)
65 μm PDMS/DVB	Adsorbent	Volatiles, amines and amides	50-300	250
85 μm PA	Absorbent	Polar semi-volatiles	80-300	280
100 μm PDMS	Absorbent	Volatiles	60-275	250
7 μm PDMS	Absorbent	Non-polar high MW	125-600	320

2.3 Process parameters

A number of parameters, including the influence of extraction (adsorption or absorption) temperature (T_{ext} = 25 °C or 50 °C), extraction time (t_{ext} = 10 min or 20 min), salt presence, pH (pH below 2, ≈6, or above 12 determined by MColorpHast™ pH Indicator Strips), type of fiber used (see Section 2.2), and extraction method (HS and DI), were screened for their influence on SPME of WSO from the HTL aqueous phase. The pH of the water samples was adjusted by addition of HCl (below pH = 2) or NaOH (above pH = 12). Salinity was changed by addition of 1 g of NaCl. Not all combinations of the factors were examined. An initial screening of the performance of the fibers under selected standard conditions was performed for both HS (T_{ext} = 25 °C, t_{ext} = 20 min, no salt, pH ≈ 6) and DI (T_{ext} = 25 °C, t_{ext} = 10 min, no salt, pH ≈ 6). This was followed by an examination of the effects of pH on HS extraction from the fibers, and a study of the influence of salt on HS and DI uptake from the 65 μm PDMS/DVB fiber. The effect of time and temperature of extraction was determined for HS method and all the fibers. The combinations of factors chosen for analysis were selected and performed in triplicate. SPME of organics from the biocrude was evaluated with regard to the fiber type, but not the extraction conditions. Due to the properties of the biocrude and poor durability of the fibers, it was not possible to study the influence of pH, the presence of salt, or the extraction method (HS or DI). The biocrude was extracted at T_{ext} = 25 °C for 10 min.

2.4 Apparatus

The samples were all analyzed with a Perkin Elmer Clarus GC 580 and MS SQ 8 S with EI ionization and quadrupole ion analyzer. The gas chromatograph was equipped with a PerkinElmer Crossbond column (30 m X 0.25 mm ID) coated with 0.25 μm stationary phase (95 % dimethyl polysiloxane and 5 % diphenyl) and the carrier gas used was helium (constant flow 1 cm^3/min). Detector temperature was 180 °C. Electron impact mass spectra were recorded at 70 eV ionization energy. The injector was used in split mode (50:1). The applied SPME method involved desorption at T_{inj} = 200 °C followed by a heating ramp of 10 °C/min from T_{start} = 40 °C (hold for 2 min) to 200 °C (hold for 2 min). A solvent delay time of 1 min was used, to avoid overloading the mass spectrometer with organic solvents. The samples extracted with LLE were analyzed using the following method: T_{inj} = 300 °C, split 30:1, heating ramp of 20 °C/min from T_{start} = 75 °C (hold 1.5 min) to 275 °C (hold for 10 min), solvent delay 2.5 min, scan m/z 75 - 600. A provisional

identification of the compounds was performed with the NIST database.

3 Results and Discussion

3.1 Water phase characterization

In the water phase, more than 140 compounds of diverse polarity were found and tentatively identified with the NIST database. The identifications were evaluated with regard to the values of reverse match factor (RMF), which is considered a particularly useful tool for samples with a complex matrix. In general, the identifications were of high quality. Quantitatively speaking, the distribution of the obtained RMF values was [786, 866, 895] for the 1st (Q1), 2nd (Q2), and 3rd (Q3) quartiles of the identified compounds, respectively. This means, that only 25% of the identifications had a RMF value below 786. The minimum value was 732. Most of the compounds were identified with a RMF of 866 (median), while 25 % of the RMFs were above 895. The compounds could be divided into four distinct groups of organics with nearly consecutive retention times:

1. Low molecular weight (MW) polar aliphatics (RT $\approx$ 1 - 5 min)
2. Cyclic compounds - homo- and heterocyclic (RT $\approx$ 5 - 10 min)
3. Phenol derivatives (RT $\approx$ 10 - 14 min)
4. High MW compounds (RT $\approx$ 14 - 20 min)

A systematic evaluation of the most significant peaks and the abundance of the corresponding compounds found in the water phase is shown in Tables B.6 and B.7. Only a limited number of high MW compounds is listed, as their overall impact on the samples' content was low. The group of polar aliphatics was represented by small alcohols, ketones, and esters. The most common cyclic compounds included methylated cyclopentanone and cyclopentenone derivatives, and a number of heterocyclic compounds, e.g. furans and dioxins. The major constituents of the water phase obtained with SPME were in accordance with previous results using standard separation methods [52–56]. However, the results have also shown that a combined SPME GC-MS method is much more efficient at identification of the polar WSOs compared to the standard extraction methods (Figure B.1), which tend to underestimate the complexity of the aqueous phase. LLE can still be useful for determination of certain compounds, e.g. methylated benzenediols (DEE), benzopyrans (DEE and TMS), and glycerol (TMS). The most descriptive WSO analysis should therefore combine the results from SPME, liquid-liquid extraction, and derivatization.

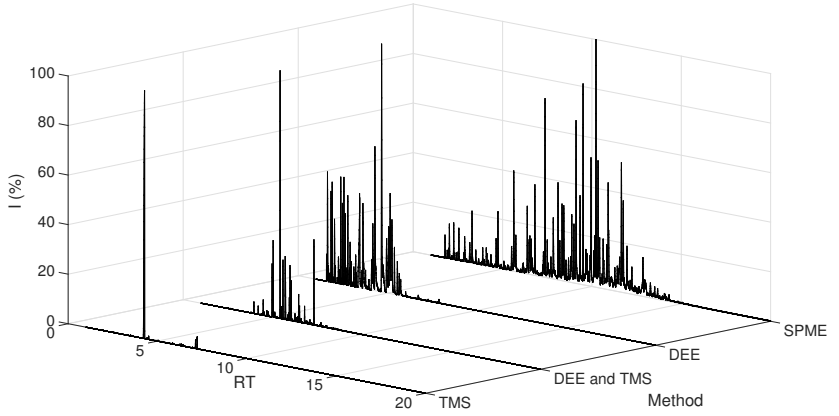

Fig. B.1: Comparison between LLE results for the water phase (extraction with DEE and TMS) and the current SPME results (HS, 65 μm PDMS/DVB, T_{ext} = 50 °C, no salt, pH≈6, t_{ext} = 10 min).

3.2 Biocrude characterization

The biocrude samples were analyzed with 65 μm PDMS/DVB, 85 μm PA, and 100 μm PDMS fibers, covering a wide range of possible compounds including volatiles and semi-volatiles, polar and non-polar compounds. Compared to the traditional methods of biocrude analysis, SPME yielded a more detailed description of the oil (Figure B.2), identifying, once again, more than 140 number of compounds over a wide range of retention times (Table B.8). SPME on the biocrude was clearly dependent on the type of fiber applied, with 65 μm PDMS/DVB being the most efficient one. On average, approx. 85% of the most significant peaks could be explained (Table B.2). The distribution of the obtained RMF values was [778, 847, 896] for the 1st (Q1), 2nd (Q2), and 3rd (Q3) quartiles of the identified compounds, respectively. The biocrude contained a number of components found in the water phase, which was not surprising, considering their common origin. Small acids, alcohols, ketones, and aldehydes, that were seen in WSO, were, to a certain degree, replaced by C4-C8 branched aliphatic alkanes and alkenes, while the amount of cyclopentenone derivatives was reduced by their conversion to cycloalkanes. The aromatic compounds were present as well, but as toluene and naphthalene, and not phenol derivatives. A small amount of oxygenated compounds could still be found in the biocrude, mostly in the form of ether links. At high RT values (RT $\geq$ 9 min), high MW molecules have begun to emerge.

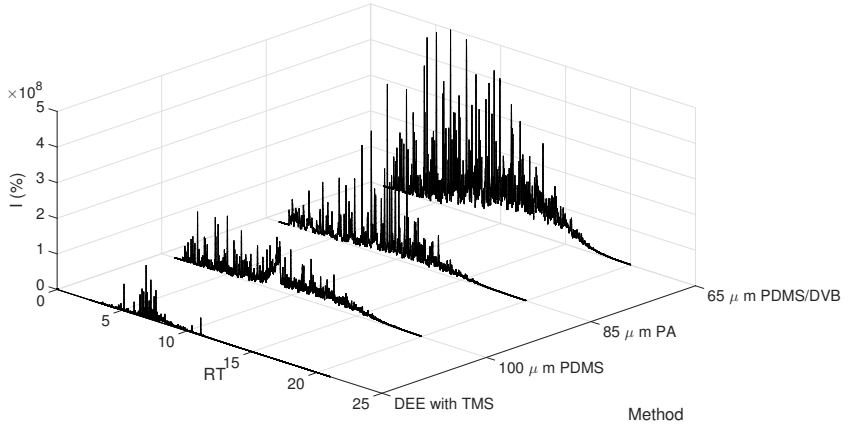

Fig. B.2: Comparison between LLE results for the biocrude (extraction with DEE and TMS) and the current SPME results obtained with different fibers (HS, T_{ext} = 25 °C, t_{ext} = 10 min) for characterization of the biocrude from HTL.

Table B.2: The distribution of the compounds found in the biocrude with SPME GC-MS (HS, 65 μm PDMS/DVB, T_{ext} = 25 °C, t_{ext} = 10 min).

Compounds	Peak A (%)
Aliphatic	3.41 %
Cyclic compounds	34.9 %
Aromatic	46.5 %
Explained	84.8 %

3.3 Reaction mechanisms

The lignocellulosic biomass is degraded by depolymerization of protolignin, and the resulting biopolymers (lignin oligomers, cellulose, and hemicellulose) are further hydrolyzed into monomers and dimers of phenylpropane (e.g. anisoles, alkylphenols, guaiacols and catechols), glucose, and C5-sugars. More stable conversion products may remain as oligomeric and dimeric units. At this point, the compounds are dissolved in the water phase and can follow a number of pathways, depending on the reaction conditions [57–60]. From the obtained products, it was clear that the formed mono-sugars were converted into WSO both through the retro-aldol condensation and the dehydration reaction.The former mechanism took place with base as catalyst and resulted in formation of low MW compounds, e.g. butanone, pentanol, hexanone. In the latter scheme, sugars were initially converted with acid as catalyst into furan, and then into cyclopentanone and cyclopentenone derivatives (2,4-dimethyl-cyclopentanone, 3,4-dimethyl-2-cyclopenten-1-one, and 4,4-dimethyl-2-cyclopentene-1-one). These smaller units continued to be dehydrated and decar-

boxylated into oxygen free alkanes and cycloalkanes (hexane, 1,2,3,4-tetramethylcyclobutene), which were then polymerized into complex high MW structures like 4-isopropylidene-2-methyl-cyclopentan-1-al. It is well known, that the dehydration reactions, if left unchecked, will result in formation of unstable structures that tend to repolymerize into solid char. An alternative origin of the high MW compounds could be assigned to the incomplete depolymerization of the biomass. The aromatic phenol derivatives could have originated both from the cleavage of the ether links from the protolignin feed, but also from the conversion of cellulose through condensation and cyclization of unstable glucose conversion intermediates [61]. The former mechanism is more probable, as the reported intermediate WSO compounds were rich in oxygen, which would fit with the original structure of lignin. The phenolic compounds were reduced further to toluene and its derivatives by removal of oxygen through dehydration or decarboxylation. These compounds were not polymerized into polyaromatic structures, but tended to be joined with the aliphatic alkanes of small MW forming long tails. Upon cooling the homogeneous reaction mixture is separated into WSO and the biocrude fractions. The reaction pathways for biomass conversion in HTL are summarized on Figure B.3.

3.4 Method development for aqueous phase

Fibers and methods (HS and DI) The effectivity of each SPME sampling procedure was estimated with the total area of GC-MS peaks as indicator for the amounts of transferred (adsorbed or absorbed) compounds. The extraction depended both on the fiber type and the process conditions applied (column pH $\approx$ 6 in Table B.3). Among the investigated fibers, the adsorbent 65 μm PDMS/DVB fiber has shown the largest HS uptake at the selected standard conditions, while the transfer to the 7 μm PDMS fiber was more than 40 times smaller. The 65 μm PDMS/DVB fiber is an adsorbent fiber, in which DVB particles are suspended in a PDMS liquid phase. The mechanism of extraction for this fiber type involves physical entrapment of the analytes in micro- meso-, and macrophores of the coating. The small and middle-sized compounds, so commonly found in the HTL aqueous phase, were easily trapped internally, while high MW compounds were adsorbed on the surface and held there by hydrogen bonding and Van der Walls interactions. Absorbent fibers (85 μm PA, 7 μm PDMS, and 100 μm PDMS) are covered by one type of a liquid sponge-like coating. In this case, extraction is based on partitioning of analytes retained by the coatings' thickness. As shown by the results, the absorbent fibers were generally less effective for extraction, either uptake or retention, of the WSO compounds. The same compounds were extracted by the different fibers. The uptake by HS and DI was approximately the same for all fibers (twice as big for the double amount of sample: 100 μm PDMS - $1.39{\cdot}10^8$, 85 PA - $1.56{\cdot}10^8$, and 7 μm PDMS - $1.76{\cdot}10^7$, 65 μm PDMS/DVB - $1.38{\cdot}10^8$). HS was the preferred method of extraction rather than DI, which, in most cases, led to the introduction of water into the column and convolution of the peaks.

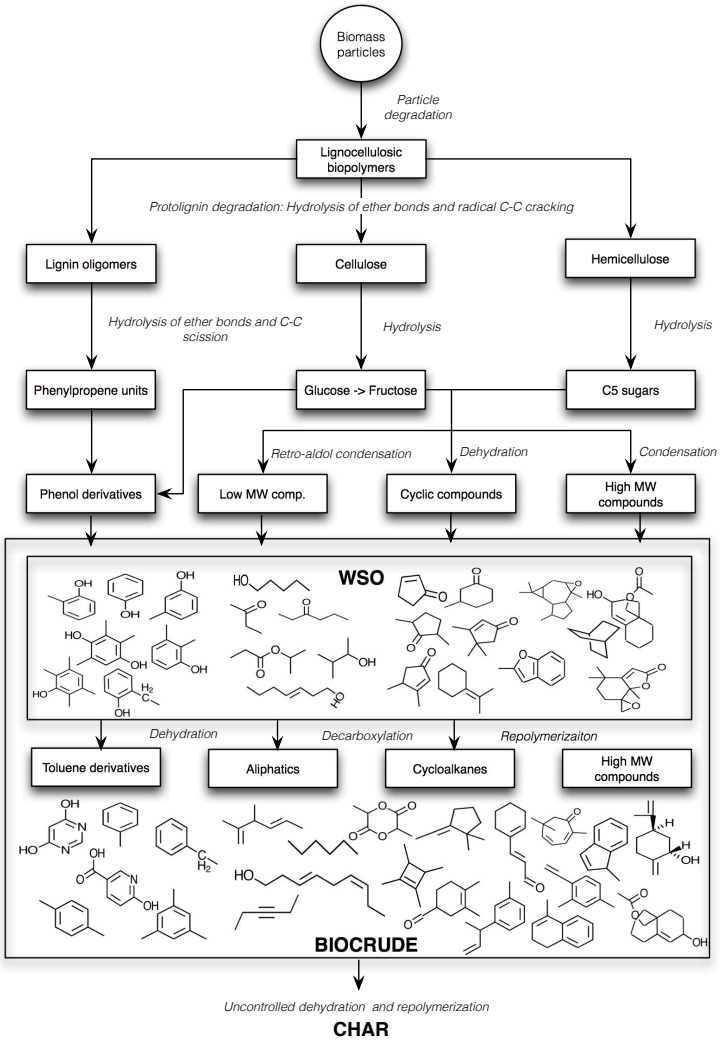

Fig. B.3: Reaction pathways showing the most common compounds identified by SPME.

The variability in extraction efficiency by SPME could be assessed in more detail by application of quantitative analysis, e.g. internal standard method. The applied semi-quantitative peak area method gives only a rough estimate of the amounts of compounds in the samples.

pH (HS) and NaCl (HS and DI for 65 μm PDMS/DVB) Since only neutral, non-ionized species are transferred to the SPME fibers, a strong dependence between the extraction yield and the pH of a sample is expected for acidic and basic species present. A low pH value would lead to a full conversion of the acidic analytes into neutral forms and their enhanced extraction. At high pH values, the extraction efficiency of bases would increase. Modification of pH led to a significant decrease of the HS uptake on the 65 μm PDMS/DVB fiber for acidic pH values, and a similar moderate reduction in the basic environment (Table B.3 and Figure B.4).

Table B.3: SPME GC-MS results for the aqueous phase, different fibers, and pH values (HS, T_{ext} = 25 °C, no salt, t_{ext} = 20 min). Fiber 85 μm PA was investigated at pH ≈ 6 and pH ≤ 2. Fiber 7 μm PDMS was investigated at pH ≈ 6 and pH ≥ 12.

	pH≈6		Acidic pH≤2		Basic pH≥12	
Fiber type	Peak A	RSD%	Peak A	RSD%	Peak A	RSD%
65 μm PDMS/DVB	$2.10{\cdot}10^8$	19.4	$1.38{\cdot}10^8$	32.9	$1.86{\cdot}10^8$	8.12
100 μm PDMS	$4.12{\cdot}10^7$	17.4	$5.45{\cdot}10^7$	46.5	$4.78{\cdot}10^7$	10.6
85 μm PA	$9.32{\cdot}10^7$	22.0	$1.45{\cdot}10^8$	65.7	-	-
7 μm PDMS	$5.85{\cdot}10^6$	23.1	-	-	$7.03{\cdot}10^6$	7.09

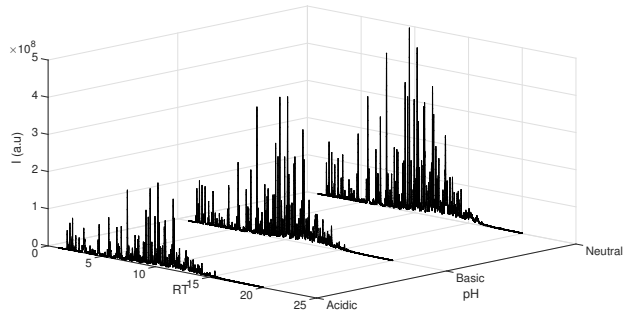

Fig. B.4: Comparison between SPME of WSO from the water phase for different pH values (HS, 65 μm PDMS/DVB, T_{ext} = 25 °C, no salt, t_{ext} = 20 min).

However, there was no statistically significant difference for HS extraction for the absorbent fibers obtained at different pH values. DI sampling was not studied for different pH levels in order to avoid fiber damage due to the direct contact of the coating with samples at very low or high pH values. As reported previously [62, 63], addition of salt may result in a change of the partial pressure of analytes, solubility and surface tension, increasing the yield of analyte uptake. The presence of NaCl resulted in a slightly increase of the uptake on the 65 μm PDMS/DVB fiber with HS (the peak area under the chromatograms with and without salt was $2.67{\cdot}10^8$ contra $2.10{\cdot}10^8$, respectively). The uptake on the 65 μm PDMS/DVB fiber by DI resulted in an even more significant increase in extraction when salt was added ($2.01{\cdot}10^8$ contra $1.38{\cdot}10^8$, respectively).

Adsorption time (HS) Time of adsorption is the period when the the fiber is exposed to the sample. Ideally, an interfacial equilibrium position should be reached within this period, which is essential for obtaining the maximum efficiency, precision, and low detection limits. For HS and 65 μm PDMS/DVB fiber, the time of adsorption influenced the amount of organics deposited on the fibers, generally increasing the latter with the former. As shown in Table B.4, for the low MW acids, ketones, aldehydes, and alcohols, the uptake increased initially (t_{ext} = 10 min), and then decreased again (t_{ext} = 20 min), most probably due to the competition between the compounds for the adsorption sites and desorption of the more volatile compounds. Increasing the time of adsorption had a slightly negative effect on the overall HS uptake of compounds on the 100 μm PDMS fiber (total peak area was $1.45{\cdot}10^8$ for t = 10 min and $1.38{\cdot}10^8$ tor t = 20 min), but had no effect at the remaining fibers. It was noted, that the uptake of high MW compounds was rather poor at T_{ext} = 25 °C independently of t_{ext} (Figure B.5).

Table B.4: SPME GC-MS results for the aqueous phase and different adsorption times (HS, 65 μm PDMS/DVB, T_{ext} = 25 °C, no salt, pH ≈ 6).

t_{ext}	5 min		10 min		20 min	
	Peak A	RSD (%)	Peak A	RSD (%)	Peak A	RSD (%)
Aliphatic low MW	$1.29{\cdot}10^7$	5.96	$1.69{\cdot}10^7$	17.1	$1.32{\cdot}10^7$	7.45
Cyclic compounds	$7.20{\cdot}10^7$	9.29	$8.24 \cdot 10^7$	18.2	$9.73{\cdot}10^7$	13.5
Aromatic	$2.42{\cdot}10^7$	6.48	$4.89{\cdot}10^7$	19.9	$6.74 \cdot 10^7$	13.5
Total	$1.09{\cdot}10^8$		$1.48 \cdot 10^8$		$1.78{\cdot}10^8$	

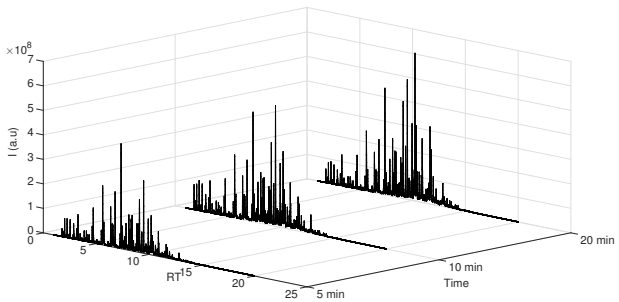

Fig. B.5: Comparison between SPME of WSO from the water phase for different adsorption times (HS, 65 μm PDMS/DVB, T_{ext} = 25 °C, no salt, pH ≈ 6).

Adsorption temperature (HS) An increased temperature of adsorption (T_{ext}) is expected to decrease the time required to reach the equilibrium zone and increase the uptake of the compounds. This can be explained by the increased diffusion and partial pressure of volatile species at elevated temperatures. However, too high temperatures could lead to thermal desorption of the more volatile compounds. The

positive correlation between the uptake and T_{ext} was proved for specified groups of compounds transferred to the 65 μm PDMS/DVB fiber by HS (Table B.5), for which the uptake increased with temperature. The trend was strongest for the low MW organics and the aromatics. The same results were achieved with HS for the 85 μm PA fiber (for T = 25 °C the peak area was $2.14{\cdot}10^8$, while for T = 50 °C the peak area was $5.71{\cdot}10^8$). However, increasing the temperature of adsorption had the reverse effect on the HS uptake by the 100 μm PDMS (for T = 25 °C the peak area was $1.45{\cdot}10^8$, while for T = 50 °C the peak area was $4.12{\cdot}10^7$), and the 7 μm PDMS (for T = 25 °C the peak area was $1.18{\cdot}10^8$, while for T = °C the peak area was $3.53{\cdot}10^7$) fibers, decreasing the adsorbed amounts with increasing temperature. It must also be noted that at high T_{ext}, the relative standard deviation of the measurements increased with increasing temperature. The best reproducibility was achieved at low temperatures and extraction times. Quantification with SPME is challenging due to the fact that results depend heavily on the equilibrium (or pre-equilibrium) state in the vial, and are therefore sensitive to minuscule changes in extraction conditions.

Table B.5: SPME GC-MS results for the water phase and different adsorption temperatures (HS, 65 μm PDMS/DVB, no salt, pH ≈ 6, t_{ext} = 10 min).

T_{ext}	25 °C		50 °C	
	Peak A	RSD (%)	Peak A	RSD (%)
Aliphatic low MW	$1.69{\cdot}10^7$	17.1	$2.29{\cdot}10^7$	16.1
Cyclic compounds	$8.24 \cdot 10^7$	18.2	$9.06{\cdot}10^7$	15.5
Aromatics	$4.89{\cdot}10^7$	19.9	$9.60{\cdot}10^7$	22.2
Total	$1.48{\cdot}10^8$		$2.09{\cdot}10^8$	

4 Conclusions

A combination of SPME and GC-MS was shown to be an excellent low-tech method providing detailed characterization of the organics in the water phase and biocrude from HTL. The method is fast, does not require organic solvents, and can be applied in combination with standard GC-MS equipment. The results from the analysis of the aqueous phase have shown that its composition is far more complex than previously anticipated. Four significant groups of compounds were identified in the water phase and the biocrude: aliphatics, cyclic compounds, aromatics, and high MW compounds. The difference between the composition of the water phase and the biocrude was related to the compounds' polarity and oxygen content. SPME of organics from the biocrude depended on the fiber type. The adsorbent fiber 65 μm poly(dimethylsiloxane) divinylbenzene (PDMS/DVB), which was designed for extraction of diverse volatiles, was the best choice for analysis of both the water and the oil phases. Extraction from the water phase was strongly dependent on both the fiber type and the process conditions, especially the adsorption time and

temperature. Optimal SPME of WSO was achieved with HS, T_{ext} = 50 °C, t_{ext} = 10 min, and pH ≈ 6. Addition of salt resulted in a slight, but statistically insignificant, increase in the mass transfer.

5 Acknowledgements

The research was conducted as a part of the Center for BioOils (C3BO) project, which was financially supported by The Danish Council for Strategic Research (grant no. 1305-00030B).

6 Supporting Information

Table B.6: Compounds identified by SPME GC-MS analysis in the water phase (HS, 65 μm PDMS/DVB, T_{ext} = 50 °C, no salt, pH≈6, t_{ext} = 10 min). Q represents the quartile of identification quality.

Nr.	RT	Compound	Peak A (%)	Q
1	1.81	Acetone	0.54	Q3
2	2.01	2-Propyl propionate	0.89	Q3
3	2.30	2-Butanone	1.07	Q3
4	2.56	Methyl propionate	0.79	Q3
5	2.88	2-Butanone, 3-methyl-	0.80	Q3
6	3.13	2-Butanol, 3-methyl-	0.61	Q1
7	3.21	2-Pentanone	1.06	Q2
8	3.88	1-Butanol, 2-methyl	0.43	Q3
9	4.68	3-Hexanone	0.69	Q3
10	4.78	Cyclopentanone	1.78	Q3
11	5.53	2-Cyclopenten-1-one	0.78	Q2
12	5.66	Cyclopentanone, 2-methyl-	3.01	Q3
13	5.77	Clopentanone, 3-methyl	0.77	Q3
14	6.34	3-Hepten-1-ol	1.22	Q1
15	6.41	Cyclopentanone, 2,5-dimethyl-	0.58	Q3
16	6.51	Cyclohexanone, 3-methyl-	0.73	Q2
17	6.55	Cyclopentanone, 2,4-dimethyl-	0.76	Q2
18	6.75	Cyclopentanol, 2,4-dimethyl-	2.18	Q1
19	7.40	2-Cyclopenten-1-one, 3,4-dimethyl-	4.56	Q2
20	7.52	Cyclopentene-4-methyl	0.71	Q2

Table B.7: Compounds identified by SPME GC-MS analysis in the water phase (HS, 65 μm PDMS/DVB, T_{ext} = 50 °C, no salt, pH≈6, t_{ext} = 10 min). Q represents the quartile of identification quality.

Nr.	RT	Compound	Peak A (%)	Q
21	7.86	2-Cyclopenten-1-one, 3-methyl-	0.98	Q2
22	7.95	2-Cyclopenten-1-one, 3,4,4-trimethyl-	1.63	Q2
23	8.15	Phenol	0.82	Q2
24	8.34	2-Cyclopenten-1-one, 3,4-dimethyl-	1.54	Q2
25	8.44	2-Cyclopenten-1-one, 2,3-dimethyl-	1.84	Q2
26	8.84	4,4-Dimethyl-2-cyclopentene-1-one	0.95	Q3
27	9.01	1-Methyl-2-(4-methylpentyl)cyclopentane	1.41	Q2
28	9.13	2-Cyclopenten-1-one, 2,3-dimethyl-	3.80	Q2
29	9.37	Phenol, 2-methyl-	2.95	Q3
30	9.53	2-Cyclopenten-1-one, 2,3,4-trimethyl-	4.61	Q2
31	9.70	Phenol, 3-methyl-	1.63	Q2
32	9.97	2-Cyclopenten-1-one, 3,4,5-trimethyl-	3.16	Q3
33	10.12	Bicyclo(2,2,2)octane	0.72	Q2
34	10.17	1-Isopropylcyclohex-1-ene	0.96	Q2
35	10.24	Phenol, 2,3-dimethyl-	4.88	Q2
36	10.29	Benzofuran, 2-methyl-	2.24	Q1
37	10.44	2-Cyclopenten-1-one, 2,3,4,5-tetramethyl-	0.77	Q2
38	10.65	Cyclohexane, (1-methylethylidene)-	1.16	Q2
39	10.69	Phenol, 2-ethyl-	1.10	Q1
40	10.85	Phenol, 3,5-dimethyl-	4.04	Q2
41	11.05	1-Cyclohexene-1-carboxaldehyde, 2,6,6-trimethyl-	3.73	Q1
42	11.29	1,3-Hexadiene, 3-ethyl-2,5-dimethyl-	0.97	Q1
43	11.44	Phenol, 2-ethyl-4-methyl-	0.99	Q2
44	11.57	2-Cyclopenten-1-one, 2,3,4,5-tetramethyl-	2.81	Q1
45	11.66	1,4-Benzenediol, 2,3,5-trimethyl-	2.90	Q1
46	11.73	Phenol, 2,3,6-trimethyl-	4.39	Q1
47	11.94	p-Propargyloxytoluene	1.65	Q1
48	12.04	Phenol, 3-ethyl-5-methyl-	1.03	Q1
49	12.09	1,5,5-Trimethyl-6-methylene-cyclohexene	0.73	Q1
50	12.19	Phenol, 3-ethyl-5-methyl-	0.92	Q2
51	12.25	3-Cyclohexene-1-carboxaldehyde, 1,3,4-trimethyl-	1.42	Q1
52	12.66	Phenol, 3,4,5-trimethyl-	1.28	Q2
53	12.80	Phenol, 2-ethyl-4,5-dimethyl-	0.74	Q2
54	12.86	Thymoquinone	3.59	Q2
55	13.01	Phenol, 2-methyl-5-(1-methylethyl)-	0.48	Q1
56	13.28	Bicyclo[3.1.1]hept-3-ene-spiro-2,4'-(1',3'-dioxane), 7,7-dimethyl-	1.70	Q1
57	13.52	Duroquinone	0.87	Q2
58	13.95	Phenol, 2,3,5,6-tetramethyl-	0.81	Q3
59	14.05	Phenol, 2-methoxy-4-propyl-	0.65	Q1
60	14.32	11-Oxatetracyclo[5.3.2.0(2,7).0(2,8)]dodecan-9-one	0.94	Q1

Table B.8: Compounds identified by SPME GC-MS analysis in the biocrude (HS, 65 μm PDMS/DVB, T_{ext} = 25 °C, t_{ext} = 10 min). Q represents the quartile of identification quality.

Nr.	RT	Name	Peak A %	Q
1	2.03	4,6-Dihydroxypyrimidine	1.97	Q2
2	2.40	3-Hexyne	1.97	Q2
3	2.75	Cyclopentene, 1-methyl-	1.93	Q2
4	3.29	n-Hexane	2.79	Q3
5	4.35	Toluene	3.85	Q3
6	4.83	1,4-Hexadiene, 2,3-dimethyl-	2.00	Q3
7	5.06	Cyclobutene, 1,2,3,4-tetramethyl-	1.62	Q2
8	5.62	Cyclopentanone, 2-methyl-	3.10	Q3
9	5.78	Cyclopentane, 2-ethylidene-1,1-dimethyl-	0.75	Q2
10	6.00	Ethylbenzene	1.15	Q3
11	6.14	p-Xylene	3.46	Q3
12	6.25	1,3-Hexadiene, 3-ethyl-2-methyl-, (Z)-	1.35	Q2
13	6.86	2-Cyclopenten-1-one, 2-methyl	2.86	Q2
14	7.38	2-Cyclopenten-1-one, 3,4-dimethyl-	5.09	Q2
15	7.65	3,6-Nonadien-1-ol, (E,Z)-	1.44	Q1
16	7.78	3-Cyclohexen-1-carboxaldehyde, 3,4-dimethyl-	2.00	Q1
17	8.10	Phenol	6.30	Q1
18	8.34	Benzene, 1,3,5-trimethyl-	3.09	Q2
19	8.85	Benzene, 1,4-diethyl-	2.01	Q2
20	9.07	3-Cyclohex-1-enyl-prop-2-enal	4.93	Q2
21	9.33	Phenol, 3-methyl-	7.25	Q2
22	9.50	2-Cyclopenten-1-one, 3,4,4-trimethyl-	3.18	Q3
23	9.65	2,4-Cycloheptadien-1-one, 2,6,6-trimethyl-	4.04	Q1
24	9.93	Indan, 1-methyl-	4.73	Q2
25	10.21	Phenol, 2,5-dimethyl-	3.37	Q3
26	10.57	Phenol, 2-ethyl-	0.91	Q2
27	10.74	3-Cyclohexen-1-ol, 5-methylene-6-(1-methylethenyl)-, acetate	2.50	Q3
28	10.92	2,4-Dimethylstyrene	1.85	Q2
29	11.48	Benzene, 1-methyl-3-(1-methyl-2-propenyl)-	1.54	Q1
30	11.79	Acetic acid, 7-hydroxy-1,3,4,5,6,7-hexahydro-2H-naphthalen-4a-ylmethyl ester	0.81	Q1
31	12.22	Cyclopentan-1-al, 4-isopropylidene-2-methyl-	1.03	Q1
32	12.74	Naphthalene, 1,2-dihydro-4-methyl-	0.77	Q1
33	13.26	Benzene, 1,4-bis(1-methylethenyl)-	2.08	Q1

References

[1] T. H. Pedersen and L. A. Rosendahl, "Production of fuel range oxygenates by supercritical hydrothermal liquefaction of lignocellulosic model systems," *Biomass Bioenergy*, vol. 83, pp. 206–215, 2015.

[2] D. L. Barreiro, W. Prins, F. Ronsse, and W. Brilman, "Hydrothermal liquefaction (HTL) of microalgae for biofuel production: State of the art review and future prospects," *Biomass Bioenergy*, vol. 53, pp. 113–127, 2013.

[3] J. Akhtar and N. A. S. Amin, "A review on process conditions for optimum bio-oil yield in hydrothermal liquefaction of biomass," *Renew. Sustainable Energy Rev.*, vol. 15, no. 3, pp. 1615–1624, 2011.

[4] Y. Yu, X. Lou, and H. Wu, "Some recent advances in hydrolysis of biomass in hot-compressed water and its comparisons with other hydrolysis methods," *Energy Fuels*, vol. 22, no. 1, pp. 46–60, 2007.

[5] A. Demirbaş, "Current technologies for the thermo-conversion of biomass into fuels and chemicals," *Energ. Source.*, vol. 26, no. 8, pp. 715–730, 2004.

[6] S. S. Toor, L. A. Rosendahl, J. Hoffmann, T. H. Pedersen, R. P. Nielsen, and E. G. Søgaard, "Hydrothermal Liquefaction of Biomass," in *Application of Hydrothermal Reactions to Biomass Conversion.* Springer, 2014, pp. 189–217.

[7] Z. Zhu, L. Rosendahl, S. S. Toor, D. Yu, and G. Chen, "Hydrothermal liquefaction of barley straw to bio-crude oil: Effects of reaction temperature and aqueous phase recirculation," *Appl. Energ.*, vol. 137, pp. 183–192, 2015.

[8] Z. Zhu, S. S. Toor, L. Rosendahl, and G. Chen, "Analysis of product distribution and characteristics in hydrothermal liquefaction of barley straw in subcritical and supercritical water," *Environ. Prog. Sustain. Energy*, vol. 33, no. 3, pp. 737–743, 2014.

[9] F. Goudriaan and D. Peferoen, "Liquid fuels from biomass via a hydrothermal process," *Chem. Eng. Sci.*, vol. 45, no. 8, pp. 2729–2734, 1990.

[10] F. Behrendt, Y. Neubauer, M. Oevermann, B. Wilmes, and N. Zobel, "Direct liquefaction of biomass," *Chem. Eng.Technol.*, vol. 31, no. 5, pp. 667–677, 2008.

[11] A. A. Peterson, F. Vogel, R. P. Lachance, M. Fröling, M. J. Antal Jr, and J. W. Tester, "Thermochemical biofuel production in hydrothermal media: A review of sub-and supercritical water technologies," *Energy Environ. Sci.*, vol. 1, no. 1, pp. 32–65, 2008.

[12] Z. Shuping, W. Yulong, Y. Mingde, I. Kaleem, L. Chun, and J. Tong, "Production and characterization of bio-oil from hydrothermal liquefaction of microalgae Dunaliella tertiolecta cake," *Energy*, vol. 35, no. 12, pp. 5406–5411, 2010.

[13] C. Xu and N. Lad, "Production of heavy oils with high caloric values by direct liquefaction of woody biomass in sub/near-critical water," *Energy Fuels*, vol. 22, no. 1, pp. 635–642, 2007.

[14] A. Hammerschmidt, N. Boukis, E. Hauer, U. Galla, E. Dinjus, B. Hitzmann, T. Larsen, and S. D. Nygaard, "Catalytic conversion of waste biomass by hydrothermal treatment," *Fuel*, vol. 90, no. 2, pp. 555–562, 2011.

[15] S. Yin, R. Dolan, M. Harris, and Z. Tan, "Subcritical hydrothermal liquefaction of cattle manure to bio-oil: Effects of conversion parameters on bio-oil yield and characterization of bio-oil," *Bioresour. Technol.*, vol. 101, no. 10, pp. 3657–3664, 2010.

[16] T. Minowa, M. Murakami, Y. Dote, T. Ogi, and S.-y. Yokoyama, "Oil production from garbage by thermochemical liquefaction," *Biomass Bioenergy*, vol. 8, no. 2, pp. 117–120, 1995.

[17] C. Tuck, E. Pérez, I. Horváth, R. Sheldon, and M. Poliakoff, "Valorization of biomass: deriving more value from waste," *Science*, vol. 337, no. 6095, pp. 695–699, 2012.

[18] C. Xu and J. Lancaster, "Conversion of secondary pulp/paper sludge powder to liquid oil products for energy recovery by direct liquefaction in hot-compressed water," *Water Res.*, vol. 42, no. 6, pp. 1571–1582, 2008.

[19] N. Sudasinghe, B. Dungan, P. Lammers, K. Albrecht, D. Elliott, R. Hallen, and T. Schaub, "High resolution FT-ICR mass spectral analysis of bio-oil and residual water soluble organics produced by hydrothermal liquefaction of the marine microalga Nannochloropsis salina," *Fuel*, vol. 119, pp. 47–56, 2014.

[20] S. R. Villadsen, L. Dithmer, R. Forsberg, J. Becker, A. Rudolf, S. B. Iversen, B. B. Iversen, and M. Glasius, "Development and application of chemical analysis methods for investigation of bio-oils and aqueous phase from hydrothermal liquefaction of biomass," *Energy Fuels*, vol. 26, no. 11, pp. 6988–6998, 2012.

[21] J. Li, C. Wang, and Z. Yang, "Production and separation of phenols from biomass-derived bio-petroleum," *J. Anal. Appl. Pyrolysis*, vol. 89, no. 2, pp. 218–224, 2010.

[22] S. Karagöz, T. Bhaskar, A. Muto, and Y. Sakata, "Comparative studies of oil compositions produced from sawdust, rice husk, lignin and cellulose by hydrothermal treatment," *Fuel*, vol. 84, no. 7, pp. 875–884, 2005.

[23] P. J. Valdez, J. G. Dickinson, and P. E. Savage, "Characterization of product fractions from hydrothermal liquefaction of Nannochloropsis sp. and the influence of solvents," *Energy Fuels*, vol. 25, no. 7, pp. 3235–3243, 2011.

[24] X. Yuan, J. Wang, G. Zeng, H. Huang, X. Pei, H. Li, Z. Liu, and M. Cong, "Comparative studies of thermochemical liquefaction characteristics of microalgae using different organic solvents," *Energy*, vol. 36, no. 11, pp. 6406–6412, 2011.

[25] I. Leonardis, S. Chiaberge, T. Fiorani, S. Spera, E. Battistel, A. Bosetti, P. Cesti, S. Reale, and F. De Angelis, "Characterization of bio-oil from hydrothermal liquefaction of organic waste by NMR spectroscopy and FTICR mass spectrometry," *ChemSusChem*, vol. 6, no. 1, pp. 160–167, 2013.

[26] T. T. Kekäläinen, T. Venäläinen, and J. Jänis, "Characterization of birch wood pyrolysis oils by ultrahigh-resolution FT-ICR mass spectrometry: Insights into thermochemical conversion," *Energy Fuels*, 2014.

[27] J. M. Jarvis, A. M. McKenna, R. N. Hilten, K. Das, R. P. Rodgers, and A. G. Marshall, "Characterization of pine pellet and peanut hull pyrolysis bio-oils by negative-ion electrospray ionization Fourier transform ion cyclotron resonance mass spectrometry," *Energy Fuels*, vol. 26, no. 6, pp. 3810–3815, 2012.

[28] M. Garcia-Perez, A. Chaala, H. Pakdel, D. Kretschmer, and C. Roy, "Characterization of bio-oils in chemical families," *Biomass Bioenergy*, vol. 31, no. 4, pp. 222–242, 2007.

[29] T. Ba, A. Chaala, M. Garcia-Perez, D. Rodrigue, and C. Roy, "Colloidal properties of bio-oils obtained by vacuum pyrolysis of softwood bark. Characterization of water-soluble and water-insoluble fractions," *Energy Fuels*, vol. 18, no. 3, pp. 704–712, 2004.

[30] C. Branca, P. Giudicianni, and C. Di Blasi, "GC/MS characterization of liquids generated from low-temperature pyrolysis of wood," *Ind. Eng. Chem. Res.*, vol. 42, no. 14, pp. 3190–3202, 2003.

[31] S. Vitolo and P. Ghetti, "Physical and combustion characterization of pyrolytic oils derived from biomass material upgraded by catalytic hydrogenation," *Fuel*, vol. 73, no. 11, pp. 1810–1812, 1994.

[32] K. Sipilä, E. Kuoppala, L. Fagernäs, and A. Oasmaa, "Characterization of biomass-based flash pyrolysis oils," *Biomass Bioenergy*, vol. 14, no. 2, pp. 103–113, 1998.

[33] H. Pakdel, H. Zhang, and C. Roy, "Detailed chemical characterization of biomass pyrolysis oils, polar fractions," in *Advances in Thermochemical Biomass Conversion.* Springer, 1993, pp. 1068–1085.

[34] A. G. Marshall and R. P. Rodgers, "Petroleomics: The next grand challenge for chemical analysis," *Acc. Chem. Res.*, vol. 37, no. 1, pp. 53–59, 2004.

[35] T. M. Schaub, R. P. Rodgers, A. G. Marshall, K. Qian, L. A. Green, and W. N. Olmstead, "Speciation of aromatic compounds in petroleum refinery streams by continuous flow field desorption ionization FT-ICR mass spectrometry," *Energy Fuels*, vol. 19, no. 4, pp. 1566–1573, 2005.

[36] K. Qian, W. K. Robbins, C. A. Hughey, H. J. Cooper, R. P. Rodgers, and A. G. Marshall, "Resolution and identification of elemental compositions for more than 3000 crude acids in heavy petroleum by negative-ion microelectrospray high-field fourier transform ion cyclotron resonance mass spectrometry," *Energy Fuels*, vol. 15, no. 6, pp. 1505–1511, 2001.

[37] A. A. Herod, K. D. Bartle, and R. Kandiyoti, "Characterization of heavy hydrocarbons by chromatographic and mass spectrometric methods: An overview," *Energy Fuels*, vol. 21, no. 4, pp. 2176–2203, 2007.

[38] K. Qian, R. P. Rodgers, C. L. Hendrickson, M. R. Emmett, and A. G. Marshall, "Reading chemical fine print: Resolution and identification of 3000 nitrogen-containing aromatic compounds from a single electrospray ionization Fourier transform ion cyclotron resonance mass spectrum of heavy petroleum crude oil," *Energy Fuels*, vol. 15, no. 2, pp. 492–498, 2001.

[39] F. Taner, A. Eratik, and I. Ardic, "Identification of the compounds in the aqueous phases from liquefaction of lignocellulosics," *Fuel Process. Technol.*, vol. 86, no. 4, pp. 407–418, 2005.

[40] P. Desbene, M. Essayegh, B. Desmazieres, and F. Villeneuve, "Analysis of biomass pyrolysis oils by a combination of various liquid chromatographic techniques and gas chromatography-mass spectrometry," *J. Chromatogr. A*, vol. 553, pp. 211–221, 1991.

[41] E. A. Smith, S. Park, A. T. Klein, and Y. J. Lee, "Bio-oil analysis using negative electrospray ionization: Comparative study of high-resolution mass spectrometers and phenolic versus sugaric components," *Energy Fuels*, vol. 26, no. 6, pp. 3796–3802, 2012.

[42] S. Chiaberge, I. Leonardis, T. Fiorani, P. Cesti, S. Reale, and F. D. Angelis, "Bio-oil from waste: A comprehensive analytical study by soft-ionization FTICR mass spectrometry," *Energy Fuels*, vol. 28, no. 3, pp. 2019–2026, 2014.

[43] L. A. Stanford, S. Kim, G. C. Klein, D. F. Smith, R. P. Rodgers, and A. G. Marshall, "Identification of water-soluble heavy crude oil organic-acids, bases, and neutrals by electrospray ionization and field desorption ionization Fourier transform ion cyclotron resonance mass spectrometry," *Environ. Sci. Technol.*, vol. 41, no. 8, pp. 2696–2702, 2007.

[44] K. Anastasakis and A. Ross, "Hydrothermal liquefaction of the brown macro-alga Laminaria Saccharina: Effect of reaction conditions on product distribution and composition," *Bioresource Technol.*, vol. 102, no. 7, pp. 4876–4883, 2011.

[45] B. Scholze and D. Meier, "Characterization of the water-insoluble fraction from pyrolysis oil (pyrolytic lignin). Part I. PY–GC/MS, FTIR, and functional groups," *J. Anal. Appl. Pyrol.*, vol. 60, no. 1, pp. 41–54, 2001.

[46] H. Prosen and L. Zupančič-Kralj, "Solid-phase microextraction," *Trac-Trend. Anal. Chem.*, vol. 18, no. 4, pp. 272–282, 1999.

[47] S. Vichi, A. I. Castellote, L. Pizzale, L. S. Conte, S. Buxaderas, and E. López-Tamames, "Analysis of virgin olive oil volatile compounds by headspace solid-phase microextraction coupled to gas chromatography with mass spectrometric and flame ionization detection," *J. Chromatogr. A*, vol. 983, no. 1, pp. 19–33, 2003.

[48] J. C. Demyttenaere, C. Dagher, P. Sandra, S. Kallithraka, R. Verhé, and N. De Kimpe, "Flavour analysis of Greek white wine by solid-phase microextraction–capillary gas chromatography–mass spectrometry," *J. Chromatogr. A*, vol. 985, no. 1, pp. 233–246, 2003.

[49] J. Pawliszyn, *Handbook of solid phase microextraction.* Elsevier, 2011.

[50] A. Kruse and A. Gawlik, "Biomass conversion in water at 330 - 410 °C and 30 - 50 MPa. Identification of key compounds for indicating different chemical reaction pathways," *Ind. Eng. Chem. Res.*, vol. 42, no. 2, pp. 267–279, 2003.

[51] T. H. Pedersen, I. Grigoras, J. Hoffmann, S. S. Toor, I. M. Daraban, C. U. Jensen, S. Iversen, R. B. Madsen, M. Glasius, K. R. Arturi, R. P. Nielsen, E. G. Søgaard, and L. A. Rosendahl, "Continuous hydrothermal co-liquefaction of aspen wood and glycerol with water phase recirculation," *Appl. Energ.*, vol. 162, pp. 1034–1041, 2016.

[52] M. Sasaki, Z. Fang, Y. Fukushima, T. Adschiri, and K. Arai, "Dissolution and hydrolysis of cellulose in subcritical and supercritical water," *Ind. Eng. Chem. Res.*, vol. 39, no. 8, pp. 2883–2890, 2000.

[53] A. Demirbaş, M. Balat, and K. Bozbaş, "Direct and catalytic liquefaction of wood species in aqueous solution," *Energ. Source.*, vol. 27, no. 3, pp. 271–277, 2005.

[54] S. Karagöz, T. Bhaskar, A. Muto, Y. Sakata, T. Oshiki, and T. Kishimoto, "Low-temperature catalytic hydrothermal treatment of wood biomass: analysis of liquid products," *Chem. Eng. J.*, vol. 108, no. 1, pp. 127–137, 2005.

[55] Y. Qian, C. Zuo, J. Tan, and J. He, "Structural analysis of bio-oils from sub-and supercritical water liquefaction of woody biomass," *Energy*, vol. 32, no. 3, pp. 196–202, 2007.

[56] P. Sun, M. Heng, S.-H. Sun, and J. Chen, "Analysis of liquid and solid products from liquefaction of paulownia in hot-compressed water," *Energ. Convers. Manage.*, vol. 52, no. 2, pp. 924–933, 2011.

[57] B. M. Kabyemela, T. Adschiri, R. M. Malaluan, and K. Arai, "Kinetics of glucose epimerization and decomposition in subcritical and supercritical water," *Ind. Eng. Chem. Res.*, vol. 36, no. 5, pp. 1552–1558, 1997.

[58] B. M. Kabyemela, T. Adschiri, R. Malaluan, and K. Arai, "Degradation kinetics of dihydroxyacetone and glyceraldehyde in subcritical and supercritical water," *Ind. Eng. Chem. Res.*, vol. 36, no. 6, pp. 2025–2030, 1997.

[59] M. Balat, "Mechanisms of thermochemical biomass conversion processes. Part 3: Reactions of liquefaction," *Energ. Source. Part A*, vol. 30, no. 7, pp. 649–659, 2008.

[60] S. Yin, Y. Pan, and Z. Tan, "Hydrothermal conversion of cellulose to 5-hydroxymethyl furfural," *Int. J. Green Energy*, vol. 8, no. 2, pp. 234–247, 2011.

[61] D. A. Nelson, P. M. Molton, J. A. Russell, and R. T. Hallen, "Application of direct thermal liquefaction for the conversion of cellulosic biomass," *Ind. Eng. Chem. Prod. RD.*, vol. 23, no. 3, pp. 471–475, 1984.

[62] D.-H. Cho, S.-H. Kong, and S.-G. Oh, "Analysis of trihalomethanes in drinking water using headspace-SPME technique with gas chromatography," *Water Res.*, vol. 37, no. 2, pp. 402–408, 2003.

[63] S. Zhou, J. Huang, X. Gao, and L. Zhao, "SPME-GC-MSD for determination of nine phenyl compounds in snow water in Beijing China," *Chromatographia*, vol. 62, no. 1-2, pp. 109–111, 2005.

Paper C

Hydrothermal liquefaction of lignin in near-critical water in a new batch reactor: Influence of phenol and temperature

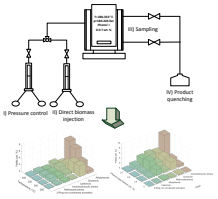

Katarzyna R. Arturi, Morten Strandgaard, Rudi P. Nielsen, Erik G. Søgaard, and Marco Maschietti

The paper has been published in the
Journal of Supercritical Fluids Vol. 123, pp. 28–39, 2017.

Abstract

The hydrothermal conversion of Kraft lignin (6 wt.%) in the presence of K_2CO_3 (1.7 wt.%) was studied as a function of temperature (T = 280 - 350 °C) and phenol mass fraction (w_{Ph} = 0.0 - 9.7 wt.%). The process was carried out in a new batch reactor with injection of lignin slurry enabling fast heating of the biomass, effective control of reaction pressure, and withdrawal/quenching of the products. An aqueous phase and biocrude were obtained, both containing a broad spectrum of aromatic monomers and dimers. The former group consisted mostly of methoxybenzenes, guaiacols, catechols, and alkylphenols, while the latter included anisolic/phenolic dimers. For a given w_{Ph} (3.4 wt.%), the total yield of monomeric aromatics (Y_T) was maximized at 320 °C. At T = 300 °C and without phenol, Y_T was low, whereas it increased steeply up to w_{Ph} = 6.5 wt.%.

Keywords: Kraft lignin, hydrothermal conversion, aromatic monomers, biocrude, co-solvent, injection.

1 Introduction

Lignin is the second most common terrestrial biopolymer on Earth, and the most significant naturally occurring source of aromatics in nature. It accounts for 15 to 40 % of the biomass (on a dry mass basis) and approx. 40 % of its energy content [1–3]. The largest manufacturer of lignin is the pulp industry, with the kraft process being the dominating technology. The amount of lignin extracted in the pulping process in the western hemisphere is estimated to be in the order of 50 million tons per year.

Currently, more than 98 % of the extracted lignin is utilized at the pulp mills as a low value fuel for production of steam and power [1, 2]. The remaining amount, accounting for approx. 1 million tons per year, is made available for a number of low-value commercial uses, such as dispersant in cement, binder for animal feed pellets, additive for drilling fluids in the oil industry, or dust suppressing agent for roads [1]. Since the energy efficiency of pulp mills has been increasing in recent years, it is anticipated that growing amounts of lignin will be available for external uses in the years to come [4].

In addition, lignin-rich residue streams are also obtained in the production of bioethanol from lignocellulosic feedstock, with a number of industrial plants already operational, under construction, or at demonstration stage. Therefore, valorization of the excess lignin is deemed a major factor in maximizing sustainability and profitability of lignocellulosic biorefinery units [3].

In recent years numerous chemical process routes for conversion of lignin into valuable products, e.g. drop-in biocrude and chemical feedstocks, have been studied on laboratory scale [5–9]. One of the most promising technologies for converting lignin is hydrothermal liquefaction (HTL) performed in near-critical water (T = 240

- 370 °C and p = 10 - 30 MPa), which has been reported in the literature in a number of variants [10–16]. The properties of near-critical water (NCW) as a reaction medium are appealing for a number of reasons: NCW exhibits an increased solvent power towards low-polarity compounds, while still being a good solvent for polar compounds and salts; the ionic product is higher than at lower temperatures, which leads to catalytic effects towards many ionic reactions; the density of the reaction medium is adjustable, with relatively small variations of temperature and pressure [17–21]. Moreover, application of NCW as reaction medium renders the energy intensive process step of drying the biomass obsolete. In addition, the relatively mild temperatures of NCW allow the integrity of aromatic rings to be retained, thus favoring process routes leading to aromatic monomeric compounds.

The addition of K_2CO_3 to the NCW reaction medium was shown to increase the yields of liquid products and to decrease char formation during conversion of lignocellulosic biomass, with higher yields of liquid products compared to additions of other alkali salts (Na_2CO_3) and strong bases (KOH, NaOH) [22–24]. In the case of hydrothermal conversion of lignin, the beneficial effect of K_2CO_3 was observed to increase the yields of monomeric aromatic compounds [14, 25].

Moreover, the use of organic co-solvents in hydrothermal liquefaction led to a reduction in char formation during conversion of lignocellulosic biomass. This effect was explained with the increase of biomass solubility in the reaction medium and with the action of the co-solvent as capping agent or scavenger of the unstable fragments produced in the depolymerization of biomass [26–29]. In the case of lignin conversion, phenol was clearly associated with lower char formation due to its role as capping agent [26–28].

The role of phenol as capping agent was described extensively in studies on hydrothermal conversion of a lignin model compound by Lin et al. [30–32]. In addition, Fang et al. [28] also observed that the use of phenol as co-solvent favor the solubilization of lignin in the reaction medium. The combined use of K_2CO_3 and phenol in the NCW reaction medium gave promising results in the conversion of Kraft lignin to bio-oil and water-soluble aromatic chemicals [14, 15, 25]. While the presence of phenol in NCW conversion of lignin showed favorable results, the effect of its amount in the reacting system has not been investigated yet.

Laboratory experiments on NCW conversion of biomass are often performed in batch mode on small scale reactors ($\leq$ 100 mL). These systems have the advantage of minimizing practical problems common for the continuous systems (e.g. clogging of flow control valves), and are therefore to be preferred in the initial screening of an innovative process. However, typical laboratory batch equipment for NCW conversion suffers from a number of limitations, which makes the interpretation of the results somewhat uncertain. More specifically, laboratory batch systems often require the biomass to be charged in the reactor before the heating and pressurization and they lack the means for reaction products quenching, thus leading to

uncertainties in the interpretation of the reaction time and temperature. Product quenching is typically only possible in micro-reactors, which can be heated and cooled in thermostatic baths. However, in these cases, the reactor volume is typically extremely small (few mL) and does not allow accurate yield calculations of different product fractions. In addition, batch laboratory reactors used for conversion by NCW are often not equipped with means for controlling reaction pressure, thus leading to non-negligible density variations of the reaction medium due to the relatively high compressibility of NCW.

Among these factors, the slow heating time of hydrothermal batch reactors is one of the major drawbacks when operating on lignocellulosic materials, leading to results very different from those obtained in continuous stirred tank reactors (CSTR) or plug flow reactors (PFR) with product recycle, where a fast heating of the feed is achieved. As a consequence, results obtained in laboratory scale batch reactors often do not provide an accurate basis for developing continuous flow processes. For example, Kruse et al. [33] found "completely different results" when comparing hydrothermal gasification of lignocellulosic biomass in supercritical water in a batch reactor and in a CSTR.

A possible way to overcome this drawback is to preliminary fill the batch reactor with water (or water + additives), heat and pressurize the reactor and then inject the biomass. This solution, together with the relative technical details, was described by Modell [34]. A batch system with biomass injection was also reported by Schmieder et al. [35], even though without details on the operating procedure. A more detailed description of the advantages that can be obtained with a batch reactor equipped with an injection system was provided by Barbier et al. [36], who tested a new reactor on glucose decomposition in supercritical water. However, not many details on the specific issues that can be encountered when injecting a biomass slurry were provided in a subsequent publication which comprised lignin conversion [37].

The aim of the present work is demonstration of a new laboratory batch reactor encompassing fast biomass heating, pressure control, and product quenching. Fast biomass heating is achieved through feed injection into the pre-heated and pre-pressurized reactor. Pressure control during reaction is obtained by injecting/withdrawing small and finely regulated amounts of water into/from the system. Additionally, sampling ports for immediate withdrawal and quenching of the products make it possible to stop the hydrothermal conversion at the desired reaction time. In this work, this new batch reactor was applied to the conversion of Kraft lignin in NCW, in the presence of K_2CO_3 and phenol. The effect of reaction temperature and phenol mass fraction in the feed was studied.

2 Materials and Methods

2.1 Materials

The biomass used in this study was Kraft pine lignin Indulin® AT (Specialty Chemicals Division, MeadWestvaco Corporation South Carolina, USA). The biomass was in the form of a free flowing brown powder with no insolubles in warm aqueous solution of 5 % NaOH. The moisture content of the lignin powder was 3.6 wt.%, the ash content was 1.9 wt.%. The average molar mass was 8000 g/mol. The elemental composition of dry lignin on an ash-free basis was as follows: 64.4 % carbon, 6.7 % hydrogen, 1.8 % sulfur, and 27.1 % oxygen.

The organic solvents were purchased from Sigma-Aldrich: tetrahydrofuran (THF, anhydrous, ≥ 99.9 %, inhibitor-free), acetone (used for cleaning purposes, ACS reagent, ≥ 99.5 %), diethyl ether (DEE, Laboratory Reagent, ≥ 99.5 %, GC). K_2CO_3 (anhydrous, free-flowing, Redi-Dri™, ACS reagent, ≥ 99 %) was used as catalyst. Additional chemicals were used: liquefied phenol (≥ 89 %, water approx. 10 %) as co-solvent, N_2 (≥ 99.998 %) for purging the reactor of oxygen before heating up, and syringol (2,6-dimethoxyphenol, 99 %) as internal standard (IS). Distilled water was used in all experiments as the primary reaction solvent.

2.2 Experimental apparatus

The new experimental set-up presented in this work (Figure C.1), built by SITEC-Sieber Engineering AG, was specifically conceived and designed for biomass hydrothermal conversion studies. The core part of the set-up is the reactor (R1, 99 ml, wetted parts in Inconel 625), which can operate up to 400 °C and 300 bar.

The reactor is heated with four electrical heating cartridges immersed in the reactor shell (500 W each). The inner temperature is measured with a thermocouple type K (class 1, accuracy ± 0.5 %) and it is controlled by a mixed cascade/slave PID controller. The reactor pressure is measured at a top connection by a pressure gauge with an accuracy of ± 1 %. The reactor is equipped with a magnetic stirring system, coupled with a heating plate providing supplementary heat to the reactor. Heat dispersion is limited by a high-temperature insulation jacket wrapped around the reactor. The reactor is connected with two high-pressure precision hand pumps (P1 and P2; stroke capacity: 100 ml; capacity per revolution: 2 ml; maximum operating pressure: 300 bar). The pump P1 can be used for injecting/withdrawing water in/from the system for the purpose of precise pressure control. P1 is protected by a filter (F1) to avoid contact with slurry particles. P2 was specifically designed with a protecting sealing part for enabling it to pump slurry in and out of the system. The pressure at the discharge of the hand pumps is measured by two pressure gauges. The set-up is also equipped with a dedicated flushing line for recovering slurry residuals not fed into the reactor. The maximum pressure that can be reached in the system is limited by a pneumatic valve and a rupture disc set

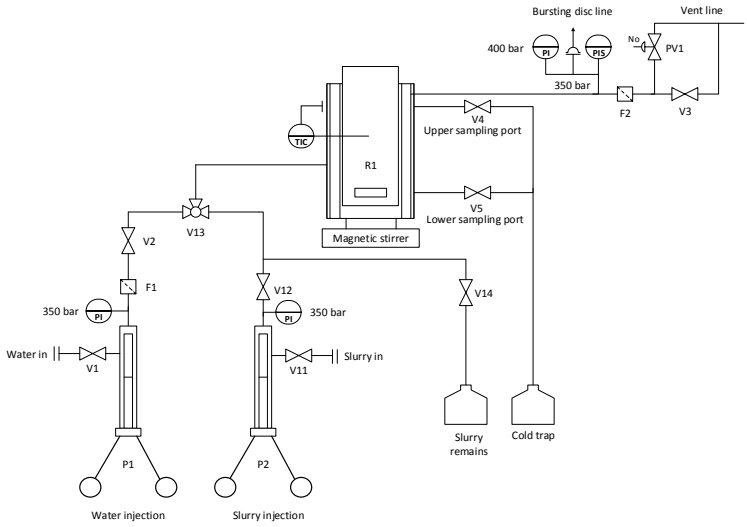

Fig. C.1: P& I diagram for the applied batch/semi-batch reactor system. R1: reactor, P1, P2: hand-driven pumps; F1, F2: filters; V1-V5, V11-V12: closing valves; V13: three-way valve; PV1: pneumatic safety valve; PI: pressure indicator; PIS: pressure indicator switch; TIC: temperature indicator and controller.

to break at 350 bar. The reactor is equipped with two sampling ports, a lower and an upper one, through which the reaction products can be withdrawn and conveyed to a cold trap for quenching.

2.3 Procedure

The reactor charge was split into two parts. The first portion consisted of a solution of water, phenol, and K_2CO_3, which was charged into R1 before heating of the system; the second portion was a slurry composed of water, lignin and K_2CO_3 (the lignin slurry), which was injected into the preheated and pressurized reactor. The lignin slurry was prepared in advance by dispersing the Kraft lignin in a solution of water and K_2CO_3. The dispersion was carried out using an IKA Ultra Turrax (30 min, 20000 rpm). Before the injection, the slurry was stirred again for 15 min.

At the beginning of each experimental run, the top lid of the reactor was removed and the reactor was charged with the first portion of the feed. The reactor was then sealed by screwing the upper cap securely into place and then flushed with N2 for 30 min. The mixture in R1 was heated at constant volume, and therefore pressurized until a pre-heating temperature (T_{PH}) slightly above the selected reaction temperature (T_R) was reached [34]. The amount of the first portion was selected in order to be in the proper range leading to a two-phase (vapor-liquid) mixture until T_{PH} was reached. The second portion of the feed (i.e. the lignin slurry) was injected into the reactor through the pump P2 (cold injection). Importantly, the presence of

a vapor-liquid mixture inside the reactor in the first step of the slurry injection led to condensation of the vapor, thus preventing the drastic temperature drop that would have happened with a cold injection into a homogeneous system. This step of the injection process proceeded until the reaction mixture was completely condensed and was characterized by small pressure and temperature variations. The subsequent step (i.e. cold injection into a condensed system) was relatively short, being characterized by a steep pressure increase until the reaction pressure and temperature were reached.

A number of preliminary experimental runs were dedicated to locating optimal values for the amount of the first portion of the feed, depending on the desired reaction conditions. Larger quantities of the first portion require small injections of more concentrated slurry (i.e. the second portion), thus leading to shorter injection times and smaller temperature fluctuations, but also to possible practical problems in pumping the slurry. On the other hand, smaller amounts of the first portion lead to easier pumping of the slurry but also to higher injection times and larger temperature fluctuations. A smooth operating procedure, characterized by no tube blocking, reasonable injection times and small temperature fluctuations, was found charging a first portion of 45.0 g and injecting a slurry of lignin of approximately 12 wt.% as the second portion. The preliminary investigation included nine injections of lignin slurry (12 wt.%) carried out at ambient conditions, with the aim of determining the actual composition of the slurry after the injection into the reactor. The injected mass was collected, dried in an oven for 24 hours at 90 °C and subsequently weighed. For all the nine injections, the dry matter content was on average 11.67 wt.% with a standard deviation of 0.27 wt.%. Detailed data are provided as supplementary content (Table C.6).

Typical injection times were in the range 3 - 5 minutes. Temperature fluctuations during the injection were in the range $T_R \pm 15$ °C, with the values stabilizing in the range $T_R \pm 2$ °C after less than 2 minutes from the end of the injection. After the completion of the injection, the pressure in the reactor was kept within ± 5 bar during the whole reaction time. The pressure control was obtained with water injection/withdrawal lower than 0.05 mL, as measured from the hand pump revolution. This value led to a negligible effect on the overall composition of the reacting phase.

After the desired reaction time (15 min), the reaction mixture was depressurized by fast discharge (approx. 30 s) of the reactor content through the lower sampling valve (V5). At the level of lignin concentration used in this work, clogging of the valve V5 happened only sporadically and could be solved opening the upper sampling valve (V4) and closing and opening again the valve V5. The mixture was quenched in a cold trap containing 100 mL of water (measured at ambient temperature) and immersed in an ice bath with salt. Some preliminary runs with depressurization and quenching of pure water from near-critical states to ambient conditions allowed optimization of the design of the cold trap in order to achieve negligible losses of water vapor, together with maximum product temperatures not exceeding 60 °C. At

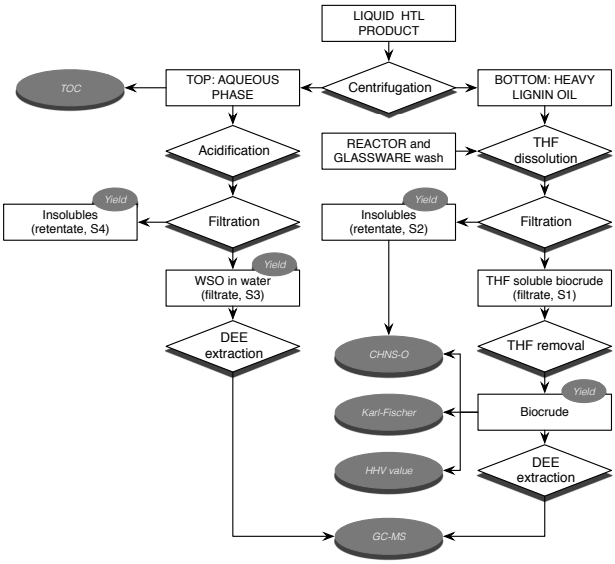

Fig. C.2: Separation and analysis of the products from HTL of lignin.

these conditions, the loss of water-soluble aromatic compounds for evaporation can be considered negligible. The reaction products collected in the trap consisted of two distinct liquid phases, an aqueous phase and oil. Solid particles were also visible. The content of the trap was weighed, and then the products were centrifuged at 5000 rpm for 180 minutes (Figure C.2).

The centrifugation gave an aqueous phase at the top and oil phase at the bottom (heavy lignin oil). The bottom fraction was recovered using THF; the reactor and tubing were also washed with THF. The two obtained THF mixtures were mixed and filtrated under vacuum through a Pyrex glass filter (porosity 2) yielding THF soluble biocrude (filtrate, S1) and solids particles (retentate, S2). The solids recovered on the filter papers were dried overnight in oven at 105 °C before weighing. The solvent was removed from S1 by evaporation at room temperature for 24 hours, thus obtaining the biocrude. The aqueous phase obtained after the centrifugation was acidified down to pH 2 and left at rest for 3 hours. The resulting mixture was filtrated under vacuum through a pre-weighed Whatman No. 5 filter paper, giving an aqueous phase (filtrate, S3) containing water soluble organics (WSO) and solids (retentate, S4). The total solid product obtained as a sum of S2 and S4 is designated in this work as insolubles. The aqueous phase was stored at room temperature, protected from light, for subsequent analysis. It appeared to be stable for weeks, with respect to visual appearance (i.e. no color change). Nevertheless, it was typically analyzed not more than a couple of days after the reaction.

2.4 Experimental conditions

In the current study, the influence of phenol mass fraction (w_{Ph} values between 0 wt.% and 9.7 wt.%, runs a-b-c-d) and temperature (T values between 282 °C and 355 °C, runs e-f-g-h) on the hydrothermal conversion of Kraft lignin was studied (see Table C.1). Full data of the two portions charged in the reactor are provided as supplementary content (Table C.6). The value of pressure (p) was adjusted with the temperature in order to limit, as much as possible, the density variation of the primary solvent (water). In all experimental runs, this density value was between 605 kg/m^3 and 765 kg/m^3. The actual overall density measured according to the loaded mass varied from 791 kg/m^3 to 879 kg/m^3. The latter values are higher because the actual reacting system is not pure water and contains higher density substances, and because of the fluid in the dead-space of the equipment, which is at ambient temperature. The mass fraction of lignin and homogeneous catalyst (K_2CO_3) were fixed at approx. 6.0 wt.% and 1.7 wt.%, respectively. In the runs where temperature was varied, the mass fraction of phenol was held at approx. 3.4 wt.%. The reaction temperature and pressure reported in Table C.1 are average values measured during the reaction time. As noted above, fluctuations were however small. No runs without lignin were performed, as previous studies have shown that phenol is stable at the applied hydrothermal conditions [14].

Table C.1: Process conditions in the experimental runs.

Run	a	b	c	d	e	f	g	h
	T = 300 °C with phenol at:				Phenol = 3.4 wt.% with T at:			
	0 wt.%	3.4 wt.%	6.5 wt.%	9.7 wt.%	280 °C	300 °C	320 °C	350 °C
Lignin (dry, wt.%)	6.0	6.0	6.0	6.2	6.0	6.0	5.9	5.7
K_2CO_3 (wt.%)	1.6	1.7	1.9	1.7	1.7	1.7	1.7	1.7
Pressure (bar)	195	201	197	198	181	201	215	240
Temperature (°C)	298	300	299	299	282	300	321	355

2.5 Analysis

The aqueous samples were added a known amount of internal standard (IS: syringol), extracted with DEE in a separating funnel (10 mL:10 mL, 1 hr, stirring), filtrated through 0.45 μm sterile filter, and injected for analysis in GC-MS. The oil samples were extracted with DEE by mixing approx. 1 g of oil with 20 mL of the solvent, followed by filtration through 0.45 μm sterile filter, and addition of IS. Syringol is similar in both structure and the properties to the compounds present, yet is typically not present in softwood lignin and not formed in the conversion of lignin in NCW, therefore giving similar response factors (RF) without interfering with the reaction products [14]. Before adding the IS to a sample, an injection without IS was carried out to verify the absence of peaks at the retention time of the IS. The GC-MS analyses were carried out in triplicate. The Relative Standard Deviation (RSD) of the peak area was checked on a number of representative components, resulting to be below 5 %. The samples were analyzed and identified with a PerkinElmer Clarus GC 580 and MS SQ 8 S with electron impact (EI) ionization and quadrupole

ion analyzer. The gas chromatograph was equipped with a PerkinElmer Crossbond column (30 m X 0.25 mm ID) coated with 0.25 μm stationary phase (95 % dimethyl polysiloxane and 5 % diphenyl) and the carrier gas used was helium (constant flow 1 mL/min). Detector temperature was 180 °C. Electron impact mass spectra were recorded at 70 eV ionization energy. The GC settings were as follows: injection temperature 300 °C, split ratio 50/1, heating starts at 70 °C (hold 4.0 min), ramp to 300 °C (5 K/min, hold for 10 min), solvent delay 3.0 min, and scan m/z 40-400. Spectral interpretation was performed with NIST 2011 database.

Elemental analysis of the lignin and the biocrude was conducted in triplicate on a PerkinElmer 2400 Series II CHNS/O elemental analyzer. Approx. 5 mg of the sample were used in each analysis. In between each 5th run, the apparatus was checked with a standard compound. Oxygen was calculated by subtraction on a ash-free dry basis. The higher heating value (HHV) of the produced biocrude was determined by IKA C 2000 basic oxygen (p = 30 bar) bomb calorimeter (triplicate measurements). The total carbon content (TC) and the total inorganic carbon content (TIC) of the aqueous phase were measured in triplicate with an AI-Analyzer Multi N/C 2100S, and the total organic carbon content (TOC) was calculated by difference. Injection volume was 500 μl. The applied gas was oxygen with p_{O_2} approx. 5 bar, gas ow 160 mL/min, and oven temperature 800 °C. The average RSD on triplicate TOC measurements was 1.2 %. The water content in the biocrude was determined in triplicate by a volumetric Karl Fischer unit. Approx. 0.5 g of sample was dissolved in 5 g THF and then filtrated. The water content in THF was measured and then subtracted. The water content in lignin was determined thermogravimetrically (TGA, N2 flow 30 cc/min, heating 10 K/min from 25 °C to 115 °C). The average SD was 0.3 %.

3 Results and Discussion

The conversion of Kraft lignin in near-critical water, followed by quenching in the water trap and centrifugation of the reaction products, resulted in an aqueous phase and a black oil, heavier than the aqueous phase and containing suspended solids. TOC of the aqueous phase after centrifugation was measured and the expected TOC values at the reactor exit (i.e. before quenching) were recalculated taking into account the dilution in the trap. These values resulted to be between 31 g/L and 35 g/L for runs e-f-g-h, whereas they increased from 21 g/L to 70 g/L for runs a-b-c-d, as w_{Ph} in the feed increased. The aqueous phase after acidification and removal of the insolubles was characterized by GC-MS identification and quantitation of the water soluble organics (WSO). With regard to the oil, its THF-soluble fraction was indicated as biocrude and characterized by means of overall parameters (elemental analysis, HHV, water content). In addition, the lighter fraction of the biocrude, defined as the fraction soluble in DEE, was characterized by means of GC-MS identification and quantitation.

3.1 Aqueous phase characterization

A typical chromatogram obtained from the GC-MS analysis of the aqueous phase, as well as the chemical structures of the most abundant compounds, are presented in Figure C.3. The majority of the identified conversion products could be classified into five main groups of compounds: methoxybenzenes (M), guaiacols (G), catechols (C), alkylphenols (A), and phenolic dimers (APD). Alkyl side chains of the monomeric compounds were of methyl and ethyl type only. The mass fractions of the identified compounds at the reactor exit were calculated from the GC-MS quantitation, also taking into account the dilution in the cold water trap. Results are shown in Table C.2. As can be seen, the total mass fraction of WSO on a phenol-free basis increased with both w_{Ph} (at constant temperature) and temperature (at constant w_{Ph}), until maximum values were reached for w_{Ph} of 6.5 wt.% and temperature of 320 °C. In the run without phenol in the feed, a very small amount of WSO was found in the produced aqueous phase, indicating an inefficient conversion process. With regard to the mass fractions of single classes of compounds, some major trends could be identified. As temperature increased, the aqueous phase was enriched in catechols (up to 320 °C) and alkylphenols, whereas the content of guaiacols reduced. In addition, the mass fraction of guaiacols, alkylphenols, and dimers showed a maximum at w_{Ph} of 6.5 wt.%, whereas catechols mass fractions increased in the whole range of w_{Ph} values. The content of methoxybenzenes in the aqueous phase was very small, but they were found in remarkable amount in the oil (see Section 3.2).

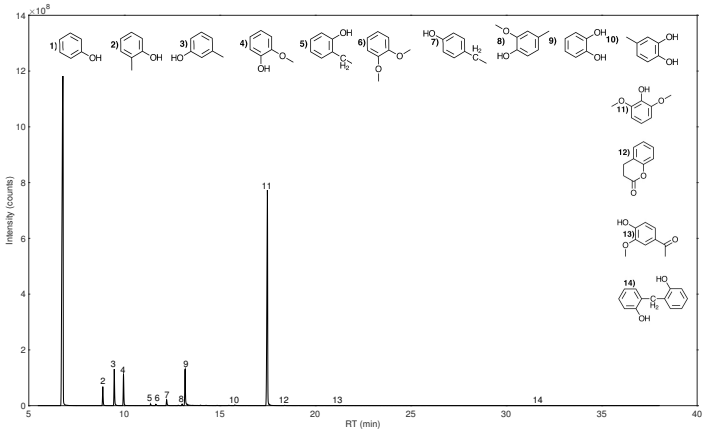

Fig. C.3: Typical chromatogram obtained for the aqueous phase (example from run g). 1: phenol, 2: o-cresol, 3: m/p-cresol, 4: guaiacol, 5: 2-ethylphenol, 6: veratrol, 7: 4-ethylphenol, 8: methylguaiacol, 9: catechol, 10: 4-methylcatechol, 11: syringol (internal standard), 12: hydrocoumarin, 13: acetovanillone, 14: phenolic dimers. Peaks 12-14 are not visible due to the scale of the plot.

Guaiacols are the main primary products of softwood lignin decomposition, obtained via hydrolysis and cleavage of ether and C-C bonds. Catechols and alkylphenols are also reported as primary products of lignin decomposition through the same reaction mechanisms, but they can also be formed by secondary reactions such as demethoxylation of guaiacols and alkylation of hydroxylated benzenes [7]. Phenolic dimers can also be formed by secondary re-polymerization reactions from phenol and 1-ring aromatic reaction intermediates [26, 30]. Methoxybenzenes (e.g. anisole) were reported as one of the products of hydrothermal conversion of lignin in the presence of phenol [14, 15, 27]. A similar reacting mixture was reported by Nguyen et al. [15], who converted Kraft Lignoboost softwood lignin (average molecular weight 3900 g/mol) in near-critical water, in the presence of phenol (4.1 wt.%) and K_2CO_3 (1.6 wt.%), on a continuous flow unit (1 kg/h of feed slurry) equipped with a PFR filled with ZrO_2 particles, and operated with recycle (10:1) in order to achieve fast heating of the feed slurry.

Table C.2: Full quantification of WSO. All values are expressed as mass fractions.

Run		a	b	c	d	e	f	g	h
		T = 300 °C with phenol at:				Phenol = 3.4 wt.% with T at:			
RT (min)	Identification	0 wt.%	3.4 wt.%	6.5 wt.%	9.7 wt.%	280 °C	300 °C	320 °C	350 °C
5.1	Anisole	0.0000	0.0127	0.0000	0.0000	0.0000	0.0127	0.0000	0.0000
6.7	Phenol	0.0392	1.72	3.23	4.23	1.37	1.72	1.61	1.63
8.8	o-Cresol	0.0001	0.0139	0.0224	0.0095	0.0020	0.0139	0.0478	0.0669
9.4	m/p-Cresol	0.0003	0.0314	0.0511	0.0201	0.0054	0.0314	0.0915	0.1214
9.9	Guaiacol	0.0090	0.160	0.160	0.119	0.183	0.160	0.0766	0.0159
11.3	2-Ethylphenol	0.0000	0.0026	0.0033	0.0013	0.0008	0.0026	0.0041	0.0066
11.5	Veratrol	0.0000	0.0057	0.0021	0.0004	0.0024	0.0057	0.0043	0.0038
12.1	4-Ethylphenol	0.0001	0.0100	0.0145	0.0063	0.0030	0.0100	0.0168	0.0231
13.0	Methylguaiacol	0.0003	0.0047	0.0023	0.0005	0.0019	0.0047	0.0039	0.0014
13.2	Catechol	0.0050	0.0478	0.0611	0.102	0.0066	0.0478	0.103	0.0723
14.1	2-Coumaranone	0.0000	0.0017	0.0051	0.0040	0.0009	0.0017	0.0000	0.0007
15.8	4-Methylcatechol	0.0000	0.0000	0.0000	0.0000	0.0000	0.0000	0.0029	0.0065
18.4	Hydrocoumarine	0.0000	0.0016	0.0034	0.0027	0.0006	0.0016	0.0012	0.0009
18.8	Vanillin	0.0090	0.0000	0.0000	0.0000	0.0047	0.0000	0.0000	0.0000
20.9	Acetovanillone	0.0010	0.0017	0.0029	0.0006	0.0030	0.0017	0.0000	0.0000
31.5	Phenolic dimer I	0.0000	0.0019	0.0049	0.0028	0.0012	0.0019	0.0001	0.0000
32.0	Phenolic dimer II	0.0000	0.0021	0.0085	0.0072	0.0025	0.0021	0.0001	0.0000
	Total	0.0558	2.02	3.57	4.51	1.59	2.02	1.96	1.95
	Phenol	0.0392	1.72	3.23	4.23	1.37	1.72	1.61	1.63
	Phenol-free total	0.0166	0.298	0.342	0.277	0.218	0.298	0.352	0.321
	Methoxybenzenes	0.0000	0.0183	0.0021	0.0004	0.0024	0.0183	0.0043	0.0038
	Guaiacols	0.0093	0.165	0.162	0.119	0.185	0.165	0.0804	0.0172
	Catechols	0.0049	0.0477	0.0610	0.1022	0.0066	0.0477	0.1058	0.0788
	Alkylphenols	0.0003	0.0578	0.0912	0.0372	0.0111	0.0578	0.160	0.219
	APD	0.0000	0.0039	0.0133	0.0100	0.0036	0.0039	0.0002	0.0000

With the exception of small components (C1 - C3) not identified in this work, 14 peaks corresponding to aromatic components match in the aqueous phases produced in the two works, representing from 92 % to 95 % of the total phenol-free components identified by Nguyen et al. [15] when operating the reactor in the range 290 – 350 °C. From a quantitative standpoint, the data of this work related to phenol mass fraction in the range 3.2 wt.% - 3.6 wt.% (see Table C.2) show that the total phenol-free mass fraction of aromatic components increased from 0.22 wt.% to 0.35

wt.%, as temperature increases from 280 to 320 °C, which is in line with the values observed by Nguyen et al. [15] (0.27 wt.% to 0.45 wt.% as temperature increased from 290 °C – 330 °C). On the other hand, the further increase at 350 °C is not observed in this work. The qualitative trends of the different classes of compounds also match, with strong increases of mass fractions of catechols and alkylphenols and strong decreases of mass fractions of guaiacol, vanillin, acetovanillone and phenolic dimers, as temperature increases.

3.2 Biocrude characterization

As can be seen from Table C.3, the elemental composition of the obtained biocrudes showed an increase in carbon combined with a decrease in sulfur and oxygen with respect to the lignin feed, which is a significant improvement from a drop-in fuel standpoint.

Table C.3: Properties and composition of the biocrude from different runs. Elemental composition and HHV are reported on a water-free basis. The initial HHV of lignin was 26.75 MJ/kg. The initial composition of lignin was: 64.4 % carbon, 6.7 % hydrogen, 1.8 % sulfur, and 27.1 % oxygen.

Run	a	b	c	d	e	f	g	h
	T = 300 °C with phenol at:				Phenol = 3.4 wt.% with T at:			
	0 wt.%	3.4 wt.%	6.5 wt.%	9.7 wt.%	280 °C	300 °C	320 °C	350 °C
Water (wt. %)	2.73	4.54	1.61	1.23	1.23	4.54	1.71	5.19
C (%)	69.9	67.3	72.0	72.3	68.9	67.3	72.4	72.1
H (%)	5.7	6.1	6.4	6.2	6.5	6.1	5.8	5.5
N (%)	0.21	0.00	0.00	0.40	0.00	0.00	0.04	0.01
S (%)	0.61	0.68	0.65	0.59	0.72	0.68	0.41	0.41
O (%)	23.6	25.9	21.0	20.5	23.9	25.9	21.4	22.0
HHV (MJ/kg)	29.8	30.4	31.1	31.2	30.4	30.4	30.7	32.1

As can be calculated, this qualitative result is also valid for the elemental composition of biocrudes on a phenol-free basis. This is significant in the context of a process where the unconverted phenol is recovered from the biocrude prior to its recirculation to the reactor. Consistently with the elemental composition results, the HHV of the biocrudes showed a significant increase compared to the heating value of the feed. The trends in CHNS/O composition and HHV were most noticeable for high w_{Ph} values and high reaction temperatures. The water content of the biocrudes, after centrifugation and solvent evaporation, was relatively low (1 - 5 wt.%). The results obtained in this work for a given mass fraction of phenol in the feed are very much in line with the results obtained by Nguyen et al. [15] in similar conditions (see Section 3.1): in this work the average carbon and sulfur mass fraction variations, and HHV variations (i.e. dry biocrude values – dry lignin values) were +9 %, -69 %, +15 %, respectively; in the work of Nguyen et al. [15], considering the runs in the range 290 °C – 350 °C, the analogous average values were + 11 %, -75 %, +13 %, respectively. On the other hand, the water content of the biocrude produced in this work was remarkably lower (1 – 5 wt.% vs. 11 – 19 wt.%). The higher speed of the centrifugation applied in this work (5000 rpm, instead of 4700 rpm [15]) can

explain, at least in part, the lower water content due to an improved separation of dispersed water.

A typical chromatogram obtained from the GC-MS analysis of the DEE-soluble fraction of the biocrudes, also referred to as the light oil fraction, as well as the chemical structures of the most common compounds are presented in Figure C.4. In general, the compounds identified in the aqueous phase were also detected in the light oil, with their distribution between the phases depending on their polarity. In line with this trend, the light oil was richer in methoxybenzenes, guaiacols, and alkylphenols, whereas it showed only small amounts of catechols.

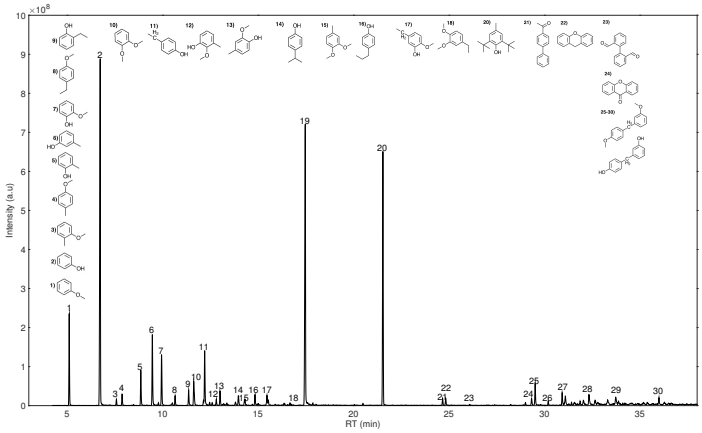

Fig. C.4: Typical chromatogram obtained for the DEE-souble part of the biocrude (example from run g). 1: anisole, 2: phenol, 3: 2-methylanisole, 4: 4-methylanisole, 5: o-cresol, 6: m/p-cresol, 7: guaiacol, 8: 4-ethylanisole, 9: 2-ethylphenol, 10: veratrol, 11: 4-ethylphenol, 12: methylguaiacol, 13: methylguaiacol, 14: p-cumenol, 15: methylveratrol,16: 4-propylphenol, 17: 4-ethylguaiacol, 18: 4-ethylveratrole, 19: syringol (internal standard), 20: butylated hydroxytoluene (BHT), 21: ethanone, 1-[1,1'-biphenyl]-x-yl , 22: 9H-xanthene, 23: 1,1'-biphenyl-2,2'-dicarboxaldehyde, 24: xanthone, 25-30: APD.

Alkyl side chains to aromatic rings were mostly of methyl and ethyl type, even though propyl groups were also found. This pattern is also very much in line with that found by Nguyen et al. [15]. More specifically, 13 of the identified peaks corresponding to 1-ring aromatic components match with the experimental results reported by Nguyen et al. [15], together with two phenolic dimer types (C6-C1-C6 and C6-C2-C6) identified in both works. The matching components represent from 88 % to 95 % of the whole oil reported by Nguyen et al. [15]. The major difference of the oil produced in the present work is represented by the relatively high amount of butylated hydroxytoluene (BHT), with mass fractions increasing with temperature from 1.0 wt.% to 3.2 wt.% and between 1.0 wt.% and 1.9 wt.% in the runs with varying phenol in the feed. Interestingly, this component was not found by Nguyen et al. [14, 15]. However, BHT was sporadically reported in experimental works of lignin depolymerization and conversion, in relation to a number of process variants.

For example, it was reported as one of the major products of near-critical water conversion of lignin in a batch reactor (280 °C, no catalyst, 15 min of reaction time) by Karagöz et al. [38]; it was obtained from conversion of lignin in water/methanol mixtures (250 °C, acid catalysts, 30 min of reaction time) [39]; it was reported as one of the products of fast pyrolysis of lignin [40]. The mechanisms of its formation in lignin conversion processes are not clear [38, 39]. Minor differences with respect to the oil reported by Nguyen et al. [15] are given by a higher relative amount of 2-ring non-condensed aromatics (2-NCAR), e.g. 9H-xanthene and xanthone, and a number of dimers of anisolic nature which were found in this work and that were not observed by Nguyen et al. [14, 15]. Phenol content in the light oil varied in the range 0.19 wt.% to 15.1 wt.%, depending naturally on the initial mass fraction of the co-solvent in the feed (Table C.4). On a phenol-free basis, the mass fraction of the components detected in the light oil ranged from 1.8 wt.% to 14.7 wt.%, with higher values obtained at high co-solvent contents in the feed. The major trends in the light oil composition profile were that the mass fractions of methoxybenzenes, guaiacols, 2-NCAR, and dimers increased with w_{Ph}, with the increase being particularly remarkable for the dimers. The alkylphenols increased up to w_{Ph} 6.5 wt.%. With regard to the effect of temperature, values rising up to 320 °C resulted in strong increases in mass fractions of alkylphenols, methoxybenzenes, dimers and 2-NCAR. This is also in line with the trend reported in the literature [15]. However, with the exception of 2-NCAR and alkylphenols, the further increase in the mass fractions of these compounds at 350 °C [15] was not observed here.

Table C.4: Quantification of the classes of compounds in the DEE-soluble fraction of the biocrude from different runs. All values are expressed as mass fractions.

Run	a	b	c	d	e	f	g	h
	T = 300 °C with phenol at:				Phenol = 3.4 wt.% with T at:			
	0 wt.%	3.4 wt.%	6.5 wt.%	9.7 wt.%	280 °C	300 °C	320 °C	350 °C
Total	4.49	15.4	18.4	32.9	12.2	15.4	18.2	17.9
Phenol	0.19	4. 18	6.99	15.13	3.33	4.18	4.31=	3.70
Phenol-free total	1.84	4.80	8.05	14.74	3.14	4.80	10.14	9.03
Methoxybenzenes	0.221	0.929	2.30	3.02	0.484	0.929	1.55	1.17
Guaiacols	0.496	0.925	1.19	1.40	0.861	0.925	1.10	0.330
Catechols	0.0000	0.0000	0.0000	0.0671	0.0000	0.0000	0.0000	0.0000
Alkylphenols	1.06	1.83	2.91	2.20	1.06	1.83	5.36	5.57
2-NCAR	0.0133	0.112	0.113	0.407	0.0637	0.112	0.299	0.733
APD	0.0261	0.940	1.42	7.55	0.641	0.940	1.63	0.840

3.3 Yields of products fractions and C-balances

In addition to the characterization of the products, the results from each run were assessed with respect to two different parameters: carbon balances and yields of well-defined product fractions. The C-balances were determined from the carbon input into the reactor feed and the carbon output, which was calculated taking into account the TOC measurements of the aqueous phase obtained by centrifugation and the elemental analysis of both the insolubles (S2, S4) and the biocrude. In all runs, the C-recovery in the product fractions was between 82.8 % and 102.3 % (Table

C.5), thus showing a good control over the carbon flow in the process. With regard to yields, they were calculated for three products fractions: biocrude, WSO, and insolubles. The biocrude is considered on a water-free and phenol-free basis; WSO are considered on a phenol-free basis. All yields are referred to the dry lignin fed to the system. The choice of expressing biocrude and WSO yields on a phenol-free basis is justified by the fact that an industrial application of this process would require a downstream recovery step of unconverted phenol to be recirculated to the reactor unit and therefore it is not appropriate to consider phenol as one of the products.

Table C.5: Summary of the yields of products and C-balances.

Run	a	b	c	d	e	f	g	h
	T = 300 °C with phenol at:				Phenol = 3.4 wt.% with T at:			
	0 wt.%	3.4 wt.%	6.5 wt.%	9.7 wt.%	280 °C	300 °C	320 °C	350 °C
Biocrude (wt. %)	33.9	77.3	87.6	102.3	50.6	77.3	50.4	48.3
WSO (wt. %)	0.2	4.4	4.9	3.5	3.4	4.4	5.0	5.2
Insolubles (wt. %)	54.4	11.3	7.12	1.4	22.4	11.3	12.6	15.9
C-recovery (%)	86.2	102.3	82.8	95.5	89.4	102.3	84.9	84.3

However, since phenol takes part in the reaction as capping agent, phenol-free yields higher than 100 % are possible according to this definition. As can be seen from Table 5, in the absence of phenol in the feed, the process was not efficient, with low yields of biocrude and WSO and high yield of insolubles (54.4 %). The insolubles decreased remarkably with increasing w_{Ph}, as a consequence of an increased production of monomeric aromatic compounds (see Section 3.4) and favored solubilization in the biocrude. In line with this explanation, the yields of biocrude increased notably with rising w_{Ph}. Bearing in mind that the yield of biocrude is defined on a phenol-free basis, this result clearly indicates an increased production of liquid products (or products forming liquid phases when mixed with phenol). On the other hand, the trend of the yield of WSO is more complex, showing a steep increase at lower w_{Ph} values, while exhibiting a maximum for w_{Ph} of 6.5 wt.%. The decrease of WSO at the highest phenol level is likely to be determined by the increased production of methoxybenzenes and phenolic dimers (see Section 3.4, which are less soluble in water. Other factors may also play a role, such as shifts in phase equilibrium distribution of monomeric phenolic components when more phenol is dissolved in the biocrude. With regard to the reaction temperature, the process did not work efficiently at 280 °C, in spite of the presence of phenol in the feed. The yield of WSO showed a monotonic increase with temperature, up to 5.2 % at the highest temperature. The yields of biocrude exhibited a maximum at 300 °C, whereas the yields of insolubles followed an opposite trend, with a minimum showed at 300 °C. The presence of a minimum yield of the insolubles inside the temperature range can be explained with the competition between hydrolysis and cleavage of ether and C-C bonds, leading to lignin depolymerization, and condensation reactions, which are enhanced at higher temperatures and eventually yield secondary products of higher molecular weight [7].

3.4 Yields of chemical classes of compounds

The yields of single classes of chemicals were calculated combining the components identified and quantitated both in the acidified aqueous phase (i.e. the WSO) and in the light oil (i.e. the DEE-soluble fraction of the biocrude) using GC-MS. The yield of each chemical class (n) was defined according to Equation C.1 [25].

$$Y_n = \frac{m_{n,WSO} + m_{n,BC}}{m_l(1 - w_l)} \tag{C.1}$$

where $m_{n,WSO}$ and $m_{n,BC}$ are the masses of the nth-class of compounds in the acidified aqueous phase and biocrude, respectively. The results are represented in Figure C.5 and C.6, which show the dependence of the yields on phenol mass fraction and temperature, respectively. As can be seen, in the absence of phenol the production of water-soluble and/or DEE-soluble monomeric and dimeric aromatic compounds was practically absent, with a total yield of monomeric compounds (Y_T = Y_M + Y_A + Y_G + Y_C + unclassified monomeric aromatics) equal to 0.8 %, along with 0.01 % of 2-ring aromatics (Y_{2-NCAR} and Y_{APD}). The addition of phenol up to 6.5 wt.% to the reacting system led to a substantial increase in both the total yield (from 0.8 % to 12.5 %), as well as the yield of monomeric compounds (from 0.8 % to 10.8 %). As can be seen from the trends of the single classes, increasing further the phenol mass fraction (from 6.5 % to 9.7 %) produced a further, although limited, increase in the yield of monomeric compounds (from 10.8 % to 11.5 %), together with a remarkable increase of the yield of dimers (from 1.6 % to 9.7 %). More specifically, looking at the trends for the single chemical classes of monomers, Y_G and Y_A showed a maximum for phenol mass fraction at 6.5 %, whereas Y_C and Y_M increased progressively. At constant w_{Ph} (approx. 3.4 wt.%), the total yield of the classified compounds, as well as the total yield of the monomers, showed a maximum at 320 °C, with the values being 8.7 % and 9.3 %, respectively. Y_G and Y_A were very sensitive to temperature, with guaiacols decreasing with it, whereas the opposite trend was found for alkylphenols. The decrease of guaiacols and increase of alkylphenols with temperature is a typical pattern of lignin depolymerization and conversion processes, due to the enhancement of demethoxylation and alkylation reactions at higher temperatures [7]. Since demethoxylation reactions produce phenols and catechols from guaiacols, higher amounts of phenol as co-solvent are expected to favor the formation of catechols, which is in line with the results shown in Fig. C.5. The marked increase of the yield of alkylphenols as phenol concentration increases up to 6.5 wt.% (see Fig. C.5) is in line with the function of phenol as capping agent [26–28], which is realized reacting with unstable fragments and thus competing with condensation reactions [7, 30, 32]. However, phenol can also react with 1-ring aromatic reaction intermediates to form relatively stable dimeric aromatic compounds [31] This pathway seems to prevail at the highest phenol mass fraction used in this work, thus explaining the marked increase in phenolic dimers with a corresponding small further increase in the yield of monomeric aromatic components. Comparing results referring to similar operating conditions with the work of Nguyen et al. [15] on a continuous flow unit developed at Chalmers Uni-

versity of Technology, the yields of monomeric compounds in this work was found to be somewhat lower, between 7 % and 11 %, instead of 10 % to 20 %. However, the two processes present a number of differences which probably explain the observed data: the feed Kraft lignin used in this work has a higher average molar mass (8000 vs 3900); the reactor of the continuous flow unit was operated as a PFR with recycle, which means that the feed stream is not only rapidly heated but also pre-mixed with reaction products, which is not the case in a batch operation; the PFR was filled with solid material (ZrO_2); the operating pressure in this work was in the range 20 - 24 MPa, instead of 25 MPa.

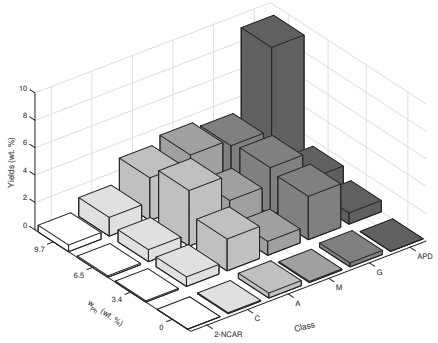

Fig. C.5: Overall yields of the main chemical families: methoxybenzenes (M), guaiacols (G), catechols (C), alkylphenols (A), two-ring non-condensed aromatic dimers (2-NCAR), and anisolic and phenolic dimers (APD) as a function of phenol mass fraction in the feed. Reaction temperature: 300 °C. Mass fraction of K_2CO_3: in the range 1.6 wt.% - 1.9 wt.%.

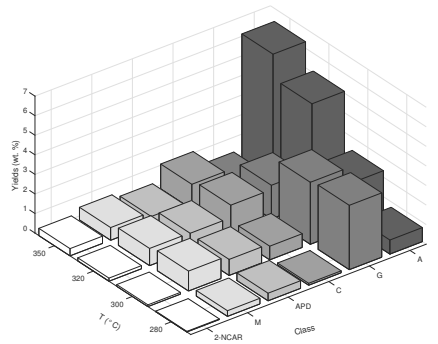

Fig. C.6: Overall yields of the main chemical families: methoxybenzenes (M), guaiacols (G), catechols (C), alkylphenols (A), two-ring non-condensed aromatic dimers (2-NCAR), and anisolic and phenolic dimers (APD) as a function of reaction temperature. Mass fraction of phenol: 3.2 wt.% - 3.6 wt.%. Mass fraction of K_2CO_3: 1.7 wt.%.

4 Conclusions

The results obtained in this work show that the new equipment, comprising a batch reactor with biomass injection system, is an effective tool for studying the hydrothermal conversion of biomass slurries in near-critical water medium. The equipment allowed fine control of reaction time and density of the reaction medium through combination of fast heating of the biomass, pressure control, and products withdrawal/quenching. In particular, the fast heating of the injected slurry is a key aspect allowing better match of laboratory scale batch results with results on continuous flow pilot units, thus reducing uncertainties associated with the process scale up. The lignin conversion products obtained in this work showed a very good match with the products obtained on a continuous flow small scale pilot unit running a similar, albeit not same, process [15]. The yields of 1-ring aromatic components in similar conditions were somewhat lower (7 % - 11 % instead of 10 % - 20 %), which could however be explained by the differences between the two systems. Besides the reaction temperature, this work focused on the effect of phenol mass fraction in the feed of the reacting system. In the absence of phenol, the process is not efficient. Increasing phenol mass fraction, the insolubles reduce and the phenol-free yield of lignin-derived 1-ring aromatic components increases. This is due both to physical factors, i.e. improved solubilization of the reaction products in phenol-containing phases, and to chemical factors, i.e. the role of phenol as capping agent favoring the formation of 1-ring aromatics with respect to re-polymerization reactions. Interestingly, the results of this work show that the yield of 1-ring aromatic components sharply increases with small addition of phenol in the reacting system (e.g. from 0.8 wt.% to 7.3 wt.% as the phenol/lignin ratio increases from 0 to 0.56), whereas at higher phenol levels this yield shows a plateau (e.g. from 10.8 wt.% to 11.8 wt.% as the phenol/lignin ratio increases from 1.1 to 1.6). In particular, at the higher phenol/lignin ratios, the yield of alkylphenols shows a maximum and starts to decrease, whereas the yields of phenolic dimers sharply increases. This suggests that the secondary re-polymerization reactions of phenol and 1-ring aromatic intermediates become predominant with respect to reactions of phenol and smaller reactive fragments. Therefore, an optimal phenol/lignin ratio is envisaged in a process aimed at producing 1-ring aromatics, without increasing too much the yield of phenolic dimers.

5 Acknowledgments

This work was supported by the Danish Council for Strategic Research (DSF grant no. 1305-00030B), Danish Agency for Science, Technology and Innovation (grant no. 11-118412); and by Marie Curie Career Integration Grant (FP7-PEOPLE-2012-CIG, project no. 321816).

6 Supporting Information

Table C.6: Studies with injection of slurries.

#	Mass of injected slurry (g)	Dry mass of injected slurry (g)	Dry mass content (wt.%)
1	8.43	1.03	12.18
2	10.94	1.31	11.99
3	10.90	1.28	11.70
4	10.59	1.24	11.74
5	10.72	1.25	11.63
6	9.17	1.05	11.48
7	10.52	1.20	11.37
8	7.84	0.89	11.36
9	4.88	0.56	11.58

Table C.7: Process conditions in the experimental runs.

Run	a	b	c	d	e	f	g	h
	T = 300 °C with phenol at:				Phenol = 3.4 wt.% with T at:			
	0 wt.%	3.4 wt.%	6.5 wt.%	9.7 wt.%	280 °C	300 °C	320 °C	350 °C
Portion 1 (g)	45.0	45.0	45.0	45.0	45.0	45.0	45.0	45.0
Lignin (g)	0	0	0	0	0	0	0	0
Phenol (g)	0.00	3.01	5.71	8.92	2.94	3.01	2.00	2.99
K_2CO_3 (g)	0.73	0.76	0.84	0.76	0.75	0.76	0.77	0.77
Portion 2 (g)	47.2	44.6	43.2	47.1	45.9	44.6	42.0	38.1
Lignin (g)	5.55	5.41	5.34	5.75	5.45	5.41	5.10	4.69
Phenol (g)	0	0	0	0	0	0	0	0
K_2CO_3 (g)	0.77	0.75	0.80	0.79	0.76	0.75	0.71	0.65

References

[1] B. Saake and R. Lehnen, *Lignin, Ullmann's Encyclopedia of Industrial Chemistry.* Wiley-VCH, 2012.

[2] A. J. Ragauskas, G. T. Beckham, M. J. Biddy, R. Chandra, F. Chen, M. F. Davis, B. H. Davison, R. A. Dixon, P. Gilna, M. Keller, P. Langan, A. K. Naskar, J. N. Saddler, T. J. Tschaplinski, G. A. Tuskan, and C. E. Wyman, "Lignin valorization: Improving lignin processing in the biorefinery," *Science*, vol. 344, no. 6185, p. 1246843, 2014.

[3] S. Xie, A. J. Ragauskas, and J. S. Yuan, "Lignin conversion: Opportunities and challenges for the integrated biorefinery," *Ind. Biotechnol.*, vol. 12, no. 3, pp. 161–167, 2016.

[4] J. Lora, "Industrial commercial lignins: sources, properties and applications," in *Monomers, polymers and composites from renewable resources*, M. N. Belgacem and A. Gandini, Eds. Elsevier, 2008, ch. 4.

[5] J. Zakzeski, P. C. A. Bruijnincx, A. L. Jongerius, and B. M. Weckhuysen, "The catalytic valorization of lignin for the production of renewable chemicals," *Chem. Rev.*, vol. 110, no. 6, pp. 3552–3599, 2010.

[6] M. P. Pandey and C. S. Kim, "Lignin depolymerization and conversion: A review of thermochemical methods," *Chem. Eng. Technol.*, vol. 34, no. 1, pp. 29–41, 2011.

[7] S. Kang, X. Li, J. Fan, and J. Chang, "Hydrothermal conversion of lignin: A review," *Renew. Sustainable Energy Rev.*, vol. 27, pp. 546–558, 2013.

[8] P. Azadi, O. R. Inderwildi, R. Farnood, and D. A. King, "Liquid fuels, hydrogen and chemicals from lignin: A critical review," *Renew. Sustainable Energy Rev.*, vol. 21, pp. 506–523, 2013.

[9] C. Xu, R. A. D. Arancon, J. Labidi, and R. Luque, "Lignin depolymerisation strategies: towards valuable chemicals and fuels," *Chem. Soc. Rev.*, vol. 43, no. 22, pp. 7485–7500, 2014.

[10] Wahyudiono, M. Sasaki, and M. Goto, "Recovery of phenolic compounds through the decomposition of lignin in near and supercritical water," *Chem. Eng. Process.*, vol. 47, no. 9, pp. 1609–1619, 2008.

[11] M. Tymchyshyn and C. C. Xu, "Liquefaction of bio-mass in hot-compressed water for the production of phenolic compounds," *Bioresource Technol.*, vol. 101, no. 7, pp. 2483–2490, 2010.

[12] J.-M. Lavoie, W. Baré, and M. Bilodeau, "Depolymerization of steam-treated lignin for the production of green chemicals," *Bioresour. Technol.*, vol. 102, no. 7, pp. 4917–4920, 2011.

[13] R. Beauchet, F. Monteil-Rivera, and J. Lavoie, "Conversion of lignin to aromatic-based chemicals (L-chems) and biofuels (L-fuels)," *Bioresource Technol.*, vol. 121, pp. 328–334, 2012.

[14] T. D. H. Nguyen, M. Maschietti, T. Belkheiri, L.-E. Åmand, H. Theliander, L. Vamling, L. Olausson, and S.-I. Andersson, "Catalytic depolymerisation and conversion of Kraft lignin into liquid products using near-critical water," *J. Supercrit. Fluids*, vol. 86, pp. 67–75, 2014.

[15] T. D. H. Nguyen, M. Maschietti, L.-E. Åmand, L. Vamling, L. Olausson, S.-I. Andersson, and H. Theliander, "The effect of temperature on the catalytic conversion of Kraft lignin using near-critical water," *Bioresource Technol.*, vol. 170, pp. 196–203, 2014.

[16] V. Roberts, V. Stein, T. Reiner, A. Lemonidou, X. Li, and J. A. Lercher, "Towards quantitative catalytic lignin depolymerization," *Chem. Eur. J.*, vol. 17, no. 21, pp. 5939–5948, 2011.

[17] C. A. Eckert and K. Chandler, "Tuning fluid solvents for chemical reactions," *J. Supercit. Fluid.*, vol. 13, no. 1, pp. 187–195, 1998.

[18] A. A. Peterson, F. Vogel, R. P. Lachance, M. Fröling, M. J. Antal Jr, and J. W. Tester, "Thermochemical biofuel production in hydrothermal media: A review of sub-and supercritical water technologies," *Energy Environ. Sci.*, vol. 1, no. 1, pp. 32–65, 2008.

[19] G. Brunner, "Near critical and supercritical water. Part I. Hydrolytic and hydrothermal processes," *J. Supercrit. Fluids*, vol. 47, no. 3, pp. 373–381, 2009.

[20] ——, "Near and supercritical water. Part II: Oxidative processes," *J. Supercrit. Fluids*, vol. 47, no. 3, pp. 382–390, 2009.

[21] A. G. Carr, R. Mammucari, and N. Foster, "A review of subcritical water as a solvent and its utilization for the processing of hydrophobic organic compounds," *Chem. Eng. J.*, vol. 172, no. 1, pp. 1–17, 2011.

[22] S. Karagöz, T. Bhaskar, A. Muto, Y. Sakata, T. Oshiki, and T. Kishimoto, "Low-temperature catalytic hydrothermal treatment of wood biomass: analysis of liquid products," *Chem. Eng. J.*, vol. 108, no. 1, pp. 127–137, 2005.

[23] S. Karagöz, T. Bhaskar, A. Muto, and Y. Sakata, "Hydrothermal upgrading of biomass: Effect of K_2CO_3 concentration and biomass/water ratio on products distribution," *Bioresource Technol.*, vol. 97, no. 1, pp. 90–98, 2006.

[24] T. Bhaskar, A. Sera, A. Muto, and Y. Sakata, "Hydrothermal upgrading of wood biomass: influence of the addition of K_2CO_3 and cellulose/lignin ratio," *Fuel*, vol. 87, no. 10, pp. 2236–2242, 2008.

[25] M. Maschietti, T. D. H. Nguyen, T. Belkheiri, L.-E. Åmand, H. Theliander, L. Vamling, L. Olausson, and S.-I. Andersson, "Catalytic hydrothermal conversion of LignoBoost Kraft lignin for the production of bio-oil and aromatic chemicals," in *Proceedings of the International Chemical Recovery Conference*, vol. 2, 2014, pp. 252–261.

[26] M. Saisu, T. Sato, M. Watanabe, T. Adschiri, and K. Arai, "Conversion of lignin with supercritical water-phenol mixtures," *Energy Fuels*, vol. 17, no. 4, pp. 922–928, 2003.

[27] K. Okuda, M. Umetsu, S. Takami, and T. Adschiri, "Disassembly of lignin and chemical recovery–rapid depolymerization of lignin without char formation in water–phenol mixtures," *Fuel Process. Technol.*, vol. 85, no. 8, pp. 803–813, 2004.

[28] Z. Fang, T. Sato, R. L. Smith, H. Inomata, K. Arai, and J. A. Kozinski, "Reaction chemistry and phase behavior of lignin in high-temperature and supercritical water," *Bioresour. Technol.*, vol. 99, no. 9, pp. 3424–3430, 2008.

[29] T. H. Pedersen, I. Grigoras, J. Hoffmann, S. S. Toor, I. M. Daraban, C. U. Jensen, S. Iversen, R. B. Madsen, M. Glasius, K. R. Arturi, R. P. Nielsen, E. G. Søgaard, and L. A. Rosendahl, "Continuous hydrothermal co-liquefaction of aspen wood and glycerol with water phase recirculation," *Appl. Energ.*, vol. 162, pp. 1034–1041, 2016.

[30] L. Lin, Y. Yao, M. Yoshioka, and N. Shiraishi, "Liquefaction mechanism of lignin in the presence of phenol at elevated temperature without catalysts. Studies on ß-o-4 lignin model compound. I. Structural characterization of the reaction products," *Holzforschung-Int. J. Biol. Chem. Phys. Technol. Wood*, vol. 51, no. 4, pp. 316–324, 1997.

[31] L. Lin, M. Yoshioka, Y. Yao, and N. Shiraishi, "Liquefaction mechanism of lignin in the presence of phenol at elevated temperature without catalysts. Studies on ß-0-4 lignin model compound. III. Multi-condensation," *Holzforschung-Int. J. Biol. Chem. Phys. Technol. Wood*, vol. 51, no. 4, pp. 333–337, 1997.

[32] ——, "Liquefaction mechanism of lignin in the presence of phenol at elevated temperature without catalysts. Studies on ß-o-4 lignin model compound. II. Reaction pathway," *Holzforschung-Int. J. Biol. Chem. Phys. Technol. Wood*, vol. 51, no. 4, pp. 325–332, 1997.

[33] A. Kruse, T. Henningsen, A. Sinag, and J. Pfeiffer, "Biomass gasification in supercritical water: Influence of the dry matter content and the formation of phenols," *Ind. Eng. Chem. Res.*, vol. 42, no. 16, pp. 3711–3717, 2003.

[34] M. Modell, "Gasification and liquefaction of forest products in supercritical water," in *Fundamentals of Thermochemical Biomass Conversion.* Springer, 1985, pp. 95–119.

[35] H. Schmieder, J. Abeln, N. Boukis, E. Dinjus, A. Kruse, M. Kluth, G. Petrich, E. Sadri, and M. Schacht, "Hydrothermal gasification of biomass and organic wastes," *J. Supercrit. Fluids*, vol. 17, no. 2, pp. 145–153, 2000.

[36] J. Barbier, N. Charon, N. Dupassieux, A. Loppinet-Serani, L. Mahé, J. Ponthus, M. Courtiade, A. Ducrozet, A. Fonverne, and F. Cansell, "Hydrothermal conversion of glucose in a batch reactor. A detailed study of an experimental key-parameter: The heating time," *J. Supercrit. Fluids*, vol. 58, no. 1, pp. 114–120, 2011.

[37] J. Barbier, N. Charon, N. Dupassieux, A. Loppinet-Serani, L. Mahé, J. Ponthus, M. Courtiade, A. Ducrozet, A.-A. Quoineaud, and F. Cansell, "Hydrothermal conversion of lignin compounds. A detailed study of fragmentation and condensation reaction pathways," *Biomass Bioenergy*, vol. 46, pp. 479–491, 2012.

[38] S. Karagöz, T. Bhaskar, A. Muto, and Y. Sakata, "Comparative studies of oil compositions produced from sawdust, rice husk, lignin and cellulose by hydrothermal treatment," *Fuel*, vol. 84, no. 7, pp. 875–884, 2005.

[39] A. K. Deepa and P. L. Dhepe, "Lignin depolymerization into aromatic monomers over solid acid catalysts," *ACS Catalysis*, vol. 5, no. 1, pp. 365–379, 2014.

[40] R. Lou, S.-b. Wu, and G.-j. Lv, "Effect of conditions on fast pyrolysis of bamboo lignin," *J. Anal. Appl. Pyrolysis*, vol. 89, no. 2, pp. 191–196, 2010.

Paper D

Hydrothermal conversion of Fallopia japonica in near-critical water: A study of liquefaction routes in the presence of co-solvents

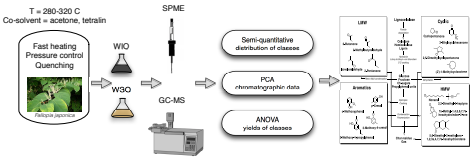

Katarzyna R. Arturi, Sergey Kucheryavskiy, Marco Maschietti, Rudi P. Nielsen, and Erik G. Søgaard

The manuscript has been submitted to
Bioresource Technology in February 2017

The layout has been revised.

Abstract

Reaction routes behind liquefaction of Fallopia japonica in near-critical water were studied as a function of temperature (T = 280 - 320 °C) and the polarity of co-solvents (acetone and tetralin). The experiments were performed in a state-of-the-art cold-injection batch reactor combining fast heating, pressure control, and products quenching. Using this approach, well-defined reaction conditions (temperature, pressure, and residence time) are achieved and the influence of heating rates on the chemistry of conversion is avoided. The presence of co-solvents stabilized low molecular weight products, leading to lower quantities of high molecular weight compounds and their derivatives. The addition of tetralin resulted in enhanced production of aromatics through improved solubilization of lignin and aromatization of furans. Additionally, it also promoted retro-aldol condensation of sugars into low molecular weight compounds and repressed hydrogenation of furans into cyclics.

Hydrothermal liquefaction; Cold-injection; Tetralin; Acetone; Lignocellulose; Biomass conversion; Near-critical eater, PCA

1 Introduction

Liquefaction is a thermochemical technique for conversion of mixed and complex biomass feedstocks into drop-in biofuels and chemical feedstock using near- or supercritical water (T_{cr} = 374 °C, p_{cr} = 22.1 MPa) [1–3]. The process takes place in a benign and environmentally friendly solvent, the properties of which can be adjusted depending on pressure and temperature. The fact that hydrothermal liquefaction (HTL) is carried out in water entails that the moisture content of the biomass not only is not an obstacle associated with massive energy penalties, but is considered an advantage. With changes in temperature and pressure, the hydrogen bonds between water molecules are disrupted and the regular network of molecules is replaced with clusters of 5 - 20 H_2O units [4]. Ionic product (IP), which expresses the degree of water auto-dissociation, increases from 10^{-14} to 10^{-11} between the ambient conditions and approx. T = 280 °C, and then decreases up to the supercritical point and beyond, a phenomenon explained by the decreasing stabilization power of the ionic species [5, 6]. In addition to IP, the properties influencing the fluidity of the reaction medium and the mass transfer of the solutes, i.e. density (ρ) and viscosity (μ), decrease with increasing temperature. Last, but not least, the values of dielectric constant (the relative dielectric permittivity, ϵ) decrease from approx. 80 at ambient conditions to 10 - 25 in the near-critical region, and further to 1 - 2 above the supercritical temperature, changing the dissociation of salts from excellent, to moderate, to non-existent [4]. At the same time, the reaction medium becomes increasingly miscible with non-polar organics.

Liquefaction of biomass in a water medium involves depolymerization of biopolymers followed by secondary transformations of monomers into intermediates and products distributed between biocrude, aqueous, gaseous, and solid fractions. Reaction mechanisms for liquefaction induced depolymerization include base-catalyzed hydrolysis, dehydration, addition of water, rearrangements, Friedel-Crafts alkylation, aldol condensation, and Cannizzaro reaction [7], with the final outcome of mixture auto-stabilization being a competition between depolymerization and repolymerization pathways. While the former process leads to high yields of light molecular weight monomers and intermediates of varying polarity, the latter results in the formation of biochar. The reaction pathways of a liquefaction process can be influenced by variation of process parameters, e.g. temperature, solvent density, presence of catalyst, addition of co-solvents, and reaction time. The role of co-solvents is to solubilize the biomass and its conversion products, in addition to acting as scavengers of unstable radical intermediates [8, 9], thus resulting in enhancing both the yields of lower molecular weight compounds, as well as the quality of the liquefaction products [10]. While various polar solvents, e.g. phenol, alcohols, glycols, and acetone, have shown promise as solvents and co-solvents [11–13], non-polar organics have only been considered to a lesser extent for the purpose [14–17]. In particular, proton donating solvents such as tetralin, which is an excellent additive for facilitating liquefaction of coal [18], could be potentially interesting for HTL.

In recent years, liquefaction studies have focused on utilization of sustainable, cheap, and abundant feeds [19, 20] such as lignocellulose, which is the most common raw material in both agriculture, as well as forestry sectors worldwide [21]. Moreover, the sustainability of the liquefaction could be increased further by application of currently underutilized resources [22] including invasive plant species, e.g. *Fallopia japonica*. As recently pointed out by [23], the use of non-indigenous and environmentally malign plants for the production of energy would turn an ecological burden into a useful resource. *Fallopia japonica* is a large, herbaceous perennial knotweed native to East Asia, Japan, China, and Korea, but also emerging in North America and Europe. It has tolerance to a wide range of soil types, pH values, salinity, and temperature regions (above -35 °C). It grows fast and requires relatively small water input [24]. Different processes [25, 26] have been considered for exploiting the potential of *Fallopia*, including pyrolysis [27]. However, so far the application of HTL on this raw material has not been studied.

While accounts of hydrothermal liquefaction in continuous units of varying sizes have been reported in the literature [2], the majority of the liquefaction studies for screening new processes are performed in a batch mode, where the relative ease of processing is nearly always accompanied by a limited process control. In a typical batch experiment, biomass is loaded into a cold, constant-volume reactor, heated for a period with the pressure rising autogenously, left for a short reaction time (τ), and then cooled by natural diffusion of heat. While the value of τ in liquefaction normally varies in the range 10 - 30 min, heating and cooling intervals add up to several hours. As was shown numerous times in the literature, the applied heating

rates have an impact on the reaction pathways behind liquefaction [28, 29]. Additionally, the lack of pressure control, an important reaction variable influencing the fluid density and thus its properties, introduces an additional level of uncertainty into the liquefaction batch results. Long heating and cooling times, with consequent unreliable definition of reaction time at a given temperature, together with unsteady pressure, make most laboratory batch reactors not accurate for studying liquefaction conversion processes. The limitations pertaining to heating time can be overcome by slurry cold-injection batch reactors, where the biomass feed dispersed in water is injected into the pre-heated pre-pressurised reaction medium [30–33]. A precise, accurate, and reproducible assessment of the output from liquefaction on a batch scale is a crucial pre-request for optimizing the continuous scale processes and the subsequent commercialization of the technology.

In this study, a cold-injection batch reactor equipped with means for pressure control and products quenching was used [34]. Applying this approach, well-defined reaction times at a well-defined reaction temperature and pressure are achieved. In particular, the long heating times and random temperature gradients affecting the chemistry of conversion are avoided, providing a reliable source of knowledge about reactions taking place during HTL. We have carried out the hydrothermal conversion of *Fallopia japonica* in order to study the liquefaction mechanisms of lignocellulosic biomass in the presence of co-solvents of different polarity (acetone and tetralin). Biomass as a basis for a biorefinery-based future is more likely to succeed if it is based on locally available and ample raw materials, such as *Fallopia*. Therefore, it is important to assess the potential of these raw materials as a source of value-added products.

2 Materials and Methods

2.1 Materials

The biomass used in this study was a freshly harvested *Fallopia Japonica*, both leaves and branches. The plants were cut into smaller pieces, dried in an oven at 105 °C for 24 h, ground down to a particle size of 100 μm, dried again at the same conditions, and milled further into particles of roughly 10 μm in diameter. The average moisture content of the biomass was approx. 2 wt.%. The ash content of the biomass was approx. 5 wt.% (dry basis). The elemental composition of the final feed was 49 wt.% carbon, 7 wt.% hydrogen, 43 wt.% oxygen, 0.9 wt.% nitrogen, and 0.1 wt.% sulfur. The values were determined by a Perkin Elmer 2400 Series II CHNS/O analyzer (oxygen calculated by difference) and re-calculated on a dry, ash-free basis. All used chemicals were obtained from Sigma Aldrich. Following organic solvents and co-solvents were used: acetone (co-A, ACS reagent, ≥ 99.5 %), diethyl ether (DEE, ≥ 99.5 %, GC), and tetralin (co-T, ≥ 99.5 %). Bromobenzene was used as an internal standard (IS, ≥ 99.5). K_2CO_3 (anhydrous, free-flowing, Redi-Dri^{TM}, ≥ 99 %) was used as a catalyst. Sodium carboxymethyl cellulose (CMC, MW approx. 250

000 g/mol) was employed as a dispersant to prevent biomass sedimentation and to increase the stability of the slurry. Distilled water was the primary reaction solvent. N_2 (99.9 % pure) was applied for purging the reactor system.

2.2 Equipment and procedure

Liquefaction experiments were performed in a batch reactor (99 mL), equipped with magnetic stirrer and temperature control system, connected with two hand-pumps, which allow injection of biomass slurry feed in the pre-heated and pre-pressurised reactor, as well as fine control of the reaction pressure by means of extremely small injections/withdrawals of fluid. The reactor was also equipped with multiple ports and a system of valves allowing withdrawal of the reaction products, from the reactor at high-temperature and pressure and quenching of the products. On the whole, this laboratory set-up allowed to study biomass conversion processes with an accurate control on reaction time, temperature and pressure (Figure D.7 of the Supporting Information). Details on the equipment are provided elsewhere [34].

The study was based on a full factorial experimental design (Table D.1) consisting of 12 runs with variations of temperature (280, 300, 320 °C) and co-solvents (co-A: 0 - 1 wt.% & co-T: 0 - 1 wt.%). The experimental procedure was as follows: a 45 g mixture of water, K_2CO_3, and co-solvent was injected into the reactor with one of the two hand-pumps; the reactor was then purged with N_2 and then heated up to a temperature 30 °C above the desired reaction temperature and pressurised. A feed slurry containing biomass, water, K_2CO_3, and CMC was mixed using an IKA Ultra Turrax (30 min, 20000 rpm) and then injected through the second pump until the selected pressure values were reached (190, 220, and 250 bar for 280, 300, 320 °C, respectively). The compositions of the reaction mixtures are summarized in Table D.1.

Table D.1: Composition of the reaction mixture in each run.

T (°C)	co-A (wt.%)	co-T (wt.%)	Biomass (wt. %)	K_2CO_3 (wt.%)	CMC (wt.%)
280	0.0	0.0	2.49	1.07	0.12
300	0.0	0.0	2.33	1.09	0.11
320	0.0	0.0	2.19	1.11	0.10
280	1.00	0.0	2.20	1.07	0.09
300	0.91	0.0	2.31	1.11	0.11
320	1.11	0.0	2.29	1.09	0.11
280	0.0	1.00	2.49	1.10	0.11
300	0.0	0.93	2.31	1.13	0.11
320	0.0	1.07	1.97	1.09	0.09
280	1.01	1.02	2.46	1.09	0.11
300	1.02	1.02	2.33	1.08	0.12
320	1.01	1.07	2.12	1.12	0.10

The injection of biomass resulted in a relatively small pressure and temperature drop followed by their increase up to the target operating values of the reaction. The whole injection process lasted from about 3 - 5 min. The heating and pressure profiles for the system are presented in Figure D.8 (Supporting Information). After the reaction time (τ = 10 min), the products were rapidly depressurized and cooled down in a cold trap. The gas products were not collected.

2.3 Analysis strategy

Once the reaction mixture was cooled down to room temperature, the products were separated by centrifugation (6000 rpm, 4 hr) into aqueous (top) and non-aqueous (bottom) fractions. The aqueous fraction was filtered under vacuum (Whatman No. 5) and separated into a solid (#S1) and a liquid fraction (#F1). The organic content of the #F1 was designated water soluble organics (WSO). The non-aqueous phase was redissolved in acetone, filtered (vacuum, Whatman No. 5), and separated into a retentate (#S2) and filtrate (#F2). The two solid fractions #S1 and #S2 were combined (#S) and dried in an oven at 105 °C overnight. The separation procedure is summarized in Figure D.9 (Supporting Information). The organic content of #F2 after removal of the solvent (vacuum evaporation at T = 35 °C and p $\approx$ 500 mbar) was designated biocrude (BC). Water insoluble organics (WIO) fraction was defined as a combination of solids and biocrude.

The moisture content in the biomass, solid, and the biocrude samples was determined thermogravimetrically (TGA, N_2 flow 35 cc/min, heating 10 K/min from 25 °C to 110 °C). The yields of WIO, #S, and BC (Y_{WIO} ,Y_S, and Y_{BC}, respectively) were calculated on a co-solvent free and dry biomass basis. The yields of WSO (Y_{WSO}) were determined measuring the total organic carbon of #F1 (TOC, AI-Analyzer Multi N/C 2100S (pO_2 = 5 bar, flow O_2 = 160 ml/min, T_{oven} = 800 °C) and the carbon content of #F1 solid residue obtained after evaporation at 105 °C for 3 hr. The composition of the WSO and WIO fractions, including their content of co-solvents, was determined with gas chromatography-mass spectrometry (GC-MS). Additionally, the WIO fraction was characterized with Fourier transform infrared spectroscopy (FT-IR, Thermo-Nicolet Avatar 370 with ATR module, scan range: 400 - 4000 cm^{-1}, resolution: 1 cm^{-1}, scans no.: 64).

2.4 Sampling and GC-MS

The sampling method before GC-MS was optimized for each fraction: solid-phase microextraction (SPME) for WSO [35] and liquid-liquid extraction (LLE) for WIO. The SPME equipment used in this study (manual sampling holder with needles 23 gauge and 65 μm poly(dimethylsiloxane) divinylbenzene PDMS/DVB adsorbent fiber) were purchased from Supelco (Bellefonte, PA, USA). The fibers were conditioned daily in the GC injector according to the recommendations of the manufacturer (30 min at T = 250 °C) before use. In between the runs, the fiber was cleaned (10 min at 225 °C), and a possible carry over was assessed by a blank run. A set

of 15 initial extractions was used to develop an optimal SPME extraction procedure (extraction temperature, time of extraction, presence of salt, pH changes). The aim was to increase the partition coefficients and decrease the time required for obtaining equilibrium. Based on the results, the variation of pH (below 2 and above 10) was the only factor with no tangible influence on the extraction results. The final optimized method maximized the concentration of the volatile components in the head-space. A sample (5 ml of the water phase) was placed in a 22 ml glass vial containing a magnetic stirrer, added 50 mg of internal standard solution (IS), 1 g of NaCl, and sealed using a PTFE coated silicone rubber septum. The vial was placed in a thermostated bath adjusted to T = 50 °C. The fiber was exposed to the head-space (HS) of the sample for 10 min. After the sampling, the SPME fiber was retracted into the syringe, injected through septum into the GC, and desorbed for 1 min. The apparatus used for gas chromatography mass spectrometry was a Perkin Elmer Clarus GC 580 and MS SQ 8 S with an EI quadrupole ion analyzer. A Perkin Elmer Crossbond column (30 m X 0.25 mm ID, 0.25 μm 95 % dimethyl polysiloxane and 5 % biphenyl) with helium as a carrier carrier gas (1 ml/min) was used to separate the analytes. For SPME, the analytes were desorbed at T = 200 °C in a split mode (50:1) with 1 min solvent delay. The GC-MS program was optimized for the applied SPME fiber (T = 40 °C hold for 2 min followed by a heating ramp of 10 K/min to T = 200 °C hold for 2 min). WIO samples were extracted with DEE (1:1), injected at T = 300 °C in split mode (30:1) with solvent delay of 2.5 min, and heated (T = 75 °C held for 1.5 min followed by a heating ramp of 10 K/min to T = 275 °C held for 10 min). MS spectra were recorded at 70 eV ionization energy and scanned for m/z 75 - 600. The main components were identified on the basis of the NIST database.

2.5 Data analysis

All analytical measurements were performed in triplicate. The results were examined with analysis of variance (ANOVA) and multivariate data analysis (MDA), both of which have shown to be useful in the describing of liquefaction results [36]. Principal component analysis (PCA) was applied for the detection of hidden patterns in the GC-MS data of WSO compounds. In this method, the chromatographic data was projected to a set of orthogonal vectors (principal components, PC) oriented in the original variable space along directions of maximum variation, allowing to find hidden structures (groups or trends). The analyzed data set was constructed of the process variables (temperature and the presence of co-solvents as dummy ±1 variables). The results of PCA were evaluated by score plots (projection of the samples to the principal components) and loading plots (contribution of each variable) for pairs of principal components (PCs). More details about PCA can be found elsewhere [37]. ANOVA was applied for detection of statistically significant effects of temperature and co-solvents on both the mass yields, as well as the yields of chemical classes of compounds. All calculations were made in R (version 3.2.2), a free software environment for statistical computing, supported by mdatools package (DOI: 10.5281/zenodo.59547). All figures were prepared in Matlab R2016a.

3 Results and Discussion

3.1 Yields of products

The yields of WSO (Y_{WSO}) formed by liquefaction of *Fallopia japonica* increased with reaction temperature, with and without co-solvents (Figure D.1). Although there is no consensus on the matter, the temperatures between 300 and 330 °C are often considered the most optimal conditions for a successful HTL conversion of lignocellulosic biomass into biocrude oil [38]. Processing with co-solvents raised Y_{WSO} additionally, especially at the highest operating temperature (T = 320 °C). For the yields of WIO (Y_{WIO}), the trends were generally opposite with regard to the reaction temperature. Since the WIO fraction is expected to be a mixture of unreacted biomass, heavy biocrude compounds, and repolymerized solid char, the value of Y_{WIO} combined three different phenomena: conversion of biomass, formation of biocrude, and condensation routes leading to solid biochar. At low temperatures, a major contribution to the high Y_{WIO} was expected to be attributed to an ineffective biomass conversion. With increasing reaction temperature and in the presence of co-solvents, a decrease in the yields of WIO was accompanied by changes in its composition: the amount of solids (biomass and char) in WIO generally decreased, while the biocrude fraction increased (Figure D.10 of the Supporting Information). The WIO's content of BC was, in most cases, maximized at T = 300 °C. With tetralin as a co-solvent and at T = 300 °C, as much as 98 % of the WIO fraction was biocrude. The following decrease in the BC amounts at T = 320 °C indicated that the process entered into the domain of dehydration reactions resulting in char formation. Similar trends were noticed in the absence of co-solvents.

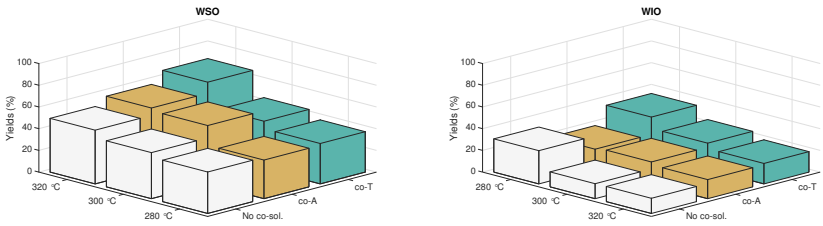

Fig. D.1: Mass yields of WSO and WIO obtained at different conversion conditions.

3.2 WSO

The SPME extract of the aqueous fraction was analyzed with GC-MS, and the identified peaks were divided into four chemical classes: low molecular weight aliphatics (LMW), cyclic carbonyl compounds (C), aromatics (A), and high molecular weight (HMW) compounds. The last-mentioned group represented a broad spectrum of chemical species of generally high molecular weight and structure indicating secondary reactions pathways following depolymerization. Aromatics were

formed due to depolymerization of lignin or aromatization of sugars [39]. The latter process involved dehydration of glucose to anhydrosugars (e.g. levoglucosan and levoglucosenone), and further to furans (e.g. furfurals). The last step combined dehydration and rearrangement of the formed oxygenates to aromatic compounds. Alternatively, the furans could have been hydrogenated into the cyclic derivatives of e.g. cyclopentanone. The LMW compounds were mainly the result of retro-aldol condensation reactions, but could also have originated as products from other conversion pathways. The HMW compounds, which can be considered precursors of the solid char, were formed by repolymerization of the secondary reaction products including aliphatic, cyclic, and aromatic units. The reaction pathways involved in hydrothermal conversion of lignocellulosic biomass are summarized in Figure D.2. The list of the most common WSO found in the samples is compiled in Table D.2. The full list of the WSO used in the subsequent analysis is specified in Table D.4 of the Supporting Information.

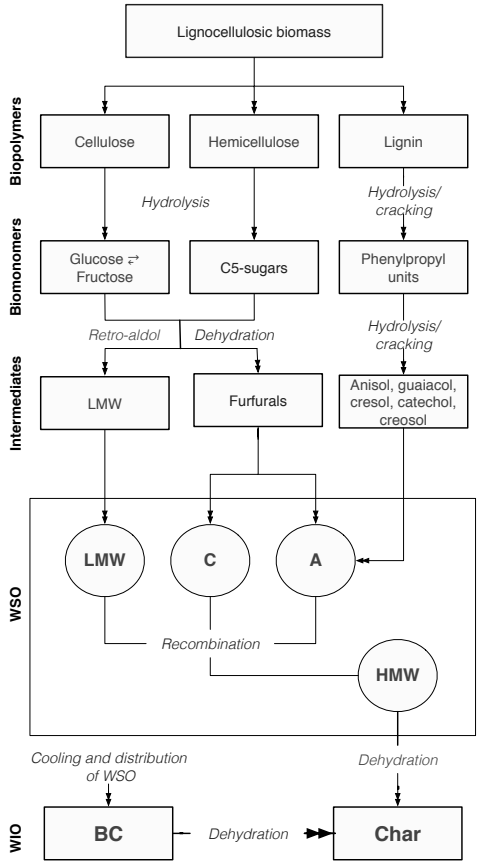

Fig. D.2: Reaction routes behind HTL of lignocellulose biomass.

Table D.2: Examples of WSO representing different classes of compounds (extracted with SPME and identified by GC-MS). Both acetone as well as tetralin were identified in the aqueous samples.

RT (min)	Compound	Class	Formula	MW
2.27	2-Butanone	LMW	C_4H_8O	72
2.79	Butanal, 3-methyl-	LMW	$C_5H_{10}O$	86
3.18	2-Pentanone	LMW	$C_5H_{10}O$	86
3.83	Pentyl formate	LMW	$C_6H_{12}O_2$	116
3.89	2-Methylbutan-1-ol	LMW	$C_5H_{12}O$	88
5.63	Cyclopentanone, 2-methyl-	C	$C_6H_{10}O$	98
9.26	2-Cyclopenten-1-one, 3-(1-methylethyl)-	C	$C_8H_{12}O$	124
9.32	2-Cyclohexen-1-one, 3,4-dimethyl-	C	$C_8H_{12}O$	124
9.50	2-Cyclopenten-1-one, 2,3,4-trimethyl-	C	$C_8H_{12}O$	124
9.70	p-Cresol	A	C_7H_8O	108
10.85	Phenol, 3,5-dimethyl-	A	$C_8H_{10}O$	122
11.56	Creosol	A	$C_8H_{10}O_2$	138
11.12	Phenol, 3-ethyl-	A	$C_8H_{10}O$	122
12.84	Phenol, 4-ethyl-2-methoxy-	A	$C_9H_{12}O_2$	152
13.59	6-Methyl-1,2,3,5,8,8a-hexahydronaphthalene	HMW	$C_{11}H_{16}$	148
15.08	Bicyclo[4.3.0]non-3-ene, 3,4-dimethyl-7-exo-methylene-	HMW	$C_{12}H_{18}$	162

The distribution of the chemical classes in WSO was determined on the basis of the relative peak areas (with respect to the total peak area). Peak areas of components belonging to the same class were lumped together. The area used in the assessment accounted for approx. 75 % of the total chromatographic area. The results are compiled in Figure D.3. The LMW compounds comprised the smallest part of the products (0.5 - 1.1 %), while the aromatics constituted the largest part (33 - 69 %). The cyclic compounds (8 - 23 %) and the high molecular weight compounds (7 - 26 %) accounted for the rest. Several interesting tendencies were noted in the obtained results, e.g. an increased abundance of cyclic and HMW compounds in the absence of co-solvents, especially at the lowest reaction temperature (T = 280 °C). Formation of cyclics indicated the dominance of dehydration/rearrangement routes over the retro-aldol condensation leading to LMW. The addition of co-solvents shifted the conversion pathways towards the formation of aromatics, most noticeable at T = 300 °C. The formation of both C as well as the HMW was repressed in the presence of co-solvents, which acted as scavengers of the reactive and unstable secondary reaction products.

Combination of chromatography and multivariate PCA proved to be a valuable tool for identification of hidden trends in the large data sets obtained from the GC-MS analyses. The results were evaluated by reviewing the score plots for different sets of principal components with the data points (i.e. the samples) colored according to the varying parameters of the experimental runs, i.e. the presence of acetone, tetralin, and temperature. For score plots with hidden patterns, the significant variables (i.e. the peaks) responsible for the groupings were retrieved from the corresponding loading plots.

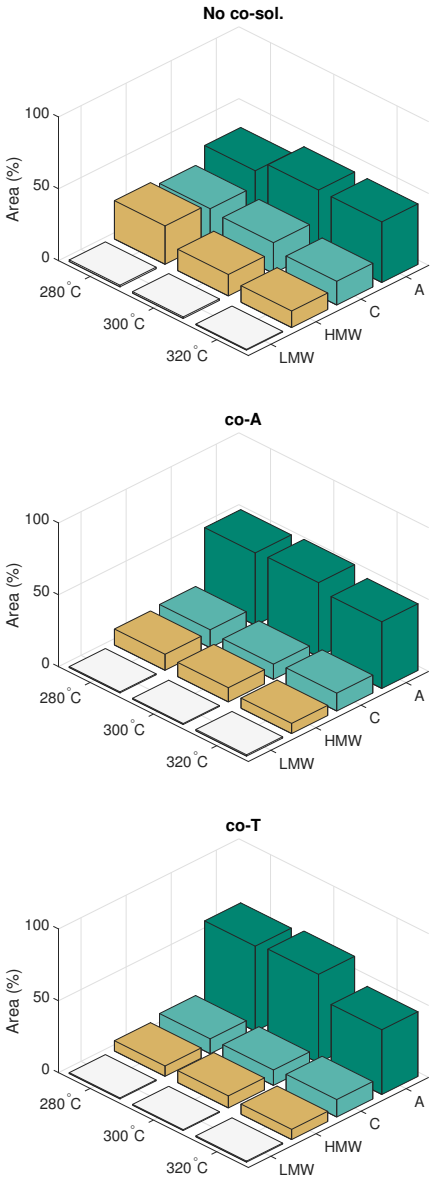

Fig. D.3: Distribution of the chemical classes in WSO.

The results have shown a clear pattern along the principal component responsible for the greatest variation in the data (PC1, 68.94 %) according to the presence of tetralin in the runs (Figure D.4). The points associated with negative scores represent the runs without the co-solvent and are explained by the negative loadings in the figure. The opposite applied for the runs with tetralin, i.e. the data points with positive scores corresponded to the positive loading values. While tetralin was the most significant peak in the second group (RT = 11.22 min), a number of other peaks responsible for the shift in reaction routes were identified as well. The PCA loadings confirmed the change in the abundance of aromatics and HMW gleaned from the semi-quantitative analysis of class distribution, showing an increase in the first group and a decrease in the second. Statistical analysis was employed to find out how temperature and the presence of co-solvents influence the distribution of chemical classes in WSO.

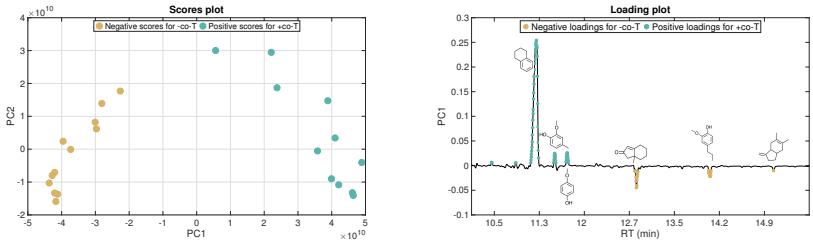

Fig. D.4: PC1 vs. PC2 score plot (left) and PC1 line loading plot (right) colored according to the presence of tetralin co-solvent.

The significant effects were identified using ANOVA and Tukeys's test for multiple comparisons. The graphical representation of the effects is shown in Figure D.5. The two top figures show the effect of tetralin on the yields of low molecular weight compounds (LMW = f(co-T)) and aromatics (A = f(co-T)), respectively. The bottom figure shows the effect of temperature on the overall yields (Total = f(T)). While the overall yields of WSO compounds increased with temperature, addition of tetralin seemed to increase the yields of A and LMW compounds.

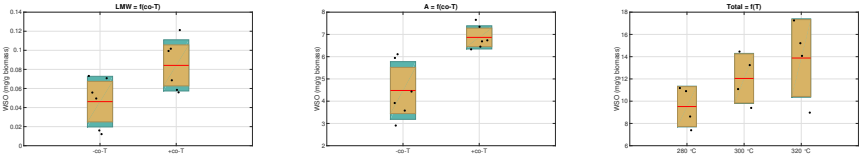

Fig. D.5: Box-plots for the most significant effects identified with ANOVA analysis of the yields of different classes of WSO.

3.3 WIO

The central part of the identified WIO consisted of alkanes and alkenes of varying chain length, semi-polar aromatics, and polymerized structures (Table D.3). In addition to that, a limited number of nitrogen-containing heterocyclic compounds were identified as well. The saturated and unsaturated hydrocarbons were by-products of retro-aldol conversion of the sugars (glucose and fructose) followed by deoxygenation. The heterogeneous nitrogen compounds were formed through a reaction between the cyclic compounds and amino acids from the hydrolysis of proteins. Due to the similarities in composition and structure, it is likely that HMW from WSO are the precursors of the WIO, the biocrude, as well the solid char, with process conditions deciding the position of the equilibrium between those three phases. The aromatic element in WIO was of limited polarity compared to the corresponding WSO aromatic fraction. It is also evident, that the co-solvents acted as precursors to some of the identified WIO, e.g. naphthalene and 3,3,6,8-tetramethyl-1-tetralone were formed from tetralin and acetone, respectively.

Table D.3: The most common compounds identified by GC-MS in the DEE soluble fraction of WIO. Tetralin was identified, but not reported among the results.

RT (min)	Compound	Formula	MW
4.92	4,4-Dimethyl-2-pentene	C_7H_{14}	98
5.65	4-Methyl-3-heptanol	$C_8H_{18}O$	130
6.95	2-Methylhepta-2,4-dien-6-one	$C_8H_{12}O$	124
7.79	Benzaldehyde	C_7H_6O	106
8.13	Phenol	C_6H_6O	94
9.95	2-Methoxyphenol	$C_7H_8O_2$	124
10.12	2-Nonen-1-ol	$C_9H_{18}O$	142
11.50	Naphthalene	$C_{10}H_8$	128
11.67	Decanal	$C_{10}H_{20}O$	156
12.81	4-Ethyl-2-methoxyphenol	$C_9H_{12}O_2$	152
13.81	2,6-Dimentoxyphenol	$C_8H_{10}O_3$	154
15.88	Butylated hydroxytoluene	$C_{15}H_{24}O$	220
17.04	3,3,6,8-Tetramethyl-1-tetralone	$C_{14}H_{18}O$	202
19.52	3,7,11,15-Tetramethyl-2-hexadecene	$C_{20}H_{40}$	280

The FT-IR resulted in an additional description of the WIO fraction composition (Figure D.6). The broad band at 3350 cm^{-1} was a combination of vibrations of hydroxy groups (-OH from the chemisorbed water and reaction products), aromatic C-H, and N-H from amines and amides. The presence of ether bonds was demonstrated through the bands in the range 2850 - 2925 cm^{-1} (symmetric vibration of -CH) and 1030 cm^{-1} (stretch C-O vibration). The bands in the range 1400 - 1600 cm^{-1} and 600 - 1000 cm^{-1} represented the aromatic double C=C and out-of-plane vibrations of alkyl constituents attached to the aromatic rings, respectively. The presence of similar alkene derived C=C was evidenced by the 800 - 900 cm^{-1} bands representing the =C-H bonds. There was no evidence of either carbonyl

functional groups nor the presence of cyclics. An increasing reaction temperature resulted in decreasing bands at 2925 cm^{-1} accompanied by a higher absorbance at 3350 cm^{-1} (up to 300 °C), 1400 - 1600 cm^{-1}, and 600 - 1000 cm^{-1}. This tendency can be interpreted as enhanced degradation of ether bonds and aromatization of WIO with rising T values. In the presence of co-solvents, the bands responsible for the aromatic structures were enlarged further.

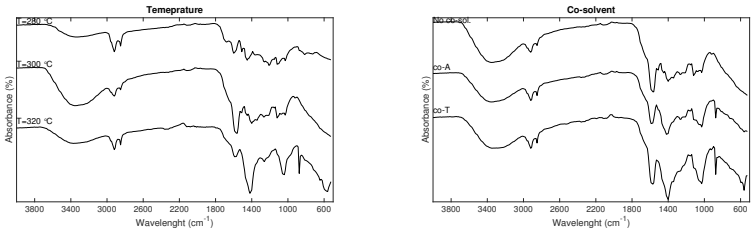

Fig. D.6: FT-IR analysis of the WIO fraction: the influence of temperature and co-solvents.

4 Conclusions

While the yields of WSO increased with reaction temperature, the opposite occurred for WIO. BC was maximized in most cases at T = 300 °C. Formation of biochar was repressed until T = 320 °C. The addition of co-solvents enhanced the conversion of biomass and entailed significant reaction route shifts. Tetralin resulted in an increased production of aromatics (solubilization of lignin and aromatization of furans) and LMW (retro-aldol condensation), while the formation of cyclics (dehydration) and repolymerization of HMW were repressed. In the absence of co-solvents, dehydration/rearrangement routes leading to the formation of HMW and biochar were of significance.

5 Acknowledgments

This research was supported by the Danish Council for Strategic Research (DSF grant no. 1305-00030B), Danish Agency for Science, Technology and Innovation (grant no. 11-118412), and by Marie Curie Career Integration Grant (FP7-PEOPLE-2012-CIG, project no. 321816).

6 Supporting Information

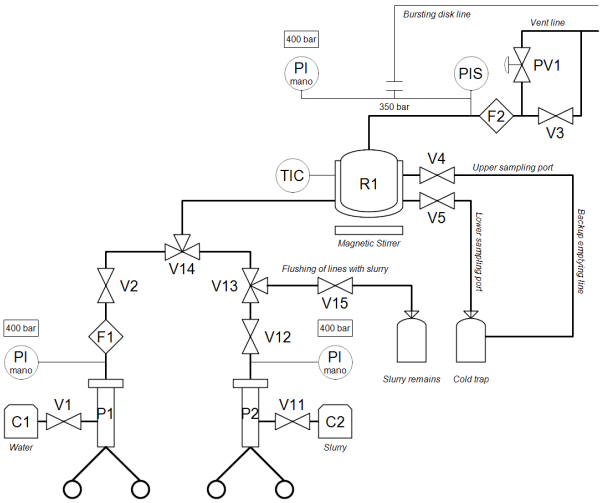

Fig. D.7: P&I (process & instrumentation diagram) for the applied reactor system. R1: reactor, P1, P2: hand-driven pumps; F1, F2: filters; V1-V5, V11-V12: closing valves; V13: three-way valve; PV1: pneumatic safety valve; PI: pressure indicator; PIS: pressure indicator switch; TIC: temperature indicator and controller.

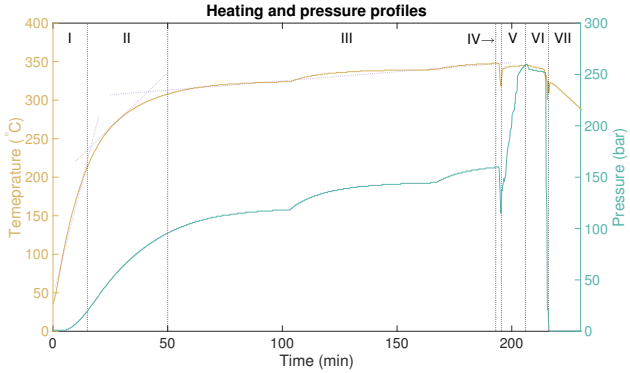

Fig. D.8: Heating and pressure profiles for the SITEC setup. The regions of interest: I - heating rate 13 K/min, II - heating rate 3 K/min, III - heating rate 0.3 K/min, IV - cold injection of biomass slurry, V - return to the initial conditions, VI - reaction time, VII - cooling and depressurization. The slope changes at t = 105 and 175 min correspond to regulation of the SP-point and the subsequent changes in the heating rates. During the presented run, the obtained reaction temperature was slightly above the selected reaction temperature, so the resulting decrease in both temperature and pressure was an operation adjustment. In a typical run, the variations in temperature and pressure during the reaction time were ± 5 °C and ± 10 bar, respectively.

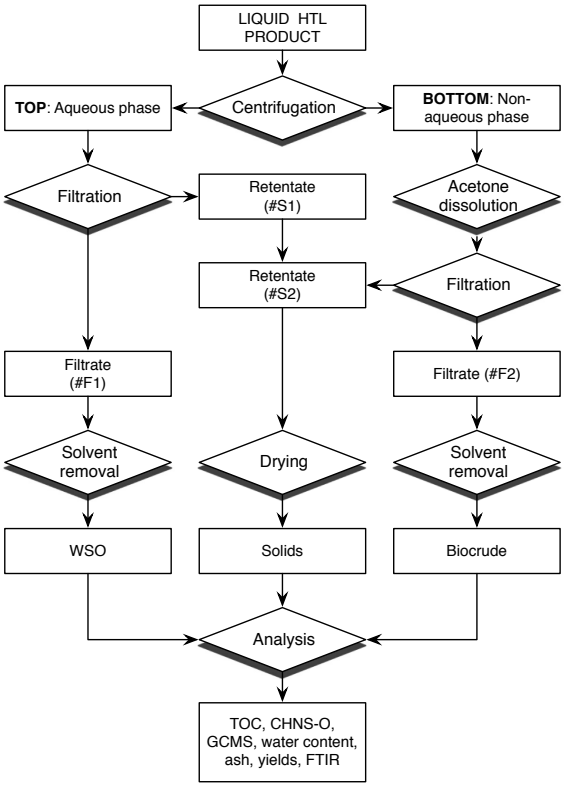

Fig. D.9: Product separation scheme.

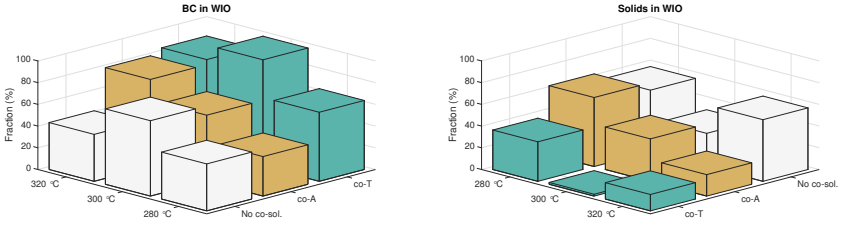

Fig. D.10: Distribution of the biocrude and solid fraction in WIO.

Table D.4: Full list of WSO compounds (except co-solvents) used in the statistical analysis of the classes.

RT (min)	Compound	Class	Formula	MW
2.27	2-Butanone	LMW	C_4H_8O	72
2.79	Butanal, 3-methyl-	LMW	$C_5H_{10}O$	86
2.90	Butanal, 2-methyl-	LMW	$C_5H_{10}O$	86
3.18	2-Pentanone	LMW	$C_5H_{10}O$	86
3.83	Pentyl formate	LMW	$C_6H_{12}O_2$	116
3.89	2-Methylbutan-1-ol	LMW	$C_5H_{12}O$	88
3.95	1H-Pyrrole, 1-methyl-	C	C_5H_7N	81
4.21	Di-tert-butyl ether	LMW	$C_8H_{18}O$	130
4.38	Piperidine, 1-methyl-	C	$C_6H_{13}N$	99
4.75	Cyclopentanone	C	C_5H_8O	84
4.88	3-Penten-2-one, 4-methyl-	LMW	$C_6H_{10}O$	98
5.16	1H-Pyrrole, 1-ethyl-	C	C_6H_9N	95
5.63	Cyclopentanone, 2-methyl-	C	$C_6H_{10}O$	98
5.74	Cyclopentanone, 3-methyl-	C	$C_6H_{10}O$	98
5.92	Piperidine, 1-ethyl-	C	$C_7H_{15}N$	113
6.07	Pyridine, 3-methyl-	A	C_6H_7N	93
6.52	Cyclopentanone, 2,5-dimethyl-	C	$C_7H_{12}O$	112
6.60	Cyclopentanone, 2,3-dimethyl-	C	$C_7H_{12}O$	112
6.66	Cyclopentanone, 2,4-dimethyl-	C	$C_7H_{12}O$	112
6.81	2-Cyclopenten-1-one, 2-methyl-	C	C_6H_8O	96
7.01	Anisole	A	C_7H_8O	108
7.38	1-Cyclohexylethanol	C	$C_8H_{16}O$	128
7.51	2-Ethylcyclopentanone	C	$C_7H_{12}O$	112
7.70	3-Ethylcyclopentanone	C	$C_8H_{12}O$	124
7.79	Benzaldehyde	A	C_7H_6O	106
8.14	Phenol	A	C_6H_6O	106
8.34	Cyclopropane, 1,1-dimethyl-2-pentyl-	HMW	$C_{10}H_{16}O_3$	184
8.43	2-Cyclopenten-1-one, 2,3-dimethyl-	C	$C_7H_{10}O$	110
8.54	Cyclohexanone, 3-ethyl-	C	$C_8H_{14}O$	126
8.83	2-Cyclopenten-1-one, 3,4-dimethyl-	C	$C_7H_{10}O$	110
8.88	1-Acetylcyclohexene	HMW	C_9H_{16}	124
8.99	1-Methylcyclooctene	C	C_9H_{16}	124
9.12	2-Cyclopenten-1-one, 2,3-dimethyl-	C	$C_7H_{10}O$	110
9.26	2-Cyclopenten-1-one, 3-(1-methylethyl)-	C	$C_8H_{12}O$	124
9.32	2-Cyclohexen-1-one, 3,4-dimethyl-	C	$C_8H_{12}O$	124
9.40	2,4-Pentadien-1-ol, 3-propyl-, (2Z)-	LMW	$C_6H_{10}O$	98
9.50	2-Cyclopenten-1-one, 2,3,4-trimethyl-	C	$C_8H_{12}O$	124
9.70	p-Cresol	A	C_7H_8O	108
9.97	2-Methoxyphenol (guaiacol)	A	$C_7H_8O_2$	124
10.12	Nonanal	HMW	$C_9H_{18}O$	142
10.66	3-Hydroxy-2-(2-methylcyclohex-1-enyl)propionaldehyde	A	$C_{10}H_{16}O_2$	152
10.23	2-Cyclopenten-1-one, 2,3,4,5-tetramethyl-	C	$C_9H_{14}O$	168
10.70	cis-p-Mentha-2,8-dien-1-ol	A	$C_{10}H_{16}O$	152
10.80	Benzene, 1,2-dimethoxy-	A	$C_8H_{10}O_2$	138
10.85	Phenol, 3,5-dimethyl-	A	$C_8H_{10}O$	122
10.90	2-Cyclopenten-1-one, 3,4,5-trimethyl-	C	$C_8H_{12}O$	124
11.56	Creosol	A	$C_8H_{10}O_2$	138
11.12	Phenol, 3-ethyl-	A	$C_8H_{10}O$	122
12.02	Ethyl 4-methoxybenzoate	A	$C_{10}H_{12}O_3$	180
12.45	2-Cyclopenten-1-one, 2-pentyl-	C	$C_{10}H_{16}O$	152
12.84	Phenol, 4-ethyl-2-methoxy-	A	$C_9H_{12}O_2$	152
12.89	2H-Inden-2-one, 1,4,5,6,7,7a-hexahydro-7a-methyl-, (S)-	HMW	$C_{10}H_{14}O$	150
13.59	6-Methyl-1,2,3,5,8,8a-hexahydronaphthalene	HMW	$C_{11}H_{16}$	148
14.04	Phenol, 2-methoxy-4-propyl-	A	$C_{10}H_{14}O_2$	166
14.57	2-Cyclopenten-1-one, 3-methyl-2-(2,4-pentadienyl)-, (Z)-	HMW	$C_{11}H_{14}O$	162
14.72	Octahydro-7H-cyclopenta[a]pentalen-7-one	HMW	$C_{11}H_{14}O$	172
15.08	Bicyclo[4.3.0]non-3-ene, 3,4-dimethyl-7-exo-methylene-	HMW	$C_{12}H_{18}$	162
15.83	Phenol, 2,4-bis(1,1-dimethylethyl)-	A	$C_{14}H_{22}O$	206

References

[1] S. S. Toor, L. Rosendahl, and A. Rudolf, "Hydrothermal liquefaction of biomass: a review of subcritical water technologies," *Energy*, vol. 36, no. 5, pp. 2328–2342, 2011.

[2] T. H. Pedersen, I. Grigoras, J. Hoffmann, S. S. Toor, I. M. Daraban, C. U. Jensen, S. Iversen, R. B. Madsen, M. Glasius, K. R. Arturi, R. P. Nielsen, E. G. Søgaard, and L. A. Rosendahl, "Continuous hydrothermal co-liquefaction of aspen wood and glycerol with water phase recirculation," *Appl. Energ.*, vol. 162, pp. 1034–1041, 2016.

[3] Y. Yu, X. Lou, and H. Wu, "Some recent advances in hydrolysis of biomass in hot-compressed water and its comparisons with other hydrolysis methods," *Energy Fuels*, vol. 22, no. 1, pp. 46–60, 2007.

[4] N. Akiya and P. E. Savage, "Roles of water for chemical reactions in high-temperature water," *Chem. Rev.*, vol. 102, no. 8, pp. 2725–2750, 2002.

[5] A. Kruse and E. Dinjus, "Hot compressed water as reaction medium and reactant: Properties and synthesis reactions," *J. Supercrit. Fluids*, vol. 39, no. 3, pp. 362–380, 2007.

[6] R. P Nielsen and E. G Søgaard, "Features of near-and supercritical water," *Curr. Phys. Chem.*, vol. 3, no. 4, pp. 501–507, 2013.

[7] M. Balat, "Mechanisms of thermochemical biomass conversion processes. Part 3: Reactions of liquefaction," *Energ. Source. Part A*, vol. 30, no. 7, pp. 649–659, 2008.

[8] S. Cheng, I. D'cruz, M. Wang, M. Leitch, and C. Xu, "Highly efficient liquefaction of woody biomass in hot-compressed alcohol- water co-solvents," *Energy Fuels*, vol. 24, no. 9, pp. 4659–4667, 2010.

[9] X. Yuan, H. Li, G. Zeng, J. Tong, and W. Xie, "Sub-and supercritical liquefaction of rice straw in the presence of ethanol–water and 2-propanol–water mixture," *Energy*, vol. 32, no. 11, pp. 2081–2088, 2007.

[10] Z. Liu and F. Zhang, "Effects of various solvents on the liquefaction of biomass to produce fuels and chemical feedstocks," *Energ. Convers. and Manage.*, vol. 49, no. 12, pp. 3498–3504, 2008.

[11] X. Yuan, J. Wang, G. Zeng, H. Huang, X. Pei, H. Li, Z. Liu, and M. Cong, "Comparative studies of thermochemical liquefaction characteristics of microalgae using different organic solvents," *Energy*, vol. 36, no. 11, pp. 6406–6412, 2011.

[12] H. Huang, X. Yuan, G. Zeng, J. Wang, H. Li, C. Zhou, X. Pei, Q. You, and L. Chen, "Thermochemical liquefaction characteristics of microalgae in sub-and supercritical ethanol," *Fuel Process. Technol.*, vol. 92, no. 1, pp. 147–153, 2011.

[13] P. D. Patil, V. G. Gude, A. Mannarswamy, S. Deng, P. Cooke, S. Munson-McGee, I. Rhodes, P. Lammers, and N. Nirmalakhandan, "Optimization of direct conversion of wet algae to biodiesel under supercritical methanol conditions," *Bioresour. Technol.*, vol. 102, no. 1, pp. 118–122, 2011.

[14] R. W. Thring, E. Chornet, and R. P. Overend, "Thermolysis of glycol lignin in the presence of tetralin," *Can. J. Chem. Eng.*, vol. 71, no. 1, pp. 107–115, 1993.

[15] S. B. Lalvani, P. Rajagopal, B. Akash, J. A. Koropchak, and C. B. Muchmore, "Liquefaction of newsprint and cellulose in tetralin under moderate reaction conditions," *Fuel Process. Technol.*, vol. 35, no. 3, pp. 219–232, 1993.

[16] T.-o. Matsui, A. Nishihara, C. Ueda, M. Ohtsuki, N.-o. Ikenaga, and T. Suzuki, "Liquefaction of micro-algae with iron catalyst," *Fuel*, vol. 76, no. 11, pp. 1043–1048, 1997.

[17] A. Koriakin, H. V. Nguyen, D.-W. Kim, and C.-H. Lee, "Thermochemical decomposition of microcrystalline cellulose using sub-and supercritical tetralin and decalin with Fe_3O_4," *Ind. Eng. Chem. Res.*, vol. 54, no. 18, pp. 5184–5194, 2015.

[18] S. Sangon, S. Ratanavaraha, S. Ngamprasertsith, and P. Prasassarakich, "Coal liquefaction using supercritical toluene–tetralin mixture in a semi-continuous reactor," *Fuel Process. Technol.*, vol. 87, no. 3, pp. 201–207, 2006.

[19] D. Elliott, D. Beckman, A. Bridgwater, J. Diebold, S. Gevert, and Y. Solantausta, "Developments in direct thermo-chemical liquefaction of biomass: 1983-1990," *Energy Fuels*, vol. 5, no. 3, pp. 399–410, 1991.

[20] D. C. Elliott, "Historical developments in hydroprocessing bio-oils," *Energy Fuels*, vol. 21, no. 3, pp. 1792–1815, 2007.

[21] A. J. Ragauskas, C. K. Williams, B. H. Davison, G. Britovsek, J. Cairney, C. A. Eckert, W. J. Frederick, J. P. Hallett, D. J. Leak, and C. L. Liotta, "The path forward for biofuels and biomaterials," *Science*, vol. 311, no. 5760, pp. 484–489, 2006.

[22] C. Tuck, E. Pérez, I. Horváth, R. Sheldon, and M. Poliakoff, "Valorization of biomass: deriving more value from waste," *Science*, vol. 337, no. 6095, pp. 695–699, 2012.

[23] K. Van Meerbeek, L. Appels, R. Dewil, A. Calmeyn, P. Lemmens, B. Muys, and M. Hermy, "Biomass of invasive plant species as a potential feedstock for bioenergy production," *Biofuel. Bioprod. and Bior.*, vol. 9, no. 3, pp. 273–282, 2015.

[24] A. G. Aguilera, P. Alpert, J. S. Dukes, and R. Harrington, "Impacts of the invasive plant Fallopia japonica (houtt.) on plant communities and ecosystem processes," *Biol. Invasions*, vol. 12, no. 5, pp. 1243–1252, 2010.

[25] Z. Hromádková, J. Hirsch, and A. Ebringerová, "Chemical evaluation of Fallopia species leaves and antioxidant properties of their non-cellulosic polysaccharides," *Chem. Pap.*, vol. 64, no. 5, pp. 663–672, 2010.

[26] D. Donnez, P. Jeandet, C. Clément, and E. Courot, "Bioproduction of resveratrol and stilbene derivatives by plant cells and microorganisms," *Trends Biotechnol.*, vol. 27, no. 12, pp. 706–713, 2009.

[27] W. B. Widayatno, G. Guan, J. Rizkiana, X. Hao, Z. Wang, C. Samart, and A. Abudula, "Steam reforming of tar derived from Fallopia japonica stem over its own chars prepared at different conditions," *Fuel*, vol. 132, pp. 204–210, 2014.

[28] E. Kamio, S. Takahashi, H. Noda, C. Fukuhara, and T. Okamura, "Effect of heating rate on liquefaction of cellulose by hot compressed water," *Chem. Eng. J.*, vol. 137, no. 2, pp. 328–338, 2008.

[29] A. Sinag, A. Kruse, and J. Rathert, "Influence of the heating rate and the type of catalyst on the formation of key intermediates and on the generation of gases during hydropyrolysis of glucose in supercritical water in a batch reactor," *Ind. Eng. Chem. Res.*, vol. 43, no. 2, pp. 502–508, 2004.

[30] M. Modell, "Gasification and liquefaction of forest products in supercritical water," in *Fundamentals of Thermochemical Biomass Conversion*. Springer, 1985, pp. 95–119.

[31] H. Schmieder, J. Abeln, N. Boukis, E. Dinjus, A. Kruse, M. Kluth, G. Petrich, E. Sadri, and M. Schacht, "Hydrothermal gasification of biomass and organic wastes," *J. Supercrit. Fluids*, vol. 17, no. 2, pp. 145–153, 2000.

[32] J. Barbier, N. Charon, N. Dupassieux, A. Loppinet-Serani, L. Mahé, J. Ponthus, M. Courtiade, A. Ducrozet, A. Fonverne, and F. Cansell, "Hydrothermal conversion of glucose in a batch reactor. A detailed study of an experimental key-parameter: The heating time," *J. Supercrit. Fluids*, vol. 58, no. 1, pp. 114–120, 2011.

[33] A. J. Mørup, P. R. Christensen, D. F. Aarup, L. Dithmer, A. Mamakhel, M. Glasius, and B. B. Iversen, "Hydrothermal liquefaction of dried distillers grains with solubles: A reaction temperature study," *Energy Fuels*, vol. 26, no. 9, pp. 5944–5953, 2012.

[34] K. R. Arturi, M. Strandgaard, R. P. Nielsen, E. G. Søgaard, and M. Maschietti, "Hydrothermal liquefaction of lignin in near-critical water in a new batch reactor: Influence of phenol and temperature," *J. Supercrit. Fluids*, vol. 123, pp. 28–39, 2017.

[35] K. R. Arturi, K. R. Toft, R. P. Nielsen, L. A. Rosendahl, and E. G. Søgaard, "Characterization of liquid products from hydrothermal liquefaction (HTL) of biomass via solid-phase microextraction (SPME)," *Biomass Bioenergy*, vol. 88, pp. 116–125, 2016.

[36] K. R. Arturi, S. Kucheryavskiy, and E. G. Søgaard, "Performance of hydrothermal liquefaction (HTL) of biomass by multivariate data analysis," *Fuel Process. Technol.*, vol. 150, pp. 94–103, 2016.

[37] K. H. Esbensen, D. Guyot, F. Westad, and L. P. Houmoller, *Multivariate data analysis-in practice: an introduction to multivariate data analysis and experimental design*. CAMO Software, 2002.

[38] J. Akhtar and N. A. S. Amin, "A review on process conditions for optimum bio-oil yield in hydrothermal liquefaction of biomass," *Renew. Sustainable Energy Rev.*, vol. 15, no. 3, pp. 1615–1624, 2011.

[39] J. Russell, R. Miller, and P. Molton, "Formation of aromatic compounds from condensation reactions of cellulose degradation products," *Biomass*, vol. 3, no. 1, pp. 43–57, 1983.

Paper E

Recovery of value-added chemicals by solvolysis of unsaturated polyester resin

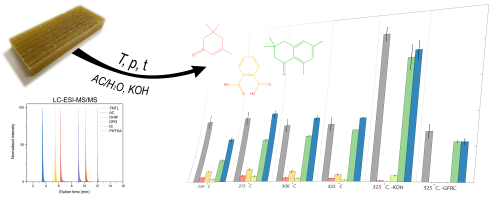

Katarzyna R. Arturi, Hülya U. Sokoli, Erik G. Søgaard, Frédéric Vogel, and Saša Bjelić

The manuscript has been submitted to the *Journal of Cleaner Production* in February 2017.

The layout has been revised.

Abstract

This work describes the composition of the products from solvolysis of thermoset polyester in an acetone/water mixture. A qualitative and quantitative evaluation of the compositions of the aqueous and oil phases was achieved by the combination of liquid chromatography with electrospray ionization mass spectrometry (LC-ESI-MS/MS), gel permeation chromatography (GPC), and total organic carbon (TOC). Close to 100 % of the organic carbon in the aqueous phase was explained by the monomers phthalic acid and dipropylene glycol, co-solvent acetone, and a secondary reaction product, isophorone. In the oil, the most abundant compounds were isophorone, 3,3,6,8-tetramethyl-1-tetralone, and dihydroisophorone. While the first two compounds were intermediates in the self-condensation of acetone, dihydroisophorone has not been reported previously as the by-product of the conventional acetone self-condensation reaction pathway. The identified compounds represented a broad spectrum of value-added products that could be recycled for production of polymers, used as a building blocks, or as fine chemicals. Keywords: thermosetting resin, chemical properties, chemical analysis, recycling.

1 Introduction

The production of polymer materials has been increasing exponentially since the 1950's, and in 2015, it exceeded 322 million tons [1]. With plastics, a broad range of target properties can be obtained to replace naturally derived materials such as wood, glass, or ceramics, often for a lower price. However, the fossil origin of polymers, the lack of biodegradability, and the resulting accumulation in the environment decrease their overall appeal [2]. Three major strategies have been developed to reduce the amount of plastic waste: reuse of the products as a whole, extraction of the energy contained in them by burning, and chemical disassembling into monomeric building blocks [3]. While all those valorization approaches promote the sustainability of plastics, only the chemical route offers a prospect of closing the loop on the polymer life cycle by perpetually reusing the raw material [4].

One of the most common chemical recycling methods is solvolysis in near- and supercritical fluids, typically water or alcohols [5–8]. The process has been studied and described in great detail for simple condensation and addition thermoplastics, such as polyethylene terephthalate (PET), which is hydrolyzed into monomeric building blocks at high pressure and high temperature conditions [9]. For heterogeneous polymer-based materials, e.g. composites incorporating polymeric resins reinforced with fibers, solvolytic treatment has been shown to result in a broad spectrum of secondary reaction products in addition to the monomers [10], and was therefore applied mainly as a tool for recovery of the valuable inorganic filaments [11–15]. Glass and carbon reinforced composites incorporating a polyester (GFRC, fiberglass) and epoxy (CFRC) polymer matrix are the two most common types of composite materials with extensive applications in transportation and construction industries [4]. GFRC is a strong lightweight raw material, that has been

developed as a cheap and more flexible alternative to CFRC. The resin in GFRC is typically a styrene-based emulsion of unsaturated polyester (UP) chains polymerized from dibasic acids (e.g. phthalic and maleic acids) and polyhydric alcohols (e.g. ethylene and propylene glycols). The composite is prepared by lamination curing, i.e. formation of styrene bridges (cross-links) between the unsaturated parts of the polyester chains. The presence of cross-links and the heterogeneous composition of GFRC pose a significant challenge for solvolytic extraction of its building blocks and limit its recycling possibilities. However, in the light of growing demand for composite materials combined with legislative pressure preventing land-filling of composite wastes, more efforts should be expended on developing methods for effective recovery of valuable chemicals from these materials [16, 17].

The knowledge about the reaction products and mechanisms behind the solvolytic depolymerization of thermoset polyester-based plastics is limited. Most studies focus on degradation of the organic matrix and recovery of the glass fibers [18]. Analytic assessment of the composition of the liquefied resin is typically performed by gas chromatography-mass spectroscopy (GC-MS) [3, 10, 19], which results in a limited insight into the content of the semi- and non-volatile fraction of the reaction products expected from the depolymerization (e.g. phthalic acid). Perhaps the most extensive analytic work on the subject was reported by [20], who combined the standard GC-MS analysis with Fourier transform infrared spectroscopy (FT-IR) and size exclusion chromatography (SEC, GPC), offering a broader understanding of the reaction routes and the composition of the products from solvolysis of thermoset polyesters. As was pointed out by the authors, with production of valuable chemicals being a partial aim, the focus of evaluations should be shifted towards a more detailed assessment of the nature and quantity of the recovered monomers.

The objective of this work was to perform a qualitative and quantitative evaluation of the composition of the products from solvolysis of an UP-based GFRC. The liquefaction process was performed in the presence of KOH as a catalyst and acetone as a co-solvent, a combination that has previously shown to couple an effective low-temperature recovery of glass fibers, retaining excellent mechanical properties, with production of high heating value oils [21]. However, in order to maximize the sustainability of the solvolytic recycling process, the degradation products should be assessed as a potential source for value-added monomeric building blocks and chemicals, in addition to the recovery of fibers and the production of oil. The assessment is performed by combination of state of the art analytic tools including liquid chromatography with electrospray ionization and a hybrid orbitrap-quadrupole mass spectrometric detection (LC-ESI-MS/MS), gel permeation chromatography (GPC, also referred to as SEC), and total organic carbon content (TOC). A credible quantitative characterization of the products from solvolysis of GFRC is an essential requirement for a realistic estimation of the potential for recycling of building blocks and production of chemicals from thermoset polyesters.

2 Materials and Methods

2.1 Materials

Vanillin-(phenyl-$^{13}C_6$) from Sigma Aldrich was used as an internal standard (IS). Phthalic acid (PHTHA), isophorone (ISP), dipropylene glycol (DPG), 3,3,6,8-tetramethyl-1-tetralone (TMTL), dihydroisophorone (DHISP), and acetone (AC) were used for calibration and quantification by an external standard method. Solvents purchased from Sigma Aldrich included acetonitrile (ACN), methanol (MeOH), formic acid (HCOOH), and high purity water. All were of high performance liquid chromatography (HPLC) grade (purity $\geq$ 99.99 %).

2.2 Solvothermal experiments

The aqueous and oil samples produced by solvolysis of GFRC containing UP resin (maleic acid, phthalic acid, and propylene glycol cross-linked with styrene) were obtained from Sokoli et al. [21]. In short: a block of GFRC weighting approx. 80 g (27 wt.% UP resin) was liquefied in 240 ml of a 50/50 vol.% AC/H_2O reaction medium with 8 g of KOH added. The reactor was a non-stirred 280 ml high pressure batch reactor (316 stainless steel, BC-1, HIP - High Pressure Equipment, USA) with an electrical heating mantle. The heating time varied in the range 45 - 60 min depending on the reaction temperature. After the reaction time of 30 min, the reaction products were cooled down (120 min), depressurized, and separated into three distinctive fractions: glass fibers, an aqueous, and an oil phase. No solid residue was produced, except for the glass fibers. The gas phase was not collected. The composition of the conversion products was studied as a function of temperature (250 - 325 °C) at constant pressure (30 MPa). In addition, two control experiments without the catalyst (acetone and GFRC present, no KOH) and without the composite material (acetone and KOH present, no GFRC) at T = 325 °C were performed as well. The physical appearance of the samples is shown in Figure E.1.

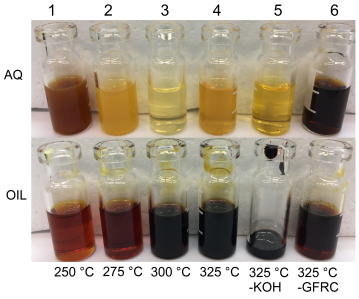

Fig. E.1: The physical appearance of the samples. Top row - aqueous samples. Bottom row - oil samples. Samples 1 - 4 (250 - 325 °C) represent runs with GFRC, AC, and KOH. Run 325 °C, -KOH was performed with GFRC and AC (without KOH). Run 325 °C, -GFRC was performed with AC and KOH (without GFRC).

2.3 LC-ESI-MS/MS

The aqueous (AQ) and oil (OIL) samples from HTS of GFRC were diluted (AQ: 1:500 in MeOH, OIL: 1:100 in ACN), filtrated (0.22 μm), and the IS was added. The quantification procedure was performed in accordance with the U.S. Environmental Protection Agency [22] method validations guidelines with regard to calibration and quality control (QC). Each calibration was based on five levels of standards, while the QC for assessment of accuracy and precision were based on three levels of controls. The presence of carry-over was assessed from the blank samples run after the runs with highest concentration of calibration standards. The standards and quality controls were filtrated and the IS was added prior to the analysis, which took place in a Thermo Scientific Dionex Ultimate 3000 Series RS system (Thermo, Switzerland) including a pump, a column compartment, and an auto-sampler.

The following program using mobile phase A (1 % ACN and 0.2 % HCOOH in high purity water) and mobile phase B (99 vol.% ACN in high purity water) at flow rate of 0.250 ml/min was applied: 1 % B (2 min), from 1 to 99 % B (10 min), and 99 % B (4 min). 1 μl of the prepared solutions was injected. Separation of the analytes was achieved with an ACQUITY UPLC® CHS^{TM} C18 VanGuard^{TM} pre-column and column (150 mm x 2.1 mm x 5 mm, particle size 1.7 μm) from Waters (Switzerland). The temperature of the columns was 50 °C. The chromatographic separation of the analytes is demonstrated in Figure E.6. A heated electrospray ionization (ESI, 3.5 kV spray voltage) in positive mode was used for the ionization of the target analytes. Data acquisition was performed using Thermo Scientific^{TM} Q-Extractive^{TM} hybrid quadrupole-orbitrap mass spectrometer controlled by Xcalibur 4.1 software. Mass spectra were acquired in full scan mode with an isolation window of 1 m/z from 50-750 m/z (AC, ISP, DHISP, and TMTL) or 100 to 1500 m/z (PHTHA and DPG). The resolution was set to 70000.

Raw mass spectral data files were collected in triplicate including a blank between each run. The data were imported into Compound Discoverer^{TM} 2.0 software (Thermo, Switzerland) and processed according to the work flow shown in Figure E.5 (SI). Standard settings were used except for the following variables: 10^5 counts intensity threshold for precursors, 0.1 min maximum shift alignment, and 2.5 ppm mass tolerance. Chromatographic peaks detected in one of the input files but missing in others were checked by "Fill Gaps" option. The composition (of a general formula $C_cH_hO_o$) was predicted based on exact mass and isotopic patterns. Additionally, the identity of the compounds was determined by a search within mzCloud [23] and ChemSpider [24] databases. The results were summarized by descriptive statistics and were used as an input to differential analysis. Thermo Xcalibur software suite was used for calculations of quantification.

2.4 GPC

Gel permeation chromatography (GPC) for the determination of the molecular weight distribution of the compounds present in the oil phase was performed using Agilent 1260 Infinity LC (Agilent, Switzerland) with two PolarSil linear S columns (PSS, Germany) operated at 55 °C and a refractive index detector. 5 g/L LiBr in DMSO solution was used both as a sample solvent and as an eluent of the analytes (conc. 33 g/L). The injection volume of 80 μl was combined with a flow of 1 ml/min. MW of the compounds in the samples was determined by a calibration standard in the range 152 to 211000 g/mol (poly(vinyl pyridine) extended with vanillin).

2.5 Organic carbon analysis

The content of organic carbon in the samples was measured by a Vario EL Cube elemental analyzer (Elementar, Germany). Approx. 5 mg of oil and 40 mg of aqueous phase were weighted in triplicate and measured against sulfanilamide (puriss. p.a. ≥99 %, Sigma Aldrich) as a standard. The following settings were applied: pressure 1250 mbar, flow of He carrier gas 250 ml/min, flow of O_2 carrier gas 50 ml/min (for first 90 s), combustion tube temperature 1150 °C, reduction tube temperature 850 °C.

3 Results and Discussion

3.1 Aqueous phase composition

The LC-ESI-MS/MS analyses have shown that the aqueous phase is a mixture of hundreds of compounds, with phthalic acid (PHTHA), isophorone (ISP), dipropylene glycol (DPG), and acetone (AC) being the most prominent constituents that were quantified (Table E.1).

Table E.1: Quantification (g/L) of the major constituents of the aqueous (AQ) and oil (OIL) fractions. The values are expressed as means with standard deviations. Columns 1 - 4 (250 - 325 °C) represent runs with GFRC, AC, and KOH. Run 325 °C, -KOH was performed with GFRC and AC (without KOH). Run 325 °C, -GFRC was performed with AC and KOH (without GFRC).

	250°C	275°C	300°C	325°C	325°C -KOH	325°C -GFRC
AQ						
ISP	12.3 ± 0.2	14 ± 2	7.7 ± 0.9	6.3 ± 0.2	2.0 ± 0.2	-
PHTHA	37 ± 2	39 ± 3	31 ± 4	20 ± 2	2.2 ± 0.1	-
DPG	10 ± 1	17 ± 2	9 ± 1	3.8 ± 0.4	16.8 ± 0.8	-
AC	8.2 ± 0.4	14.4 ± 0.3	14.8 ± 0.2	16.1 ± 0.4	37 ± 4	11.7 ± 0.3
OIL						
ISP	300 ± 20	300 ± 20	230 ± 3	220 ± 10	38 ± 3	80 ± 8
DHISP	90 ± 20	85 ± 7	76 ± 1	75 ± 5	-	23 ± 3
TMTL	230 ± 30	230 ± 20	140 ± 10	179 ± 8	-	500 ± 40

While PHTHA and DPG are monomeric units of the polyester chain, ISP is not an indigenous ingredient of the resin, so its presence must be attributed to secondary reactions. The concentrations of PHTHA decreased with temperature from 37 g/L at T = 250 °C to 20 g/L at T = 325 °C. The obtained tendency was in accordance with previous results, which indicated that PHTHA tends to be converted into secondary reaction products with increasing temperatures [20], especially above T = 325 °C. Without the KOH, the concentrations of PHTHA were significantly lower (2.2 g/L), indicating an inefficient hydrolysis of the polyester chains leading to the release of this compound. In the absence of GFRC, no PHTHA was detected in the aqueous phase. The amounts of ISP followed a similar trend with regard to the temperature, being reduced by half from 12.3 g/L to 6.3 g/L between 250 and 325 °C. While minor amounts of the compound were detected in the run without KOH, none was present without the composite material. The concentrations of DPG were maximized at T = 275 °C (17 g/L) and were also significant in the absence of catalyst, which indicated an effective non-catalyzed hydrolysis of the bonds in the polyester chain leading to the release of DPG units. DPG was calibrated with an isomeric mixture of 4-oxa-2,6-heptanediol, 2-(2-hydroxy-propoxy)-propan-1-ol, and 2-(2-hydroxy-1-methyl-ethoxy)-propan-1-ol, all of which were also detected in the analyzed samples. AC content in the samples was in the range 8.2 - 16.1 g/L, generally increasing with reaction temperature. In the runs without KOH, the concentration of AC were significantly higher (37 g/L), which showed that part of the co-solvent was converted during the catalyzed hydrothermal solvolysis. Neither maleic acid, nor styrene were identified among the reaction products. The combined quantification results accounted for 69 - 106 % of the organic carbon present in the aqueous phase (Figure E.2). The overall content of carbon varied from 8.9 to 10.9 wt.% with decreasing reaction temperature. The high carbon content in the run without the catalyst could be clearly attributed to the presence of unconverted acetone.

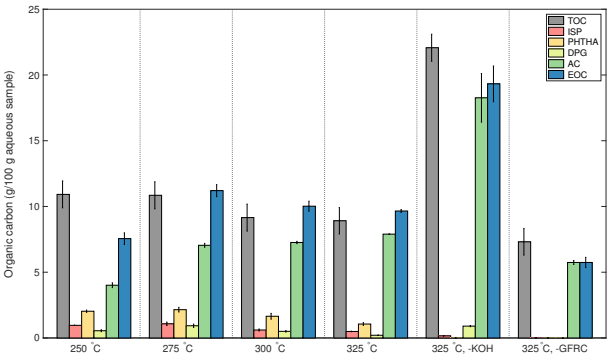

Fig. E.2: Carbon content present in the aqueous phase and the fractions of carbon explained by the quantification of individual compounds. EOC - explained organic carbon. Groups 1 - 4 (250 - 325 °C) represent runs with GFRC, AC, and KOH. Run 325 °C, -KOH was performed with GFRC and AC (without KOH). Run 325 °C, -GFRC was performed with AC and KOH (without KOH).

3.2 Oil phase composition

The analyzed oil fraction was a complex mixture containing a broad spectrum of chemicals making a full quantification of this fraction a task involving evaluation of hundreds of chemical species. The most prominent peaks were identified as ISP, dihydroisophorone (DHISP), and 3,3,6,8-tetramethyl-1-tetralone (TMTL). The quantification results for the oil fraction (Table E.1) show that all were found in significant amounts. Concentration of DHISP were the lowest decreasing with temperature from 90 g/L at T = 250 °C to 75 g/L at T = 325 °C. While the compounds were absent from the oil produced without the catalyst, low concentrations were identified in the absence of GFRC materials indicating AC as its origin. TMTL was the second most abundant compound present in the oil fraction ranging from 230 g/L to 179 g/L and following the same temperature trends as DHISP. Interestingly, TMTL concentrations of 500 g/L were found in the oil produced without the composite, thus further confirming AC to be responsible for the formation of the major oil constituents in this study, in accordance with partial identifications reported by Sokoli et al. [21]. ISP concentrations were the highest among the identified compounds (300 - 220 g/L) and were also decreasing with temperature. The obtained quantification results accounted for 45 - 60 % of the organic carbon present in the oil phase, which itself was constant at 80 %.

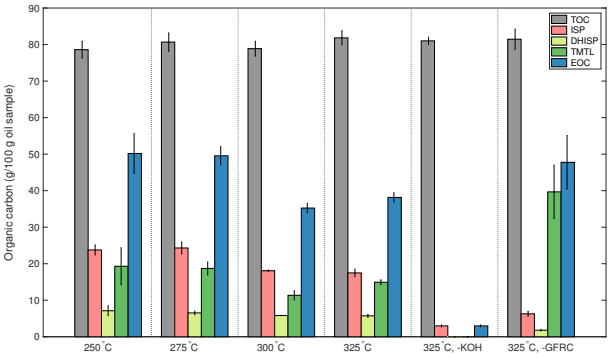

Fig. E.3: Carbon content present in the oil phase and the fractions of carbon explained by the quantification of individual compounds. EOC - explained organic carbon. Groups 1 - 4 (250 - 325 °C) represent runs with GFRC, AC, and KOH. Run 325 °C, -KOH was performed with GFRC and AC (without KOH). Run 325 °C, -GFRC was performed with AC and KOH (without GFRC).

In addition to the quantified compounds, a number of moderately sized peaks have been identified in the oil (listed in Table E.2 of SI). The assessment of the molecular weight distribution of the oil constituents shows a narrow distribution of MW values (200 - 500 g/mol) (Figure E.4). At higher reaction temperatures (T ≥ 300 °C), an additional fraction of high molecular weight compounds (MW = 500 - 10000 g/mol) is present, indicating repolymerization reactions [25]. The main GPC peak representing MW values around 150 g/mol expresses the presence of ISP and DHISP. While the absence of GFRC material resulted in even narrower distribution

of molecular weights, the lack of catalyst had the opposite effect, most probably due to an ineffective degradation of the polymer (Figure E.3).

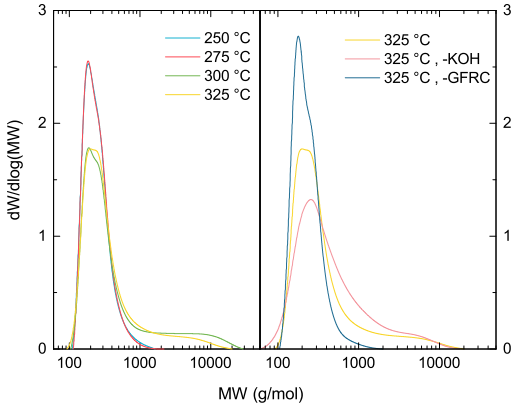

Fig. E.4: GPC results for the oil phase. (left) The MW distribution for the runs with GFRC, AC, and KOH in the temperature range 250 - 325 °C. (right) Comparison of the run at T = 325 °C with the blank runs, i.e. 325 °C, -KOH (GFRC and AC present, without KOH) and 325 °C, -GFRC (AC and KOH present, without GFRC). Please note: the MW distributions for 250 and 275 °C are virtually indistinguishable.

3.3 Reaction mechanisms

Near- and supercritical fluids (e.g. water, alcohols, glycols) are excellent media for numerous thermal transformations including hydrolysis, condensation, dehydration, and many others [26, 27]. While the production of monomers such as PHTHA and DPG can be easily explained by the hydrolysis of ester bonds in the polyester chain, the pathways for the formation of secondary intermediates are not so clear. The presence of ISP in the control run without GFRC indicated that AC, and not the composite, was its source. According to the literature, ISP can be formed through self-condensation of AC involving aldol condensation (from AC to diacetone alcohol to triacetone alcohol), dehydration (from triacetone dialcohol to phorone), and 1,6-Michael cyclization (from phorone to ISP) [28]. In addition, TMTL is formed according to a similar reaction pathway as a result of condensation of ISP with mesityl oxide (formed by dehydration of diacetone alcohol). The conversion pathway has been shown to take place over a wide range of experimental conditions [28–31], including solvolysis [21]. A scheme with summarized reaction pathways is provided in the SI (Figure E.7). The presence of GFRC and variations in temperature seem to influence the equilibrium of the AC-ISP-TMTL system. Without the composite material, TMTL is the major reaction product. In the absence of catalyst, ISP at a low concentration is the only product, indicating the importance of KOH for this pathway. With GFRC and KOH, ISP is the major reaction product, followed by TMTL. While DHISP is not a part of the previously reported reaction pathway, it is clearly formed by reduction of ISP. Interestingly, neither maleic acid nor styrene

were found among the reaction products in the aqueous and oil fractions. Cross-linking between styrene and the double bond of maleic acid make these areas of the polymer impervious to hydrothermal treatment as they are not hydrolyzable. Breakdown of the surrounding ester bonds would therefore result in the release of these parts of the thermoset resin as phenylethylene-succinate co-polymers. It can be argued that due to their lack of polarity, they would be solubilized by acetone in the oil fraction. Previous studies of thermoset polyesters have described this fraction of liquefaction products as oligomers of low molecular weight ($\leq$ 2000 g/mol) with a great tendency to internal cyclization [25]. Furthermore, due to the randomness of the curing process, those styrene-maleic acid co-polymers would not have any defined structure, but would be represented by a broad spectrum of possible combinations.

4 Conclusions

Maximizing the sustainability of GFRC recycling via solvolysis in near-critical water requires utilization of all available product streams: both the the glass fibers and the resin degradation products. In order to assess the potential for production of value-added building blocks and other chemicals from the organic matrix, a state of the art analytic tools such as high resolution LC-MS/MS should be applied for the identification and quantification of the non-volatile reaction products. Moreover, the method can be successfully applied for the measurements of semi-volatiles. The reaction products from solvolysis of UP-based GFRC resulted in formation of a broad spectrum of chemical species distributed between two distinctive phases: an aqueous and an oil fraction. Already at this stage of the process, a polarity based separation of the monomeric building blocks and secondary reaction products was observed. The former group of chemicals, including PHTHA and DPG, represented the hydrolyzable building blocks of the polyester chain that could be recycled directly and were found exclusively in the aqueous phase. The second group of compounds, which included valuable secondary reaction products such as ISP, DHISP, and TMTL, dominated the content of the oil fraction, the majority of which was formed due to self-condensation of acetone. The combination of the selected analytic methodology with verified quantification procedures resulted in high quality data, as indicated by the explanation of nearly 100 % of the organic carbon in the aqueous phase. With production of various valuable chemicals being a partial aim of GFRC solvolysis, a shift towards detailed quantitative assessments of the conversion products in studies is required in order to evaluate the true sustainability of these processes.

5 Acknowledgments

This research was supported by the Danish Council for Strategic Research (DSF grant no. 1305-00030B) and Danish Agency for Science, Technology and Innova-

tion (grant no. 11-118412). Part of this work was supported by and performed within the Swiss Competence Center for Energy Research BIOSWEET. Funding from the Commission for Technology and Innovation (CTI, Bern, Switzerland) and from the Energy System Integration Platform at PSI is gratefully acknowledged. The authors would also like to thank Timon Käser and David Scholz for the help with TOC and GPC measurements, respectively.

6 Supporting information

Table E.2: The major compounds identified in the products from solvolysis of GFRC. The chemicals quantified in the aqueous and oil fractions are followed by a list of additional tentative identifications in the oil phase.

Name	Formula	MW (g/mol)	Sample
Quantified			
Phthalic acid (PHTHA)	$C_8H_6O_4$	166	AQ
Dipropylene glycol (DPG)	$C_6H_{14}O$	102	AQ
3,5,5-Trimethylcyclohex-2-en-1-one (isophorone, ISP)	$C_9H_{14}O$	138	AQ & OIL
3,3,5-Trimethylcyclohexan-1-one (dihydroisophorone, DHISP)	$C_9H_{16}O$	140	OIL
3,3,6,8-Tetramethyl-1-tetralone (TMTL)	$C_{14}H_{18}O$	202	OIL
Identified			
Tetrapropylene glycol	$C_{12}H_{26}O_5$	250	OIL
Hexapropylene glycol	$C_{18}H_{40}O_7$	368	OIL
Phenyl butenone	$C_{10}H_{10}O$	146	OIL
Dimethyl octahydro keto isopropenyl naphthalene	$C_{15}H_{22}O$	218	OIL
Trimethyl cyclohexylideneacetone	$C_{12}H_{18}O$	178	OIL
Tert-butyl tetrahydro naphthalene	$C_{14}H_{20}$	188	OIL
Isopropenyl dimethyl hexahydro naphthalenone	$C_{15}H_{22}O$	218	OIL
Acetyl ethyl tetramethyl tetralin	$C_{18}H_{26}O$	258	OIL

Table E.3: Parameters describing the quality of the obtained calibrations for each quantified compound.

Compound	Range (mg/ml)	R^2	CV (%) range
AQ			
ISP	0.04 - 0.01	0.99	5.96-15.17
PHA	0.01 - 1.00	0.97	0.82-22.78
DPG	0.0001 - 0.01	0.99	5.27-8.10
AC	0.80 -19.8	0.98	5.5 - 8.0
OIL			
ISP	0.05 - 2.50	0.97	3.89-15.59
DHISP	0.01 - 5.0	0.97	1.87-13.60
TMTL	0.001 - 0.1	0.98	16.94-24.41

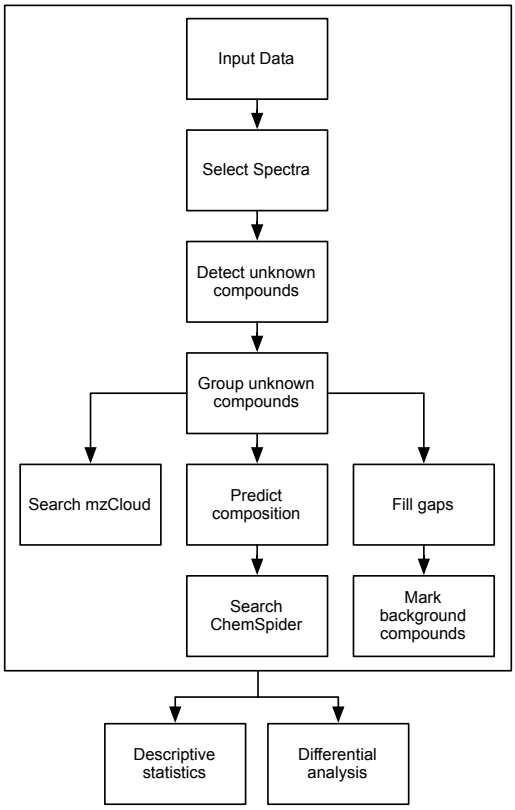

Fig. E.5: Work flow used to process the obtained data in Compound Discoverer^{TM} 2.0 (Thermo Fisher Scientific Inc.). A standard method was applied except for the values of intensity threshold for precursors (10^5 counts), maximum shift alignment (0.1 min), mass tolerance (2.5 ppm).

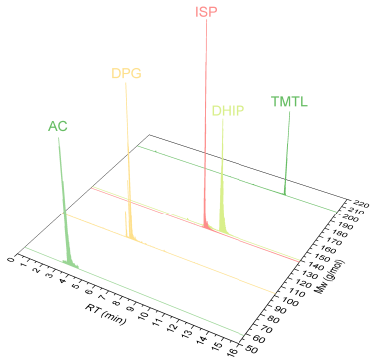

Fig. E.6: Extracted ion chromatographs of the quantified substances. The data were normalized to 100 %.

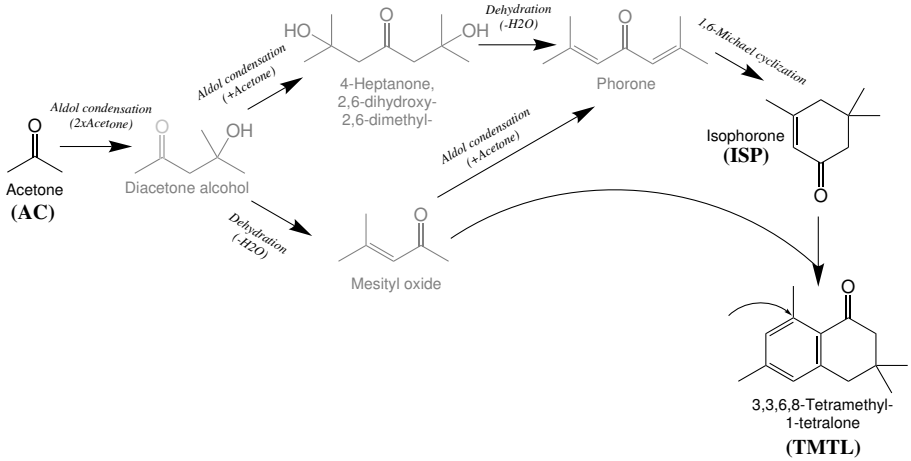

Fig. E.7: Reaction pathways for acetone self-condensation leading to formation of isophorone and 3,3,6,8-tetramethyl-1-tetralone [28]. The grayed out compounds represent the reaction intermediates not identified in this study.

References

[1] Plastics Europe, "World Plastic Production 1950–2015," https://committee.iso.org, 2016, [Online].

[2] E. L. Teuten, J. M. Saquing, D. R. Knappe, M. A. Barlaz, S. Jonsson, A. Björn, S. J. Rowland, R. C. Thompson, T. S. Galloway, and R. Yamashita, "Transport and release of chemicals from plastics to the environment and to wildlife," *Philos. Trans. R. Soc. London, Ser. B*, vol. 364, no. 1526, pp. 2027–2045, 2009.

[3] T. Iwaya, S. Tokuno, M. Sasaki, M. Goto, and K. Shibata, "Recycling of fiber reinforced plastics using depolymerization by solvothermal reaction with catalyst," *J. Mater. Sci.*, vol. 43, no. 7, pp. 2452–2456, 2008.

[4] M. Goto, "Chemical recycling of plastics using sub-and supercritical fluids," *J. Supercrit. Fluids*, vol. 47, no. 3, pp. 500–507, 2009.

[5] J.-i. Ozaki, S. K. I. Djaja, and A. Oya, "Chemical recycling of phenol resin by supercritical methanol," *Ind. Eng. Chem. Res.*, vol. 39, no. 2, pp. 245–249, 2000.

[6] R. Piñero-Hernanz, C. Dodds, J. Hyde, J. García-Serna, M. Poliakoff, E. Lester, M. J. Cocero, S. Kingman, S. Pickering, and K. H. Wong, "Chemical recycling of carbon fibre reinforced composites in near-critical and supercritical water," *Composites Part A*, vol. 39, no. 3, pp. 454–461, 2008.

[7] Y. Shibasaki, T. Kamimori, J.-i. Kadokawa, B. Hatano, and H. Tagaya, "Decomposition reactions of plastic model compounds in sub-and supercritical water," *Polym. Degrad. Stab.*, vol. 83, no. 3, pp. 481–485, 2004.

[8] Y. Liu, M. Farnsworth, and A. Tiwari, "A review of optimisation techniques used in the composite recycling area: State-of-the-art and steps towards a research agenda," *J. Clean. Prod.*, vol. 140, pp. 1775–1781, 2017.

[9] A. Ikeda, K. Katoh, and H. Tagaya, "Monomer recovery of waste plastics by liquid phase decomposition and polymer synthesis," *J. Mater. Sci.*, vol. 43, no. 7, pp. 2437–2441, 2008.

[10] T. Sugeta, S. Nagaoka, K. Otake, and T. Sako, "Decomposition of fiber reinforced plastics using fluid at high temperature and pressure," *Jpn. J. Poly. Sci. Technol.*, vol. 58, no. 10, pp. 557–563, 2001.

[11] G. Jiang, S. J. Pickering, E. H. Lester, T. Turner, K. Wong, and N. Warrior, "Characterization of carbon fibers recycled from carbon fibre/epoxy resin composites using supercritical n-propanol," *Compos. Sci. Technol.*, vol. 69, no. 2, pp. 192–198, 2009.

[12] L. Yuyan, S. Guohua, and M. Linghui, "Recycling of carbon fibre reinforced composites using water in subcritical conditions," *Mater. Sci. Eng., A*, vol. 520, no. 1, pp. 179–183, 2009.

[13] Y. Bai, Z. Wang, and L. Feng, "Chemical recycling of carbon fibers reinforced epoxy resin composites in oxygen in supercritical water," *Mater. Des.*, vol. 31, no. 2, pp. 999–1002, 2010.

[14] C. Morin, A. Loppinet-Serani, F. Cansell, and C. Aymonier, "Near-and supercritical solvolysis of carbon fibre reinforced polymers (CFRPs) for recycling carbon fibers as a valuable resource: State of the Art," *J. Supercrit. Fluids*, vol. 66, pp. 232–240, 2012.

[15] D. Liu, L. Song, P. Wu, Y. Liu, Q. Li, and Z. Yan, "Direct hydro-liquefaction of sawdust in petroleum ether and comprehensive bio-oil products analysis," *Bioresource Technol.*, vol. 155, pp. 152–160, 2014.

[16] F. La Mantia, *Handbook of plastics recycling*. iSmithers Rapra Publishing, 2002.

[17] J. Rybicka, A. Tiwari, and G. A. Leeke, "Technology readiness level assessment of composites recycling technologies," *J. Clean. Prod.*, vol. 112, pp. 1001–1012, 2016.

[18] G. Oliveux, J.-L. Bailleul, E. L. G. La Salle, N. Lefèvre, and G. Biotteau, "Recycling of glass fibre reinforced composites using subcritical hydrolysis: Reaction mechanisms and kinetics, influence of the chemical structure of the resin," *Polym. Degrad. Stab.*, vol. 98, no. 3, pp. 785–800, 2013.

[19] A. Kamimura, K. Yamada, T. Kuratani, Y. Taguchi, and F. Tomonaga, "Effective depolymerization waste FRPs by treatment with DMAP and supercritical alcohol," *Chem. Lett.*, vol. 35, no. 6, pp. 586–587, 2006.

[20] G. Oliveux, J.-L. Bailleul, and E. L. G. La Salle, "Chemical recycling of glass fibre reinforced composites using subcritical water," *Composites Part A*, vol. 43, no. 11, pp. 1809–1818, 2012.

[21] H. U. Sokoli, M. E. Simonsen, R. P. Nielsen, K. R. Arturi, and E. G. Søgaard, "Conversion of the matrix in glass fiber reinforced composites into a high heating value oil and other valuable feedstocks," *Fuel Process. Technol.*, vol. 149, pp. 29–39, 2016.

[22] U.S. Environmental Protection Agency, "Validation and Peer Review of U.S. Environmental Protection Agency Chemical Methods of Analysis."

[23] HighChem Ltd., Bratislava, Slovakia, "mzCloud - Advanced Mass Spectral Database," https://www.mzcloud.org/, 2016, [Online].

[24] Royal Society of Chemistry, Thomas Graham House, Cambridge, UK, "Chemspider," http://www.chemspider.com/, 2016, [Online].

[25] M. Vallee, G. Tersac, N. Destais-Orvoen, and G. Durand, "Chemical recycling of class A surface quality sheet-molding composites," *Ind. Eng. Chem. Res.*, vol. 43, no. 20, pp. 6317–6324, 2004.

[26] G. Brunner, "Near critical and supercritical water. Part I. Hydrolytic and hydrothermal processes," *J. Supercrit. Fluids*, vol. 47, no. 3, pp. 373–381, 2009.

[27] ——, "Near and supercritical water. Part II: Oxidative processes," *J. Supercrit. Fluids*, vol. 47, no. 3, pp. 382–390, 2009.

[28] K. Ramanamurty and G. Salvapati, "New dimensions on value added aldol chemicals of acetone," *J. Sci. Ind. Res.*, vol. 59, no. 5, pp. 339–349, 2000.

[29] J. A. Bertrand, D. Cheung, A. D. Hammerich, H. O. House, W. T. Reichle, D. Vanderveer, and E. J. Zaiko, "Structure of the substance $C_{27}H_{38}O$ formed by the base-catalyzed self-condensation of isophorone."

[30] H.-G. Franck, J. Turowski, R. Kemalettin Erünlü, G. Storch, M. Zander, and R. Lemke, "3,3,6,8-Tetramethyl-tetralon-(1), ein Kondensationsprodukt des Acetons," *Liebigs Ann.*, vol. 724, no. 1, pp. 94–101, 1969.

[31] K. Ramanamurty and G. Salvapathi, "Catalytic cyclocondensation of acetone to isophorone," *Indian J. Chem., Sect. B: Org. Chem. Incl. Med. Chem*, vol. 38, pp. 24–28, 1999.

ISSN (online): 2446-1636
ISBN (online): 978-87-7112-908-3

AALBORG UNIVERSITY PRESS